

IMPACT OF CLIMATE VARIABILITY ON STREAMFLOW AND WATER QUALITY IN  
THE NORTH CENTRAL UNITED STATES

A Dissertation  
Submitted to the Graduate Faculty  
of the  
North Dakota State University  
of Agriculture and Applied Science

By

Karen Renee Ryberg

In Partial Fulfillment of the Requirements  
for the Degree of  
DOCTOR OF PHILOSOPHY

Major Program:  
Environmental and Conservation Sciences  
Option:  
Environmental Science

April 2015

Fargo, North Dakota

North Dakota State University  
Graduate School

---

**Title**

Impact of Climate Variability on Streamflow and Water Quality in the North  
Central United States

---

**By**

Karen Renee Ryberg

---

The Supervisory Committee certifies that this *disquisition* complies with North Dakota State  
University's regulations and meets the accepted standards for the degree of

**DOCTOR OF PHILOSOPHY**

SUPERVISORY COMMITTEE:

Wei Lin

---

Chair

F. Adnan Akyüz

---

Rhonda Magel

---

Aldo V. Vecchia

---

Approved:

April 1, 2015

---

Date

Eakalak Khan

---

Department Chair

## ABSTRACT

Long-term precipitation, temperature, and streamflow records were used to compare changes in precipitation and potential evapotranspiration to changes in runoff within 25 stream basins. Historical changes in the region appear to be more consistent with complex transient shifts in seasonal climatic conditions than with gradual climate change. Annual peak streamflow data were divided into two populations, snowmelt/spring and summer/fall, to test the hypotheses that, because of changes in precipitation regimes, the odds of summer/fall peaks have increased and, because of temperature changes, snowmelt/spring peaks happen earlier. The odds of summer/fall peaks occurring have increased across the study area. In northern portions of the study region, snowmelt/spring peaks are occurring earlier by 8.7 to 14.3 days. Tree-ring chronologies and historical precipitation data in a region around the Souris River Basin, were analyzed to model past long-term variations of precipitation. Results show that precipitation varies on multi-decadal time scales.

The Red River of the North drains much of eastern North Dakota and northwestern Minnesota and flows north into Manitoba, Canada, ultimately into Lake Winnipeg, so phosphorus transport is an International concern. Phosphorus changes over time were determined and phosphorus concentrations at the International border, when adjusted for variability in streamflow (flow-normalized), have generally increased from 1972-2012; however, most of that increase happened in the 1970s. Flux, the total amount of phosphorus transported, has increased dramatically in recent decades; however, when adjusted for streamflow variability (so that flux is from variation caused by the occurrence of high- or low-flow conditions), the flow-normalized flux has declined in recent years. This indicates that an important reason for increased flux is climatic – the wet conditions experienced since 1993.

These changes have implications for water interests, such as potential changes in lead-time for flood forecasting or changes in the operation of flood-control dams or wastewater treatment plants. Results suggest that the recent wet period may be a part of natural variability on a very long time scale and that this not only has implications for flood risk, but for nutrient export to Canada.

## ACKNOWLEDGEMENTS

I thank members of my committee, Drs. Wei Lin (advisor), Adnan Akyüz, Rhonda Magel, and Aldo (Skip) Vecchia, for their support and feedback in this process. Thank you also to Gregg Wiche, Director of the U.S. Geological Survey (USGS) North Dakota Water Science Center, who encouraged me to pursue a Ph.D. and provided work flexibility. Much of this work has been submitted as journal articles. I would like to thank the valuable input of those that reviewed the research before journal submission. Bob Hirsch and Greg McCabe both of the USGS reviewed *Impact of Climate Variability on Runoff in the North-Central United States*. Glenn Hodgkins of the USGS and Steve Buan of the NOAA North Central River Forecast Center reviewed *Changes in Seasonality and Timing of Peak Streamflow in Snow and Semi-Arid Climates of the North Central United States, 1910-2012*. Greg Pederson and Kevin Vining both of the USGS reviewed *Tree-Ring Based Estimates of Long-Term Seasonal Precipitation in the Souris River Region of Saskatchewan, North Dakota, and Manitoba*. Galen Hoogestraat and Bob Hirsch both of the USGS reviewed the dissertation chapter *Total Phosphorus Changes in the Red River of the North at Emerson, Manitoba, and Fargo, North Dakota-Moorhead, Minnesota, 1970-2012*. Rochelle Nustad and Laura Medalie, both of the USGS, provided reviews of a conference proceedings paper based on *Total Phosphorus Changes in the Red River of the North at Emerson, Manitoba, and Fargo, North Dakota-Moorhead, Minnesota, 1970-2012*.

## **DEDICATION**

This dissertation is dedicated to all my ancestors who valued education and whose ambitions brought them to North Dakota.

## TABLE OF CONTENTS

ABSTRACT .....	iii
ACKNOWLEDGEMENTS .....	v
DEDICATION .....	vi
LIST OF TABLES .....	xii
LIST OF FIGURES.....	xiii
LIST OF ABBREVIATIONS.....	xviii
LIST OF SYMBOLS .....	xxiii
LIST OF APPENDIX TABLES .....	xxvii
LIST OF APPENDIX FIGURES.....	xxviii
CHAPTER 1. INTRODUCTION .....	1
1.1. Introduction .....	1
1.2. Research Questions, Hypotheses, and Objectives .....	4
1.2.1. Research Questions.....	4
1.2.2. Hypotheses.....	4
1.2.3. Objectives .....	4
1.3. Dissertation Organizations .....	5
CHAPTER 2. LITERATURE REVIEW .....	7
2.1. Climate Effects on Flooding and Runoff.....	7
2.2. Changes in Regional Precipitation and Temperature .....	10
2.3. Long-Term Review of Previous Wet and Dry Periods.....	11
2.5. Climate Effects on Water Quality .....	37
2.5. Phosphorus in the Red River of the North Basin.....	40
2.5.1. Phosphorus in the Red River of the North Basin in the United States .....	44
2.5.2. Phosphorus in the Red River of the North Basin in Canada.....	49

CHAPTER 3. IMPACT OF CLIMATE VARIABILITY ON RUNOFF IN THE NORTH CENTRAL UNITED STATES .....	53
3.1. Introduction .....	53
3.2. Data and Methodology .....	56
3.3. Results .....	67
3.3.1. Comparison of Precipitation and Runoff Trends Between Groups .....	67
3.3.2. Analysis of Climate and Runoff Changes for Individual Basins .....	72
3.4. Discussion and Conclusions .....	84
CHAPTER 4. CHANGES IN SEASONALITY AND TIMING OF PEAK STREAMFLOW IN SNOW AND SEMI-ARID CLIMATES OF THE NORTH- CENTRAL UNITED STATES, 1910-2012.....	88
4.1. Introduction .....	89
4.2. Data and Methodology .....	92
4.2.1. Logistic Regression to Examine Seasonality of Peaks .....	96
4.2.2. Linear Regression to Examine Timing of Peaks within Seasons .....	98
4.3. Results of Logistic Regression to Examine Seasonality of Peaks .....	99
4.3.1. Interpretation of the Model .....	102
4.4. Changes in Timing of Peaks .....	103
4.4.1. Snowmelt/Spring Peaks .....	104
4.4.2. Summer/Fall Peaks .....	105
4.5. Discussion and Conclusions .....	107
CHAPTER 5. TREE-RING BASED ESTIMATES OF LONG-TERM SEASONAL PRECIPITATION IN THE SOURIS RIVER REGION OF SASKATCHEWAN, NORTH DAKOTA, AND MANITOBA .....	110
5.1. Introduction .....	111
5.1.1. Definition of Study Area.....	112
5.2. Data and Methodology .....	113

5.2.1. Hierarchical Agglomerative Cluster Analysis .....	115
5.2.2. Tree-Ring Analysis .....	116
5.2.3. Modeling Precipitation .....	119
5.3. Results of Cluster Analysis.....	124
5.4. Results of Precipitation Modeling .....	130
5.5. Conclusions .....	141
<b>CHAPTER 6. TOTAL PHOSPHORUS CHANGES IN THE RED RIVER OF THE NORTH AT EMERSON, MANITOBA, AND FARGO, NORTH DAKOTA- MOORHEAD, MINNESOTA, 1970-2012 .....</b>	<b>143</b>
6.1. Background.....	143
6.2. Discharge History and Variability Analysis .....	150
6.2.1. Red River at Emerson, Manitoba.....	153
6.2.2. Red River at Fargo, North Dakota-Moorhead, Minnesota .....	156
6.3. Total Phosphorus Data.....	160
6.3.1. Red River of the North at Emerson, Manitoba .....	161
6.3.2. Red River at Fargo, North Dakota, and Moorhead, Minnesota.....	164
6.4. Weighted Regression on Time, Discharge, and Season - WRTDS.....	168
6.4.1. Flow Normalization .....	171
6.5. Results of WRTDS Analysis .....	174
6.5.1. WRTDS Results for Red River at Emerson, Manitoba .....	174
6.5.2. WRTDS Results for the Red River at Fargo, North Dakota-Moorhead Minnesota.....	182
6.6. Discussion.....	189
6.7. Future Research .....	191
<b>CHAPTER 7. SUMMARY AND CONCLUSIONS .....</b>	<b>192</b>
7.1. Future Research .....	198

REFERENCES.....	199
APPENDIX A. SUPPORTING MATERIAL FOR CHAPTER 4 CHANGES IN SEASONALITY AND TIMING OF PEAK STREAMFLOW IN SNOW AND SEMI-ARID CLIMATES OF THE NORTH-CENTRAL UNITED STATES, 1910-2012.....	
A.1. Study Area .....	227
A.2. Streamgauge Selection.....	231
A.2.1. Additional Comments on Streamgauge Selection .....	233
A.3. Information about Regions .....	235
A.4. Creation of Annual Snowmelt/Spring and Summer/Fall Peak Streamflow Series.....	238
A.5. Regression to Examine Timing and Magnitude of Peaks at Individual Streamgages.....	238
A.5.1. Changes in Timing and Magnitude of Snowmelt/Spring Peaks at Individual Streamgages .....	239
A.5.2. Changes in Timing and Magnitude of Summer/Fall Peaks at Individual Streamgages.....	241
A.5.3. Summary of Changes in Timing and Magnitude at Individual Streamgages .....	243
APPENDIX B. WAVELET ANALYSIS AND MULTIREOLUTION DECOMPOSITION FOR TREE-RING BASED ESTIMATES OF LONG-TERM SEASONAL PRECIPITATION IN THE SOURIS RIVER REGION OF SASKATCHEWAN, NORTH DAKOTA, AND MANITOBA.....	
	244
APPENDIX C. DISCHARGE ANALYSIS FOR LONG-TERM STREAMGAGES ON THE RED RIVER OF THE NORTH AND SELECTED TRIBUTARIES.....	
	252
C.1. Red River of the North at Wahpeton, North Dakota.....	255
C.2. Red River of the North at Hickson, North Dakota.....	257
C.3. Red River of the North at Fargo, North Dakota.....	258
C.4. Sheyenne River at West Fargo, North Dakota.....	260
C.5. Red River of the North at Halstad, Minnesota.....	263
C.6. Red Lake River at Crookston, Minnesota.....	264
C.7. Red River of the North at Grand Forks, North Dakota.....	266
C.8. Pembina River at Neche, North Dakota.....	269

C.9. Red River of the North at Emerson, Manitoba ..... 271

APPENDIX D. DIAGNOSTIC PLOTS FOR WEIGHTED REGRESSIONS ON TIME,  
DISCHARGE, AND SEASON (WRTDS) ANALYSES OF TOTAL PHOSPHORUS IN  
THE RED RIVER OF THE NORTH AT EMERSON, MANITOBA, AND FARGO,  
NORTH DAKOTA-MOORHEAD, MINNESOTA ..... 273

## LIST OF TABLES

<u>Table</u>	<u>Page</u>
2.1. Wet and dry periods in the north central United States before 1900. ....	13
3.1. Twenty-five U.S. Geological Survey (USGS) streamgaging stations chosen to compare changes in runoff with changes in precipitation in the study area. ....	58
3.2. Long-term mean precipitation and runoff, 1915-2010, for basin groups A, B, C, and D, for season 1, January-June, Season 2, July-December, and annual season. ....	69
3.3. Change in runoff from dry (1953-64) to wet (1982-93 and 1998-2009) periods for season 1 (January-June) and season 2 (July-December) for basin groups B, C, and D. ....	81
3.4. Coefficient of determination ( $R^2$ ) for linear regression models relating seasonal 7-day high runoff to seasonal runoff for groups B, C, and D. ....	84
4.1. Regions associated ecological regions (Commission for Environmental Cooperation, 1997) and climate classes (Kottek et al., 2006), and the Julian date that separates the snowmelt/spring peak date density from the rain/summer peak date density. ....	96
4.2. Final logistic regression model measures of significance when using dataset 3 (test dataset). ....	101
4.3. Logistic regression model coefficients, odds ratio, and 99-percent confidence intervals. ....	102
5.1. Information and associated statistics for precipitation models. ....	133
6.1. Changes in total phosphorus flow-normalized concentration between three time points in period 1, 1970-1993, and three time points in period 2, 1993-2012, for the Red River at Emerson, Manitoba. ....	182
6.2. Changes in total phosphorus flow-normalized flux between three time points in period 1, 1970-1993, and three time points in period 2, 1993-2012, for the Red River at Emerson, Manitoba. ....	182
6.3. Changes in total phosphorus flow-normalized concentration between three time points in period 1, 1970-1993, and three time points in period 2, 1993-2012, for the Red River of the North at Fargo, North Dakota-Moorhead, Minnesota. ....	189
6.4. Changes in total phosphorus flow-normalized flux between three time points in period 1, 1970-1993, and three time points in period 2, 1993-2012, for the Red River of the North at Fargo, North Dakota- Moorhead, Minnesota. ....	189

## LIST OF FIGURES

<u>Figure</u>	<u>Page</u>
2.1. Red River flood, spring 1881, Fargo, North Dakota. Courtesy of the Elwyn B. Robinson Department of Special Collections, Chester Fritz Library, University of North Dakota, OGL # 797-245. ....	35
2.2. The Northern Pacific railroad bridge over the Red River at Fargo, North Dakota, and Moorhead, Minnesota, 1897. The bridge was weighted down with locomotives and loaded boxcars. The tracks were washed out east and west of the cities. Buildings in the background include the Union elevator, erected in 1879 and Moorhead saloons. Courtesy of the North Dakota State University Archives, Fargo, N.D. (328.2.4). ....	36
2.3. U.S. consumption (agricultural use) of phosphate as a plant nutrient (U.S. Department of Agriculture Economic Research Service, 2013). ....	42
2.4. U.S. consumption (agricultural use) of plant nutrients (fertilizer) as a percent of total consumption (U.S. Department of Agriculture Economic Research Service, 2013). ....	42
3.1. Isohyetal lines (1895-2010), U.S. Geological Survey streamgages, and their basins, grouped into four regions based on similarity of topography, climate, and historic patterns of runoff. Precipitation data interpolated to a grid then contoured using ArcMap10 inverse-distance weighting and extended to rectangular boundary of states polygons. ....	59
3.2. Isohyetal lines (1895-2010), U.S. Geological Survey streamgages, and their basins, grouped. ....	61
3.3. Land-cover (Homer et al., 2004) map for study area. ....	63
3.4. Basin group ratio of 12-year mean to long-term mean for season 1, January-June, and season 2, July-December, precipitation and runoff. Note: Ratio is positive and centered around one. The scales were transformed to depict the precipitation and runoff on the same scale, still centered around one. ....	68
3.5. Average runoff for season 1 (January-June) and season 2 (July-December) for selected 12-year periods for basin groups B, C, and D. ....	73
3.6. Average precipitation versus potential evapotranspiration (Thornthwaite method) for season 1 (January-June) and season 2 (July-December) for selected 12-year periods for basin groups B, C, and D (open symbols, pre-1970; solid symbols, post-1970). ....	74
3.7. Average precipitation versus runoff and runoff plus estimated evapotranspiration (left-hand graphs) and fitted runoff versus observed runoff (right-hand graphs) for season 1 (January-June) and season 2 (July-December) for selected 12-year periods for basin groups B, C, and D. ....	77

3.8. Residuals from nonlinear water-balance model for estimating runoff for season 1 (January-June) and season 2 (July-December) for selected 12-year periods for basin groups B, C, and D.....	78
3.9. Observed 7-day high runoff (left-hand graphs) and fitted versus observed 7-day high runoff (right-hand graphs) for season 1 (January-June) and season 2 (July-December) for selected 12-year periods for basin groups B, C, and D.....	83
4.1. Regions based on climate, ecoregions, and major river basins (shown in Appendix A), and streamgages.....	90
4.2. Geographically related areas of similar Julian date density patterns. The vertical line and number indicate the date that separate potentially snowmelt/spring peaks from those that occur later in the year because of rain (summer/fall) peaks (R1-R7, regions 1-7 in figure 4.1). .....	95
4.3. Trends in Julian date by region for snowmelt/spring peaks (R1-R7, regions 1-7 in figure 4.1).....	105
4.4. Trends in Julian date by region for summer/fall peaks (R1-R7, regions 1-7 in figure 4.1). .....	106
5.1. Locations of the Souris River Basin, study area boundary (four-degree buffer around Souris River Basin), meteorological stations, and potential tree-ring sites. The tree-ring sites ultimately used are labeled with the site name.....	113
5.2. Example multiresolution decomposition of tree-ring chronology at Boundary Bog, Saskatchewan, Canada.....	120
5.3. Dendrogram for cluster analysis with horizontal line indicating five groups of meteorological stations. ....	125
5.4. Boxplots of mean seasonal total precipitation for each group of meteorological stations. ....	127
5.5. The five clusters of meteorological stations in the study area.....	129
5.6. Group 1 (southeast), Season 2 (March-June) modeled and observed 12-year moving average precipitation.....	136
5.7. Group 5 (southern Manitoba and southeastern Saskatchewan), season 3 (July-October) modeled and observed 12-year moving average precipitation.....	138
5.8. Twelve-year moving average annual precipitation for group 1 (southeast) and group 3 (southwest).....	140

6.1. Red River of the North Basin, upstream of the confluence with the Assiniboine Basin at Winnipeg, Manitoba, Canada. (Political divisions, major rivers and lakes, and ecological regions from Commission for Environmental Cooperation (1997); selected streamgauge and water-quality sampling site locations from U.S. Geological Survey Water Data for the Nation, <a href="http://dx.doi.org/10.5066/F7P55KJN">http://dx.doi.org/10.5066/F7P55KJN</a> .)	145
6.2. U.S. total consumption of the plant nutrient phosphate (U.S. Department of Agriculture Economic Research Service, 2013).	147
6.3. U.S. consumption of plant nutrients (fertilizer) as a percent of total consumption (U.S. Department of Agriculture Economic Research Service, 2013).	147
6.4. Estimated total phosphorus flux from wastewater treatment plants in the Red River of the North Basin.	149
6.5. Time series plot of daily mean discharge for the Red River of the North at Emerson, Manitoba.	153
6.6. Running standard deviation of the logarithm of daily mean discharge (Q) for the Red River of the North at Emerson, Manitoba.	154
6.7. Plots of discharge statistics annual 1-day maximum daily mean discharge (maximum day), annual mean of the daily mean discharges (mean daily), annual median of the daily mean discharges (median daily), and annual minimum 7-day mean of the daily mean discharges (7-day minimum) for the Red River of the North at Emerson, Manitoba.	155
6.8. Decadal boxplots of daily mean discharge for the Red River of the North at Emerson, Manitoba.	156
6.9. Time series plot of daily mean discharge for the Red River at Fargo, North Dakota, and Moorhead, Minnesota.	157
6.10. Running standard deviation of logarithm of daily mean discharge for the Red River at Fargo, North Dakota, and Moorhead, Minnesota.	157
6.11. Plots of discharge statistics annual 1-day maximum daily mean discharge (maximum day), annual mean of the daily mean discharges (mean daily), annual median of the daily mean discharges (median daily), and annual minimum 7-day mean of the daily mean discharges (7-day minimum) for the Red River at Fargo, North Dakota, and Moorhead, Minnesota.	159
6.12. Decadal boxplots of daily mean discharge for the Red River at Fargo, North Dakota-Moorhead, Minnesota. Twelve discharge values of zero were replaced with 0.1 because of the use of a logarithmic scale.	160

6.13. Total phosphorus concentration versus discharge, concentration versus time, boxplots of concentration by month, and boxplots of the sampled discharges and all daily discharges for the Red River of the North at Emerson, Manitoba. ....	162
6.14. Observed log flux (load) versus discharge for the Red River of the North at Emerson, Manitoba. ....	163
6.15. Decadal boxplots of total phosphorus for the Red River of the North at Emerson, Manitoba, including some samples prior to the 1970-2012 analysis period. Number of samples per period written above each boxplot. ....	164
6.16. Total phosphorus concentration versus discharge, concentration versus time, boxplots of concentration by month, and side-by-side boxplots of the sampled discharges and all daily discharges for the Red River of the North at Fargo, North Dakota-Moorhead, Minnesota. ....	166
6.17. Observed log flux (load) versus log discharge for the Red River of the North at Fargo, North Dakota-Moorhead, Minnesota. ....	167
6.18. Decadal boxplots of total phosphorus for the Red River of the North at Fargo, North Dakota-Moorhead, Minnesota. Number of samples per period written above each boxplot. ....	168
6.19. Observed and estimated total phosphorus concentrations and fluxes in the Red River of the North at Emerson, Manitoba, 1970-1993. ....	175
6.20. Observed and estimated total phosphorus concentrations and fluxes in the Red River of the North at Emerson, Manitoba, 1993-2012. ....	176
6.21. Estimated total phosphorus concentration change the Red River of the North at Emerson, Manitoba, from 1970 to 1993. ....	177
6.22. Estimated total phosphorus concentration change the Red River of the North at Emerson, Manitoba, from 1993 to 2012. ....	178
6.23. Estimated January 1, April 1, July 1, and October 1 total phosphorus concentration over time, at the 25th, 50th, and 75th percentiles of discharge for each month for the period 1970-1993, Red River of the North at Emerson, Manitoba. ....	180
6.24. Estimated January 1, April 1, July 1, and October 1 total phosphorus concentration over time, at the 25th, 50th, and 75th percentiles of discharge for each month for the period 1993-2012, Red River of the North at Emerson, Manitoba. ....	181
6.25. Observed and estimated total phosphorus concentrations and fluxes in the Red River of the North at Fargo, North Dakota-Moorhead, Minnesota, 1970-1993. ....	183
6.26. Observed and estimated total phosphorus concentrations and fluxes in the Red River of the North at Fargo, North Dakota-Moorhead, Minnesota, 1993-2012. ....	184

6.27. Estimated total phosphorus concentration change in the Red River of the North at Fargo, North Dakota-Moorhead, Minnesota, from 1970 to 1993.....	185
6.28. Estimated total phosphorus concentration change in the Red River of the North at Fargo, North Dakota-Moorhead, Minnesota, from 1993 to 2012.....	186
6.29. Estimated January 1, April 1, July 1, and October 1 total phosphorus concentration over time at the 25th, 50th, and 75th percentiles of discharge for each month for the period 1970-1993, Red River of the North at Fargo, North Dakota-Moorhead, Minnesota.....	187
6.30. Estimated January 1, April 1, July 1, and October 1 total phosphorus concentration over time at the 25th, 50th, and 75th percentiles of discharge for each month for the period 1993-2012, Red River of the North at Fargo, North Dakota-Moorhead, Minnesota.....	188

## LIST OF ABBREVIATIONS

10 <sup>3</sup> ft <sup>3</sup> /s .....	1,000 cubic feet per second
10 <sup>3</sup> kg/yr. ....	1,000 kilograms per year
10 <sup>6</sup> kg/yr. ....	1,000,000 kilograms per year
AC .....	Agglomerative coefficient
AHCCD.....	Adjusted and Homogenized Canadian Climate Data
ANOVA .....	Analysis of variance
BB.....	Boundary Bog tree-ring chronology
BCV.....	Burning Coal Vein tree-ring chronology
BSk.....	Köppen-Geiger climate class for zone described as Arid, Steppe, cold arid
C .....	Celsius
CB.....	Cedar Butte tree-ring chronology
cfs .....	cubic feet per second
Conc. ....	Concentration
DDLf .....	Dry, drought, low streamflow
df.....	degrees of freedom
Dfa.....	Köppen-Geiger climate class for zone described as snow, fully humid, hot summer
Dfb.....	Köppen-Geiger climate class for zone described as snow, fully humid, warm summer
dplR.....	Dendrochronology Program Library in R
Dwa .....	Köppen-Geiger climate class for zone described as snow, winter dry, hot summer
Dwb .....	Köppen-Geiger climate class for zone described as snow, winter dry, warm summer
EC.....	Environment Canada

eds.....	editors
EGRET .....	Exploration and Graphics for RivEr Trends
ENSO .....	El Niño Southern Oscillation
EPS .....	Express population signal
Eq. ....	Equation
Eqs. ....	Equations
Est.....	Estimated
ET .....	Evapotranspiration
exp .....	exponential
F.....	Fahrenheit
F.....	Flood
ft <sup>3</sup> /s .....	cubic feet per second
FWA .....	Flow-weighted average
GAGES-II.....	Geospatial Attributes of Gages for Evaluating Streamflow, version II
GCM.....	Global circulation model
GIS .....	Geographic information system
GRACE .....	Gravity Recovery and Climate Experiment
HACA.....	Hierarchical agglomerative cluster analysis
HCDN-209 .....	Hydro-Climatic Data Network – 2009
HR .....	High runoff
HUC .....	Hydrologic unit code
IA.....	Iowa
INT .....	Intercept term
IPCC .....	Intergovernmental Panel on Climate Change
ISRB .....	International Souris River Board

ITRDB.....	International Tree-Ring Data Bank
KG.....	Köppen-Geiger
kg/day.....	Kilograms per day
km <sup>2</sup> .....	kilometers squared
LLJ.....	Low-level jet
LR.....	Low runoff
mg/L.....	milligrams per liter
mm.....	millimeters
MN.....	Minnesota
MO.....	Missouri
MPCA.....	Minnesota Pollution Control Agency
NASA.....	National Aeronautics and Space Administration
NAWQA.....	National Water Quality Assessment
NCDC.....	National Climatic Data Center
ND.....	North Dakota
NDDH.....	North Dakota Department of Health
NDSU.....	North Dakota State University
NE.....	Nebraska
NOAA.....	National Oceanic and Atmospheric Administration
NRC.....	National Research Council
O.....	Other
OBS.....	Observed runoff change
Obs.....	Observed
OGL.....	Abbreviation used in front of numbers identifying resources from the University of North Dakota Orin G. Libby Manuscript Collection

OK.....	Oklahoma
P.....	Phosphorus
pdf.....	probability density function
PDO.....	Pacific Decadal Oscillation
PET.....	Potential evapotranspiration
PET1.....	Potential evapotranspiration, season 1 (January-June)
PET2.....	Potential evapotranspiration, season 2 (July-December)
PHDI.....	Palmer Hydrologic Drought Index
PHDI2.....	Palmer Hydrologic Drought Index lagged two months
PR1.....	Precipitation, season 1 (January-June)
PR2.....	Precipitation, season 2 (July-December)
RES.....	Runoff change in the residuals
RO1.....	Runoff, season1 (January-June)
RO2.....	Runoff, season 2 (July-December)
RO7DH.....	7-day high runoff
ROFIT.....	Fitted runoff from water-balance model
RORES.....	Residuals from water-balance model
RWI.....	Ring-width index
S.....	Snow
SD.....	South Dakota
SD.....	Sustained drought
SNR.....	Signal to noise ratio
SSS.....	Subsample signal strength

SWMM.....	Storm Water Management Model
tons/d.....	Tons per day
TP.....	Total phosphorus
TRNP.....	Theodore Roosevelt National Park tree-ring chronology
U.S.....	United States
USGS.....	U.S. Geological Survey.
USHCN.....	United States Historical Climatology Network
WBD.....	Watershed boundary dataset
WBM.....	Runoff change explained by water-balance model
WI.....	Wisconsin
WRTDS.....	Weighted Regressions on Time, Discharge, and Season
WS.....	Wet or snowy period
WWTP.....	Wastewater treatment plant

## LIST OF SYMBOLS

$\int_0^{\infty} [.] dQ$ .....	integral of quantity in brackets from 0 to infinity with respect to daily mean streamflow
$f_{T_s}(Q)$ .....	probability density function of discharge, specific to a particular time or year, designated as $T_s$ , and $T_s$ is restricted to values between 0 and 1 (the fractional part of the time variable $T$ )
$R_a^2$ .....	adjusted coefficient of determination in simple linear regression and adjusted coefficient of multiple determination in multiple linear regression
$\chi^2$ .....	chi-squared
[.] <sup>+</sup> .....	quantity in brackets if the quantity is positive, zero otherwise
° .....	degree
∈ .....	epsilon, error term in regression model
+ .....	addition
× .....	multiplication
< .....	less than
= .....	equals
> .....	greater than
− .....	when used with formulas or numbers, subtraction or a negative number
/ .....	division
∞ .....	infinity
≤ .....	less than or equal to
≥ .....	greater than or equal to
Ave{.}	average of quantity in brackets
<i>BIC</i> .....	Schwartz's information criterion

$\cos$ .....	cosine function
$C_p$ .....	Mallow's $C_p$ criterion
D4.....	16-year ( $2^4$ ) wavelet voice
D5.....	32-year ( $2^5$ ) wavelet voice
D6.....	64-year ( $2^6$ ) wavelet voice
D7.....	128-year ( $2^7$ ) wavelet voice
$e$ .....	a constant, 2.7183..., the base of the natural logarithm
$E[C_{fn}(T)]$ .....	flow-normalized concentration for time $T$
$E[F_{fn}(T)]$ .....	flow-normalized flux for time $T$
$E[.]$ .....	expected value of quantity in brackets
$e_1$ .....	error term for 7-day high runoff linear regression model 1
$e_2$ .....	error term for 7-day high runoff linear regression model 2
$e_3$ .....	error term for 7-day high runoff linear regression model 3
$G_i$ .....	the $i$ th group
$I\{\cdot\}$ .....	indicator function that is 1 for a specified condition and zero otherwise
J1.....	fitted regression coefficient
J2.....	fitted regression coefficient
$k$ .....	growth per year after the initial growth spurt
K1.....	fitted regression coefficient
L1.....	fitted regression coefficient
$\log$ .....	logarithm
$\log(c)$ .....	logarithm of water-quality constituent concentration

$\log(c)_d$	daily estimate of the logarithm of water-quality constituent concentration
$N$	total number of observations
$nYrs$	number of years in tree-ring chronology
$Q$	daily mean discharge
$q$	logarithm of daily mean discharge
$R^2$	coefficient of determination in simple linear regression and coefficient of multiple determination in multiple linear regression
$RW(t)$	Ring-width growth at time $t$
$\sin$	sine function
$S_j$	the $j$ th season
$t$	time $t$
$T$	time, in decimal years
$trunc$	function that takes a single numeric argument $x$ and returns a numeric vector containing the integers formed by truncating the values in $x$ toward 0.
$w(Q,T)$	WRTDS estimate of concentration as a function of $Q$ (discharge) and $T$ (time)
$\mathbf{X}$	matrix representation of explanatory variables in regression model
$\mathbf{X}\beta$	matrix algebra representation of the observations of the explanatory variables and model parameters
$\mathbf{Y}$	matrix representation of response variables in regression model
$\alpha$	alpha, model coefficient
$\beta$	beta, model coefficient
$\gamma$	gamma, the initial year
$\delta$	delta, represents slope of the decrease in growth of ring-widths

$\pi$ ..... pi, a constant, 3.1416...

## LIST OF APPENDIX TABLES

<u>Table</u>	<u>Page</u>
A.1. Köppen-Geiger classification system (Kottek et al., 2006) representing the five climate classes in the study area. ....	228
A.2. Examples of streamgages in same 8-digit hydrologic unit with overlapping periods of record where both were retained for the study. ....	233
A.3. Additional information about each region in the study area. ....	236
C.1. U.S. Geological streamgage numbers and names, listed in downstream direction along the Red River of the North, used for discharge analysis. ....	252

## LIST OF APPENDIX FIGURES

<u>Figure</u>	<u>Page</u>
A.1. Water-Resources Regions (Seaber et al., 1987) within the study area.....	227
A.2. Köppen-Geiger climate classes (Kottek et al., 2006) used within the study area. The white hole in Wyoming extending slightly into Montana is an arid climate with desert precipitation and cold arid temperature and was left out because of the desert designation. ....	229
A.3. Level II Ecological regions (Commission for Environmental Cooperation, 1997) within the study area. The white holes within the study area are mountainous ecological regions that were removed.....	230
A.4. Seven groups used in study, each of similar climate and topography.....	231
A.5. Average streamgage locations for each region (region 2 divided into eastern and western parts) for the period 1910-1961 and 1962-2012. ....	237
A.6. Trends in snowmelt/spring Julian date and magnitude of peaks at long-term streamgages, after adjusting for antecedent conditions. ....	240
A.7. Trends in summer/fall Julian date and magnitude of peaks at long-term streamgages, after adjusting for antecedent conditions. ....	242
B.1. Multiresolution decomposition for Boundary Bog tree-ring chronology (MacDonald and Case, 2014).....	245
B.2. Multiresolution decomposition for Burning Coal Vein tree-ring chronology (Meko and Sieg, 2014a).....	245
B.3. Multiresolution decomposition for Theodore Roosevelt National Park tree-ring chronology (Meko and Sieg, 2014b).....	246
B.4. Multiresolution decomposition for Cedar Butte tree-ring chronology (Meko and Sieg, 2014c). ....	246
B.5. Wavelet analysis for Boundary Bog tree-ring chronology (MacDonald and Case, 2014). ....	248
B.6. Wavelet analysis for Burning Coal Vein tree-ring chronology (Meko and Sieg, 2014a).....	249
B.7. Wavelet analysis for Theodore Roosevelt National Park tree-ring chronology (Meko and Sieg, 2014b). ....	250
B.8. Wavelet analysis for Cedar Butte tree-ring chronology (Meko and Sieg, 2014c). ....	251

C.1. Discharge for period of record ending September 30, 2014, Red River of the North at Wahpeton, North Dakota. ....	255
C.2. Running standard deviation of logarithm of daily mean discharge (Q) for the Red River of the North at Wahpeton, North Dakota. ....	255
C.3. Annual 1-day maximum daily mean discharge (maximum day), annual mean of the daily mean discharges (mean daily), annual median of the daily mean discharges (median daily), and annual minimum 7-day mean of the daily mean discharges (7-day minimum), Red River of the North at Wahpeton, North Dakota. ....	256
C.4. Discharge for period of record ending September 30, 2014, Red River of the North at Hickson, North Dakota. ....	257
C.5. Running standard deviation of logarithm of daily mean discharge (Q) for the Red River of the North at Hickson, North Dakota. ....	257
C.6. Annual 1-day maximum daily mean discharge (maximum day), annual mean of the daily mean discharges (mean daily), annual median of the daily mean discharges (median daily), and annual minimum 7-day mean of the daily mean discharges (7-day minimum), Red River of the North at Hickson, North Dakota. ....	258
C.7. Discharge for period of record ending September 30, 2014, Red River of the North at Fargo, North Dakota. ....	259
C.8. Running standard deviation of logarithm of daily mean discharge (Q) for the Red River of the North at Fargo, North Dakota. ....	259
C.9. Annual 1-day maximum daily mean discharge (maximum day), annual mean of the daily mean discharges (mean daily), annual median of the daily mean discharges (median daily), and annual minimum 7-day mean of the daily mean discharges (7-day minimum), Red River of the North at Fargo, North Dakota. ....	260
C.10. Discharge for period of record ending September 30, 2014, Sheyenne River West at Fargo, North Dakota. ....	261
C.11. Running standard deviation of logarithm of daily mean discharge (Q) for the Sheyenne River at West Fargo, North Dakota. ....	261
C.12. Annual 1-day maximum daily mean discharge (maximum day), annual mean of the daily mean discharges (mean daily), annual median of the daily mean discharges (median daily), and annual minimum 7-day mean of the daily mean discharges (7-day minimum), Sheyenne River at West Fargo, North Dakota. ....	262
C.13. Discharge for period of record ending September 30, 2014, Red River of the North at Halstad, Minnesota. ....	263

C.14. Running standard deviation of logarithm of daily mean discharge (Q) for the Red River of the North at Halstad, Minnesota. ....	263
C.15. Annual 1-day maximum daily mean discharge (maximum day), annual mean of the daily mean discharges (mean daily), annual median of the daily mean discharges (median daily), and annual minimum 7-day mean of the daily mean discharges (7-day minimum), Red River of the North at Halstad, Minnesota. ....	264
C.16. Discharge for period of record ending September 30, 2014, Red Lake River at Crookston, Minnesota. ....	265
C.17. Running standard deviation of logarithm of daily mean discharge (Q) for the Red Lake River at Crookston, Minnesota. ....	265
C.18. Annual 1-day maximum daily mean discharge (maximum day), annual mean of the daily mean discharges (mean daily), annual median of the daily mean discharges (median daily), and annual minimum 7-day mean of the daily mean discharges (7-day minimum), Red Lake River at Crookston, Minnesota. ....	266
C.19. Discharge for period of record ending September 30, 2014, Red River of the North at Grand Forks, North Dakota. ....	267
C.20. Running standard deviation of logarithm of daily mean discharge (Q) for the Red River of the North at Grand Forks, North Dakota. ....	267
C.21. Annual 1-day maximum daily mean discharge (maximum day), annual mean of the daily mean discharges (mean daily), annual median of the daily mean discharges (median daily), and annual minimum 7-day mean of the daily mean discharges (7-day minimum), Red River of the North at Grand Forks, North Dakota. ....	268
C.22. Discharge for period of record ending September 30, 2014, Pembina River at Neche, North Dakota. ....	269
C.23. Running standard deviation of logarithm of daily mean discharge (Q) for the Pembina River at Neche, North Dakota. ....	269
C.24. Annual 1-day maximum daily mean discharge (maximum day), annual mean of the daily mean discharges (mean daily), annual median of the daily mean discharges (median daily), and annual minimum 7-day mean of the daily mean discharges (7-day minimum), Pembina River at Neche, North Dakota. ....	270
C.25. Discharge for period of record ending September 30, 2014, Red River of the North at Emerson, Manitoba. ....	271
C.26. Running standard deviation of logarithm of daily mean discharge (Q) for the Red River of the North at Emerson, Manitoba. ....	271

C.27. Annual 1-day maximum daily mean discharge (maximum day), annual mean of the daily mean discharges (mean daily), annual median of the daily mean discharges (median daily), and annual minimum 7-day mean of the daily mean discharges (7-day minimum), Red River of the North at Emerson, Manitoba.....	272
D.1. WRTDS diagnostic plots for 1970-1993 total phosphorus model for the Red River of the North at Emerson, Manitoba.....	274
D.2. WRTDS diagnostic plots for 1993-2012 total phosphorus model for the Red River of the North at Emerson, Manitoba.....	275
D.3. WRTDS diagnostic plots for 1970-1993 total phosphorus model for the Red River of the North at Fargo, North Dakota-Moorhead, Minnesota.....	276
D.4. WRTDS diagnostic plots for 1993-2012 total phosphorus model for the Red River of the North at Fargo, North Dakota-Moorhead, Minnesota.....	277

## **CHAPTER 1. INTRODUCTION**

### **1.1. Introduction**

There is much speculation about the impact of climate change on water quantity and water quality. However, natural variability is an important component that is not yet fully understood and likely explains many of the extreme events and longer-term wet and dry periods experienced by the north central United States (U.S.). This work seeks to study changes in water quantity and water quality in the north central U.S., explain the changes in terms of climate change (natural or anthropogenic) and land-use change and place the changes in the context of the many hydrologic predictions for future climates.

Brekke et al. (2009) stated, from a Federal perspective, that trend analysis related to climate change should be “conducted over large areas affected by similar weather systems.” The north central U.S. is notable for floods in recent years, including floods on the Souris River (Saskatchewan, Canada, North Dakota, and Manitoba, Canada) Red River of the North (North Dakota, Minnesota, and Manitoba), James River (North Dakota and South Dakota), Big Sioux River (South Dakota, Minnesota, and Iowa), Minnesota River, Iowa River, and Cedar River (Iowa). Unprecedented flooding in the Souris River Basin of Manitoba, North Dakota, and Saskatchewan, in 2011 caused extensive damage to Minot, North Dakota, and numerous smaller communities in Manitoba, North Dakota, and Saskatchewan. The region stands out in other studies as an area of increased flood magnitude (Hirsch and Ryberg, 2012; Peterson et al., 2013); however, it has received less attention than other areas of the country, such as New England and the Rocky Mountains. Researchers are interested in areas that are more populous or pristine mountain basins (unfortunately those areas often have shorter periods of observational record and can limit one to smaller basins). In addition, the climate of this region is complex with large

annual variability in temperature and precipitation (Wishart, 2004). It is far removed from the moderating effects of the oceans, but the climate is an interaction of oceanic influences with much of the moisture coming from tropical air masses from the Gulf of Mexico, drying and warming effects from air masses originating in the Pacific that cross the Rocky Mountains, and cold air masses from the arctic (Andersen et al., 2012; Jensen, no date; Wishart, 2004).

Large changes in runoff have occurred in the conterminous U.S. during the past century, with higher runoff tending to occur during the period from the 1970s to the first decade of the 21st century than in the early and mid-1900s (Lins and Slack, 1999, McCabe and Wolock, 2002). The north central U.S. has experienced particularly large increases in runoff and flood magnitudes in recent decades and there is much interest in the attribution of these changes (Hirsch and Ryberg, 2012). For future water resources management, understanding the reasons for these changes and the potential of long-term wet or dry periods is important. Are recent increases in runoff the result of natural climate variability, anthropogenic climate change, land-use changes, or some combination of all of these factors? Paleo-climatic studies from eastern North and South Dakota based on tree rings and lake sediments indicate similar transitions to wet periods have occurred several times in the past 1,000-2,000 years (Shapley et al., 2005; Laird et al., 2003). At the same time, the Intergovernmental Panel on Climate Change (IPCC) is certain that floods will increase in future climates, but because of the variety of physical processes involved in flooding and human influences such as land use change, there is a great deal of uncertainty in the exact nature of changes (Whitfield, 2012).

Documented increases in precipitation intensity and frequency have not directly translated into increases in flooding though and global circulation models indicate atmospheric forcing has had only a slight impact on runoff in the north central U.S. during the 20th century

(increase of less than 5 percent, Milly et al., 2005). Furthermore, increases in precipitation during summer and fall coincide with runoff increases in recent decades and global circulation models indicate these precipitation increases are closely related to sea-surface-temperature anomalies and are not caused by global warming (Wang et al., 2009). Others suggest that land-use change is a major contributor to changes in runoff (Schilling et al., 2008; Zhang and Schilling, 2006) and can change in long-term climate by altering climate (Pielke, Sr., 2005; Pielke, Sr. et al., 2011).

Another important consideration is the timing of changes. In the snow and semi-arid climates of the north central U.S., annual peak streamflows, the greatest flow in a stream recorded at a streamgage in a given year, can occur any day of the year, but are most likely to occur in the spring (in snow-melt dominated streams) or the summer (in rain-dominated areas). The differences in the timing of peaks are attributable to climate, and climate changes may cause changes in the timing and seasonality of annual peaks. These issues are important for a wide variety of water-resource decisions from the operation of flood-control dams to decisions about agricultural irrigation.

There is a growing awareness of the impact of climate variability or change on water quality. The Federal Advisory Committee Draft Climate Assessment Report, released for public review in 2013, states that climate-related water-quality challenges are “increasing, particularly sediment and contaminant concentrations after heavy downpours... Air and water temperatures, precipitation intensity, and droughts affect water quality in rivers and lakes. More intense runoff and precipitation generally increase river sediment, nitrogen, and pollutant loads. Increasing water temperatures and intensifying droughts can decrease lake mixing, reduce oxygen in bottom waters, and increase the length of time pollutants remain in water bodies” (National Climate Assessment and Development Advisory Committee, 2013).

## **1.2. Research Questions, Hypotheses, and Objectives**

### **1.2.1. Research Questions**

1. Are recent changes in runoff in the north central U.S. a product of natural climate variability, land use, anthropogenic climate change, or a combination of these forces?
2. Have changes in precipitation and temperature changed the peak streamflow timing and seasonality in the north central U.S.?
3. Was the Souris River flood of 2011, which caused extensive damage to Minot, North Dakota, and numerous smaller communities in Manitoba, North Dakota, and Saskatchewan, part of natural variability on a very long time scale or a product of anthropogenic climate change?
4. Can a climate signal, whether part of natural variability or part of climate change, be discerned in water quality in the study area?

### **1.2.2. Hypotheses**

It is hypothesized that transient changes between wet and dry climatic conditions occur on a time scale greater than decadal. The changes are complex, each one somewhat different from the others (in length, severity, seasonality, and regional coverage). In the north central U.S. the probability of experiencing summer or fall rain-generated peaks has increased and spring peaks may come earlier in some areas. Natural climate variability occurs on very long time scales and can make it difficult to discern variability from change. Water-quality issues in the region are impacted by climate variability and/or change.

### **1.2.3. Objectives**

The goal of this study was to contribute to the description of long-term natural climate variability in the region and its impact on surface-water quantity and quality and to develop ways

to separate out climate variability or change from potential land-use effects. These goals were accomplished by:

1. Studying the impact of climate variability on runoff in select basins of the north central U.S.
2. Separating climate and land-use/other effects in the analysis of runoff.
3. Examining changes in peak streamflow timing and seasonality and their relation to documented changes in precipitation and temperature.
4. Relating a recent historic flood to past wet and dry periods going back over 300 years.
5. Developing a model of phosphorus changes over time in the Red River of the North Basin.

### **1.3. Dissertation Organizations**

This dissertation is organized into four papers prefaced by an introduction and literature review, followed by overall conclusions and appendices. Chapter 1 is the introduction. Chapter 2 is a literature review. Chapter 3 entitled “Impact of Climate Variability on Runoff in the North Central United States” is also the basis of an article published in *the Journal of Hydrologic Engineering* (Ryberg et al., 2014). The article is co-authored with Dr. Wei Lin of North Dakota State University (NDSU) and Dr. Aldo Vecchia of the U.S. Geological Survey (USGS). Dr. Lin provided direction and review. Dr. Vecchia modeled water-balance for the study. Chapter 4 is the basis of a manuscript entitled “Changes in Seasonality and Timing of Peak Streamflow in Snow and Semi-Arid Climates of the North Central United States, 1910-2012” submitted to the journal *Hydrological Processes*. The article is co-authored by Drs. Adnan Akyüz and Lin of NDSU and Gregg Wiche of the USGS. All authors were involved in data analysis, interpretation, and review of the manuscript. Chapter 5 is the basis of a manuscript titled “Tree-Ring Based Estimates of Long-Term Seasonal Precipitation in the Souris River Region of Saskatchewan, North Dakota, and Manitoba” submitted to the *Journal of the Canadian Water Resources*

*Association.* The manuscript is co-authored by Drs. Vecchia, Akyüz, Lin, who all contributed review, direction, and assistance with interpretation. Chapter 6 presents analysis describing changes in total phosphorus in the Red River of the North Basin and will contribute to the development of a structural equation model of phosphorus in the Basin. The model will result in a future journal article. Chapter 7 presents the overall conclusions. Supplementary figures, analyses, and text are provided in Appendixes A-D. Information from Chapter 6 is the subject of a conference proceedings paper for the 2015 ASABE (American Society of Agricultural and Biological Engineers) North Central Intersectional Conference, coauthored by Drs. Akyüz and Lin.

## **CHAPTER 2. LITERATURE REVIEW**

An extensive literature review was performed at each stage of this research. The literature review includes the following five sections: climate effects on runoff and flooding, changes in regional precipitation and temperature, long-term review of previous wet and dry periods, climate effects on water quality, and phosphorus in the Red River of the North Basin.

### **2.1. Climate Effects on Flooding and Runoff**

The IPCC is certain that floods will increase in future climates, but because of the variety of physical processes involved in flooding and human influences such as land use change, there is a great deal of uncertainty in the exact nature of changes (Whitfield, 2012). Documented increases in precipitation intensity and frequency have not directly translated into increases in flooding. Peterson et al. (2013) summarized the current state of knowledge related to changes in heat waves, cold waves, floods, and droughts in the U.S. In terms of floods and droughts, they said that annual peak streamflow is not changing uniformly and that “confounding the analysis of trends in river flooding is multiyear and even multidecadal variability likely caused by both large-scale atmospheric circulation changes and basin-scale ‘memory’ in the form of soil moisture. Droughts also have long-term trends as well as multiyear and decadal variability.”

Whitfield (2012) summarized key uncertainties, hypotheses, and projections for floods in future climates. He stated that “while the Intergovernmental Panel on Climate Change (IPCC) is certain that floods will increase in future climates, there is considerable uncertainty in the exact nature of how this will evolve largely because floods are generated by a wide variety of hydroclimatological events.” The warming atmosphere increases evaporation and thus the quantity of water vapor (Andersen and Shepherd, 2013). This is considered an “intensification” of the hydrologic cycle and one of the consequences is that extreme precipitation events are

becoming more intense and frequent in some areas (Whitfield, 2012). However, studies of observed streamflow have not shown a consistent increase in flooding across the U.S. (Lins and Slack, 1999; Douglas et al., 2000; McCabe and Wolock, 2002; Kundzewicz et al., 2005; Brekke et al., 2009; Hirsch and Ryberg, 2012). “Depending upon which GCMs [global circulation models] are used and also the relative importance of snowmelt contribution in flood volumes, catchment characteristics, and location, the impacts of climate change on floods can be positive or negative” (Whitfield, 2012). Furthermore, “changes in the timing of floods are expected to be explained by changes in the generating process; for example, in warmer climates, snowmelt peaks are expected to occur earlier in the year” (Whitfield, 2012). In many regions, such as the north central U.S., “the contribution of snowmelt to spring floods is likely to decline” (Whitfield, 2012). With a warmer atmosphere, more precipitation will fall as rain instead of snow. Rain on snow events may increase and snowmelt flooding may occur earlier (because of smaller snowpacks and warmer temperatures; Whitfield, 2012).

Andersen and Shepherd (2013) also summarized projections related to floods in future climates. Some of their “key” projections that are relevant to the north central U.S. include the following. “Atmospheric circulation patterns are changing. Mid-latitude storm tracks and associated precipitation are shifting poleward and LLJs [low-level jets] are strengthening and producing more precipitation in the Great Plains... Global mean precipitation rate and runoff are increasing, particularly in northern latitudes, with variable local and regional trends... Warming causes earlier snowmelt and diminished snowpack, however, mid-winter snowfall could increase in continental regions... Regional soil moisture anomalies are increasing with implications for degree of infiltration, runoff, and enhanced atmospheric feedbacks.” In terms of surface-water runoff quantity, increases in extreme precipitation may result in more floods caused by

infiltration excess overland flow because the intensity of the precipitation will increasingly exceed the infiltration capacity.

Temperature regimes also affect flooding and runoff. While heat waves attract attention, changes in daily low temperatures may affect runoff in snow climates more. “In North America over the last 50 years, there has been a 50 percent increase in the number of unusually warm nights. Nights that fell into the top tenth percentile in terms of temperature for the climate of the 1950s now fall into the top fifteenth percentile and almost all of this increase has happened since 1975” (National Environmental Education Foundation, 2014). Higher overnight lows during the spring would lead to less freezing overnight, thereby hastening the spring runoff. Projections of warming suggest that spring flooding may come earlier (Melillo et al., 2014). Researchers have linked a warming global climate to a shift in the timing of runoff in “snowmelt-fed rivers” (Bates et al., 2008). Trends toward earlier timing of peak streamflow (which are influenced by snowmelt runoff in areas with substantial snowpack) have been observed in New England (Hodgkins et al., 2003), New York (Burns et al., 2007), eastern North America (Hodgkins and Dudley, 2006), California (Dettinger and Cayan, 1995), the western U.S. (Cayan et al., 2001; Dettinger, 2005; Stewart et al., 2005; McCabe and Clark, 2005; Regonda et al., 2005), and Canada (Burn et al., 2008; Zhang et al., 2001).

Warming will also have an effect on surface storage of water (Whitfield, 2012). In some areas, less precipitation will fall as snow and therefore less water will be stored on the landscape over winter months, increasing runoff during the winter – a phenomenon already observed in many areas. As freeze-thaw cycles change with temperature, another change in winter is an increase or decrease in ice jam formation and earlier ice jam events (Whitfield, 2012; Andersen and Shepherd, 2013). This may result in an increase in flooding in some areas and a decrease in

others. While runoff trends are expected to follow precipitation trends, there is uncertainty in part because of evapotranspiration. Temperature changes and the influence of carbon dioxide changes on plant processes affect evapotranspiration, which then affects runoff (America's Climate Choices: Panel on Advancing the Science of Climate Change et al., 2010).

Changes in temperature and precipitation (form, amount, and intensity) may contribute to greater variability in flooding, such as more independent rain-generated peak streamflow events rather than one large snowmelt peak, changes in the date of the annual streamflow peak or the center of volume for water years, floods of longer duration, or floods of greater magnitude but shorter duration. In arid areas, more days without rain may occur, resulting in longer periods of lower flow. However, these areas may also experience more intense precipitation that can result in flash flooding, fast rates of rise, and erosion. Some studies suggest climate change will result in large-scale changes to storm tracks, low-level jet streams, mesoscale meteorology, and ocean phenomena, such as El Niño, North Atlantic Oscillation, and Pacific Decadal Oscillation (Whitfield, 2012; Andersen and Shepherd, 2013). Runoff is a complex process of water cycling through the atmosphere, land cover, soils, and geologic formations; therefore, in addition to the changes in temperature and precipitation, the response of runoff to climate changes is also influenced by land-use change (America's Climate Choices: Panel on Advancing the Science of Climate Change et al., 2010). All of these processes (natural or anthropogenic) may influence runoff quantity, rate, and timing, but the changes may differ across the landscape.

## **2.2. Changes in Regional Precipitation and Temperature**

Yang et al. (2007) showed that Great Plains precipitation is strongly correlated with Niño-3.4 sea surface temperatures over time scales including semi-annual, annual, and 5.5-8.5 years. Furthermore, a number of studies have identified a decadal-scale (greater than 7 years)

signal in precipitation (Cayan et al., 1998; Garbrecht and Rossel, 2002; Small and Islam, 2008; Small and Islam, 2009; Ault and St. George, 2010). Small and Islam (2008; 2009) identified a statistically significant signal in autumn precipitation in the central U.S. with a periodicity of approximately 12 years, with the signal strongest in the Midwest and Great Plains. Precipitation increases have been reported in all seasons (Karl and Knight, 1998; Wang et al., 2009), with the largest changes observed in fall (Garbrecht and Rossel, 2002; Small and Islam, 2008; Small and Islam, 2009; Wang et al., 2009), and an expectation under atmospheric warming that “more precipitation will fall as rain rather than snow” (Andersen and Shepherd, 2013).

The average surface temperature of the Earth was 1.4°F (0.8 °C) greater during 2000-10 than it was during 1900-10 (America's Climate Choices: Panel on Advancing the Science of Climate Change et al., 2010). A warming Earth is also evidenced in proxy data from ice cores, tree rings, corals, lake sediments, and boreholes and in a decline in Northern Hemisphere snow cover, earlier thawing and later freezing of rivers and lakes (America's Climate Choices: Panel on Advancing the Science of Climate Change et al., 2010). Since 1895, U.S. average temperature has increased by 1.3° to 1.9°F. (in a manner not constant over time), with the greatest warming in winter and spring (Walsh et al., 2014). Wang et al. (2009) showed that the strongest U.S. surface air temperature warming in 1950-2000 occurred in the spring over the northwestern U.S. and the northern plains.

### **2.3. Long-Term Review of Previous Wet and Dry Periods**

Wet and dry periods from approximately 1900 to the present are well documented and data are readily available from agencies such as the USGS, the National Oceanic and Atmospheric Administration, and Environment Canada; therefore, this literature review was done on past tree-ring, precipitation, and streamflow studies in the north central U.S. that

indicated periods of wet and dry conditions prior to 1900 (Brooks et al., 2003; Carlyle, 1984; Case and MacDonald, 2003; Lapp et al., 2013; Rannie, 1998; Red River Basin Board, 2000; Severson and Sieg, 2006; St. George and Nielsen, 2002; St. George and Nielsen, 2003; St. George and Rannie, 2003; Thorleifson et al., 1998). Wet and dry periods and extreme flood and drought events for the north central U.S. and south central Canada before 1900 are summarized in table 2.1. After 1900, there are sufficient instrumental temperature, precipitation, and streamflow data sets to document such periods (such as Environment Canada, 2014; Easterling et al., 1996; Mekis and Vincent, 2011; Menne and Vose, 2011; U.S. Geological Survey, 2015e; Vincent et al., 2012).

Table 2.1. Wet and dry periods in the north central United States before 1900.

Year(s)	Conditions	Region or Basins	Notes	Sources
1406-15	DDLDF	Central North Dakota	Period of drought or dry years (Will, 1946, used bur oak from Missouri River breaks near Bismarck, ND, to identify dry and wet years), could be off +/- 5 years	Severson and Sieg, 2006
1434-52	DDLDF	Central North Dakota	Period of drought or dry years (Will, 1946, used bur oak from Missouri River breaks near Bismarck, ND, to identify dry and wet years; may have some wet years interspersed in period), could be off +/- 5 years	Severson and Sieg, 2006
1471-1501	DDLDF	Central North Dakota	Period of drought or dry years (Will, 1946, used bur oak from Missouri River breaks near Bismarck, ND, to identify dry and wet years), could be off +/- 5 years	Severson and Sieg, 2006
1472-1481	SD	Northwestern Great Plains, Canada	Positive PDO, high variance ENSO	Lapp et al., 2013
1477	DDLDF	Southern Manitoba	Annual precipitation estimated more than 2 standard deviations below mean	St. George and Nielsen, 2002
1483-1494	SD	Northwestern Great Plains, Canada	Positive PDO, high variance ENSO	Lapp et al., 2013
1485	DDLDF	Southern Manitoba	Annual precipitation estimated more than 2 standard deviations below mean	St. George and Nielsen, 2002

DDLDF, dry, drought, low flow; LR, low runoff; SD, sustained drought; F, flood; HR; High runoff; WS, wet or snowy period; S, snow; O, other; PDO, Pacific Decadal Oscillation; ENSO, El Niño Southern Oscillation.

Table 2.1. Wet and dry periods in the north central United States before 1900 (continued).

Year(s)	Conditions	Region or Basins	Notes	Sources
1498-1508	SD	Northwestern Great Plains, Canada	Positive PDO, high variance ENSO	Lapp et al., 2013
1505-18	DDLDF	Central North Dakota	Period of drought or dry years (Will, 1946, used bur oak from Missouri River breaks near Bismarck, ND, to identify dry and wet years), could be off +/- 5 years	Severson and Sieg, 2006
1510	F	Red	Flood upper Red	St. George and Nielsen, 2003
1512-1518	SD	Northwestern Great Plains, Canada	Positive PDO, low variance ENSO	Lapp et al., 2013
1525-31	DDLDF	Central North Dakota	Period of drought or dry years (Will, 1946, used bur oak from Missouri River breaks near Bismarck, ND, to identify dry and wet years), could be off +/- 5 years	Severson and Sieg, 2006
1538	F	Red	Flood upper Red	St. George and Nielsen, 2003
1539-53	DDLDF	Central North Dakota	Period of drought or dry years (Will, 1946, used bur oak from Missouri River breaks near Bismarck, ND, to identify dry and wet years; may have some wet years interspersed in period), could be off +/- 5 years	Severson and Sieg, 2006
1556	DDLDF	Southern Manitoba	Annual precipitation estimated more than 2 standard deviations below mean	St. George and Nielsen, 2002
1559-1570	SD	Northwestern Great Plains, Canada	Positive PDO, high variance ENSO	Lapp et al., 2013
1562-76	DDLDF	Central North Dakota	Period of drought or dry years (Will, 1946, used bur oak from Missouri River breaks near Bismarck, ND, to identify dry and wet years), could be off +/- 5 years	Severson and Sieg, 2006

Table 2.1. Wet and dry periods in the north central United States before 1900 (continued).

Year(s)	Conditions	Region or Basins	Notes	Sources
1576-1583	SD	Northwestern Great Plains, Canada	Positive PDO, low variance ENSO	Lapp et al., 2013
1595	DDLDF	Southern Manitoba	Annual precipitation estimated more than 2 standard deviations below mean	St. George and Nielsen, 2002
1596-1611	DDLDF	Central North Dakota	Period of drought or dry years (Will, 1946, used bur oak from Missouri River breaks near Bismarck, ND, to identify dry and wet years), could be off +/- 5 years	Severson and Sieg, 2006
1612	DDLDF	Southern Manitoba	Annual precipitation estimated more than 2 standard deviations below mean	St. George and Nielsen, 2002
1618-1623	SD	Northwestern Great Plains, Canada	Negative PDO, low variance ENSO	Lapp et al., 2013
1623-27	DDLDF	Central North Dakota	Period of drought or dry years (Will, 1946, used bur oak from Missouri River breaks near Bismarck, ND, to identify dry and wet years; may have some wet years interspersed in period), could be off +/- 5 years	Severson and Sieg, 2006
1626-1630	SD	Northwestern Great Plains, Canada	Negative PDO, low variance ENSO	Lapp et al., 2013
1633-45	DDLDF	Central North Dakota	Period of drought or dry years (Will, 1946, used bur oak from Missouri River breaks near Bismarck, ND, to identify dry and wet years), could be off +/- 5 years, could be off +/- 5 years	Severson and Sieg, 2006
1644	DDLDF	Southern Manitoba	Annual precipitation estimated more than 2 standard deviations below mean	St. George and Nielsen, 2002

Table 2.1. Wet and dry periods in the north central United States before 1900 (continued).

Year(s)	Conditions	Region or Basins	Notes	Sources
1645-1654	SD	Northwestern Great Plains, Canada	Negative PDO, high variance ENSO	Lapp et al., 2013
1646-54	DDLDF	Northern Great Plains	Period of drought or dry years (Meko, 1982, using Ponderosa pine in ND, SD, NE, WY, MT)	Severson and Sieg, 2006
1648-1746	O	Red	Interval without extreme flooding on lower Red	St. George and Nielsen, 2003
1654-63	DDLDF	Central North Dakota	Period of drought or dry years (Will, 1946, used bur oak from Missouri River breaks near Bismarck, ND, to identify dry and wet years), could be off +/- 5 years	Severson and Sieg, 2006
1658	F	Red	Flood upper Red	St. George and Nielsen, 2003
1661	DDLDF	Southern Manitoba	Annual precipitation estimated more than 2 standard deviations below mean	St. George and Nielsen, 2002
1670-1775	DDLDF	Red River	Below-normal precipitation occurring ~2 years out of 3.	St. George and Nielsen, 2002
1673	O	Missouri	First historic documentation of Missouri River flood at mouth, but not known whether this was typical or extreme; Louis Jolliet and Jacques Marquette journals; Marquette wrote "sailing quietly in clear and calm Water, we heard the noise of a rapid, into which we were about to run. I have seen nothing more dreadful. An accumulation of large and entire trees, branches, and floating islands, was issuing from The mouth of The river pekistanoul [Missouri], with such impetuosity that we could not without great danger risk passing through it. So great was the agitation that the water was very muddy, and could not become clear. Pekitanoul is a river of Considerable size, coming from the Northwest,	Marquette, 1966

Table 2.1. Wet and dry periods in the north central United States before 1900 (continued).

Year(s)	Conditions	Region or Basins	Notes	Sources
			from a great Distance; and it discharges into the Missisipi.”	
1682	F	Red	Flood upper Red	St. George and Nielsen, 2003
1682-1688	SD	Northwestern Great Plains, Canada	Positive PDO, low variance ENSO	Lapp et al., 2013
1701-1708	SD	Northwestern Great Plains, Canada	Negative PDO, low variance ENSO	Lapp et al., 2013
1703-12	DDLDF	Northern Great Plains	Period of drought or dry years (Meko, 1982, using Ponderosa pine in ND, SD, NE, WY, MT)	Severson and Sieg, 2006
1707-20	DDLDF	Central North Dakota	Period of drought or dry years (Will, 1946, used bur oak from Missouri River breaks near Bismarck, ND, to identify dry and wet years), could be off +/- 5 years	Severson and Sieg, 2006
1717-1721	SD	Northwestern Great Plains, Canada	Positive PDO, high variance ENSO	Lapp et al., 2013
1726	F	Red	Flood upper Red	St. George and Nielsen, 2003
1727	F	Red	Flood upper Red	St. George and Nielsen, 2003
1728-35	DDLDF	Central North Dakota	Period of drought or dry years (Will, 1946, used bur oak from Missouri River breaks near Bismarck, ND, to	Severson and Sieg, 2006

Table 2.1. Wet and dry periods in the north central United States before 1900 (continued).

Year(s)	Conditions	Region or Basins	Notes	Sources
			identify dry and wet years), could be off +/- 5 years	
1741	F	Red	Flood upper Red	St. George and Nielsen, 2003
1744-52	DDLF	Central North Dakota	Period of drought or dry years (Will, 1946, used bur oak from Missouri River breaks near Bismarck, ND, to identify dry and wet years), could be off +/- 5 years	Severson and Sieg, 2006
1747	F	Red	Extreme flood lower Red	St. George and Nielsen, 2003
1747	F	Red	Flood upper Red	St. George and Nielsen, 2003
mid-1700s	F	Red	Increased flood frequency lower Red	St. George and Nielsen, 2003
1752-86	O	Central North Dakota	Will, 1946, 10 wet, nine dry years	Severson and Sieg, 2006
1753	DDLF	Southern Manitoba	Annual precipitation estimated more than 2 standard deviations below mean	St. George and Nielsen, 2002
1753-62	DDLF	Northern Great Plains	Period of drought or dry years (Meko, 1982, using Ponderosa pine in ND, SD, NE, WY, MT)	Severson and Sieg, 2006
1755-1761	SD	Northwestern Great Plains, Canada	Positive PDO, high variance ENSO	Lapp et al., 2013
late 1750s	DDLF	Great Plains	Major historical drought centered in the late 1750s, worse than 1930s	Stockton and Meko, 1983, <i>in</i> Severson and Sieg, 2006
1762	F	Red	Extreme flood lower Red	St. George and Nielsen, 2003
1762	F	Red	Flood upper Red	St. George and Nielsen, 2003
1763-1825	O	Red	Interval without extreme flooding on lower Red	St. George and Nielsen, 2003

Table 2.1. Wet and dry periods in the north central United States before 1900 (continued).

Year(s)	Conditions	Region or Basins	Notes	Sources
1776	F	Red River at Winnipeg	Large flood on the Red, likely larger than 1826 flood	Severson and Sieg, 2006; Rannie, 1998; Miller and Frink, 1984; Simons and King, 1922; U.S. Geological Survey, 1952
1790	F	Red River at Winnipeg	"general overflow occurred" (U.S. Geological Survey, 1952); mentioned by Native Americans (Rannie, 1998)	Rannie, 1998; Miller and Frink, 1984; Simons and King, 1922
1791-1800	SD	Northwestern Great Plains, Canada	Positive PDO, high variance ENSO	Lapp et al., 2013
1793-1828	O	Red	Period of "high variability; numerous floods and several drought episodes"	Thorleifson et al., 1998
1795-96	LR	Red River and Assiniboine River		Rannie, 1998
1797-98	HR	Red River at Pembina		Rannie, 1998
1798-1806	WS	Red	Concentration of high runoff years; overbank at Pembina in 1798	Thorleifson et al., 1998; Rannie, 1998
winter of 1799-1800	WS	Post at Assiniboine and Red confluence	Alexander Henry, the younger, described "extraordinary heavy fall of Snow" in early November, the remainder of the season was "open and mild", excessively hot in April, followed by a 3 day snow storm, 3 feet of snow that melted quickly	Severson and Sieg, 2006
1800	DDLf	Red River in ND	Alexander Henry, the younger, reported drought conditions in August	Severson and Sieg, 2006, p. 27-28

Table 2.1. Wet and dry periods in the north central United States before 1900 (continued).

Year(s)	Conditions	Region or Basins	Notes	Sources
1799-1800	LR	Assiniboine, Red, and Clearwater Rivers		Rannie, 1998
1800-01	HR	Red, Winnipeg, and Assiniboine Rivers		Rannie, 1998
1802-30	O	Central North Dakota	Will, 1946, seven wet, seven dry years	Severson and Sieg, 2006
1802-03	HR	Northern Red River		Rannie, 1998
1803-05	DDLDF	Red	Period of successive low/very low runoff	Thorleifson et al., 1998
1803-05	LR	Lake Superior to Missouri River region, including Assiniboine		Rannie, 1998
1804-05	DDLDF	Assiniboine, Red, South Saskatchewan, Saskatchewan	“Drought was reported from the Upper Missouri in the west to Lake Nipigon in the east and low water retarded the progress of the canoe brigades throughout the area.”	Kemp, 1982, p. 36
1805-06	HR	Red River	heavy late winter snow	Rannie, 1998
1808	WS	Pembina to the Missouri River via the Souris	Alexander Henry, the younger, described very wet conditions	Severson and Sieg, 2006

Table 2.1. Wet and dry periods in the north central United States before 1900 (continued).

Year(s)	Conditions	Region or Basins	Notes	Sources
1807-08	LR	Red River and Leech Lake, Minnesota		Rannie, 1998
1809 or 1811	F, S	Red River at Pembina and South	"general overflow occurred" (U.S. Geological Survey, 1952); some discrepancy with date, may have been 1811; 1811 "exceptionally large flood" (Rannie, 1998); did not include Assiniboine	Rannie, 1998; Miller and Frink, 1984; Simons and King, 1922
1810-1812	HR	Red River		Rannie, 1998
1811-1815	WS	Red	Concentration of high runoff years	Thorleifson et al., 1998
1811-1815	SD	Northwestern Great Plains, Canada	Negative PDO, high variance ENSO	Lapp et al., 2013
1812	HR	Souris	Flooding in May	Rannie, 1998
1815	F	Red River at Pembina, Assiniboine at Portage la Prairie	"overflowing its banks to a considerable distance" in one account, but over all "difficult to access" (Rannie, 1998)	Rannie, 1998; Miller and Frink, 1984; Canada Department of Resources and Development, 1953
1814-15	HR	Assiniboine and Red Rivers		Rannie, 1998
1815-18	DDLDF	Red	Period of successive low/very low runoff	Thorleifson et al., 1998
1815-1819	DDLDF	Red River, Saskatchewan, South Saskatchewan,	"Meteorological droughts over the 1815 to 1819 period are well known from records of crop failure and grasshopper infestation at the Red River Settlement in southern Manitoba (Hope, 1938; Allsopp, 1977). During	Case and MacDonald, 2003, p.713

Table 2.1. Wet and dry periods in the north central United States before 1900 (continued).

Year(s)	Conditions	Region or Basins	Notes	Sources
		North Saskatchewan	this period, journal reports of low streamflow are also frequent (Ball, 1992). As an example, Peter Fidler, an employee of the Hudson Bay Company at Brandon House, Manitoba (now Brandon), reported in 1819 that ‘all small creeks that flowed with plentiful streams all summer have entirely dried up, for these several years loaded craft could ascend up as high as the Elbow or Carlton House but these last 3 summers it was necessary to convey all the goods from the Forks by land in carts . . .’ (in Ball, 1992, p. 189). Low flows during the same period on the Saskatchewan River are also frequently mentioned in Hudson’s Bay Company employee journals (Ball, 1992). The reconstruction of Saskatchewan River streamflow shows major hydrological drought events in 1815 and 1817; in fact, the single year drought of 1815 is the lowest flow of the full 325-year period. The South Saskatchewan River shows similarly low flows in 1815 and 1817. On the North Saskatchewan River, flows were near median levels in 1815 to 1818. However, a hydrological drought occurred in 1819. In general, for the 1815 to 1819 period, both the historical and tree ring data support the existence of hydrological drought.”	
1816-18	LR	Red, Assiniboine		Rannie, 1998
1817-26	DDLDF	Northern Great Plains	Period of drought or dry years (Meko, 1982, using Ponderosa pine in ND, SD, NE, WY, MT)	Severson and Sieg, 2006
early	DDLDF	Great Plains	Major historical drought centered in the early 1820s,	Stockton and Meko, 1983, <i>in</i>

Table 2.1. Wet and dry periods in the north central United States before 1900 (continued).

Year(s)	Conditions	Region or Basins	Notes	Sources
1820s			worse than 1930s	Severson and Sieg, 2006
1822-23	LR	Red, Saskatchewan, Minnesota Rivers		
1823	DDLf	Red River	Major Stephen Long described very dry conditions, mention the after effects of fires, Bois de Sioux and Marsh low or dry	Severson and Sieg, 2006, p. 28-29
1823-28	WS	Red	Five successive high or very high runoff years	Thorleifson et al., 1998
1823-28	HR	Red River, Assiniboine		Rannie, 1998
1824	F, WS	Red, Assiniboine	Large flood on the Red according to Red River Basin Flood Damage Reduction Work Group; according to Rannie (1998), extremely wet summer but significant flood cannot be confirmed	Severson and Sieg, 2006, p. 33; Rannie, 1998; Miller and Frink, 1984; Harrison and Bluemle, 1980
1825	F, S	Red, Assiniboine	Significant spring flooding and persistently high water levels in early autumn in Red and Assiniboine basins; Large flood on the Red according to Red River Basin Flood Damage Reduction Work Group	St. George and Rannie, 2003; Severson and Sieg, 2006, p. 33; Rannie, 1998; Miller and Frink, 1984; Harrison and Bluemle, 1980
1826	F, WS	Red, Assiniboine	Records indicate that 1825-26 was not an exceptionally cold or snowy winter, however there were reports of deep snowpack near the Red River Settlement and throughout the southern basin (Severson and Sieg, 2006). Cold, snowy April, late spring, abundant rainfall during rising phase, largest event since 1648; Extreme flood on the lower Red; Conditions in the Assiniboine	Environment Canada, 2013; Severson and Sieg, 2006, p. 33; Rannie, 1998; St. George and Rannie, 2003; St. George and Nielsen, 2003; Miller and Frink, 1984; U.S. Geological Survey, 1952

Table 2.1. Wet and dry periods in the north central United States before 1900 (continued).

Year(s)	Conditions	Region or Basins	Notes	Sources
			appear to be as extreme as those in the Red Basin (Rannie, 1998); One of the greatest floods on the Red River at Winnipeg, before floodway; Large flood on the Red according to Red River Basin Flood Damage Reduction Work Group; ice reached "extraordinary thickness" at Winnipeg (Rannie, 1998)	
December 1826	WS	Pembina region	December 20, 1826, extremely severe blizzard, livestock lost, 33 people died	Severson and Sieg, 2006, p. 35-36
Late 1820s	WS	Southern Manitoba	Pronounced wet interval	St. George and Nielsen, 2002
1828-47	O	Red	Period of "stability and no floods when runoff seems to have fluctuated within the 'normal' range"	Thorleifson et al., 1998
1833-34	LR	Red River		Rannie, 1998
1836-37	LR	Red River		Rannie, 1998
1836-51	DDLF	Central North Dakota	Period of drought or dry years (Will, 1946, used bur oak from Missouri River breaks near Bismarck, ND, to identify dry and wet years), could be off +/- 5 years	Severson and Sieg, 2006
1842-47	SD	Northwestern Great Plains, Canada	Positive PDO, low variance ENSO	Lapp et al., 2013
1844	F	Missouri	Major flood on Missouri (location not specified)	National Park Service, 2015
1847-52	HR, WS	Red	Five successive high or very high runoff years	Thorleifson et al., 1998; Rannie, 1998
1847-70	O	Red	Period of "frequently high runoff and several major floods, with one extreme drought in 1862-64"	Thorleifson et al., 1998

Table 2.1. Wet and dry periods in the north central United States before 1900 (continued).

Year(s)	Conditions	Region or Basins	Notes	Sources
1849	WS	Western Missouri, eastern Nebraska, and the northern Plains; eastern North Dakota, Minnesota	One of the wettest years (Parker 1965, Blair and Rannie, 1994). “Spring breakup of the Red River was exceptionally late, snow fell in the Red River Settlement (near modern-day Winnipeg) on several days in late May, and widespread, heavy rainfall from June to August caused unusual and protracted flooding of the Red River and its tributaries (Blair and Rannie 1994).” “The year most often identified as being wet when encountered by explorers was 1849” (Severson and Sieg, 2006).	Blair and Rannie, 1994; Parker, 1965; Severson and Sieg, 2006, p. 32-33
1849	WS	Red, eastern North Dakota	Lieutenant John Pope accompanying Major Samuel Wood on a military mission from Fort Snelling to the Red, then up the Red to the Pembina, said “The heavy and incessant rain since the 4th of June had so saturated the prairies...I was informed by the guides that such a season had not been known for twenty years, and that they had never seen the country in such conditions before.” On July 15, the party reached the Sheyenne with Wood described as “much swollen... The Shayenne is a rapid turbid stream, and was at that time deep.” After a few days, they traveled cross country and said water was standing from “two inches to two feet deep almost the entire way... we reached the Maple river which Mr. Kittson had bridged; but the water being much higher now than when he crossed it, the bridge had disappeared... There had been such torrents of rain about this time, the little branches that ordinarily furnish barely a sufficiency of water... were now swimming... we arrived at Pembina [on August 1] and	Severson and Sieg, 2006, p. 32-33

Table 2.1. Wet and dry periods in the north central United States before 1900 (continued).

Year(s)	Conditions	Region or Basins	Notes	Sources
			found the Red river and Pembina river with about twenty feet rise in them and overflowing their banks”	
1849	WS	Red, eastern North Dakota	Another unknown Sergeant on the march from the Sheyenne to the Maple described the water as 3 or 4 feet deep for a 4 mile stretch, from the Rush to the Goose he “crossed 4 miles of prairie covered with a foot and a half of water.”	Severson and Sieg, 2006, p. 32-33
1849	F	Red River at Pembina	Flooding in June, July, and August	Rannie, 1998
mid - 1800s	F, WS	Red	Increased flood frequency lower Red	St. George and Nielsen, 2003
1850	F	Red River at Pembina, Red Lake River in Minnesota	Flooding in June and July, a great deal of Minnesota flooded	Rannie, 1998
1850s	WS	Southern Manitoba	Pronounced wet interval	St. George and Nielsen, 2002
1850-54	SD	Northwestern Great Plains, Canada	Positive PDO, low variance ENSO	Lapp et al., 2013
1851	F	Red River at Pembina	Summer, no farming done at Pembina in 1851 because of 1849, 1850, and 1851 floods (Rannie, 1998)	Rannie, 1998; Miller and Frink, 1984; Harrison and Bluemle, 1980

Table 2.1. Wet and dry periods in the north central United States before 1900 (continued).

Year(s)	Conditions	Region or Basins	Notes	Sources
1852	F	Red River, Assiniboine between Portage la Prairie and White Horse Plain	R. H. Clark, Notes on Red River Floods (Winnipeg: Manitoba Department of Mines and Natural Resources, 1950), pp. 5-9 and appendixes 1-19; and Report on Investigations into Measures for the Reduction of the Flood Hazard in the Greater Winnipeg Area, Appendix B: History of Floods on the Red River (Ottawa: Department of Resources and Development, 1953), pp. 1-24. Extreme flood on the lower Red; Conditions in the Assiniboine appear to be as extreme as those in the Red Basin; One of the greatest floods on the Red River at Winnipeg, before floodway; Large flood on the Red according to Red River Basin Flood Damage Reduction Work Group	Carlyle, 1984; St. George and Nielsen, 2003; Environment Canada, 2013; Rannie, 1998; Miller and Frink, 1984; U.S. Geological Survey, 1952
1853	F, WS	Red River	"No farming was done in the Red River valley near Pembina due to the floods of this year and the previous two years" (Rannie, 1998)	Rannie, 1998; Miller and Frink, 1984; Harrison and Bluemle, 1980
mid-1800s	DDLf	Northern Great Plains, Southern Canadian Prairies, Rocky Mountain foothills	"There is ample historical documentation of meteorological drought during the mid-1800s across the northern Great Plains (e.g., Mock, 1991; Blair and Rannie, 1994). Tree ring reconstructions of precipitation have also indicated drought during the mid-19th Century in the southern Canadian Prairies (Sauchyn and Beaudoin, 1998), Rocky Mountain foothills (Case and MacDonald, 1995), and Montane regions (Watson and Luckman, 2001)."	Case and MacDonald, 2003
1853-72	DDLf	Northern Great Plains	Period of drought or dry years (Meko, 1982, using Ponderosa pine in ND, SD, NE, WY, MT)	Severson and Sieg, 2006
1856-61	WS	Red	Concentration of high runoff years	Thorleifson et al., 1998

Table 2.1. Wet and dry periods in the north central United States before 1900 (continued).

Year(s)	Conditions	Region or Basins	Notes	Sources
1856-57	HR	Red River		Rannie, 1998
1857-58	LR	Red River		Rannie, 1998
1858-72	SD	Northwestern Great Plains, Canada	Positive PDO, high variance ENSO	Lapp et al., 2013
1858-59	HR	Red River; Minnesota, upper Mississippi		Rannie, 1998
1860	F	Red River	Began to be cited as a flood year by Upham, but Rannie suggests it's unlikely (Rannie, 1998)	Rannie, 1998; Miller and Frink, 1984; Upham, 1895
1861	F	Red River	R. H. Clark, Notes on Red River Floods (Winnipeg: Manitoba Department of Mines and Natural Resources, 1950), pp. 5-9 and appendixes 1-19; and Report on Investigations into Measures for the Reduction of the Flood Hazard in the Greater Winnipeg Area, Appendix B: History of Floods on the Red River (Ottawa: Department of Resources and Development, 1953), pp. 1-24. One of the greatest floods on the Red River at Winnipeg, before floodway	Carlyle, 1984; Environment Canada, 2013; Rannie, 1998; Miller and Frink, 1984; U.S. Geological Survey, 1952
1860-61	HR	Red River		Rannie, 1998
1861-64	DDLDF	Red	Period of successive low/very low runoff	Thorleifson et al., 1998
early 1860s	DDLDF	Great Plains	Major historical drought centered in the early 1860s, worse than 1930s	Stockton and Meko, 1983, <i>in</i> Severson and Sieg, 2006
1862	DDLDF	Between Wild Rice and Sheyenne	Samuel Bond, traveling with a wagon train, said region was “dry and barren”	Severson and Sieg, 2006, p. 29

Table 2.1. Wet and dry periods in the north central United States before 1900 (continued).

Year(s)	Conditions	Region or Basins	Notes	Sources
Rivers				
1861-64	LR	Red River, Assiniboine		Rannie, 1998
1862-1949	O	Red	Interval without extreme flooding on lower Red	St. George and Nielsen, 2003
1862-64	DDLDF	Red	Extreme drought	Thorleifson et al., 1998
1863	DDLDF	Lake Traverse to the Sheyenne River, Southern North Dakota	A soldier noted that the prairie had cracks so large“ as to let one’s foot through.” A soldier with General Sibley said the roads were dry and dusty “the most so it has been for 20 years So say the inhabitant[s] of this Country. Scarcely any water and grass...” An anonymous soldier with Sibley said on July 2 that “grasshoppers [are] going east. Some starving for want of a spear of grass which cannot be found on level land.”	Severson and Sieg, 2006, p. 29-31
1863	DDLDF	Lake Traverse to the Sheyenne River, Southern North Dakota	Rained while Sibley was on the Sheyenne River July 4, Calvary went out 50 miles to see about grass. After July 18, by the time they reached Lake Jesse ( <a href="http://history.nd.gov/historicsites/jessie/index.html">http://history.nd.gov/historicsites/jessie/index.html</a> ) forage was better. William Clandening, accompanying a wagon train from Fort Abercrombie to Lake Jessie and then to the Souris River said there was no water in the Wild Rice or Maple rivers – only pools (both had had running water in 1862). Joseph Hamel, also accompanying the wagon train, said	Severson and Sieg, 2006, p. 29-31

Table 2.1. Wet and dry periods in the north central United States before 1900 (continued).

Year(s)	Conditions	Region or Basins	Notes	Sources
			near <a href="http://history.nd.gov/historicsites/jessie/index.html">http://history.nd.gov/historicsites/jessie/index.html</a> the Souris River, “The draught we had in Minnesota is prevalent this far. The prairie [prairie], on the whole, is very dry, burned by the sun. We find grass only on the bottom land and around lakes ... many dry lakes.”	
1863	O	Tewaukon Lake and the Sheyenne River	All diaries from Sibley’s command mention extreme heat in early July. July 3 “hot air strikes as if from an oven.” July 9 “it is one of the most uncomfortable days I ever saw in my life the wind is so hot that it will take a mans breath.” Followed by a sudden switch to cold temperatures	Severson and Sieg, 2006, p. 34
1863-64	O	Eastern North Dakota	Hot midsummers with cold periods in late summer	Severson and Sieg, 2006, p. 35
1864	O	Eastern ND	Temperatures 100 and above in June, sudden switch to cold in late summer	Severson and Sieg, 2006, p. 35
1865	O	Cannonball River, Devils Lake, Souris River, Forth Berthold on the Missouri	General Sully expedition, conditions described as dry with prairie pothole lakes drying out, Sheyenne, Souris, and James were not running, but difficult to determine if this was drought or normal late summer conditions. Missouri Coteau described in dismal terms by another member of the party.	Severson and Sieg, 2006, p. 31
1869-70	HR	Red River		Rannie, 1998

Table 2.1. Wet and dry periods in the north central United States before 1900 (continued).

Year(s)	Conditions	Region or Basins	Notes	Sources
1871	F	Red River		Rannie, 1998; Miller and Frink, 1984; U.S. Geological Survey, 1952
1873	F	Red River		Rannie, 1998; Miller and Frink, 1984; U.S. Geological Survey, 1952
1877-1900	DDLf	Central North Dakota	Period of drought or dry years (Will, 1946, used bur oak from Missouri River breaks near Bismarck, ND, to identify dry and wet years; may have some wet years interspersed in period), could be off +/- 5 years	Severson and Sieg, 2006
1881	F	Red, Missouri	At Grand Forks “all buildings on the bottom lands were washed away.” Very large flood on Missouri at Bismarck; Major flood on Missouri (location not specified)	Photographs in University of North Dakota archives, fig. 2.1 is an example; U.S. Geological Survey, 2015d; National Park Service, 2015
1882	F	Red, Souris	One of the greatest floods on the Red River at Winnipeg, before floodway; Large flood in North Dakota on Red; Large, poorly documented flood on the Souris in North Dakota	Environment Canada, 2013; U.S. Geological Survey, 2015b; U.S. Geological Survey, 2015c
1889-97	SD	Northwestern Great Plains, Canada	Positive PDO, high variance ENSO	Lapp et al., 2013
1892 or 1893	F	Red	Not sure if this is two events or a discrepancy with the dates One of the greatest floods on the Red River at	Environment Canada, 2013; Severson and Sieg, 2006, p. 33

Table 2.1. Wet and dry periods in the north central United States before 1900 (continued).

Year(s)	Conditions	Region or Basins	Notes	Sources
			Winnipeg, before floodway (1892); Large flood on the Red according to Red River Basin Flood Damage Reduction Work Group (1893)	
1892-1901	DDLF	Northern Great Plains	Period of drought or dry years (Meko, 1982, using Ponderosa pine in ND, SD, NE, WY, MT)	Severson and Sieg, 2006
mid 1890s	DDLF	Great Plains	Major historical drought centered in the mid 1890s	Stockton and Meko, 1983, <i>in</i> Severson and Sieg, 2006
1897	F	Red	One of the greatest floods on the Red River at Winnipeg, before floodway; Large flood in ND on the Red; Large flood on the Red according to Red River Basin Flood Damage Reduction Work Group	Environment Canada, 2013; U.S. Geological Survey, 2015b; Photographs in North Dakota State University Archives, fig. 2.2 is an example.

The early 1700s (approximately 1703-21) had periods of drought or dry years in the northern Great Plains and central North Dakota (Severson and Sieg, 2006). Lapp et al. (2013) described 24 sustained drought episodes in northwestern Canadian prairies from 1472 through 2004 and found that 1717-1721 was the most intense drought. St. George and Nielsen (2003) documented floods on the upper Red River in 1726, 1727, and 1741. The period 1753-62 was quite dry in parts of the northern Great Plains (Severson and Sieg, 2006) and from the 1820s to about 1861, conditions seem to have been fairly wet. Good historical or analytical accounts of snow amounts are harder to come by because blizzards can occur with small or large snow amounts. However, the 1820s did see numerous large floods on the Red River (most likely driven by snowmelt) and there are accounts of snowstorms. There were reports of deep snowpack near the Red River Settlement and throughout the southern Red River Basin in the winter of 1825-26 (St. George and Rannie, 2003). On December 20, 1826, a snowstorm described as “fearful” drove away the bison from the Pembina region, killed many horses, and 33 lives were lost (Severson and Sieg, 2006).

There were five successive high or very high runoff years on the Red River from 1823-28 and again on the Red River in 1847-52 (Thorleifson et al., 1998). The year 1849 stands out in Severson and Sieg (2006) as a very wet year, while 1852 saw one of the largest floods on the Red River at Winnipeg and extreme flooding on the Assiniboine River (Red River Basin Board, 2000). St. George and Nielsen (2002) found a pronounced wet interval in the 1850s in southern Manitoba. The Red River again experienced a large flood at Winnipeg in 1861 (Red River Basin Board, 2000). In 1897, the Fargo Forum and Daily Republican published an account in of the 1861 flood saying “That year the entire valley was flooded from Big Stone Lake to Winnipeg, a distance of more than 300 miles. There are but four men living in the valley now that witnessed

the great flood of '61 – the largest body of fresh water in the world at that time” (U.S. Geological Survey, 1952).

While the 1820s to 1850s were very wet in the study area and there was a large flood in the Red River in 1861, Case and MacDonald (2003) reported “There is ample historical documentation of meteorological drought during the mid-1800s across the northern Great Plains (e.g., Mock, 1991; Blair and Rannie, 1994). Tree ring reconstructions of precipitation have also indicated drought during the mid-19th Century in the southern Canadian Prairies (Sauchyn and Beaudoin, 1998), Rocky Mountain foothills (Case and MacDonald, 1995), and Montane regions (Watson and Luckman, 2001).” Various other studies report dry, drought, and or low streamflow conditions from about 1852 to about 1880 in the Red, Wild Rice (North Dakota), Sheyenne, Souris, and Missouri River Basins; the Great Plains, southern North Dakota; eastern North Dakota; and central North Dakota (Thorleifson et al., 1998; Severson and Sieg, 2006; St. George and Nielsen, 2003). Lapp et al. (2013) described the 1858-1872 drought as the “most severe and longest” of the 24 northwestern Canadian prairie droughts in their study.

There was a shift from dry to wet and historical photographs (fig. 2.1), historical gage height estimates (Missouri River at Bismarck, 1881, U.S. Geological Survey, 2015d; Souris River above Minot, 1882, U.S. Geological Survey, 2015c), and instrumental records (Red River at Grand Forks, 1882, U.S. Geological Survey, 2015b) show floods in the Missouri, Red, and Souris River Basins in 1881 and 1882 (U.S. Geological Survey, 2014b).



Figure 2.1. Red River flood, spring 1881, Fargo, North Dakota. Courtesy of the Elwyn B. Robinson Department of Special Collections, Chester Fritz Library, University of North Dakota, OGL # 797-245.

Severe flooding again occurred on the Red River in 1897 (fig. 2.2; U.S. Geological Survey, 1952; U.S. Geological Survey, 2015a and 2015b). The first peak streamflow value recorded for the Red River at Fargo, North Dakota, is from this flood (U.S. Geological Survey, 2015a), which was preceded by an “extremely severe” winter (U.S. Geological Survey, 1952).



Figure 2.2. The Northern Pacific railroad bridge over the Red River at Fargo, North Dakota, and Moorhead, Minnesota, 1897. The bridge was weighted down with locomotives and loaded boxcars. The tracks were washed out east and west of the cities. Buildings in the background include the Union elevator, erected in 1879 and Moorhead saloons. Courtesy of the North Dakota State University Archives, Fargo, N.D. (328.2.4).

Many of the resources documented in table 2.1 characterize extended wet or dry periods, or extreme events, such as floods. The extended wet and dry periods are corroborated by tree-ring records (references in table 2.1) and lake sediments from Devils Lake (Vecchia, 2008), indicating the presence of long-term climatic persistence in the interior of North America.

## 2.5. Climate Effects on Water Quality

Climate change effects on water quality are less well understood than the effects on water quantity (America's Climate Choices: Panel on Advancing the Science of Climate Change et al., 2010); however, interest in the climate effects on water quality is growing. Andersen and Shepherd (2013) indicated, “Increased runoff and flooding may alter the global risk of water contamination.” Higher temperatures and runoff exacerbated by intense precipitation can negatively affect the chemical and physical characteristics of surface water (America's Climate Choices: Panel on Advancing the Science of Climate Change et al., 2010). The Federal Advisory Committee Draft Climate Assessment Report, released for public review in 2013, states that climate-related water-quality challenges are “increasing, particularly sediment and contaminant concentrations after heavy downpours... Air and water temperatures, precipitation intensity, and droughts affect water quality in rivers and lakes. More intense runoff and precipitation generally increase river sediment, nitrogen, and pollutant loads. Increasing water temperatures and intensifying droughts can decrease lake mixing, reduce oxygen in bottom waters, and increase the length of time pollutants remain in water bodies” (National Climate Assessment and Development Advisory Committee, 2013).

A National Research Council (NRC) committee reviewed and provided guidance for the U.S. Geological Survey (USGS) National Water Quality Assessment (NAWQA) science priorities. In the letter, they stated that in areas experiencing earlier spring runoff, “higher water temperatures earlier in the season combined with nutrient wash off in early spring through melt or rain will likely lead to increased algal blooms and eutrophication frequency” (Committee on Preparing for the Third Decade (Cycle 3) of the National Water Quality Assessment (NAWQA) Program, 2010). The letter report also provided research recommendations, “Specifically, we

recommend that NAWQA reorganize its activities to focus on the two major large scale drivers affecting national water quality: (1) change in land use due to population and other demographic changes; and (2) climate variability and change...” (Committee on Preparing for the Third Decade (Cycle 3) of the National Water Quality Assessment (NAWQA) Program, 2010). The Federal Advisory Committee Draft Climate Assessment Report (National Climate Assessment and Development Advisory Committee, January 2013) outlined high priority research related to climate change. Research goal 4 is “maintain, extend, expand, and improve the observations and data systems essential to understanding climate change and responding to it.” An example of high priority research under this goal is, “evaluation of the data needs, potential components, and structure of a national indicator system. Indicators can support understanding of changes in the rate of global change, progress in adaptation/response efforts, and communication of climate change risks and opportunities. Indicators could include trends and changes in land use, air and water pollution... indicators are critically needed to assess progress in adaptation and response efforts, a ‘grand challenge’ for integrated physical and social science.” Changes in water quality explained in terms of climate could help provide indicators related to “water pollution” that others could use for adaptation and response.

As precipitation and land use intensify, unstable slopes (that are being farmed or are part of urban developments) are more vulnerable to landslides (Andersen and Shepherd, 2013). Soil moisture anomalies (the degree to which soil moisture varies from a typical value) are increasing and this may change the infiltration rate of the soil and thus the quantity of runoff (Andersen and Shepherd, 2013). These changes may also affect the vegetation grown and thus the degree to which the soil erodes and moves to surface water. With these changes and the increased potential for flash floods, the likelihood of debris flows increases, as well as large movements of sediment.

Sediment itself is a contaminant that can deposit in reservoirs, be difficult for municipal water systems to remove, or damage organisms in the streams. Sediment deposition on fish spawning beds may negatively affect some species (the fish and their predators) and an “increased amount of fine sediments within the streambed reduces its permeability to water movement, affecting the delivery and removal of gases, nutrients and metabolites” for stream biota, and potentially restricting movement of biota (Allan, 1995; Ryberg, 2006). Sediments also transport other pollutants, such as phosphorus.

Increases in runoff and flooding increase the likelihood of water contamination particularly that of water-borne diseases (Andersen and Shepherd, 2013). At some high flood levels, some sewer systems can discharge untreated wastewater (City of Winnipeg, 2014). The runoff from these urban areas that might include failed sewer systems and runoff from facilities like feedlots increase the likelihood of bacteria and other pathogens being transported in large quantities to streams.

Urban runoff can be a significant contributor of total suspended solids, organics, heavy metals, nutrients, and bacteria to streams. With predictions of greater and more intense precipitation in some parts of the country, this is a potential area of interest for the interaction of climate change and water quality. “Pervious areas are likely to have a significant influence on the runoff and pollution generation processes in changing climate and should, therefore, be examined more closely” (Borris, 2013).

With increased runoff in the past few decades (Ryberg, Lin, and Vecchia, 2014; Hirsch and Ryberg, 2012), phosphorus loads have increased dramatically in the Red River of the North, especially with respect to its discharge to Lake Winnipeg (Zhang and Rao, 2012; Gunderson, 2010). There has been pressure from Canada and from Minnesota to reduce phosphorus loads –

an expensive proposition, depending on the method (controlling sources, settling ponds, buffer strips) and not always effective during spring runoff (Gunderson, 2010).

## **2.5. Phosphorus in the Red River of the North Basin**

The Red River of the North (Red River) Basin is a hydrologic region where both water quality and water quantity are concerns. The river flows north into Manitoba, Canada, ultimately into Lake Winnipeg, so water quality is an International concern, particularly nutrients, phosphorus and nitrogen.

Phosphorus is naturally occurring, widespread, and an essential nutrient for plant growth; however, there are anthropogenic sources as well and phosphorus is often the nutrient responsible for accelerated eutrophication (Mueller and Helsel, 1996). Eutrophication is the process “by which a body of water acquires a high concentration of nutrients... These typically promote excessive growth of algae. As the algae die and decompose, high levels of organic matter and the decomposing organisms deplete the water of available oxygen, causing the death of other organisms, such as fish. Eutrophication is a natural, slow-aging process for a water body, but human activity greatly speeds up the process” (Art, 1993). Eutrophication can have the negative effects of undesirable tastes and odors, clogged pipes, and can cause declines in recreational use of water bodies, thereby negatively affecting tourism (Mueller and Helsel, 1996; Jones and Armstrong, 2001). Algal blooms also may produce toxins that are health risk for livestock, pets, and humans that drink the water (Jones and Armstrong, 2001). Lake Winnipeg, the lake into which the Red River discharges in Manitoba, Canada, was classified as eutrophic in 2000 and 2004 and hypereutrophic (with annual mean total phosphorus concentration greater than 0.1 mg/L; hypereutrophic lakes are dominated by frequent algal blooms and low

transparency) in all other years from 1999 to 2007 (Environment Canada and Manitoba Water Stewardship, 2011a).

Total phosphorus (TP) is the sum of all forms of phosphorus particulate and dissolved (that portion that can pass through a filter at the time of water-quality sampling), including phosphate, and particulate forms of phosphorus (that portion adsorbed to sediment and in plant and animal tissue). Total phosphorus is not necessarily immediately available to plants, but an indication of potentially available amounts. Sources of phosphorus include minerals, rocks, soil, and fertilizer, all of which can contribute excess phosphorus to streams through soil erosion (natural or as the result of tillage practices), and sewage effluent (Hem, 1985; Mueller and Helsel, 1996). The U.S. Department of Agriculture Economic Research Service (2013) estimated U.S. consumption of plant nutrients (nitrogen, phosphate, and potash) from 1960-2011. Figure 2.3 shows the U.S. total for phosphate. The black line is a loess smooth line (Cleveland et al., 1992) that gives a general idea of the pattern in the data, removing some of the year-to-year variability (such as 2009 which appears to be underestimated). In addition, figure 2.4 shows phosphate as a percent total of fertilizer used, with nitrogen and potash for comparison. The percent of phosphorus as total fertilizer used has consistently declined since 1960.

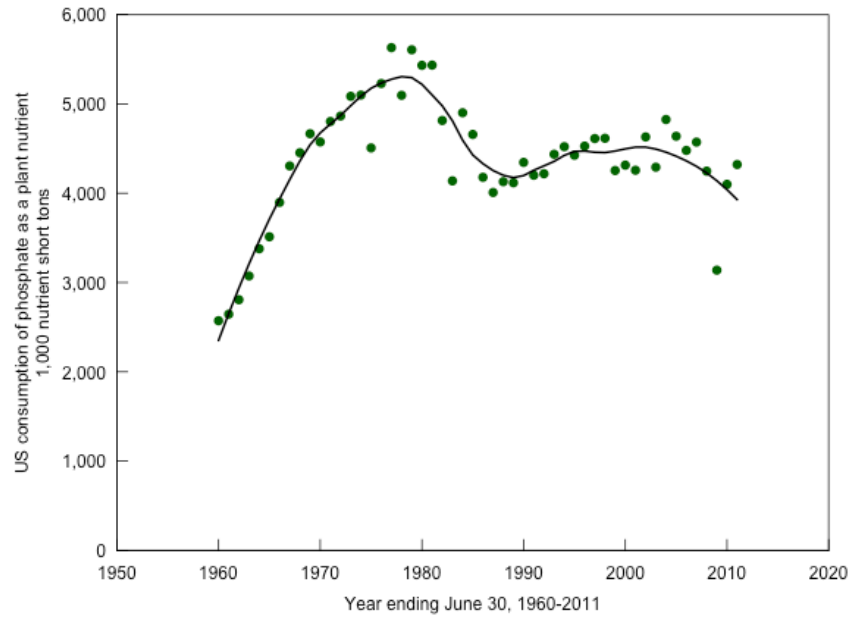


Figure 2.3. U.S. consumption (agricultural use) of phosphate as a plant nutrient (U.S. Department of Agriculture Economic Research Service, 2013).

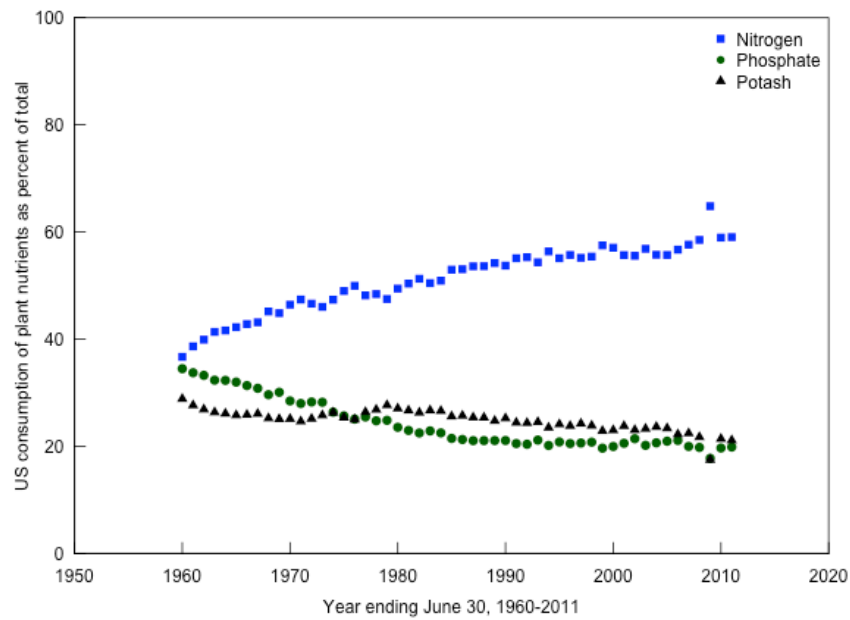


Figure 2.4. U.S. consumption (agricultural use) of plant nutrients (fertilizer) as a percent of total consumption (U.S. Department of Agriculture Economic Research Service, 2013).

According to Mueller and Helsel (1996), the natural, or background, concentration of phosphorus in streams is usually less than 0.1 mg/L. The U.S. Environmental Protection Agency recommended criteria for TP is 0.07625 mg/L in rivers and streams in ecological region VI, Corn Belt and Northern Great Plains (U.S. Environmental Protection Agency, 2002).

About 0.3 million tons of phosphorus per year was discharged in sewage effluent during the period 1978-81 and surface-water phosphorus concentrations were highest downstream from urban areas (Mueller and Helsel, 1996). From 1970 to 1992, urban streams experienced a “sustained decrease in phosphorus following mandated phosphorus controls in sewage-treatment-plant effluent. Phosphorus decreases were caused by limits on the phosphate content of detergent, which were established to reduce the amount of phosphorus input to treatment plants, and by additional treatment used in a few plants to remove phosphorus” (Mueller and Helsel, 1996). The phaseout of phosphorus in laundry detergent in the U.S. was accomplished by 1994 (Litke, 1999). Prompted by concerns about phosphorus in lakes, Minnesota banned phosphorus in lawn fertilizers in 2005 (State of Minnesota, 2005). Phosphorus was removed from dishwasher detergent in the U.S. in 2010 (Shogren, 2010).

While this research is focused on the Red River Basin at Emerson, Manitoba, and south, that is the U.S. portion of the Red River Basin, past research in the U.S. and Canada is important for understanding the larger phosphorus picture. One of the major concerns about phosphorus is that the Red River discharges into Lake Winnipeg and phosphorus loads from the Red River can have numerous consequences for the lake. Therefore, the literature review is divided into two parts, phosphorus in the Red River in the U.S. and phosphorus in the Red River and Lake Winnipeg in Canada.

### **2.5.1. Phosphorus in the Red River of the North Basin in the United States**

The main stem of the Red River flows through the Lake Agassiz Plain (fig. 2.5). This extremely flat landscape is the result of thick beds of Glacial Lake Agassiz sediment and historically was a tallgrass prairie, but has been replaced with intensive agriculture (U.S. Environmental Protection Agency, 2013). About 75-percent of annual Red River streamflow comes from the eastern tributaries in Minnesota (Tornes and Brigham, 1994), which also flow through the Lake Agassiz Plain. Some of the eastern tributaries have their sources in the north central hardwood forest, northern Minnesota wetlands, or northern lakes and forests ecological regions. The western tributaries also flow through the Lake Agassiz plain, with most of them having their source in the northern glaciated plains, an area of flat to gently rolling hills composed of glacial drift (U.S. Environmental Protection Agency, 2013).

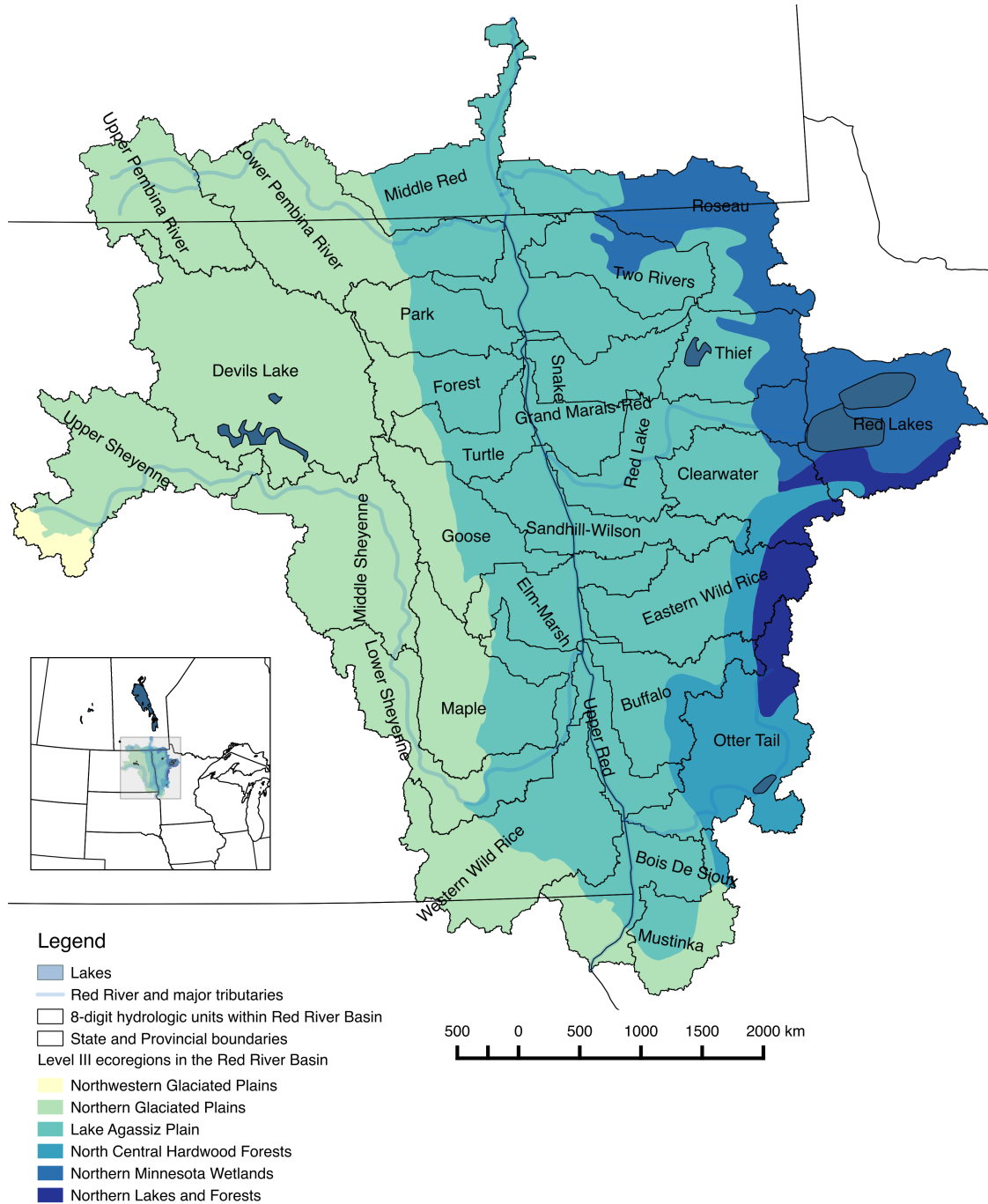


Figure 2.5. The U.S. portion of the Red River Basin and those subbasins (defined at the 8-digit hydrologic unit level) that cross the International border, upstream of the confluence with the Assiniboine River at Winnipeg, Manitoba, Canada. The level III ecoregions, rivers, lakes, and political boundaries are from the Commission for Environmental Cooperation North American Environmental Atlas, <http://www.cec.org/>, and the 8-digit hydrologic units are from the U.S. Geological Survey Watershed Boundary Dataset (WBD) <http://nhd.usgs.gov/wbd.html>.

Water quality in the Red River is affected by the lacustrine deposits of the Lake Agassiz Plain, inflow from major tributaries in North Dakota and Minnesota, runoff from agricultural areas, ground-water discharge, industrial effluents, and wastewater discharges from cities along the river, including Fargo and Grand Forks, North Dakota, and Moorhead and East Grand Forks, Minnesota, (Williams-Sether, 2004). The primary land use in the area is agriculture (Tornes, 2005) and agricultural practices are looked to as possible mechanisms for reducing phosphorus load in the Red River, in addition to point sources.

Tornes and Brigham (1994) compiled total and dissolved phosphorus concentration data for the Red River Basin collected by numerous agencies from 1970-90. They found that the streams in the Basin with the highest concentrations of TP did not have similarly high dissolved phosphorus concentrations and hypothesized that most of the phosphorus at these sites was particulate – attached to suspended sediment or contained in algal cells (Tornes and Brigham, 1994). The highest median TP in the Basin was 0.5 milligrams per liter (mg/L) in the Rabbit River in the southern end of the Basin in Minnesota. The Red River near Perley, Minnesota, and the Red River near Halstad, Minnesota, also had high phosphorus levels (median concentration greater than 0.3 mg/L). Tornes and Brigham (1994) suggested that soils or agricultural practices contributed to the high phosphorus in the Rabbit River and that effluent from Fargo, North Dakota, and Moorhead, Minnesota, wastewater treatment plants likely contributed to the high phosphorus in the Red River near Perley and Halstad. The lowest phosphorus levels (median concentration less than 0.1 mg/L) were found in Minnesota, in the Wild Rice River, South Branch Two Rivers, and the Roseau River.

Phosphorus may vary seasonally with streamflow and the growing season. Tornes and Brigham (1994) examined the seasonality of phosphorus concentrations in the Red River at

Emerson, Manitoba, using data collected by Environment Canada. They found concentrations high and variable in December and January. This is a low-flow period so the likely source of phosphorus is point sources (rather than nonpoint agricultural runoff), such as effluent from wastewater treatment plants. Concentrations decreased in February and in March, likely diluted by early snowmelt, depending on the year, and increased in April, likely representing spring runoff mobilizing phosphorus and potential releases of effluent stored during winter. Early summer also experienced high phosphorus levels, likely from storm runoff from fertilized cropland (Tornes and Brigham, 1994).

Christensen (2007) updated the study of Tornes and Brigham (1994) for data collected from 1990 through 2004, in part because of ongoing concerns about agricultural chemicals in the Red River Basin. County-based fertilizer estimates indicated that application amounts were greatest in Polk County, Minnesota, and Cass County, North Dakota, counties that both border the Red River main stem (Christensen, 2007). Christensen found that TP concentrations ranged from less than 0.005 to 4.14 mg/L and dissolved phosphorus concentrations ranged from 0.003 to 4.13 mg/L. Samples from the Pembina River generally had higher TP concentrations compared to other Red River Basin sites (Christensen, 2007), which contrasts with the 1970-90 period in which TP was generally highest in the Rabbit and Red Rivers (Tornes and Brigham, 1994). Christensen (2007) suggested that the higher TP concentrations in the Pembina River might be attributable to soil characteristics or agricultural practices and the topography, which is steeper than most of the Basin. The highest median concentrations of TP all occurred on the western (North Dakota) side of the Red River Basin in tributaries, Sheyenne, Little South Pembina, and Pembina Rivers. No large urban areas occur upstream from the sites, therefore it was hypothesized that agricultural practices were affecting water quality (Christensen, 2007).

Sether et al. (2004) calculated constituent loads and flow-weighted average concentrations for major subbasins of the upper (southern) Red River Basin for 1997-99. They found that both total and dissolved phosphorus concentrations generally increased in the downstream direction and that median concentrations for most sites exceeded the North Dakota suggested water-quality guideline of 0.1 mg/L (North Dakota Department of Health, 1991). The largest flow-weighted average (FWA) TP concentrations were about 0.5 mg/L and were found in the Sheyenne River at Harwood, North Dakota, whereas the Otter Tail River above Breckenridge, Minnesota, had the smallest FWA concentrations, about 0.1 mg/L.

Vecchia (2005) did a water-quality trend analysis, including TP at five sites, for the Red River Basin from 1970-2001. There was an uptrend in the Sheyenne River near Kindred, North Dakota, from the late 1970's to the early 1980's and there were downward trends in the Sheyenne River and in the Red Lake River at Crookston, Minnesota, from the early 1980's to the mid-1990's and the trends may have been related to livestock-management changes (Vecchia, 2005). No statistically significant trends for standardized (seasonal and annual variability removed) TP concentrations were found for the mainstem sites (Red River at Hickson, North Dakota; Halstad, Minnesota; and Emerson, Manitoba; Vecchia, 2005).

In a study to develop regression equations to continuously estimate water-quality constituents, including TP, Ryberg (2006) found that from 2003 through 2005, TP in the Red River at Fargo, North Dakota (upstream from Fargo and Moorhead, Minnesota, wastewater treatment plant effluent discharge to the river), had varied from 0.08 to 0.70 mg/L (based on 31 samples). Regression analysis showed that TP was positively correlated with streamflow and turbidity and varied seasonally with cosine and sine terms that produce a shape similar to the seasonal variability described for Tornes and Brigham (1994). Galloway (2014) updated this

study using data from 2003 through 2012 for the Red River at Fargo and at Grand Forks, North Dakota. In the Red River at Fargo from 2003-2012, TP varied from 0.07 to 1.28 mg/L (92 samples). In the Red River at Grand Forks from 2007-2010, TP varied from 0.08 to 0.68 mg/L (47 samples). At both the Fargo and Grand Forks sites, regression analysis again showed that TP was positively correlated with the streamflow and turbidity and varied seasonally (Galloway, 2014).

Galloway et al. (2012) in a study of water-quality characteristics across the State of North Dakota from 1970 through 2008 found that the highest normalized annual dissolved phosphorus yields (greater than 39 pounds per year per square mile) were concentrated on the eastern edge of the state in the Red River Basin (one site on the Goose River in North Dakota, and three sites on the main stem). The highest normalized annual TP yields (greater than 46 pounds per year per square mile) were more geographically dispersed, but included sites in the Red River Basin (Galloway et al., 2012). Trend analysis for TP was done for four sites in the Red River Basin. The only site with a statistically significant trend was the Red River at Grand Forks, North Dakota, with an estimated 60% increase (from about 0.10 to 0.16 mg/L) in concentration from 1990 to 2008 (Galloway et al., 2012).

### **2.5.2. Phosphorus in the Red River of the North Basin in Canada**

Phosphorus in the Red River of the North (Red River) is a major concern in Canada because the Red River (including the portion of the Basin drained by the Assiniboine River), along with the Saskatchewan and Winnipeg Rivers, empties into Lake Winnipeg. Lake Winnipeg is 23,750 km<sup>2</sup>, making it the tenth-largest freshwater lake in the world and the sixth largest in Canada (Environment Canada and Manitoba Water Stewardship, 2011b). Lake Winnipeg has a large, deeper north basin, into which the Saskatchewan River discharges, and a shallower south

basin, into which the Red and Winnipeg Rivers discharge (Environment Canada and Manitoba Water Stewardship, 2011b). The Winnipeg River provides almost 50-percent of the inflow to Lake Winnipeg, the Saskatchewan River provides 25-percent, and the Red River provides 16-percent of the inflow (Environment Canada and Manitoba Water Stewardship, 2011b). Where water-quality concerns are characterized separately between the north and south basins, this literature review focuses on the south because that is where the Red River discharges.

Phosphorus loads from the Red River have contributed up to three-quarters of the TP load to Lake Winnipeg (Environment Canada and Manitoba Water Stewardship, 2011b).

The outlet of the lake is the Nelson River, which flows north into Hudson Bay; this flow is regulated for hydroelectric power generation making Lake Winnipeg the third-largest hydroelectric reservoir in the world (Environment Canada and Manitoba Water Stewardship, 2011b). Lake Winnipeg also is important for fishing, recreation, and tourism. Studies of lake-bottom sediment show that phosphorus concentrations in the late 1990s and the 2000s were elevated (degree not stated) in comparison to historical records (Environment Canada and Manitoba Water Stewardship, 2011b). Elevated phosphorus has result in eutrophication that negatively affects beneficial uses of the lake.

Lake Winnipeg water quality has generally declined since the early 1900s (Environment Canada and Manitoba Water Stewardship, 2011b). Recent water-quality monitoring indicates that Lake Winnipeg is generally eutrophic or hypereutrophic and average TP from 1999 to 2007 was three times higher in the south basin (average of 0.113 mg/L) than the north basin (average of 0.044 mg/L; Environment Canada and Manitoba Water Stewardship, 2011b). Eighty-nine percent of 773 water-quality samples from 1999 through 2007 exceeded the narrative Manitoba Water Quality Guideline for TP (0.025 mg/L in lakes); 60% of the exceedances occurring in the

south basin (Environment Canada and Manitoba Water Stewardship, 2011a). The elevated concentrations in the south basin were attributed to inflow from the Red River and concentrations were generally lowest in the spring and highest in the fall (Environment Canada and Manitoba Water Stewardship, 2011a and 2011b).

Bourne et al. (2002) reported that the Red River at Selkirk transported on average 4,905 tonnes of TP per year from 1994 through 2001 and about 52-percent of this came from the U.S. During the same period, Lake Winnipeg received an average of 5,838 tonnes of TP per year, 73-percent of which came from the Red River Basin. Over the last three decades TP loads to Lake Winnipeg increased by 10-percent due to increases in the Red River (Bourne et al., 2002).

Jones and Armstrong (2001) reported that from 1978 through 1999, TP concentrations varied considerably in the Red River at Emerson, Manitoba, (just north of the Manitoba, North Dakota border) but there was not a statistically significant trend in flow-adjusted concentration (the flow adjustment removes the variability in concentration caused by variability in streamflow; the adjusted trend represents the change in TP if flow were constant). Over the same period, Jones and Armstrong (2001) found that downstream in Selkirk, Manitoba (north of the city of Winnipeg, just south of the south basin of Lake Winnipeg), there was a statistically significant uptrend in flow-adjusted concentration (28.8% increase in median concentration). This difference between the Emerson and Selkirk sites was attributed to the contributions of the Assiniboine, La Salle, and Seine Rivers, as well as other small streams and drains, and the urban storm water-runoff and treated effluent discharge from the City of Winnipeg and other area municipalities (Jones and Armstrong, 2001). The data compiled for the trends study also indicated that TP and total nitrogen concentrations in the Red River were sufficient for algal growth, although there had been few instances of excessive growth, perhaps because of turbidity

in the river which restricted light penetration and limit algal growth (Jones and Armstrong, 2001).

Jones and Armstrong (2001) also analyzed TP in the Pembina River, a tributary of the Red River with approximately half of its watershed lying in Manitoba and half in North Dakota. They found a statistically significant uptrend in flow-adjusted TP from 1974 through 1999. They suggested that anthropogenic sources of TP had increased substantially over the study period and that algal blooms occurred regularly in lakes and streams of the Pembina River system.

High TP concentrations in the south basin of Lake Winnipeg, near the mouth of the Red River, are associated with inflows with high sediment concentration, and with high suspended solids concentrations in the lake that can be caused by wind-induced resuspension of sediments because of the relatively shallow depth of the south basin (Environment Canada and Manitoba Water Stewardship, 2011a).

## **CHAPTER 3. IMPACT OF CLIMATE VARIABILITY ON RUNOFF IN THE NORTH CENTRAL UNITED STATES<sup>1</sup>**

Large changes in runoff in the north central U.S. have occurred during the past century, with larger floods and increases in runoff tending to occur from the 1970s to present. Attribution of these changes is a subject of much interest. Long-term precipitation, temperature, and streamflow records were used to compare changes in precipitation and potential evapotranspiration to changes in runoff within 25 stream basins. The basins studied were organized into four groups, each one representing basins similar in topography, climate, and historic patterns of runoff. Precipitation, potential evapotranspiration, and runoff data were adjusted for near-decadal scale variability to examine longer-term changes. A nonlinear water-balance analysis shows that changes in precipitation and potential evapotranspiration explain the majority of multi-decadal spatial/temporal variability of runoff and flood magnitudes, with precipitation being the dominant driver. Historical changes in climate and runoff in the region appear to be more consistent with complex transient shifts in seasonal climatic conditions than with gradual climate change. A portion of the unexplained variability is likely from land-use change.

### **3.1. Introduction**

Large changes in runoff have occurred in the conterminous U.S. during the past century, with higher runoff tending to occur during the period from the 1970s to the first decade of the 21st century than in the early and mid-1900s (Lins and Slack, 1999, McCabe and Wolock, 2002).

---

<sup>1</sup> The material in this chapter was co-authored by Karen R. Ryberg, Aldo V. Vecchia, and Wei Lin. Ryberg was the main analyst and writer. Vecchia assisted with the development of the non-linear water balance model. Lin and Vecchia provided feedback, and served as proofreaders and checked the results.

The north central U.S. has experienced particularly large increases in runoff and flood magnitudes in recent decades and there is much interest in the attribution of these changes (Hirsch and Ryberg 2012). For future water resources management, understanding the reasons for these changes and the potential of long-term wet or dry periods is important. Are recent increases in runoff the result of natural climate variability, anthropogenic climate change, land-use changes, or some combination of all of these factors? Paleo-climatic studies from eastern North and South Dakota based on tree rings and lake sediments indicate similar transitions to wet periods have occurred several times in the past 1,000-2,000 years (Shapley et al., 2005; Laird et al., 2003). An anticipated hydrologic impact of increases in greenhouse gas concentrations in the atmosphere is an increase in the magnitude of floods (Trenberth, 1999; Intergovernmental Panel on Climate Change, 2007; Gutowski et al., 2008). However, global circulation models indicate atmospheric forcing has had only a slight impact on runoff in the north central U.S. during the 20th century (increase of less than 5 percent, Milly et al., 2005). Furthermore, increases in precipitation during summer and fall coincide with runoff increases in recent decades and global circulation models indicate these precipitation increases are closely related to sea-surface-temperature anomalies and are not caused by global warming (Wang et al., 2009). Others suggest that land-use change is a major contributor to changes in runoff (Schilling et al., 2008; Zhang and Schilling, 2006) and changes in climate (Pielke, Sr., 2005; Pielke et al., 2011).

Another important consideration is the timing of changes. Therefore, in this study we considered seasonal climatic conditions and runoff. The precipitation, runoff, and potential evapotranspiration (PET) data for each basin were divided into two six-month seasons, January-June and July-December, because changes in the variables are non-uniform across a calendar year. These two seasons were selected because they receive roughly the same amount of

precipitation, recent increases in air temperature are generally occurring within the January-June period (Intergovernmental Panel on Climate Change, 2007), and recent changes in precipitation are generally occurring within the July-December period (Small and Islam, 2008; Small and Islam, 2009; Wang et al., 2009).

We hypothesize that transient changes between wet and dry climatic conditions occur on a time scale greater than decadal. The changes are complex, each one somewhat different from the others (in length, severity, seasonality, and regional coverage). Observed changes in runoff correspond closely with precipitation and PET amounts and regional patterns during wet or dry periods.

Seasonal precipitation, PET, total runoff (total streamflow for the season per unit basin area, expressed in millimeters, mm), and 7-day high runoff (the highest 7-day total streamflow for the season per unit basin area, expressed in mm) for two seasons (January-June and July-December) were analyzed for 25 basins extending from North Dakota and Minnesota southward to Kansas and Missouri. Basins were organized into four geographic groups so that regional differences in wet/dry precipitation conditions and associated runoff patterns could be highlighted and discussed.

Yang et al. (2007) showed that Great Plains precipitation is strongly correlated with Niño-3.4 sea surface temperatures over time scales including semi-annual, annual, and 5.5-8.5 years. Furthermore, a number of studies have identified a decadal-scale (greater than 7 years) signal in precipitation (Cayan et al., 1998; Garbrecht and Rossel, 2002; Small and Islam, 2008; Small and Islam, 2009; Ault and St. George, 2010). This study focuses on long-term (multi-decadal) variability and thus potential shorter-term, quasi-periodic signals were treated as “nuisance” variability and were smoothed out. Small and Islam (2008; 2009) identified a

statistically significant signal in autumn precipitation in the central U.S. with a periodicity of approximately 12 years, with the signal strongest in the Midwest and Great Plains. Therefore, to remove shorter-term variability and focus on multi-decadal variability, we used a 12-year moving window when analyzing precipitation, PET, and runoff.

For this paper, two approaches were used to analyze long-term variability of precipitation and runoff. In the first approach, seasonal precipitation and runoff data were standardized by dividing the data for each basin, season, and variable by its long-term mean and the standardized data were aggregated within each basin group. Graphical analysis was used to relate patterns in standardized precipitation and runoff within each group and compare and contrast patterns between groups. In the second approach, seasonal runoff data for basins in three of the basin groups were analyzed using a nonlinear water-balance model to relate seasonal runoff to seasonal precipitation and PET. Raw (unstandardized and unaggregated) data were used to highlight similarities and differences among the individual basins and to discuss whether the long-term changes in runoff appear to be influenced more by precipitation or by other factors (such as land-use changes or climate changes unrelated to precipitation). Finally, long-term changes in the relation between seasonal total and 7-day-high runoff were analyzed to determine if floods might be responding differently to climate variations than runoff.

### **3.2. Data and Methodology**

Twenty-five U.S. Geological Survey (USGS) streamgaging stations from the north central U.S. (table 3.1) were selected. Streamflow data and basin characteristics were obtained from USGS Water Data for the Nation, <http://waterdata.usgs.gov>, and from calculations within a geographic information system (GIS). These streamgages represent relatively unregulated basins (based on USGS qualification codes of peaks recorded at the gages and institutional knowledge

of the basins) with drainage areas greater than 2,000 km<sup>2</sup>, and the basins do not overlap. The basins were organized into four groups (fig. 3.1) based on topography, climate, and similarity of historical flow patterns. For each streamgage, daily-flow records were used to compute total and 7-day-high runoff for each of two seasons (January-June and July-December).

Table 3.1. Twenty-five U.S. Geological Survey (USGS) streamgaging stations chosen to compare changes in runoff with changes in precipitation in the study area.

	<b>USGS streamgage number</b>	<b>Streamgage name</b>	<b>Basin group and number</b>	<b>Drainage area, km<sup>2</sup></b>
1	04024000	St. Louis River at Scanlon, MN	A3	8,841
2	05079000	Red Lake River at Crookston, MN	A1	13,645
3	05131500	Little Fork River at Littlefork, MN	A2	4,384
4	05267000	Mississippi River near Royalton, MN	A4	30,119
5	05340500	St. Croix River at St. Croix Falls, WI	A5	15,926
6	05054000	Red River of the North at Fargo, ND	B1	17,612
7	05280000	Crow River at Rockford, MN	B4	6,850
8	05325000	Minnesota River at Mankato, MN	B5	38,694
9	06478500	James River near Scotland, SD	B2	42,748
10	06485500	Big Sioux River at Akron, IA	B3	19,904
11	06800500	Elkhorn River at Waterloo, NE	B6	17,989
12	05412500	Turkey River at Garber, IA	C4	3,858
13	05453100	Iowa River at Marengo, IA	C5	7,238
14	05464500	Cedar River at Cedar Rapids, IA	C3	16,862
15	05474000	Skunk River at Augusta, IA	C6	11,165
16	05484500	Raccoon River at Van Meter, IA	C1	8,870
17	06810000	Nishnabotna River above Hamburg, IA	C2	7,282
18	06902000	Grand River near Sumner, MO	C7	17,944
19	05514500	Cuivre River near Troy, MO	D2	2,407
20	06908000	Blackwater River at Blue Lick, MO	D1	2,895
21	06933500	Gasconade River at Jerome, MO	D6	7,340
22	07019000	Meramec River near Eureka, MO	D5	9,785
23	07068000	Current River at Doniphan, MO	D7	5,319
24	07185000	Neosho River near Commerce, OK	D3	15,348
25	07188000	Spring River near Quapaw, OK	D4	6,513

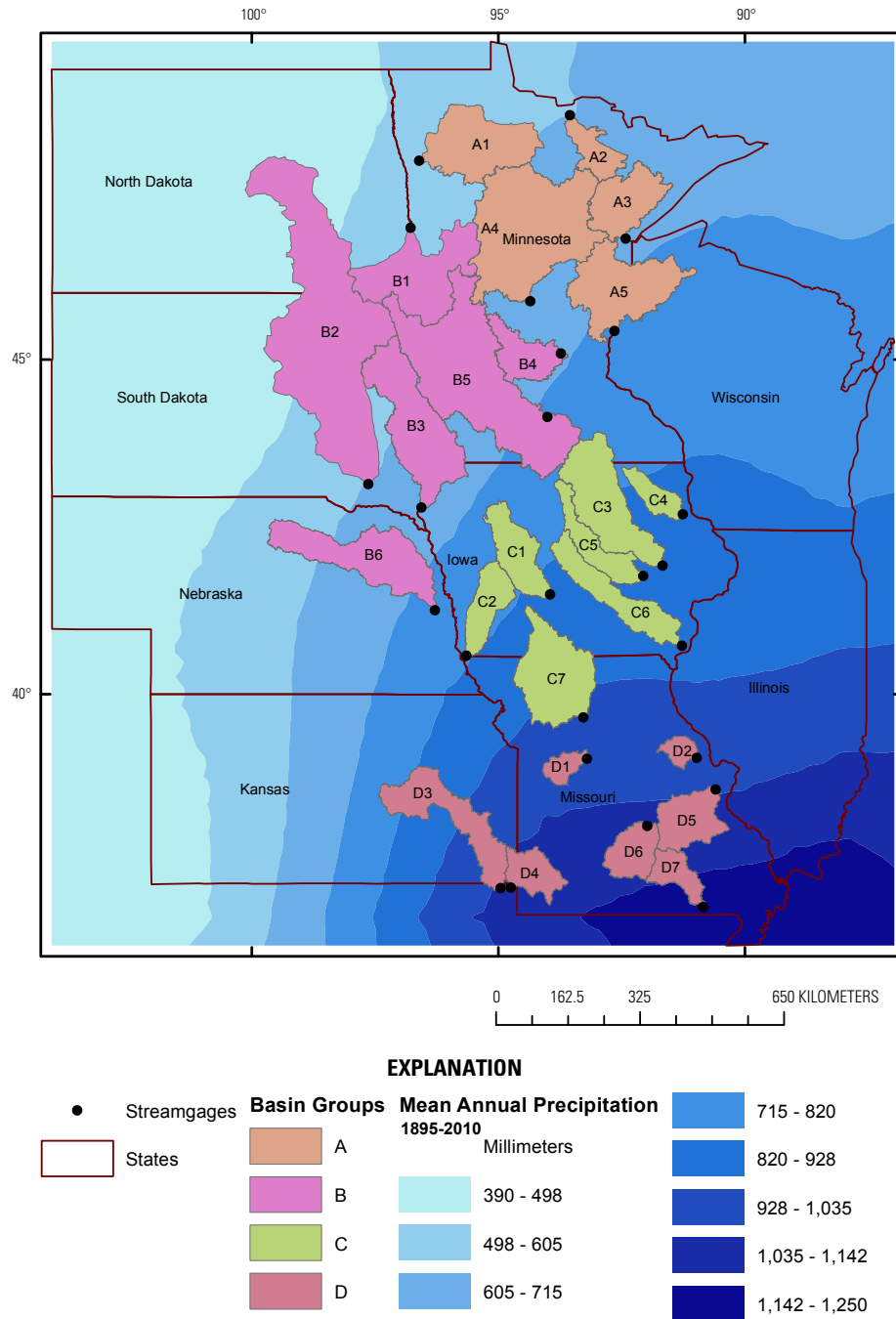


Figure 3.1. Isohyetal lines (1895-2010), U.S. Geological Survey streamgages, and their basins, grouped into four regions based on similarity of topography, climate, and historic patterns of runoff. Precipitation data interpolated to a grid then contoured using ArcMap10 inverse-distance weighting and extended to rectangular boundary of states polygons.

Map Credits: Precipitation data from U.S. Historical Climatology Network (<http://cdiac.ornl.gov/epubs/ndp/ushcn/ushcn.html>); gage locations and basin delineations from U.S. Geological Survey (<http://waterdata.usgs.gov> and geographic information system software).

Precipitation (monthly total) and temperature (monthly average of daily maximum and minimum) data used for this analysis were obtained from the United States Historical Climatology Network (USHCN) of the National Oceanic and Atmospheric Administration's National Climatic Data Center (NCDC). NCDC developed USHCN to assist in the detection of regional climate change and USHCN data have been widely used in analyzing U.S. climate (Easterling et al., 1996). The dataset begins in 1895 for all sites (with estimates for missing values) and data were available through 2010 at the time of this analysis. The north central U.S. is a region of precipitation transition from a semi-arid climate in the extreme west (approximately 390 mm of precipitation per year) to a humid climate in the extreme southeast of the region (up to approximately 1,250 mm of precipitation per year). Figure 3.1 shows the isohyetal lines for average precipitation (1895-2010) for the study area.

Gridded precipitation and temperature time series data were created by interpolating (loess smooth using latitude and longitude as independent variables and 0.125 fractional smoothing parameter, with separate interpolation for each month to maintain temporal variability) the USHCN data over 0.5 degree latitude by 0.5 degree longitude areas from latitude 48.5 degrees, longitude -102.0 degrees, in the northwest to latitude 36.5 degrees, longitude -88.0 degrees in the southeast. The interpolation process used 265 of the USHCN sites (fig. 3.2). PET was estimated from the temperature data using the Thornthwaite method (Thornthwaite and Holzman, 1942). In a GIS system, the 0.5-degree grid of the precipitation and PET data was laid over the basins and Thiessen polygons were drawn based on the grid. The Thiessen polygons were then cut to the shapes of the basins. The contributing drainage areas were calculated along with the total area of the basins. These areas were used to find the fractional area of each Thiessen polygon contributing to the total area. A weighted-average calculation was performed

on the time-series data to obtain monthly precipitation and PET values for each basin for every year of record (1895-2010). For each basin and season, precipitation, PET, runoff, and 7-day high runoff were averaged over 12-year moving windows and the moving means were used to analyze multi-decadal variability.

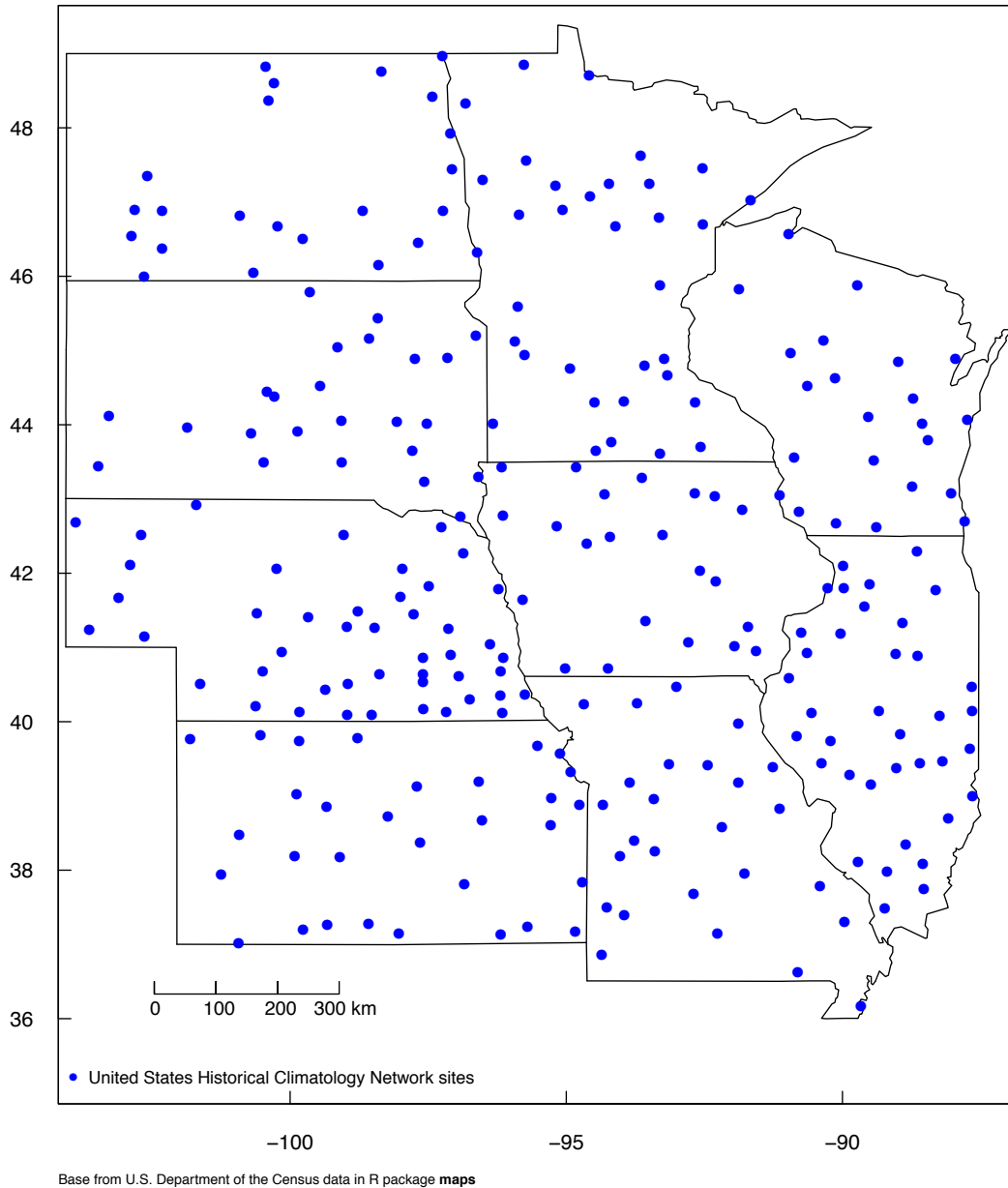


Figure 3.2. Isohyetal lines (1895-2010), U.S. Geological Survey streamgages, and their basins, grouped.

To more thoroughly evaluate the consistency (through time and from basin-to-basin) of precipitation and runoff changes and to determine if other factors besides precipitation may be affecting runoff, a water-balance analysis was used to relate changes in seasonal runoff to changes in precipitation and PET. Water-balance modeling is a common hydrologic technique to represent aspects of the hydrologic cycle (Zhang et al., 2002), in this case, runoff as a result of precipitation and evapotranspiration. This analysis included all of the basins from groups B and C, and all except one from group D (D7). Basin D7 had a much higher baseflow than other sites and was determined to have a substantial flow contribution from the underlying Karst aquifer (<http://water.usgs.gov/ogw/karst/>). Group A in general had some differences in precipitation runoff response because of land cover (group A basins included large contribution from forested areas and substantial surface-water storage, fig. 3.3) and the influence of Lake Superior. Therefore, basin group A and basin D7 were removed and the water balance for the remaining basins was examined.

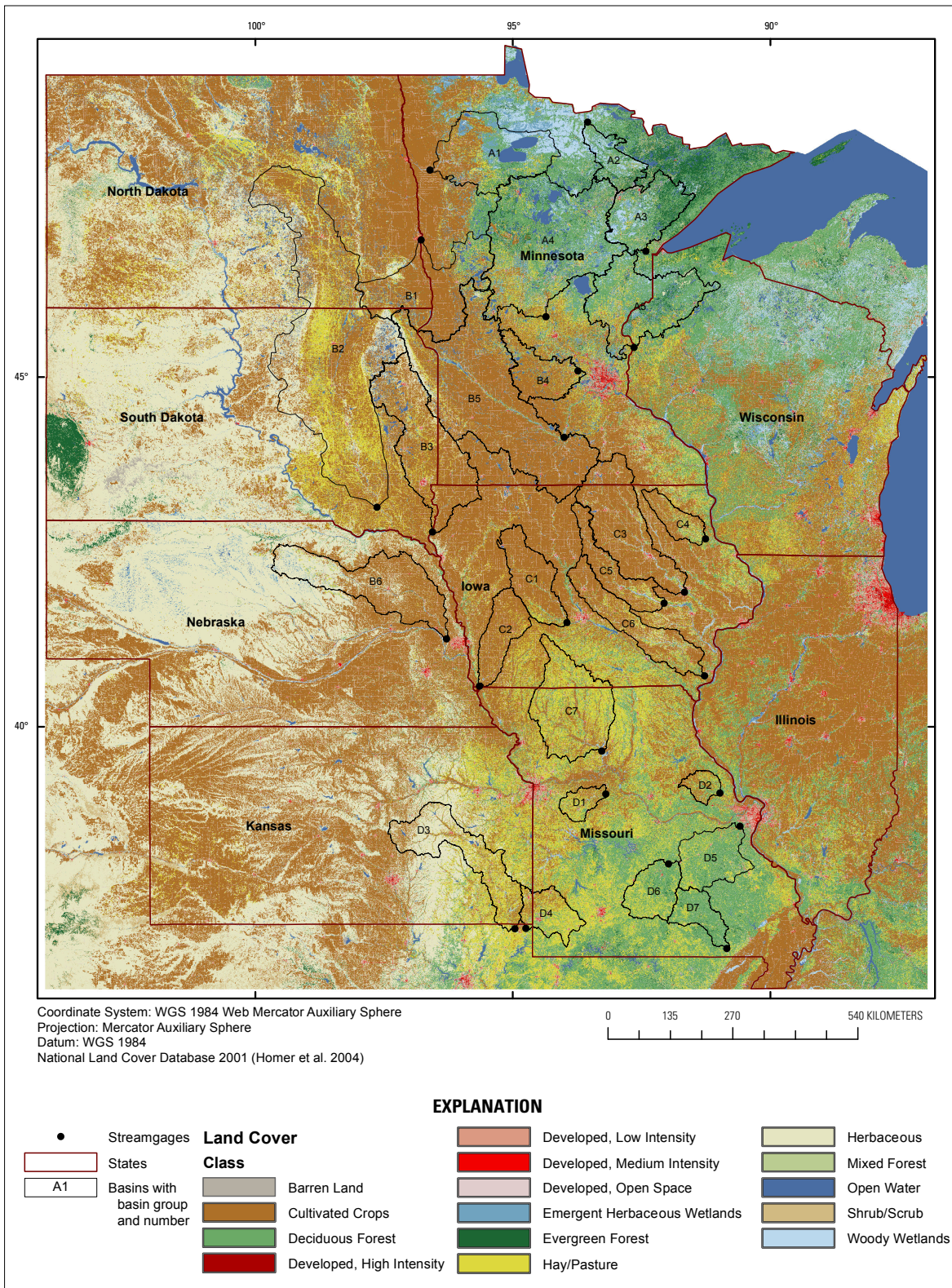


Figure 3.3. Land-cover (Homer et al., 2004) map for study area.

For the water-balance analysis, to minimize the effects of serial correlation induced from the moving averages, nonoverlapping 12-year periods were selected that were centered during a period that was not rapidly transitioning from wet-to-dry or dry-to-wet. Periods selected were 1) 1929-40, 2) 1941-52, 3) 1953-64, 4) 1970-81, 5) 1982-93, and 6) 1998-2009. Temporal and spatial variability in precipitation, PET, and runoff for the six periods were examined.

A simple, nonlinear water-balance model was used to relate runoff in the two seasons to precipitation and PET. The model is expressed as follows,

$$RO1 = PR1 - \alpha PET1 (1 - \exp(- PR1/PET1*)) \quad (\text{Eq. 3.1})$$

$$RO2 = PR2 - \beta PET2 (1 - \exp(- PR2/PET2)) \quad (\text{Eq. 3.2})$$

where RO1 and PR1 are runoff and precipitation for season 1; RO2, PR2, and PET2 are runoff, precipitation, and PET for season 2,  $\alpha$  and  $\beta$  are estimated coefficients, described later, and

$$PET1* = PET1 + [\beta PET2 - PR2]_+ \quad (\text{Eq. 3.3})$$

where PET1 is PET for season 1 and  $[\cdot]_+$  is the quantity in brackets if the quantity is positive and zero otherwise. These equations were obtained through considerable exploratory analysis of the data. In equation 3.2, runoff for season 2 is equal to precipitation for season 2 less estimated actual evapotranspiration (ET). The maximum estimated actual ET is  $\beta PET2$  and occurs when PR2 becomes large in relation to PET2. As PR2 becomes less than PET2, the estimated actual ET is reduced and approaches zero as PR2/PET2 gets small. The coefficient  $\beta$  is estimated separately for each basin to reflect static differences in basin properties (such as soil moisture storage potential, infiltration rates, slope, etc.), as well as possible bias in PET2 computed using the Thornthwaite method and is given by

$$\beta = \text{Ave}\{PR2 - RO2\} / \text{Ave}\{PET2(1 - \exp(- PR2/PET2))\} \quad (\text{Eq. 3.4})$$

where  $\text{Ave}\{\cdot\}$  is the average of the values in braces for the six non-overlapping 12-year periods for a given basin. An inherent assumption of equation 3.2 is that negligible moisture deficits remain at the end of season 1 so that estimated ET in season 2 depends only on PR2 and PET2. Runoff for season 1 (Eq. 3.1) is derived similarly to season 2, except potential moisture deficits remaining at the end of season 2 from the previous year are used to adjust estimated ET for season 1. If the maximum possible estimated ET in season 2 exceeds PR2, the difference ( $\beta\text{PET2} - \text{PR2}$ ) is added to PET1 to account for extra evaporative demand left over from season 2. If PR2 exceeds maximum evaporative demand, the difference ( $\text{PR2} - \beta\text{PET2}$ ) is assumed to be lost to precipitation runoff in season 2 and thus does not affect runoff in season 1. Coefficient  $\alpha$  is computed similarly to  $\beta$  (and after computing  $\beta$ ) as follows,

$$\alpha = \text{Ave}\{\text{PR1} - \text{RO1}\} / \text{Ave}\{\text{PET1} * (1 - \exp(-\text{PR1}/\text{PET1}^*))\}. \quad (\text{Eq. 3.5})$$

Equations 3.1 and 3.2 do not explicitly model physical processes such as infiltration, groundwater versus surface runoff, soil-moisture storage, and rain versus snowmelt. However, for the time scales considered here (six-month seasons and 12-year averages), the simple model was quite efficient for explaining long-term variation in seasonal runoff for the basins analyzed. Differences in the fitted coefficients,  $\alpha$  and  $\beta$ , between basins and potential physical processes that might cause these differences are discussed in the Results section.

Seasonal 7-day high runoff for each analysis period was computed by averaging the 12 seasonal 7-day high runoff values over the given period. A linear regression analysis was done to determine how much of the variability in 7-day high runoff could be explained by variability in total runoff and to determine the relative importance of seasonal climate effects (as expressed by the water-balance analysis) and land-use/other effects (as expressed by the residuals from the

water-balance analysis). For the hi-flow regression analysis for each season, basins within each group were combined and three linear regression models were fitted for each group,

$$RO7DH = INT + J1 ROFIT + J2 RORES + e1 \quad (\text{Eq. 3.6})$$

$$RO7DH = INT + K1 ROFIT + e2 \quad (\text{Eq. 3.7})$$

$$RO7DH = INT + L1 (ROFIT + RORES) + e3 \quad (\text{Eq. 3.8})$$

where RO7DH is 7-day high runoff; INT is an intercept term that depended on basin group as described later; ROFIT is the fitted runoff from the water-balance analysis; RORES is the residual from the water-balance analysis; J1, J2, K1, and L1 are fitted (ordinary least-squares) regression coefficients; and e1, e2, and e3 are the error terms. Statistical hypothesis tests were used to determine which of the models (Eqs. 3.6, 3.7, or 3.8) was best for explaining variability of the high-flow data and providing clues as to whether or not high flows may be responding to more subtle climatic or land-use changes than can be explained using a simple seasonal water balance.

Initially, the intercept in equations 3.6, 3.7, and 3.8 was assumed constant for each group. However, examination of model fit indicated that one station in group C (C7) and two in group D (D1 and D2) had substantially higher intercepts than the other stations. Therefore, dummy variables were included for those stations. For group C,  $INT = INT_0 + INT_1 I\{C7\}$ , and for group D,  $INT = INT_0 + INT_1 I\{D1 \text{ or } D2\}$ , where  $I\{.\}$  is the indicator function that is 1 for the specified station(s) and zero otherwise.

### 3.3. Results

#### 3.3.1. Comparison of Precipitation and Runoff Trends Between Groups

Figure 3.4 shows the group-wide averages of the ratio of the 12-year moving mean to the long-term mean for both precipitation and runoff for each season. The moving means were computed beginning with 1915 (mean for 1910-21) and ending with 2004 (mean for 1999-2010) and the long-term means were computed using data from the period 1915-2010. Although the moving means for precipitation could have been computed beginning with 1900, 1915 was used as the starting year because only two sites had streamflow data before 1910. For runoff, the moving means for each group from 1938 to 2004 generally included all of the basins in that group. However, because of missing daily streamflow data before 1938 some of the means are based on a subset (2 or more) of the basins in that group. The moving means for group D before 1928 are not shown because all of the basins in that group had missing daily streamflow data before 1923.

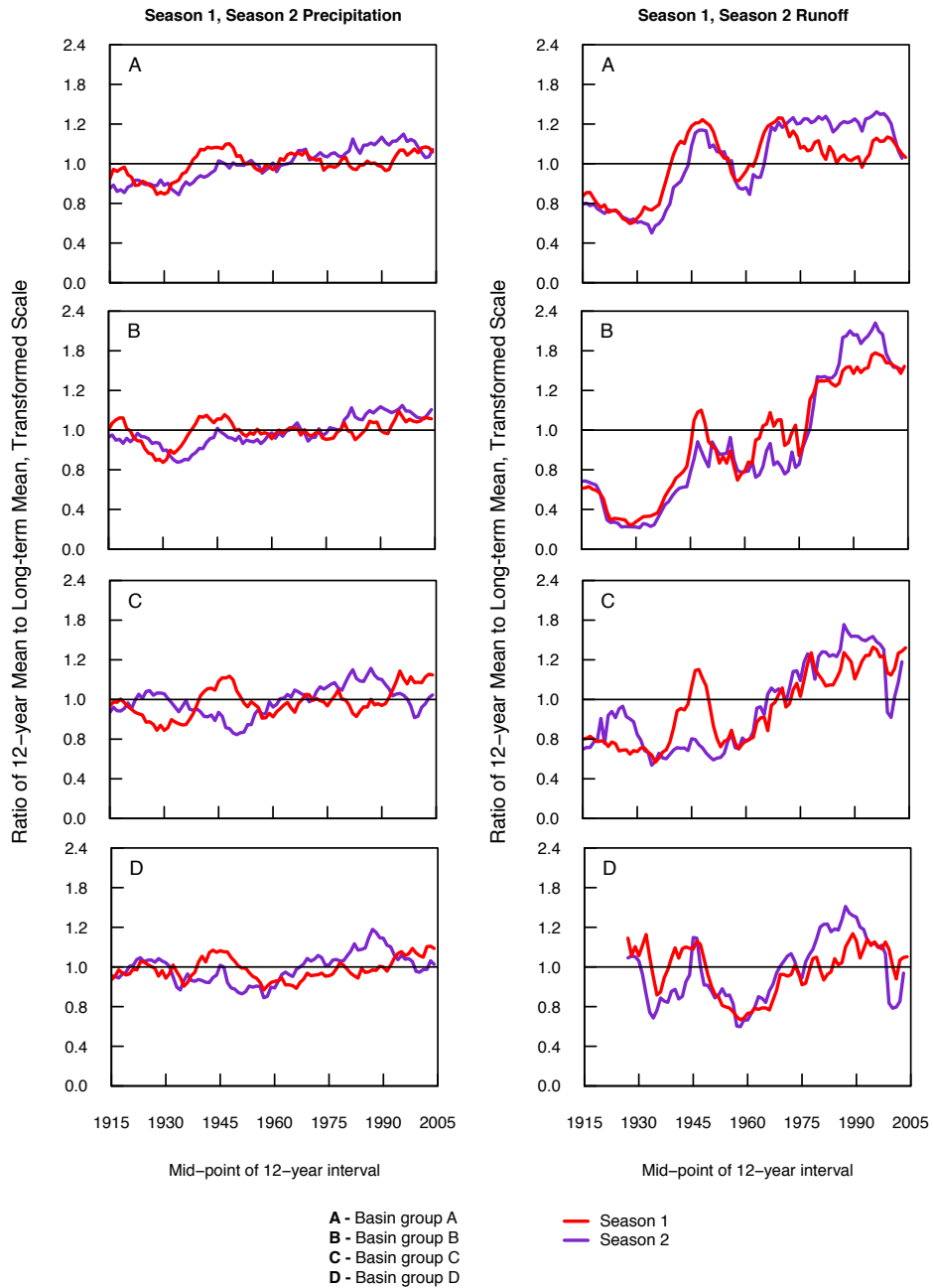


Figure 3.4. Basin group ratio of 12-year mean to long-term mean for season 1, January-June, and season 2, July-December, precipitation and runoff. Note: Ratio is positive and centered around one. The scales were transformed to depict the precipitation and runoff on the same scale, still centered around one.

Table 3.2 gives the long-term means for precipitation and runoff. For all four basin groups, long-term mean precipitation for seasons 1 and 2 are similar. However, long-term mean runoff for season 1 is about twice as high as season 2 for all groups because of higher ET in season 2 (estimated ET will be discussed in the next section).

Table 3.2. Long-term mean precipitation and runoff, 1915-2010, for basin groups A, B, C, and D, for season 1, January-June, Season 2, July-December, and annual season.

	Basin group			
	A	B	C	D
Precipitation, millimeters				
Season 1	286.4	305.6	413.4	536.9
Season 2	360.1	306.9	431.1	508.5
Annual	646.5	612.5	844.5	1,045.4
Runoff, millimeters				
Season 1	113.7	39.4	131.0	206.6
Season 2	68.2	18.4	68.2	106.6
Annual	182.3	56.9	197.1	312.5

In terms of the standardized data (standardized by dividing the data for each basin, season, and variable by its long-term mean), seasonal precipitation is less variable relative to its long-term mean than runoff in all four basin groups (fig. 3.4). However, in absolute terms precipitation is more variable than runoff. For example, the moving means for season 2 precipitation for group B ranged from about 250 mm (1933) to 340 mm (1997) compared with a range of about 4 mm (1935) to 40 mm (1997) for runoff.

There are strong similarities in the long-term seasonal precipitation patterns between the four groups (fig. 3.4). In season 1, there were two distinct wet periods for all of the groups, one spanning the mid-1940s and the other extending from the early 1990's to the end of the study period. Though definitive causes for these wet periods are not known, they are likely related to

North Atlantic winter sea surface temperature anomalies (Deser and Blackmon, 1993; Hoerling et al, 2010). In season 2, there was a distinct wet period for all groups from about 1975 to 1995. This wet period has been well documented in other studies (Garbrecht and Rossel, 2002; Small and Islam, 2009; Wang et al., 2009) and is likely related to Pacific Ocean and possibly to Atlantic Ocean surface temperature anomalies. Wet periods in either season 1 or 2 have generally coincided with normal or below normal precipitation in the other season, with the exception of recent years (2000 to the end of the study period) for groups A and B, when season 2 precipitation has remained relatively high along with the high season 1 precipitation. With respect to dry periods, in season 1 there was a distinct dry period from about the mid-1920's to the mid-1930's for groups A, B, and C, with dry season 2 conditions as well for groups A and B. These groups were part of the extreme 1930s drought in the northern Great Plains (Schubert et al., 2004; McCabe et al., 2004; Cook et al., 2011). In season 2, there was a distinct dry period during the 1950s for groups C and D with dry season 1 conditions as well for group D. These groups were part of an extensive 1950s drought in the southern Plains and Southwest U.S. (Guido, 2010; McCabe et al., 2004; Cook et al., 2011).

The long-term seasonal runoff patterns for all groups (fig. 3.4) generally were similar to precipitation patterns, but with some subtle differences between the two seasons and between groups. The effect of the 1930s drought is particularly evident, when runoff was well below normal for season 1 (groups A-C) and season 2 (groups A and B). By the mid-1940s wet period, season 1 runoff was above normal for all of the groups. Although season 1 precipitation patterns were similar for groups A-C during the 1930s and 1940s, runoff for group B was much more sensitive to the 1930s drought and took longer to recover compared with the other groups. The primary reason for this difference is that ET is higher in relation to precipitation for group B than

groups A and C. Thus, small precipitation decreases for group B, when compounded over time, can lead to much larger than normal moisture deficits and greatly reduced runoff. Conversely, precipitation increases can take much longer to overcome moisture deficits after a drought. The effect of the 1950s drought also is evident, when runoff for both seasons was well below normal for group D and below normal (but less so than the 1930s drought) for the other groups.

For groups B-D, season 2 runoff rose to by far its highest levels during the mid-1970s to mid-1990s season 2 wet period before declining to normal for groups C and D and declining but remaining above normal for group B. During this wet period, season 1 runoff for groups B-D also was at its highest levels despite normal or below normal season 1 precipitation. Season 1 runoff for groups B-D was substantially higher during the mid-1970s to mid-1990s than during the mid-1940s wet period, even though season 1 precipitation was much higher during the mid-1940s. As indicated in the next section, this apparent anomaly can be explained by a combination of moisture deficits in season 2 reducing runoff in season 1 during drier season 2 periods and land-use changes that tended to reduce ET (and hence moisture deficits) during season 2 beginning in the mid-1970s. Compared with the other groups, for group A the mid-1970s to mid-1990s season 2 wet period seems to have had much less effect on runoff. The close correspondence between season 1 precipitation and runoff patterns for group A may indicate that season 2 moisture deficits are much less prevalent for group A. However, the apparently minimal response of season 2 runoff for group A to the mid-1970s to mid-1990s season 2 wet period is difficult to explain without further analysis. Basins in group A generally have more forested land cover and lakes and less agricultural land use compared with the other groups, which may have something to do with different response of season 2 runoff to precipitation.

### 3.3.2. Analysis of Climate and Runoff Changes for Individual Basins

The previous section shows that precipitation in the north central U.S. is characterized by complex, multidecadal changes between wet and dry periods that, when aggregated over groups, produce dramatic changes in runoff that are generally consistent with the timing and direction of the precipitation changes. Potential runoff “trends” resulting from land-use changes or climate change (such as global warming) would be highly confounded with multi-decadal precipitation variability. For example, for group D the 1950s was the driest decade and the 1980s the wettest decade since precipitation records began in 1895, so it would be particularly difficult to discern a gradual effect of land-use change from 1950 to present.

Figure 3.5 shows the seasonal runoff for individual basins in groups B, C, and D (less D7) for the six selected periods (1929-40, 1941-52, 1953-64, 1970-81, 1982-93, and 1998-2009). As described earlier, basin D7 was excluded because of its connection with the underlying Karst aquifer and group A was excluded because of land-cover differences and climatic influence of Lake Superior that require a more complex water-balance analysis to describe runoff for that group. For season 1, all three groups showed considerable variability in runoff both between periods and among basins. Season 2 runoff was highly variable between periods but there was much less variability among basins compared with season 1.

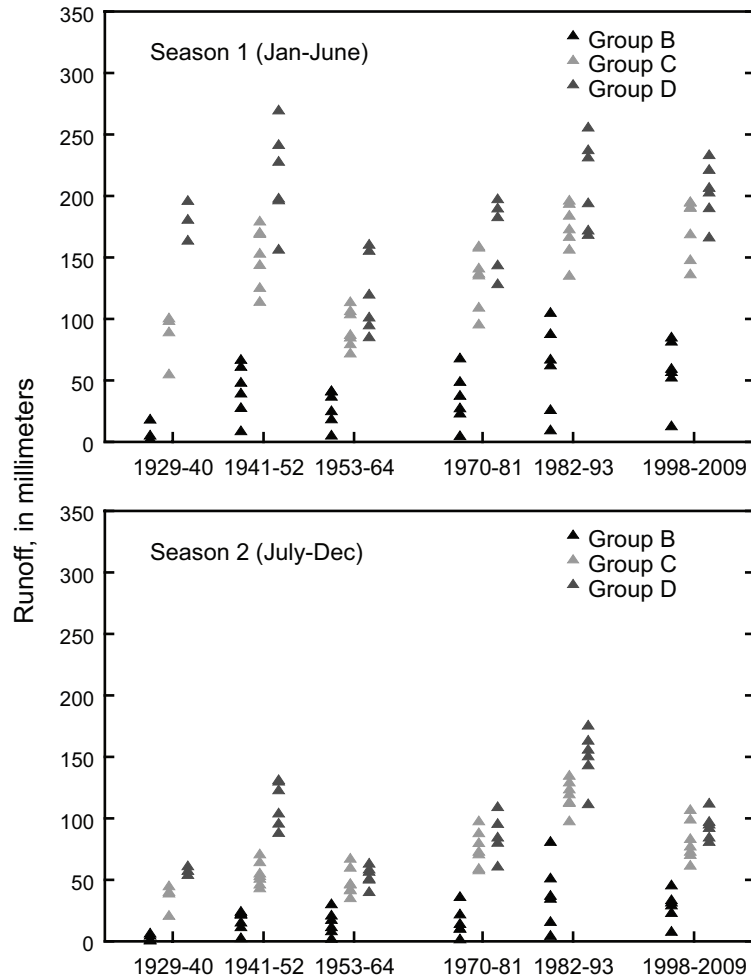


Figure 3.5. Average runoff for season 1 (January-June) and season 2 (July-December) for selected 12-year periods for basin groups B, C, and D.

Water-balance analysis can be used to relate changes in runoff evident in figure 3.5 to changes in climatic conditions, namely precipitation and PET. Figure 3.6 shows seasonal precipitation and PET totals for the 19 basins and 6 selected periods. Open symbols indicate values for the earlier periods (pre-1970) and solid symbols indicate values for the latter periods (post-1970). Although both seasons receive similar precipitation totals, large differences in PET exist. Season 1 precipitation exceeded PET for all of the basin groups. Season 2 net precipitation

(precipitation less PET) generally was negative for group B. However, for the other groups season 2 net precipitation could be positive or negative depending on wet or dry periods.

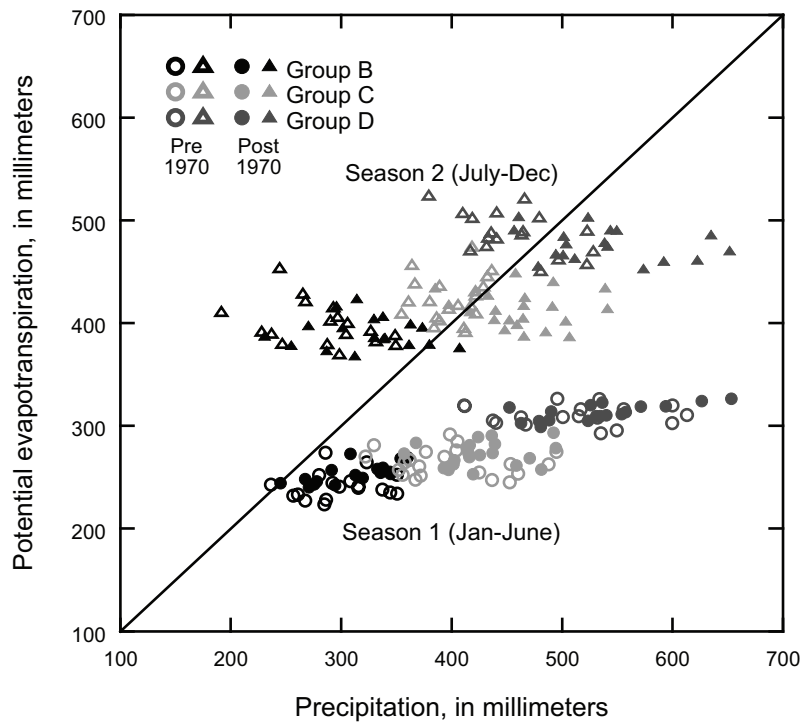


Figure 3.6. Average precipitation versus potential evapotranspiration (Thornthwaite method) for season 1 (January-June) and season 2 (July-December) for selected 12-year periods for basin groups B, C, and D (open symbols, pre-1970; solid symbols, post-1970).

The estimated coefficients for the water-balance models (Eqs. 3.1 and 3.2) for the 19 basins are given in the supplemental data of Ryberg et al. (2014, table S1). Although differences between coefficients were relatively small, fitted runoff was sensitive to small changes in these coefficients and thus there were significant differences among the basins. Since the focus of this paper is to evaluate temporal runoff changes in relation to climate variability, separate coefficients for each basin were used to remove as much of the spatial variability as possible. The timing and type of precipitation (snow versus rain) in season 1, as well as basin properties (discussed in more detail for season 2), would be expected to influence coefficients for season 1

( $\alpha$ ). While  $\alpha$  averaged 1.14, the four largest values for  $\alpha$  were all from basins in group B, where much of the precipitation in January-March is snow which remains in storage until melting during spring, exposing the snowmelt to more ET.

The term  $\beta$ PET2 is the estimated average (over a given 12-year period) of season 2 PET for a particular basin. Consistent with the definition of PET in most water-balance models,  $\beta$ PET2 is interpreted as the maximum ET rate that can occur in season 2 given unlimited supply of precipitation. The fact that all of the coefficients are substantially greater than 1.0 (average of 1.35 for all the basins) probably indicates that PET2 (the Thornthwaite estimate of PET) underestimates PET for season 2. Another study (Lu et al., 2005) confirmed the underestimation, finding that PET estimates that are based on daily rather than monthly temperature, such as the Hamon method (1961), were about 35 percent higher than estimates using the Thornthwaite method. In a study comparing the efficacy of various methods for estimating PET for rainfall-runoff models (Oudin et al., 2005), the Hamon method was among the best methods of 27 tested and outperformed more complicated methods such as the Hargreaves or Penman methods.

Other than bias in PET estimates, differences in vegetation cover and a number of physical considerations would be expected to influence  $\beta$ . Any basin property that would be expected to allow precipitation to run off quickly without being exposed to as much ET (for example, low soil-moisture infiltration rate, and high slope) would tend to lower  $\beta$ . Conversely, high soil-moisture storage capacity, high infiltration rates, and flat terrain would be expected to increase  $\beta$ . Three of the four highest values for  $\beta$  were for basins in group B, which tends to have the flattest terrain and among the highest soil-moisture storage capacities.

Figure 3.7 illustrates the water-balance model results. In the left-hand graphs, the triangles show the relation between precipitation and observed runoff in each season and the

circles show the relation between precipitation and runoff plus estimated ET. The closer estimated ET is to actual ET, the closer the upper points should align with the line of equality. The model fits well in both seasons, indicating that the nonlinear model equations provide a good representation of the water balance across the various groups and basins. The relation between precipitation and runoff, though strong, is nonlinear and has considerably more spread than the relation between precipitation and runoff plus estimated ET. Regression models using precipitation alone to estimate runoff did not represent runoff variations as well as the model using both precipitation and PET. The relation between fitted runoff (the right-hand sides of Eqs. 3.1 and 3.2) and observed runoff is shown graphically in the right-hand graphs in figure 3.7. The model explains 97 percent of the overall spatial/temporal variability in runoff for season 1 and 94 percent of the variability for season 2. With respect to the temporal variability among periods within each of the 19 basins, the model explains an average of 59 (range of 22 to 86) percent of the temporal variability for basins in group B, 87 (range of 68 to 98) percent for group C, and 84 (range of 64 to 98) percent for group D.

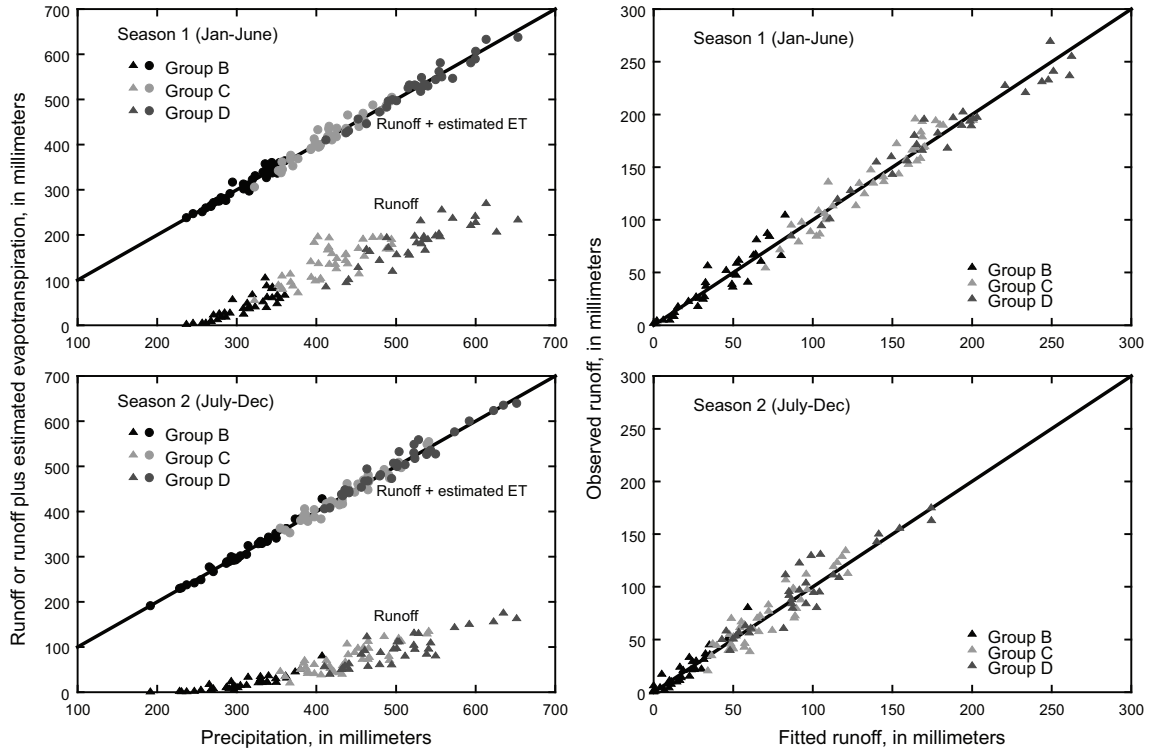


Figure 3.7. Average precipitation versus runoff and runoff plus estimated evapotranspiration (left-hand graphs) and fitted runoff versus observed runoff (right-hand graphs) for season 1 (January-June) and season 2 (July-December) for selected 12-year periods for basin groups B, C, and D.

The residuals from the water-balance equations can be examined more closely to look for indications of changes occurring in the basins through time that are not explained by climatic variability, and hence may be related to other changes such as land use (fig. 3.8). Although these changes may be small in relation to changes driven by climate variability, they nonetheless may be important considerations. Most of the basins, especially in groups B and C, have high agricultural land use (cultivated crops or hay/pasture, fig. 3.3), and large-scale changes in agricultural tillage practices and cropping patterns have occurred during the last century. Season 1 has a pattern of increasing runoff residuals for groups B and C from the mid-1950s (1953-64 analysis period) through the 1980s (1982-93 analysis period) with residuals stabilizing and remaining high during the 1998-2009 period. This is consistent with other studies (Schilling et

al., 2008; Tomer and Schilling, 2009; Zhang and Schilling, 2006) that indicate a general decrease in ET (and increase in runoff) during this time because of land-use changes. However, the increase is not as large as indicated in some previous studies. Season 2 has a similar increasing runoff pattern during the same period for group C but for all groups the season 2 runoff residuals during 1970-81 are low compared to the other analysis periods.

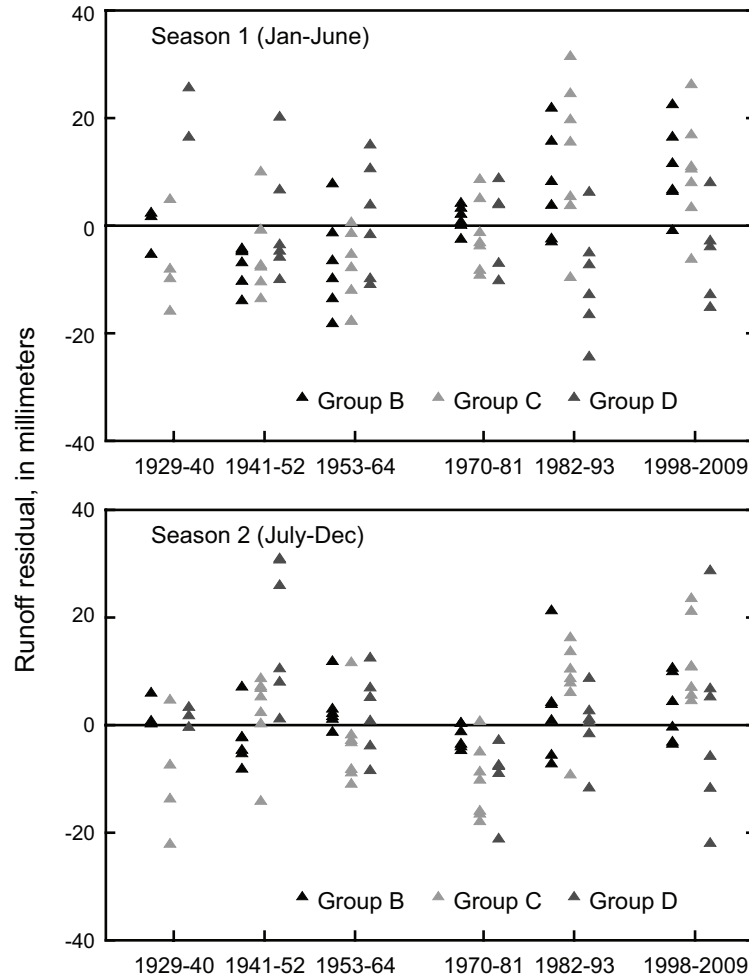


Figure 3.8. Residuals from nonlinear water-balance model for estimating runoff for season 1 (January-June) and season 2 (July-December) for selected 12-year periods for basin groups B, C, and D.

To quantify the relative changes in runoff because of seasonal climate variability or other effects such as land-use or other non-climate related changes, a dry period (1953-64) was contrasted with the two most recent wet periods (1982-93 and 1998-2009). The group averages of changes in runoff between these periods were partitioned into changes in fitted runoff from the water-balance model (seasonal climate effects) and changes in the residuals (land-use/other effects). For each group, a paired t-test was used to determine if the change in the residual runoff between the two periods was statistically different from zero. In the cases of statistically significant differences, land-use effects may have been important contributors to the changes in runoff. However, many other factors besides land-use change may cause temporal trends in the residuals. For example, changes in timing or intensity of precipitation within seasons or changes in precipitation type (rain versus snow) may not be reflected in the seasonal water-balance analysis. Therefore, since land-use effects may be confounded with other effects such as these, changes in residuals will be attributed to land-use/other effects and analysis that is more detailed may be needed to confirm that the changes are indeed dominated by land-use effects.

Table 3.3 shows the results of the partitioning analysis. For season 1, average runoff for both wet periods was about twice as high as the dry period for group B and nearly twice as high for groups C and D. For group D, the increases in runoff were not inconsistent with increases predicted from the water-balance model—the residual changes were not significantly different from zero for that group. Thus, seasonal climate effects probably were the primary cause for the runoff increases for group D. However, for the highly agricultural basins in groups B and C, land-use/other effects accounted for a significant portion of the runoff increases in season 1. For group B, land-use/other effects and seasonal climate effects contributed about equally to the approximate doubling of runoff. For group C, land-use/other effects contributed about one-

quarter and seasonal climate effects about three-quarters of the runoff increases. In absolute terms, the land-use/other effects were similar for both of the wet periods and both groups B and C, with runoff increases ranging from about 14 to 22 mm. If these changes do reflect land-use effects, then similar land-use changes occurred for groups B and C, the land-use changes lead to increases in runoff, and the changes probably occurred sometime from about the early 1950's to the mid-1980's before stabilizing and remaining relatively constant during recent decades. These observations are partially consistent with previous findings. Schilling et al. (2008) and Zhang and Schilling (2006) suggested that increases in streamflow in agricultural watersheds in the upper Mississippi Basin (including basins from group C) from the 1940s to the early 2000s resulted largely from extensive conversion of perennial vegetation to seasonal row crops and associated decreases in ET and increases in baseflow. However, these previous studies attributed most of the increasing streamflow to land-use change and did not rigorously partition climate-related change from land-use change. In this study, we show that most of the streamflow increase (about 75 percent for group C) was climate-related and a smaller portion (about 25 percent for group C) was possibly land-use-related.

Table 3.3. Change in runoff from dry (1953-64) to wet (1982-93 and 1998-2009) periods for season 1 (January-June) and season 2 (July-December) for basin groups B, C, and D.

Season	Group	Average runoff, 1953-64 (mm)	Average runoff, 1982-93 (mm)	Average runoff, 1998-09 (mm)	Runoff change, 1953-64 to 1982-93 (OBS; WBM; RES) (mm)	Runoff change, 1953-64 to 1998-2009 (OBS; WBM; RES) (mm)
1 (Jan- June)	B	27.4	59.0	57.4	(31.6; 17.3; 14.3*)	(30.0; 12.6; 17.4*)
	C	91.9	171.6	174.3	(79.6; 57.8; 21.8*)	(82.3; 63.6; 18.8*)
	D	119.0	209.3	202.9	(90.4; 101.5; -11.2)	(83.9; 89.8; -6.5)
2 (July- Dec)	B	14.5	36.8	28.0	(22.2; 22.4; -0.2)	(13.4; 13.5; -0.1)
	C	47.9	118.1	81.1	(70.3; 59.1; 11.2*)	(33.2; 17.8; 15.4*)
	D	52.8	149.5	93.1	(96.7; 98.9; -2.2)	(40.3; 42.3; -2.0)

OBS represents the observed runoff change. WBM represents the runoff change explained by the water-balance model (seasonal climate effects). RES represents the runoff change in the residuals (land-use/other effects). \* significantly different from zero ( $p < 0.05$ ) using paired  $t$ -test.

Compared to season 1, the relative changes in season 2 runoff were even larger for the 1982-93 period, with average runoff for that period about 2.5 to 3 times higher than the 1953-64 period (table 3.3). Although season 2 runoff for the 1998-2009 period was not as high as the 1982-93 period, it was still nearly twice as high as runoff during 1953-64. Like season 1, the increases in season 2 runoff for group D were consistent with increases predicted from the water-balance model, indicating the primary cause for the increases was probably climate. However, unlike season 1, for group B there was no significant land-use/other effect in the residuals for season 2. For group C, like season 1, the season 2 runoff increases apparently resulted from a combination of seasonal climate effects and land-use/other effects, with the former being dominant in the 1982-93 period. For the 1998-2009 period, seasonal climate effects and land-use/other effects contributed about equally to the increase in runoff from 1953-64.

Long-term temporal variability in seasonal 7-day high runoff for the 19 basins and 6 12-year periods analyzed previously in the water-balance analysis (fig 3.9) was similar to temporal variability in seasonal runoff (fig. 3.5). Comparison of results from the three models (Eqs. 3.6, 3.7, and 3.8) was used to determine the relative importance of climate effects and land-use/other effects for explaining variability in the 7-day high runoff. For example, if model 6 is better (describes significantly more variability) than models 7 and 8, then both ROFIT (the fitted runoff from the water-balance model) and RORES (the residuals) are important predictors of 7-day high runoff and the coefficients ( $J_1$  and  $J_2$ ) are significantly different. Thus, both seasonal climate effects and land-use/other effects are important but they affect 7-day high runoff differently. If model 6 is not better than model 7, then  $J_2$  is not significantly different from zero and only ROFIT is an important predictor of 7-day high flows. Thus, only seasonal climate effects are important. If model 6 is better than model 7 but not better than model 8, then both ROFIT and RORES are important predictors and the coefficients are not significantly different. Thus, both seasonal climate and land-use/other effects are important and both affect 7-day high runoff in a similar manner.

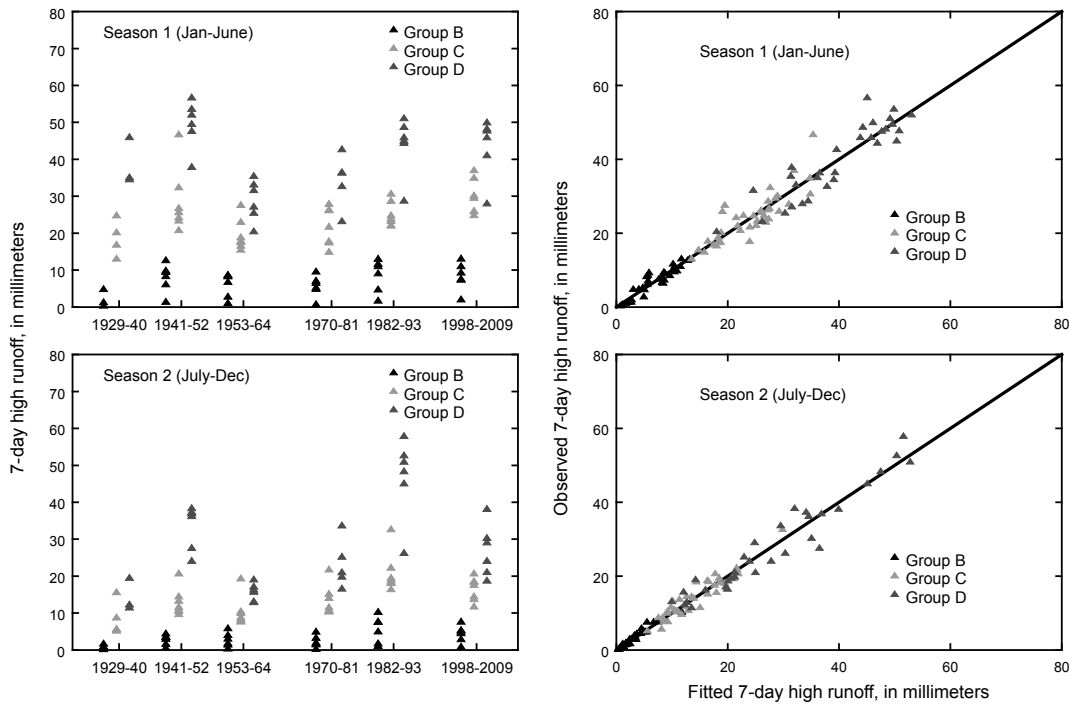


Figure 3.9. Observed 7-day high runoff (left-hand graphs) and fitted versus observed 7-day high runoff (right-hand graphs) for season 1 (January-June) and season 2 (July-December) for selected 12-year periods for basin groups B, C, and D.

Regression analysis results for the high-runoff analysis are given in table 3.4 and the fitted versus observed 7-day high runoff shown graphically in figure 3.9. For season 1, the best model for all three groups, determined by pairwise F-tests with significance level 0.05 (not by the coefficient of determination), consisted of model 7, in which just fitted runoff from the water-balance model was included. Thus, seasonal climate effects explained from 73 percent (group C) to 87 percent (group B) of the variability in 7-day high runoff for season 1 and land-use/other effects were not significant. For season 2, the best model for all three groups consisted of model 8, in which fitted runoff and residual runoff were both significant and had the same coefficient. Model 8 explained between 89 percent (group C) and 94 percent (group B) of the

variability in 7-day high runoff. Thus, both seasonal climate effects and land-use/other effects contributed to variability in 7-day high runoff for season 2. Comparing the coefficients of determination for model 8 and model 7 for season 2, for group B seasonal climate effects explained 82 percent and land-use/other effects 12 (94-82) percent of the variability in 7-day high runoff. Similarly, seasonal climate effects explained 76 percent and land-use/other effects 13 (89-76) percent of the variability for group C compared with 85 percent and 8 (93-85) percent for group D. In contrast to the previous results (table 3.3 and associated discussion), in which land-use/other effects were significant for explaining some of the variability in season 1 runoff for groups B and C, they do not appear to be significant for explaining variability in high flows. This finding is not inconsistent with other studies, such as Zhang and Schilling (2006) who argued that land-use changes would tend to affect baseflow more than high flow.

Table 3.4. Coefficient of determination ( $R^2$ ) for linear regression models relating seasonal 7-day high runoff to seasonal runoff for groups B, C, and D.

Season	Group	$R^2$ for model 6 with both fitted runoff and residual runoff (percent)	$R^2$ for model 7 with just fitted runoff (percent)	$R^2$ for model 8 with just observed (fitted plus residual) runoff (percent)
1 (Jan-June)	B	90	87*	87
	C	73	73*	70
	D	82	79*	82
2 (July-Dec)	B	94	82	94*
	C	90	76	89*
	D	93	85	93*

\* indicates best model judging by pairwise  $F$ -tests with significance level 0.05.

### 3.4. Discussion and Conclusions

Changes in runoff in the north central U.S. are closely related to changing precipitation patterns. Upward trends in precipitation appear to result from transient, abrupt, and highly persistent shifts in precipitation with durations of up to a few decades. Periods of highest flood

risk and the magnitude of large floods are consistent with seasonal changes in precipitation combined with multi-year moisture-surplus conditions that become more important in the northern and western basins. This suggests that recent increases in runoff in this area are not primarily land-use change driven. This is consistent with Tomer and Schilling (2009), for sites in Illinois, Iowa, and Missouri, where they concluded that runoff increased in the Midwest because of climate change and land-use change, but that “climate change has been the larger of the two drivers.”

Runoff patterns in figure 3.4 are smoother than precipitation patterns in all groups because the land surface provides a buffer to even out the variations in precipitation when it results in runoff. When precipitation increases during dry periods, some of the increased precipitation goes to ET, storage in soil, groundwater, and lakes rather than to the stream, until the water-storage capacity of the landscape is exceeded and excess precipitation is then lost to runoff. Likewise, when conditions are wet and precipitation decreases, moisture stored in the soil dampens the short-term variability in runoff. Nevertheless, if precipitation is intense (one anticipated impact of climate change, Bates et al., 2008) and exceeds the rate of infiltration, runoff can occur whether or not the soil is saturated.

Climate and soils conditions can help explain differences in how the four regions respond to changes in precipitation. Soils in the Dakotas dry out more often than they do in Missouri for example and initial increases in precipitation in the northwest part of the study area go into soil storage while initial increases in precipitation in the south go into runoff. If a wet period is long enough in the northwest, the excess precipitation goes into runoff as well. The wet and dry periods are different in timing and duration in the winter-spring and summer-autumn seasons confirming that precipitation changes do not change uniformly over a calendar year, emphasizing

the need for seasonal analysis. The changes are complex, each one different from the others (in length, severity, seasonality, and regional coverage).

Although anthropogenic changes may be affecting climate and runoff in subtle ways not yet evident in the runoff records or climatic data analyzed in this paper, it appears that runoff changes for this region are consistent with observations in paleo-climatic records and with natural climatic variability related to long-term fluctuations in global ocean temperature and atmospheric pressure anomalies. Paleo-climatic studies from eastern North and South Dakota (basin group B, fig. 3.1) based on tree rings and lake sediments indicate similar transitions have occurred several times in the past 1,000-2,000 years (Shapley et al., 2005; Laird et al., 2003). Intervals between extreme wet or dry periods seem to be random rather than periodic, indicating nonlinear dynamical behavior rather than predictable cycles (Vecchia, 2008). The dominant wet climatic anomaly of the 20th century and the early 21st century and the increase in autumn precipitation beginning in mid-to-late 1970s may be another transient shift, as evidenced by season 2 precipitation for groups C and D returning to normal during the 2000s (fig. 3.4).

Climate variability expressed as precipitation is a major driver of changes in runoff. An additional important climate variable is temperature, expressed in this study as PET. Recent temperature increases in season 1 would be expected to increase PET. As indicated in fig. 3.6, PET tends to be somewhat higher for comparable precipitation values during the post-1970 periods compared with the pre-1970 periods, especially for groups B and C. However, the changes are relatively small compared to the overall temporal variability of PET and very small compared with temporal variability in precipitation. Therefore, the PET increases turned out to be a negligible contributor to the water-balance analysis. Of course, larger temperature changes in future years may be important drivers of future runoff changes.

Overall, the scale of historical precipitation variability in both seasons is considerably larger than the scale of historical PET variability, so precipitation changes are expected to be the dominant driver of runoff changes. However, the water-balance analysis shows that both PET and precipitation are important for explaining historical runoff variability and they explain the majority of the spatial/temporal variability. Land-use/other effects may explain much of the remaining variability in seasonal runoff. While the water-balance may explain the climate effects on 7-day high runoff, the highly variable nature of 7-day high runoff makes it difficult to discern a relation between 7-day high runoff and relatively small land-use effects. It appears that land-use/other effects have little impact on season 1, but may have some impact on 7-day high runoff for season 2.

The potential land-use-related changes determined in this paper are smaller than indicated in Schilling et al. (2008, 2010) and more in line with Tomer and Schilling's conclusion that between climate change [or, we would argue more generally, climate variability] and land-use change, climate change has been the dominant of the two drivers of change (2009).

This paper contributes to the quantification of the climate and land-use effects on runoff. While the water-balance model worked well, potential future increases in precipitation intensity and temperature that influence runoff and ET may warrant further study.

**CHAPTER 4. CHANGES IN SEASONALITY AND TIMING OF PEAK STREAMFLOW  
IN SNOW AND SEMI-ARID CLIMATES OF THE NORTH-CENTRAL UNITED  
STATES, 1910-2012**

Changes in the seasonality and timing of peak streamflow in the north central U.S. are likely because of changes in precipitation and temperature regimes. A source of long-term information about flood events across the study area is the U.S. Geological Survey peak streamflow database. However, one challenge of answering climate-related questions with this dataset is that, even in snowmelt-dominated areas, it is a mixed population of snowmelt/spring rain generated peaks and summer/fall rain generated peaks. Therefore, a process was developed to divide the peaks into two populations, snowmelt/spring and summer/fall. The two series were then tested for the hypotheses that, because of changes in precipitation regimes, the odds of summer/fall peaks have increased and, because of temperature changes, snowmelt/spring peaks happen earlier. Over climatologically and geographically similar regions in the north central U.S., logistic regression was used to model the odds of getting a summer/fall peak. When controlling for antecedent wet and dry conditions and geographic differences, the odds of summer/fall peaks occurring have increased across the study area. Trend analysis also showed that in northern portions of the study region, snowmelt/spring peaks are occurring earlier. The timing of snowmelt/spring peaks in three regions in the northern part of the study area is becoming earlier by 8.7 to 14.3 days. These changes have implications for water interests, such as potential changes in lead-time for flood forecasting or changes in the operation of flood-control dams.

#### 4.1. Introduction

The study area used is a refinement of that of Ryberg et al. (2014) and an extension further west into the semi-arid areas of the Great Plains that is based on Water-Resources Regions (Seaber et al., 1987), Köppen-Geiger climate classes (Kottek et al., 2006), and ecological regions (Commission for Environmental Cooperation, 1997). The area includes three major water-resources regions, Missouri, Souris-Red-Rainy, and Upper Mississippi (see Appendix A, fig. A.1). Five climate classes from the Köppen-Geiger classification system occur within the study area. The two major climate types are snow and arid. The climate classes are further sub-classified by their precipitation and temperature conditions. The five climate zones are Dfa (snow, fully humid, hot summer), Dfb (snow, fully humid, warm summer), Dwa (snow, winter dry, hot summer), Dwb (snow, winter dry, warm summer), and BSk (Arid, Steppe, cold arid; see Appendix A, table A.1 and fig. A.2). The Level II ecological regions representing the Great Plains in the north central U.S. are 9.2 Temperate Prairies, 9.3 West Central Semi-Arid Prairies, and 9.4 South Central Semi-Arid Prairies (see Appendix A, fig. A.3). Using the Great Plains as a study bound eliminated mountainous areas in the western part of the study area and forested areas in the eastern part.

The intersections of the climate zones and the ecoregions within the Water-Resources Regions were used to create seven spatial regions (hereafter referred to as regions), assumed to have similar climate, topography, and water-resource regimes (fig. 4.1; see also fig. A.4 and text in Appendix A). Semi-arid is the term used by the ecological regions to describe the drier areas of the study area, while Köppen-Geiger uses arid; hereafter the term semi-arid is used to match the more commonly used terminology of the ecological regions, unless specifically talking about Köppen-Geiger climate classes or using arid in a comparative sense.

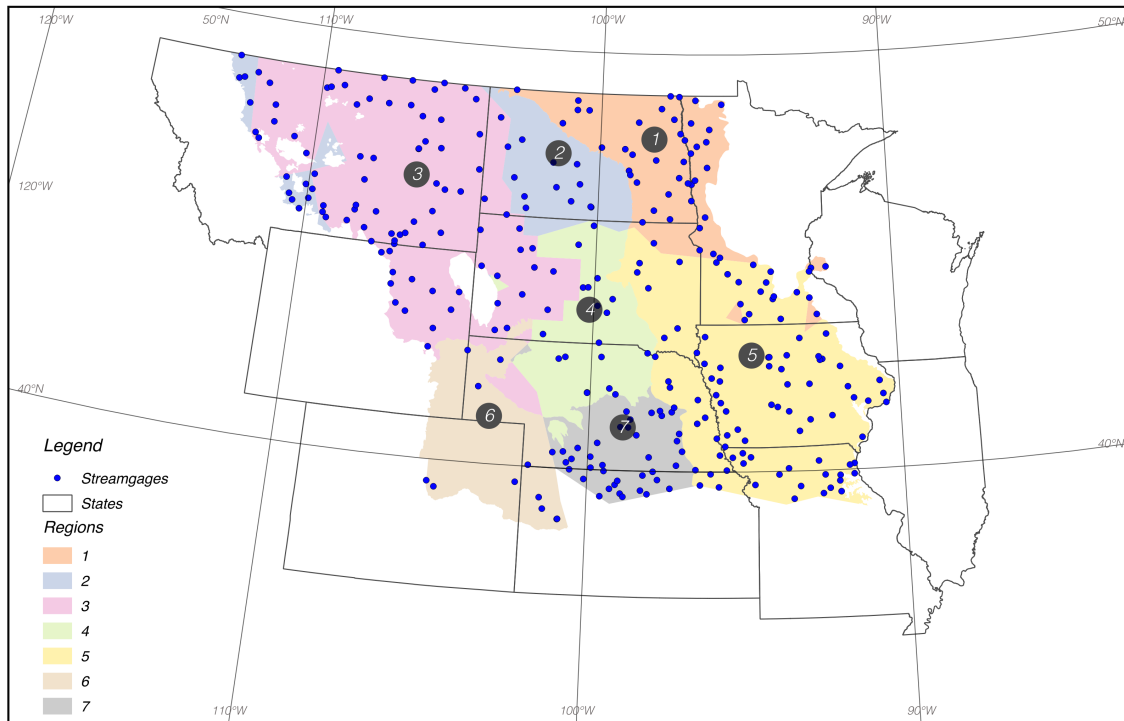


Figure 4.1. Regions based on climate, ecoregions, and major river basins (shown in Appendix A), and streamgages.

All regions experience snow, however, some have snow-melt dominated streams, and others more often have peaks caused by rain. In snow-melt dominated streams, snow accumulates throughout the winter and melts in the spring causing many of the peaks, or snow accumulates and melts, but the peaks are caused by spring rain before substantial evapotranspiration begins. However, throughout the period of recorded observation (1910-2012), even snowmelt-dominated streams have experienced winters with little snow and little spring runoff, therefore the peak may occur during the summer or fall, as can be determined by examining individual peaks in the USGS peak streamflow database, <http://nwis.waterdata.usgs.gov/usa/nwis/peak>. The semi-arid parts of the study area, while dry, are cold and can store precipitation over the winter; therefore, some peaks occur during the spring snowmelt period. This pattern of spring snowmelt gradually changes as one moves toward

the western and southern edges of the study region that may experience snow, but less than the northern most areas. The semi-arid regions in Wyoming and Nebraska and the snow climates of Nebraska and Kansas experience some peaks as spring peaks; however, the majority of peaks recorded have occurred from summer or fall rain.

Numerous studies have reported increases in precipitation and temperature. Precipitation increases have been reported in all seasons (Karl and Knight, 1998; Wang et al., 2009), with the largest changes observed in fall (Garbrecht and Rossel, 2002; Small and Islam, 2008; Small and Islam, 2009; Wang et al., 2009), and an expectation under atmospheric warming that “more precipitation will fall as rain rather than snow” (Andersen and Shepherd, 2013). Since 1895, U.S. average temperature has increased by 1.3° to 1.9°F. (in a manner not constant over time), with the greatest warming in winter and spring (Walsh et al., 2014).

Changes in peak timing due to climate change have been predicted and documented elsewhere. For instance, researchers have linked a warming global climate to a shift in the timing of runoff in “snowmelt-fed rivers” (Bates et al., 2008). Trends toward earlier timing of peak streamflow (which are influenced by snowmelt runoff in areas with substantial snowpack) have been observed in New England (Hodgkins et al., 2003), New York (Burns et al., 2007), eastern North America (Hodgkins and Dudley, 2006), California (Dettinger and Cayan, 1995), the western U.S. (Cayan et al., 2001; Dettinger, 2005; Stewart et al., 2005; McCabe and Clark, 2005; Regonda et al., 2005), and Canada (Burn et al., 2008; Zhang et al., 2001). Although some of these studies overlap the current study area, the previous studies have not focused on the north central U.S., and much of their interest has been in mountain snowmelt, therefore, this study fills a gap in the research. In addition, some of the previous studies (Zhang et al., 2001; Hodgkins et al., 2003; Hodgkins and Dudley, 2006) have used the center of volume as an indicator of changes

in streamflow related to climate. Although changes in center of volume and peak streamflow are both of interest to those trying to understand changes in hydrologic regimes, the focus of this study was the timing of peaks in the north central U.S., rather than the center of volume.

This increase in precipitation, especially in the fall, raises an issue in the detection of changes in timing of peaks: the annual peaks are a mixed population of snowmelt and rain-generated peaks. If one analyzed the mixed population together, a trend toward earlier snowmelt, or earlier spring peaks (potentially driven by warming in winter and spring), may be confounded by a concurrent increase in the percentage of annual peaks occurring in the summer or fall (potentially driven by greater or more intense precipitation in these seasons). This study categorizes peaks as those that occur in the spring from snowmelt, rain on snow, or spring rain (snowmelt/spring peaks) and those that are rain-generated from rain events in the summer and fall (summer/fall peaks). This separation into two categories allows for the examination of both the timing and seasonality issues. Because of changes in precipitation timing and in spring temperatures, changes likely have occurred in both the seasonality and timing of peaks in the north central U.S. The working hypothesis of this study is that in the north central U.S. the probability of experiencing summer or fall rain-generated peaks has increased and that spring peaks may come earlier in some areas. Understanding of this change is important for efficient water use and protection from the hydrologic extremes of floods and droughts.

#### **4.2. Data and Methodology**

In order to examine peaks for changes related to climate, annual peak streamflow values were obtained from the U.S. Geological Survey (USGS) peak streamflow database at <http://nwis.waterdata.usgs.gov/nwis/peak>. The Julian date of each peak was calculated and the historic frequency distribution of the Julian date for peak occurrence was determined for each of

the seven regions. Change points, or local minima, were identified that divide the peaks for each region into spring/snowmelt peaks (January 1 to the local minima) and summer/fall peaks (local minima to December 31). The odds of a peak occurring in the summer or fall was modeled using a logistic regression model that included a date term to determine if the odds of a peak occurring in the summer or fall are increasing.

The initial criteria for including streamgages in the study area were a defined drainage area of less than 60,000 square miles (to remove large basins with peaks that integrate a varied land mass, such as peaks on the Missouri River representing mountain and plains runoff) and at least 15 unregulated peaks. Some streamgages initially considered were on the same stream and many were in the same eight-digit hydrologic unit code (HUC, or cataloging unit: a geographic area, identified by an 8-digit code, representing part or all of a surface drainage basin, a combination of drainage basins, or a distinct hydrologic feature, Seaber et al., 1987). Therefore, to reduce spatial correlation, the potential streamgages were thinned in the following manner. For streamgages in the same HUC, the streamgage with the longest period of record for peaks was retained and the remaining streamgage(s) was (were) removed. If one or more streamgages within the same HUC had the same period of record, the streamgage with the largest drainage area was retained. This procedure resulted in the inclusion of 309 streamgages, which are shown in figure 4.1. The reduced list still provided good geographic coverage, but with much less spatial correlation. Exceptions to these rules occurred when the streamgages in the same HUC had non-overlapping period of record, or overlapped by at most 3 years. These situations occurred when streamgages were moved for a variety of reasons and this in essence extended the period of record for those HUCs. Individual peaks with particular streamflow qualification codes were eliminated from the study for reasons such as regulation and dam failure. Additional details

on the selection of streamgages and elimination of particular peaks are provided in Appendix A. Streamgage selection based on these criteria as compared to streamgages listed in Geospatial Attributes of Gages for Evaluating Streamflow database (GAGES II; Falcone, 2011) or the USGS Hydro-Climatic Data Network (HCDN-2009; Lins, 2012) is compared and contrasted in Appendix A.

The peak series was assigned to the region in which the gage was located. For each peak, the Julian date (number of days since the beginning of a particular year) was calculated. Then for each region (fig. 4.1), density plots were generated showing the frequency of Julian dates for the peaks (fig. 4.2). These plots generally show a high frequency, or density, for snowmelt- or spring rain-generated peaks, followed by a decrease in the occurrence of peaks (a sharp decrease in some areas), then an increase in the frequency of peaks later in the year at dates representing rain-generated peaks in the summer or fall. This pattern becomes less pronounced as one moves south and regions 6 and 7 show few peaks early in the year that would be indicative of snowmelt. However, all show peaks that represent a process at the end of winter, when evapotranspiration is low, caused by melting snow and/or spring rain, followed by a decreased frequency of peaks, then an increase during periods more dominated by convective processes.

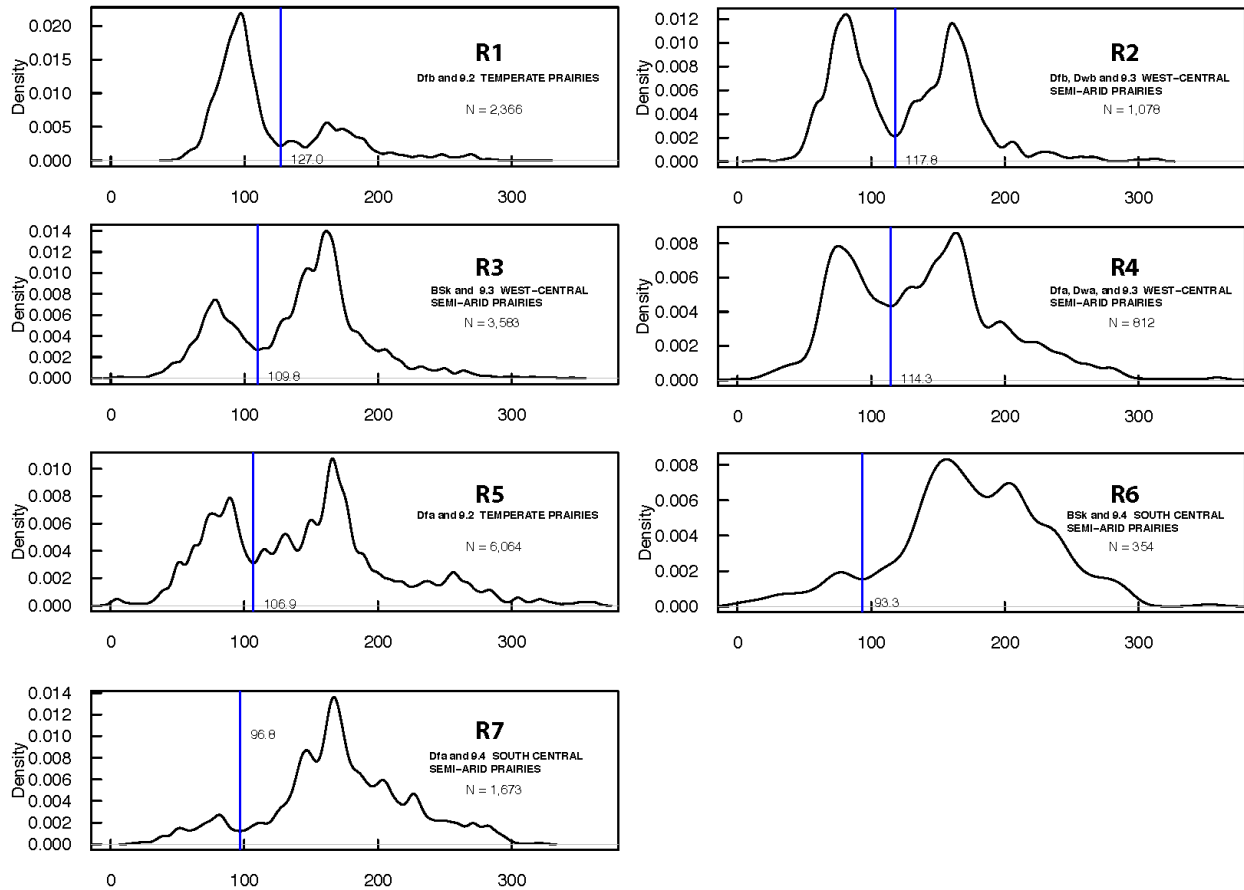


Figure 4.2. Geographically related areas of similar Julian date density patterns. The vertical line and number indicate the date that separate potentially snowmelt/spring peaks from those that occur later in the year because of rain (summer/fall) peaks (R1-R7, regions 1-7 in figure 4.1).

The Julian dates for the local minima between the early and later peak densities were used to separate the peaks into two categories, snowmelt/spring peaks and rain/summer peaks. Peaks occurring before the local minima (fig. 4.2) were assigned the category 0 and peaks after the local minima were assigned the category 1. The dates used to separate the peaks into the two categories are listed in table 4.1. Note that the density plots do not address magnitude, which could vary greatly within and between the snowmelt/spring and summer/fall peak seasons, particularly in regions 1 and 2, where large floods depend on large accumulations of snow. Summary information for each of the regions is provided in table A.3 of Appendix A.

Table 4.1. Regions associated ecological regions (Commission for Environmental Cooperation, 1997) and climate classes (Kottek et al., 2006), and the Julian date that separates the snowmelt/spring peak date density from the rain/summer peak date density.

Region	KG Class(es)	Ecological region	Local minimum, Julian date
1	Dfb	9.2 Temperate Prairies	127.0
2	Dfb, Dwb	9.3 West-Central Semi-Arid Prairies	117.8
3	BSk	9.3 West-Central Semi-Arid Prairies	109.8
4	Dfa, Dwa	9.3 West-Central Semi-Arid Prairies	114.3
5	Dfa	9.2 Temperate Prairies	106.9
6	BSk	9.4 South Central Semi-Arid Prairies	93.3
7	Dfa	9.4 South Central Semi-Arid Prairies	96.8

KG, Köppen-Geiger

#### 4.2.1. Logistic Regression to Examine Seasonality of Peaks

Logistic regression was used to build a model to explain a categorical dependent variable with two categories, snowmelt/spring peaks and summer/fall peaks, based on several potential explanatory variables. The possible outcomes are modeled using a logistic regression model, equation 4.1,

$$E[Y] = \frac{e^{X\beta}}{1 + e^{X\beta}} \quad (\text{Eq. 4.1})$$

where  $\mathbf{Y}$  is the matrix of the independent outcomes of the classification (0 or 1) and  $\mathbf{X}\beta$  is the matrix algebra representation of the observations of the explanatory variables ( $\mathbf{X}$ ) and model parameters ( $\beta$ ).

Potential explanatory variables included the region in which the streamgage was located, drainage area, altitude, and water year (because peaks are determined on a water year basis, water year is defined as the 12-month period October 1, for any given year through September 30, of the following year; the water year is designated by the calendar year in which it ends and which includes 9 of the 12 months; U.S. Geological Survey, 2014a). Water year is an important

potential explanatory variable because if the coefficient for the water year in the regression model is statistically significant, this indicates an increase or decrease over time in the probability of a peak occurring in the summer.

Ryberg et al. (2014) showed that “periods of highest flood risk and the magnitude of large floods are consistent with seasonal changes in precipitation combined with multiyear moisture-surplus conditions.” Therefore, to examine the effects of antecedent wet/dry conditions on peak-streamflow timing, additional terms were considered using the Palmer Hydrologic Drought Index (PHDI), an indicator of long-term cumulative hydrologic drought (negative PHDI) or long-term cumulative wet conditions (positive PHDI; Heim, 2002). The terms considered were the PHDI for the month in which the peak occurred, as well as PHDIs lagged 1 to 6 months before the peak. Lag effects were examined because they represent longer-term dry or wet conditions months before the generation of the peaks, and the lagged antecedent conditions, such as the accumulation of snow or the depletion of groundwater, are important for the development of floods and droughts. The PHDI indices for each U.S. climate division (<http://www.esrl.noaa.gov/psd/data/usclimdivs/data/map.html>) in the study area were downloaded using the R (R Core Team, 2014) package `climdiv` (Westerling, 2005). Each streamgauge was matched to its climate division and the PHDIs were added to the model matrix as possible explanatory variables.

The data set was quite large, 15,801 peaks, therefore a model selection and validation technique was used that split the data into three data sets of approximately the same size, a training set (dataset 1), a validation set (dataset 2), and a test set (dataset 3; Hastie et al., 2001). The data were split by year, so the first dataset had peaks for the years 1910, 1913, 1916, and so on. The second dataset contained peaks starting with the year 1911, and the third dataset had

peaks starting with year 1912. The training dataset was used to select the potential logistic regression models. The validation dataset was used to estimate prediction error for a subset of potential models. Finally, the test dataset was used to assess the final model. Splitting the dataset this way reduced serial correlation, a concern with annual streamflow records.

#### **4.2.2. Linear Regression to Examine Timing of Peaks within Seasons**

To further examine changes in timing of peaks, two annual peak time series, one of snowmelt/spring peaks the other of summer/fall peaks were created. When the peak of record for a particular year occurred during the snowmelt/spring period, that peak went into the snowmelt/spring series for that streamgauge and the maximum daily value (where available, for some years at some streamgages, the data collected was peak streamflow only and not daily mean streamflow) during the summer/fall period went into the summer/fall peak series for that streamgauge. When the annual peak occurred during summer/fall, that peak went into the summer/fall series and the maximum daily value (where available) during the snowmelt/spring period was used in the series of snowmelt/spring peaks (more details regarding this process are provided in Appendix A). Daily values were not always available for all water years, so the number of peaks in each series for a given streamgauge is not necessarily the same.

To examine changes in seasonal timing for each region, the annual peak-flow Julian date for streamgages in each region was averaged to create an average peak Julian date for each region in the snowmelt/spring peak season and the summer/fall peak season. Linear regression was performed by region to determine whether there were trends in the timing of peaks. The model used was:

$$Y = X\beta + \epsilon \quad (\text{Eq. 4.2})$$

where  $\mathbf{Y}$  is the matrix of annual regional Julian dates,  $\mathbf{X}\boldsymbol{\beta}$  is the matrix algebra representation of the observations of the explanatory variable ( $\mathbf{X}$ ; water year) and model parameters ( $\boldsymbol{\beta}$ ), and  $\epsilon$  is the model error.

The residuals of all the trend models were examined to verify the appropriateness of linear regression for this analysis. The Durbin-Watson test was performed to examine autocorrelation of the residuals. In the Durbin-Watson test (Durbin and Watson, 1950, 1950, and 1971; Zeileis and Hothorn, 2002), the null hypothesis is that the autocorrelation of the residuals is zero and it is tested against the alternative hypothesis that the residuals are autocorrelated. Therefore, a statistically significant result can indicate a model misspecification or a violation of the assumptions underlying regression (Neter et al., 1996).

#### **4.3. Results of Logistic Regression to Examine Seasonality of Peaks**

Using the training dataset, exploratory analysis (not shown) was performed using the regional membership indicators (R2-R7), altitude (ALT), the logarithm of drainage area ( $\log(\text{DA})$ ), water year (WY), and PHDI lagged 0, 1, 2, 3, 4, 5, or 6 months. PHDI lagged two months (PHDI2) contributed to a larger Nagelkerke  $R^2$  index (Nagelkerke, 1991; Harrell, 2014). Nagelkerke  $R^2$  index one of the most commonly used pseudo  $R^2$ 's and is used for model selection but not having the same interpretation as  $R^2$  in linear regression (Smith and McKenna, 2013).

Models that included all regional membership indicators R2-7, water year, and optionally one or more of PHDI2, altitude, and logarithm of drainage area were compared. The three models with the highest Nagelkerke  $R^2$  index were selected for further assessment with the validation dataset. The three models all contained the regional membership indicators and PHDI2. Model 1 had the additional variable ALT, model 2 had the additional variable  $\log(\text{DA})$ , and model 3 had both additional variables ALT and  $\log(\text{DA})$ .

The ability of the model to predict the observations in dataset 2 was measured by the Brier score (Brier, 1950). The form of the Brier score used was the modification for binary forecasts (equal to  $\frac{1}{2}$  the original proposed by Brier; Ferro, 2007). The lower the Brier score is for a set of predictions, the better the predictive capability of the model. A perfect model would have a Brier score of 0 and a model that is wrong 100% of the time would have a Brier score of 1 (in the binary modification). Models 1 and 3 had the lowest, and equal, Brier scores of 0.188. However, the  $\log(\text{DA})$  term was not statistically significant in model 3, so model 1 was chosen as the best predictive model.

Model 1 was used with dataset 3 to define the final model and provide estimates of error. Table 4.2 lists the model parameters and the  $p$ -value for the Wald test of significance. Statistical significance is defined as a  $p$ -value less than 0.01 for this study. R2 through R7 are indicator variables. If a peak occurred in region 1 (R1), all indicator variables, R2-R7, were zero. If a peak occurred in region 2, R2 was one and all other region indicators (R3-R7) were zero, and so on for each region.

Table 4.2. Final logistic regression model measures of significance when using dataset 3 (test dataset).

Explanatory Variables	<i>p</i> -value for Wald test of significance of parameters
Intercept	<0.0001
R2	0.0070
R3	0.3849
R4	0.0149
R5	<0.0001
R6	0.0012
R7	<0.0001
Altitude	<0.0001
PHDI2	<0.0001
Water Year	<0.0001
<b>Model Evaluation</b>	
Likelihood ratio test	$\chi^2=1,069$ , $df=9$ , $p$ -value <0.0001
Wald test for overall effect of explanatory variables	$\chi^2=804$ , $df=9$ , $p$ -value <0.0001
Brier score	0.182
Observations	5,153 (115 of the original removed because of missing altitude)

Additional tests were performed to verify model significance and are shown in table 4.2.

The model likelihood ratio test (Snedecor and Cochran, 1989) indicates that the model is statistically significant. The null hypothesis of the Wald test for overall effect is that all of the coefficients of the explanatory variables equal zero and the alternative is that at least one does not (Lesnoff and Lancelot, 2012) and here indicates that the selected model is better than no model. Table 4.3 contains the model parameter estimates and confidence intervals for the odds ratio.

Table 4.3. Logistic regression model coefficients, odds ratio, and 99-percent confidence intervals.

Independent Variables	Coefficients and 99-percent confidence intervals	99-percent confidence interval for $e^{\beta}$ (odds ratio)
Intercept	-42.6622 (-49.99, -35.43)	NA
R2	-0.4699 (-0.9216, -0.0232)	0.6251 (0.3979, 0.9771)
R3	0.1350 (-0.2695, 0.5390)	1.1446 (0.7638, 1.7142)
R4	0.3989 (-0.0221, 0.8228)	1.4901 (0.9782, 2.2768)
R5	1.6883 (1.4358, 1.9451)	5.4103 (4.2031, 6.9943)
R6	1.0963 (0.2709, 2.0354)	2.9932 (1.3111, 7.6554)
R7	1.8874 (1.4976, 2.2908)	6.6020 (4.4711, 9.8833)
Altitude	0.0008 (0.0006, 0.0009)	1.0008 (1.0006, 1.0009)
PHDI2	-0.2117 (-0.2478, -0.1763)	0.8092 (0.7805, 0.8384)
Water Year	0.0210 (0.0173, 0.2468)	1.0212 (1.0175, 1.0250)

#### 4.3.1. Interpretation of the Model

The model can be interpreted in terms of the odds ratio (table 4.3). For example, the odds ratio for a summer/fall peak occurrence in region 2 (R2) is the ratio of the odds of a summer/fall peak in R2 divided by the odds of a summer/fall peak in the other regions. For R2, the odds ratio is less than one, indicating summer/fall peaks are less likely than in the other regions in general.

The region variables, R2-R7, are interpreted in terms of region 1 (the temperate prairies of the Souris and Red River of the North Basins). The region variables that are positive and statistically significant show increases in the odds of summer/fall peaks when moving from region 1 to region 5, 6, and 7. Therefore, when moving south and west from regions 1 and 2, summer/fall peaks are more likely. This replicates what we know from the frequency distribution plots by region in fig. 4.2 and shows that the model detects these differences.

Altitude was statistically significant, albeit having a very small influence (with each unit increase in altitude, the odds of a summer/fall peak are 1.0008 times larger). This represents the

fact that the lowest elevation streamgages are on the eastern side of the study area (regions 1 and 5, fig. 4.1) and those experience a higher frequency of snowmelt/spring peaks (fig. 4.2) than the higher elevation streamgages that occur in Montana and Wyoming (region 3, figs. 4.1 and 4.2).

PHDI2, the antecedent wet or dry conditions, was also a significant predictor of summer peaks (table 4.2). The negative coefficient for the 2-month lagged Palmer Hydrologic Drought Index (PHDI2) indicates that when lagged antecedent conditions become wetter (such as wet fall conditions or snow accumulation), the occurrence of the peak of the year in summer or fall is less likely.

After controlling for climate and topography differences represented by region, altitude, and PHDI2, there is a positive trend over time (positive water year term) indicating that summer peaks are becoming more common. This trend is statistically significant at the 0.01 significance level. Holding all other factors constant, moving forward in time one year increases the odds of a peak occurring in the summer by 1.75 to 2.5 percent. This is a small increase; however, given the length of the period of record of this study, this increase is substantial over time.

The model replicates the fact that peaks in the more arid and southerly regions are more likely to happen in the summer (fig. 4.2). By controlling for the regional effects, the model shows that there is an increasing probability of summer/fall peaks in all regions, whether or not that is the typical time when peaks occur.

#### **4.4. Changes in Timing of Peaks**

Trends were determined for the two seasons, snowmelt/spring and summer/fall. Initial analysis included a mean regional PHDI2 term (meanPHDI2) for consistency with the previous logistic regression analysis for seasonality; however, that term was never statistically significant for the snowmelt/spring peaks and was significant only once for the summer/fall peaks (R3, but

did not change the significance of the water year trend term for that region). Therefore, meanPHDI2 was not included in the final trend models. All models, whether the trend was statistically significant or not, were tested for autocorrelation of the residuals using the Durbin-Watson test, and none of the results indicated autocorrelation at the 0.01 significance level.

#### **4.4.1. Snowmelt/Spring Peaks**

Examination of trends in the regional average Julian date of snowmelt/spring peaks shows that regions 1, 2, and 3 have statistically significant trends toward earlier snowmelt/spring peaks (fig. 4.3). These regions are on the northern tier of the study area (fig. 4.1) and those most dominated by snowmelt runoff. The difference in the mean snowmelt/spring date at the beginning of the record for region 1 (1910) and the end (2012) is 8.7 days. Region 1 overlaps with the western edge of the Hodgkins and Dudley (2006) study of changes in winter-spring center of volume (2006). In an area similar to region 1, they showed earlier winter-spring center of volume dates for 1953-2002 on the order of 1-15 days at individual streamgages (fig. 4.2 of Hodgkins and Dudley, 2006). The difference in the mean snowmelt/spring date for region 2 from the beginning of the record to the end is 10.6 days. The difference in the mean snowmelt/spring date for region 3 is 14.3 days.

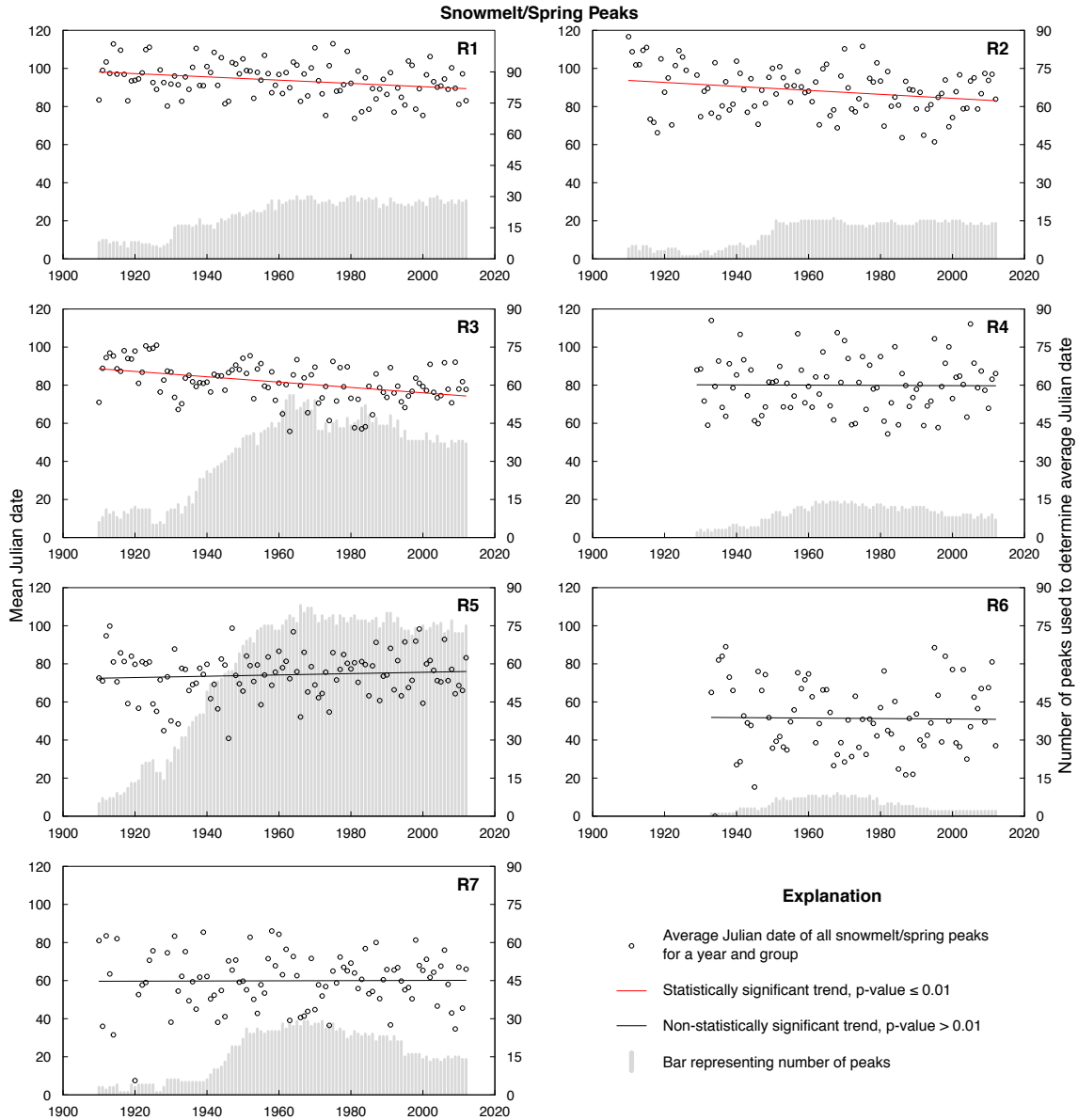


Figure 4.3. Trends in Julian date by region for snowmelt/spring peaks (R1-R7, regions 1-7 in figure 4.1).

#### 4.4.2. Summer/Fall Peaks

Examination of trends in the regional average Julian date of summer/fall peaks shows that only region 1 had a statistically significant trend and it was toward later (larger Julian date) summer/fall peaks (fig. 4.4) and the difference between the beginning and end of the period of record was 5.2 days. This is a region in which fall streamflow has been higher in recent years.

For example, on November 4, 2009, streamflow for the Red River of the North at Fargo, North Dakota, was the highest streamflow recorded for the month of November since measurements started in 1901 (U.S. Geological Survey, 2009).

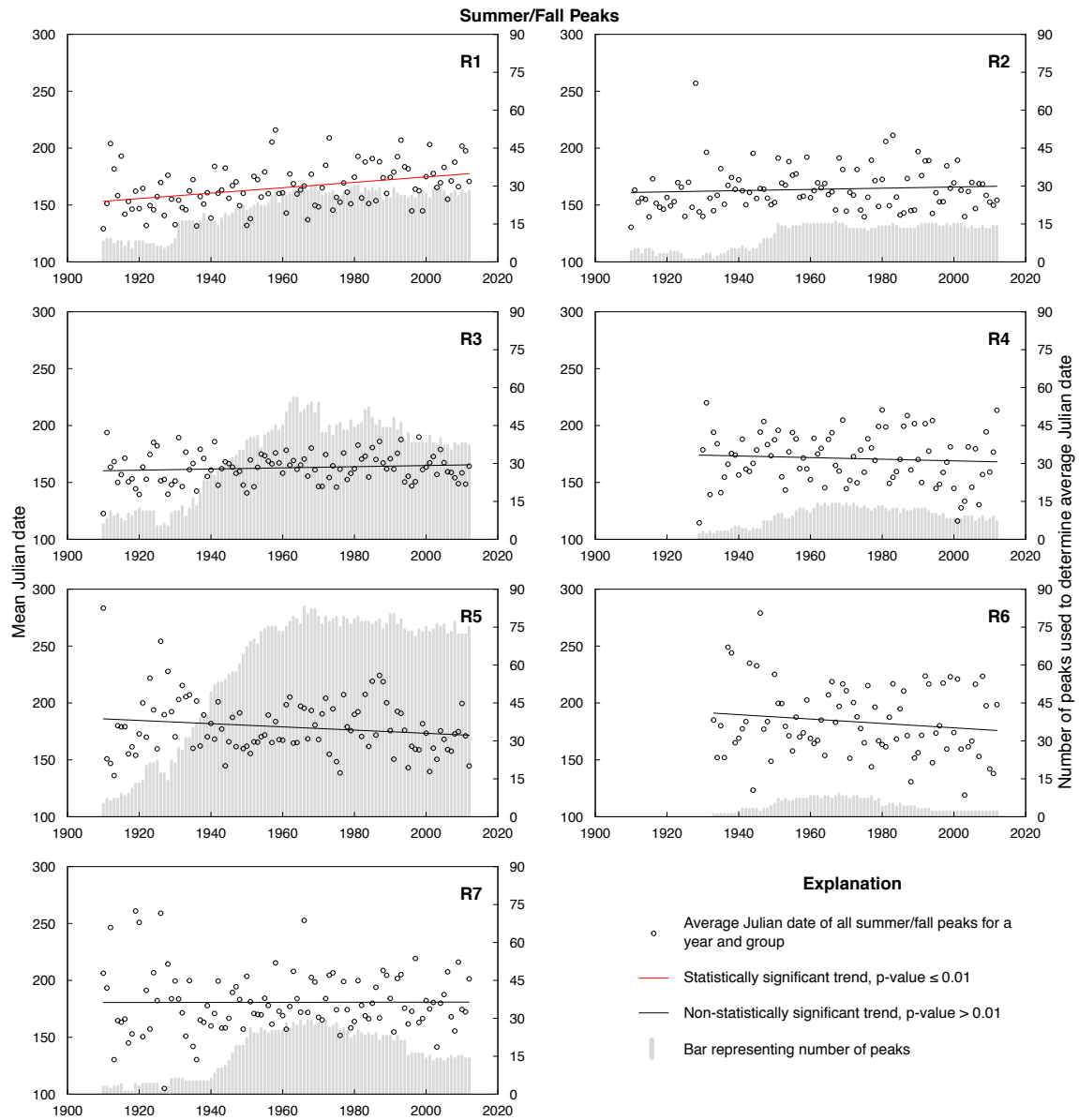


Figure 4.4. Trends in Julian date by region for summer/fall peaks (R1-R7, regions 1-7 in figure 4.1).

#### 4.5. Discussion and Conclusions

Researchers have linked a shift in the timing of runoff in “snowmelt-fed rivers” to a warming global climate (Bates et al., 2008). U.S. average temperature has increased across the country (by 1.3-1.9°F; Walsh et al., 2014) and trends toward earlier snowmelt runoff have been observed in New England, New York, and eastern North America (Hodgkins et al., 2003; Burns et al., 2007; Hodgkins and Dudley, 2006), California and the western U.S. (Dettinger and Cayan, 1995; Cayan et al., 2001; Dettinger, 2005; Stewart et al., 2005; McCabe and Clark, 2005; Regonda et al., 2005), and Canada (Burn et al., 2008; Zhang et al., 2001). At the same time, numerous studies have reported increases in precipitation in all seasons (Karl and Knight, 1998; Wang et al., 2009), with the largest trends observed in fall (Small and Islam, 2008; Small and Islam, 2009; Wang et al., 2009). Consequently, at some locations, fall streamflow has been increasing. Increases in fall precipitation may or may not be represented in annual peak streamflow, especially in snowmelt-dominated areas where the typical peak still occurs in the spring. However, there is the possibility that a trend toward earlier snowmelt, or earlier spring, may be confounded by a concurrent increase in the occurrence of annual peaks in the summer or fall.

This study divided the peaks into two regimes, spring/snowmelt peaks and summer/fall peaks (fig. 4.2). This was done to examine whether, given a warming climate and changes in precipitation, the probability of experiencing summer/fall peaks in snowmelt regions has increased with time.

When controlling for hydrologic droughts and wet periods, using the Palmer Hydrologic Drought Index lagged 2 months (PHDI2), and differences in climate and location (based on climate zones and ecological regions), there is a significant time trend. The odds of peaks

occurring in the summer or fall are increasing and this is supported by the previously documented increases in summer and fall precipitation in the central U.S. (Garbrecht and Rossel, 2002; Small and Islam, 2009; Wang et al., 2009).

The use of the PHDI2 is consistent with the results of Ryberg et al. (2014), who found, in a similar study area that did not include the semi-arid regions of this study, that “Periods of highest flood risk and the magnitude of large floods are consistent with seasonal changes in precipitation combined with multi-year moisture-surplus conditions that become more important in the northern and western basins.” The PHDI is a measure of long-term cumulative hydrological drought and wet conditions, which reflect groundwater conditions, reservoir levels, and other long-term hydrologic conditions (Heim, 2002), and should capture the multi-year moisture-surplus (moisture-deficit) conditions that contributed to flood (drought) risk. This is also consistent with Booy and Lye (1986) who found that accumulated basin storage before spring runoff is reflected in peak streamflow. The coefficient for PHDI2 was negative, indicating that when PHDI2 is positive (long-term wet conditions two months earlier than the peak, such as a wet fall or winter snow accumulation) the odds of the peak of the year occurring in the summer or fall decrease (moisture storage favors snowmelt/spring peaks).

When examining the snowmelt/spring peak series for changes in the timing of the peak at long-term streamgages, evidence was found for a general change to earlier peaks in the northern regions of the study area (regions 1, 2, and 3). Wang et al. (2009) showed the likely cause for this as they found that the strongest U.S. surface air temperature warming in 1950-2000 occurred in the spring over the northwestern U.S. and the northern plains. For summer/fall peaks there was little evidence for changes in timing beyond region 1.

This study also highlights the great deal of natural variability in the north central U.S. Over just three North American Level II ecological regions, the distribution of the date of peaks varies greatly (fig. 4.2). The distance between Fargo, North Dakota (region 1) and Hastings, Nebraska (region 7), is only about 710 kilometers (441 miles), yet the probability of peak streamflow occurring in the summer or fall is much larger in region 7, whereas region 1 is more sensitive to changes that influence the timing of snowmelt/spring peaks.

These changes provide new opportunities and risks for water managers and water users. In some cases, peak streamflow in summer and fall may be captured in reservoirs and help to extend irrigation or recreation seasons. However, changes have implications for the operation of flood-control dams. If a reservoir is normally drawn down in the fall to create storage for spring runoff, an increase in summer or fall peak streamflow may necessitate a change in the rules of operation. Lead time for flooding is also dramatically different between floods in the two seasons. Floods generated by snowmelt usually have generous lead time for forecasting and flood-fighting operations. Floods generated by intense summer or fall precipitation do not have that kind of lead time. Understanding the nature of these changes is important to efficient water use and protection from the extremes of floods and droughts.

**CHAPTER 5. TREE-RING BASED ESTIMATES OF LONG-TERM SEASONAL  
PRECIPITATION IN THE SOURIS RIVER REGION OF SASKATCHEWAN, NORTH  
DAKOTA, AND MANITOBA**

Historically unprecedented flooding occurred in the Souris River Basin of Saskatchewan, North Dakota, and Manitoba, in 2011, during a longer-term period of wet conditions in the basin. The severe flooding, and concerns about future floods and droughts, prompted the International Souris River Board (ISRB) to create a Souris River Flood Task Force, which prepared a plan of study for evaluating water-resource control measures to manage future challenges posed by floods and droughts. In order to develop a model of future flows, there is a need to evaluate effects of past multi-decadal climate variability and/or possible climate change on precipitation. In this study, tree-ring chronologies and historical precipitation data in a four-degree buffer around the Souris River Basin were analyzed to develop regression models that can be used for predicting long-term variations of precipitation. To focus on longer-term variability, 12-year moving average precipitation was modeled in five subregions (determined through cluster analysis of measures of precipitation) of the study area over three seasons (November-February, March-June, and July-October). The models used multiresolution decomposition (an additive decomposition based on powers of two using a discrete wavelet transform) of tree-ring chronologies from Canada and the U.S. and seasonal 12-year moving average precipitation based on Adjusted and Homogenized Canadian Climate Data and U.S. Historical Climatology Network data. Results for 1700–1990 show that precipitation varies on long-term (multi-decadal) time scales of 16, 32, and 64 years. Past extended pluvial and drought events, which can vary greatly with season and subregion, were highlighted by the models. Results suggest that the recent wet period may be a part of natural variability on a very long time scale.

## 5.1. Introduction

Historically unprecedented flooding occurred in the Souris River Basin of Saskatchewan, North Dakota, and Manitoba, in 2011, and caused extensive damage to Minot, North Dakota, and numerous smaller communities in Saskatchewan, North Dakota, and Manitoba. Near-record snowfall occurred over parts of the region and “record-setting rains” occurred in May and June (Service Assessment Team, 2012). In addition, the stage had been set for a very large flood by wet antecedent conditions. There was an “anomalously wet fall season” (Service Assessment Team, 2012) that continued a period of more than a decade of wet conditions, which filled available soil moisture storage, shallow groundwater aquifers, wetlands, and lakes. Observations from the Gravity Recovery and Climate Experiment (GRACE) satellites show that from 2003-12, parts of the basin experienced a freshwater storage rate of change of an additional 3 centimeters per year (NASA Earth Observatory, 2013). The severe flooding prompted the ISRB to create a Souris River Flood Task Force, which prepared a plan of study for evaluating potential reservoir operation changes and flood control measures to manage future floods and droughts (International Souris River Board, 2013). The task force plan indicated a need to evaluate the effects of multi-decadal climate variability on future flood and drought risk.

The purpose of this work is to evaluate available records from meteorological stations and tree-ring climate proxy data to determine if climate in the Souris River Basin is subject to multi-decadal to century-scale changes. This work helps provide a scientific basis for evaluating uncertainty in future climate for the Souris River Basin and helps in developing a stochastic model for simulating future streamflows that are consistent with climatic uncertainty, cover the full range of possibilities from drought to pluvial periods, and provide estimates of future risk.

### **5.1.1. Definition of Study Area**

To understand regional long-term precipitation, the study area extends beyond the Souris River Basin boundary and includes parts of other Basins in the region, such as the Missouri River, Red River of the North (Red River), Qu'Appelle River, Assiniboine River, and Saskatchewan River. The Souris River Basin boundary was provided as a GIS shapefile by Tara Gross (U.S. Geological Survey, written communication, July 11, 2014). The potential meteorological sites and the tree-ring sites were placed on the map, and then an iterative process was used to determine a regional study boundary. The final study area was a four-degree buffer around the Souris River Basin (fig. 5.1). This places the southwestern boundary just north of the Black Hills of South Dakota and Wyoming - mountainous areas. The western boundary also results in the selection of meteorological stations west of the Cypress Hills region of Saskatchewan, an area in the Northwest Forested Mountains ecological region (Commission for Environmental Cooperation, 1997). Finally, the four-degree boundary extends east into Minnesota, but excludes the forested Lake Superior region of Minnesota. The four-degree boundary provides maximal climate data and a larger set of potential tree-ring datasets in a fairly homogenous plains and prairies setting. The boundary, meteorological stations, and potential tree-ring sites are shown in figure 5.1.

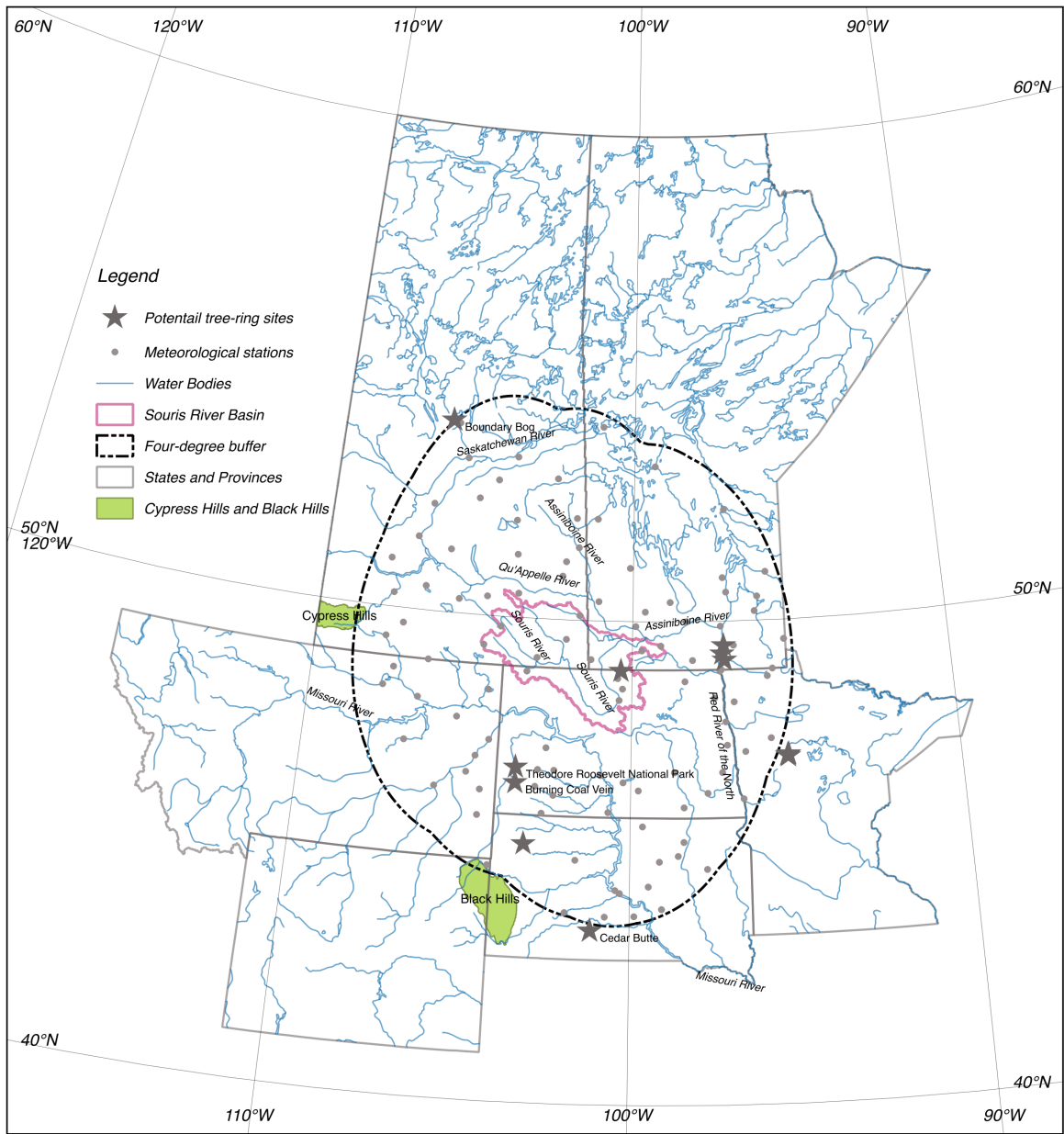


Figure 5.1. Locations of the Souris River Basin, study area boundary (four-degree buffer around Souris River Basin), meteorological stations, and potential tree-ring sites. The tree-ring sites ultimately used are labeled with the site name.

## 5.2. Data and Methodology

Monthly precipitation (Mekis and Vincent, 2011), average temperature, maximum temperature, and minimum temperature (Vincent et al., 2012) data were downloaded from the

Adjusted and Homogenized Canadian Climate Data (AHCCD) web site on July 9, 2014, from links at <https://ec.gc.ca/dccha-ahccd/default.asp?lang=En&n=B1F8423A-1> (Environment Canada, 2014). The AHCCD web site stated, "These data were created for use in climate research including climate change studies. They incorporate a number of adjustments applied to the original station data to address shifts due to changes in instruments and in observing procedures. Sometimes the observations from several stations were joined to generate a long time series" (Environment Canada, 2014).

Monthly precipitation, average temperature, maximum temperature, and minimum temperature were downloaded from the U.S. Historical Climatology Network (USHCN) on May 21, 2014, from the ftp site [http://cdiac.ornl.gov/ftp/ushcn\\_v2.5\\_monthly/](http://cdiac.ornl.gov/ftp/ushcn_v2.5_monthly/) (Menne et al., 2014). The USHCN web site provides further information about the data, "The United States Historical Climatology Network (USHCN) is a high-quality dataset of daily and monthly records of basic meteorological variables... The USHCN has been developed over the years at the National Oceanic and Atmospheric Administration's (NOAA) National Climatic Data Center (NCDC) to assist in the detection of regional climate change. Furthermore, it has been widely used in analyzing U.S. climate [sic]. The period of record varies for each station. USHCN stations were chosen using a number of criteria including length of record, percent of missing data, number of station moves and other station changes that may affect data homogeneity, and resulting network spatial coverage" (Carbon Dioxide Information Analysis Center, 2014).

Data for each of the AHCCD and USHCN meteorological stations were summarized as seasonal total precipitation and seasonal average maximum, minimum, and mean temperature. The three four-month seasons are November-February (season 1, winter, a period where much of the precipitation is stored in the basin in frozen soils or snowpack), March-June (season 2,

spring, generally the period when peak streamflow occurs, U.S. Geological Survey, 2014b), and July-October (season 3, summer/fall).

Tree-ring data were downloaded from The International Tree-Ring Data Bank (ITRDB) web site <http://www.ncdc.noaa.gov/data-access/paleoclimatology-data/datasets/tree-ring> (National Oceanic and Atmospheric Administration National Climate Data Center, 2014) on July 16, 2014. Tree-rings sites within and near the study boundary were considered for inclusion in the analysis (fig 5.1).

### **5.2.1. Hierarchical Agglomerative Cluster Analysis**

In order to group the meteorological stations into climatically similar subregions, a form of cluster analysis called hierarchical agglomerative cluster analysis (HACA) was used. In HACA, each observation (as described by the all the variables associated with it, in this case the meteorological variables association with a meteorological station) forms its own cluster, and then pairs of clusters are successively merged based on a similarity measurement and a linkage method. There are  $N-1$  (where  $N$  is the total number of observations) merges in which the closest two clusters are merged into a single cluster, resulting in one less cluster at that merge. In this analysis, the similarity was computed by the Euclidean distance between observations. The HACA routine is performed by the function *agnes* in the cluster package (Maechler et al., 2014) of R (R Core Team, 2014). The linkage method used to merge clusters was Ward's method, which uses an analysis of variance (ANOVA) approach to evaluate differences between clusters (Güler et al., 2002). The two clusters that are merged are the pair “that leads to the smallest increase in the sum of the within-group sums of squares” (Insightful Corporation, 2001). The within-group sum of squares is the sum of the squared Euclidean distances between observations at the center of its parent group.

The dendrogram reports the agglomerative coefficient (AC). The AC is a dimensionless quality index for measuring the clustering structure of the dataset and is between 0 and 1. An AC close to 1 indicates that there is a “very clear clustering structure” in the data; however, the structure needs to be analyzed to determine that it is reasonable (Kaufman and Rousseeuw, 1990).

The potential clustering variables were chosen to represent long-term differences between sites, not year-to-year differences, and included mean and median seasonal temperature, mean and median seasonal total precipitation. The sites have varying periods of record and varying start and end dates. Therefore, the cluster variables were based on data from the period 1900-2010 for sites with at least 60 years of seasonal values (some Canadian sites were operated seasonally for parts of their record and can have values for fewer than 3 seasons in some years).

### **5.2.2. Tree-Ring Analysis**

Numerous tree-ring datasets were available for use and potential datasets were initially selected based on maximizing the series end date and minimizing the series start date to be able to develop precipitation regression models on a time scale of hundreds of years. The ring-width series (the series of growth measurements from individual trees at a particular site) from potential datasets in the ITRDB were read in, plotted, detrended, and mean-value chronologies (the site-level time series) were built using the Dendrochronology Program Library in R (dplR)—a package for dendrochronologists to handle data processing and analysis (Bunn 2008; Bunn 2010; Bunn et al., 2014) for the software R (R Core Team, 2014).

The detrending process removes low-frequency variability that is caused by biological (such as differing growth rates as the tree ages) or tree-stand effects. The detrending method used was that of fitting a negative exponential curve to each series. This is "probably the most

common method for detrending" (Bunn et al., 2014) and can recover annual, decadal, to multi-centennial signals in tree-ring chronologies (Bunn et al., 2004). The model is,  $RW(t) = \gamma e^{-\delta(t)} + k$ , where  $RW(t)$  is the ring-width growth at time  $t$ ,  $\gamma$  is the initial year, the exponent  $-\delta$  is the slope of the decrease in growth of the ring-widths at time  $t$ , and  $k$  is the growth per year after the initial growth spurt (Bunn et al., 2004). Building a mean-value chronology is a process of averaging across the detrended ring-width series at each site (Bunn, 2008; Bunn, 2010; Bunn et al., 2014).

It readily became apparent that some of the tree-ring chronologies looked good from the standpoint of a long period of record; however, some were based on tree-ring series with less overlap than others, creating small sample sizes for parts of the record. Therefore, the common interval for each set of tree-ring width series was examined. There are three ways to do this: 1) find the common interval that maximizes the number of series, 2) find the common interval that maximizes the number of years, or 3) find the common interval that is the best compromise between the two (Bunn et al., 2014). The compromise option was used to identify those series with a common interval of less than 50 years, which were dropped from further consideration.

Correlation of segments within potential datasets was examined using the *corr.rwl.seg* function in the *dplR* package (Bunn et al., 2014). This function calculates "correlation serially between each tree-ring series and a master chronology built from all the other series" in the raw ring-width series. "Correlations are done for each segment of the series where segments are lagged by half the segment length" (Bunn et al., 2014), with the segment length used being the default 50 years. "Correlations are calculated for the first segment, then the second segment and so on. Correlations are only calculated for segments with complete overlap with the master chronology" (Bunn et al., 2014). This analysis highlighted some low correlations and led to an

examination of the comments in the associated correlation statistics files in the ITRDB, where available. The result of this investigation was the removal of segments from one tree-ring width series (Burning Coal Vein), as suggested by the comments (Meko and Sieg, 2014a), and then detrending the revised series.

A measure of reliability of the tree-ring signal is the express population signal (EPS) or subsample signal strength (SSS; EPS calculated over subsamples of the tree-ring period of record). These were defined by Wigley et al. (1984) and are available in dplR (Bunn et al., 2014). For the remaining possible tree-ring chronologies, EPS over 30-year moving windows that overlap by 15 years (Büntgen et al., 2014), the number of cores for each window, number of trees, and the signal to noise ratio (SNR) were examined. Examination of the EPS, SSS, and SNR highlighted the shortcomings of some of the series in that their period of record seemed promising from a total number of years standpoint, but only had one core at the beginning of the record or periods within the record of low SSS or SNR. The sites considered good candidates for modeling precipitation based on SSS being above 0.85 were:

- Boundary Bog – Tamarack (*Larix laricina*; MacDonald and Case, 2014),
- Burning Coal Vein - Ponderosa Pine (*Pinus ponderosa* Douglas ex C. Lawson; Meko and Sieg, 2014a),
- Theodore Roosevelt National Park - Rocky Mountain Juniper (*Juniperus scopulorum* Sarg.; Meko and Sieg, 2014b), and
- Cedar Butte - Ponderosa Pine (*Pinus ponderosa* Douglas ex C. Lawson; Meko and Sieg, 2014c).

These sites are labeled in figure 5.1. SSS was also used to define truncation dates for reconstruction. The final period for reconstruction was determined to be 1700 to 1990.

This resulting set of tree-ring chronologies is considered good because three different tree species that may respond to precipitation and temperature differently (Wettstein et al., 2011) are represented and each tree species may contribute differing explanatory information to the models. The study area is represented well by the inclusion of Boundary Bog at the northern edge of the study area, Cedar Butte at the southern edge, and the sites Theodore Roosevelt National Park and Burning Coal Vein closer to the center of the study area.

### **5.2.3. Modeling Precipitation**

A number of studies have identified a decadal-scale (greater than 7 years) signal in precipitation (Cayan et al., 1998; Garbrecht and Rossel, 2002; Small and Islam, 2008; Small and Islam, 2009; Ault and St. George, 2010). Small and Islam (2008; 2009) identified a statistically significant signal in autumn precipitation in the central U.S. with a periodicity of approximately 12 years, with the signal strongest in the Midwest and Great Plains. Ryberg et al. (2014) focused on long-term (multi-decadal) variability and thus shorter-term, quasi-periodic signals were treated as “nuisance” variability and smoothed out by using a 12-year moving average when analyzing precipitation, potential evapotranspiration, and runoff. Therefore, in this study 12-year moving average precipitation was modeled using the tree-ring chronologies.

Annual tree-ring chronologies (commonly used to model annual or seasonal precipitation) may not adequately represent 12-year average precipitation. Therefore, variables representing the multiresolution decomposition of the tree-ring chronologies were used. In multiresolution analysis of a time series, specific frequency components are extracted from a time series (Bunn et al., 2014). The example plot (fig. 5.2) shows a one-dimensional multiresolution analysis using a level  $J$  additive decomposition of the time series using the pyramid algorithm (Mallat, 1989) as implemented in the `dplr` package (Bunn et al., 2014). This

is an application of wavelet analysis and the additive decomposition is for each power of two in the period of record, where the number of powers is  $\text{trunc}(\log(nYrs)/\log(2))-1$ , where  $nYrs$  is the number of years in the tree-ring chronology. The R package `waveslim` (Whitcher, 2013) was used to do the multiresolution decomposition. Each frequency component is scaled for plotting by dividing by the standard deviation. Supplemental figures in Appendix A show the multiresolution decomposition for the three other tree-ring chronologies.

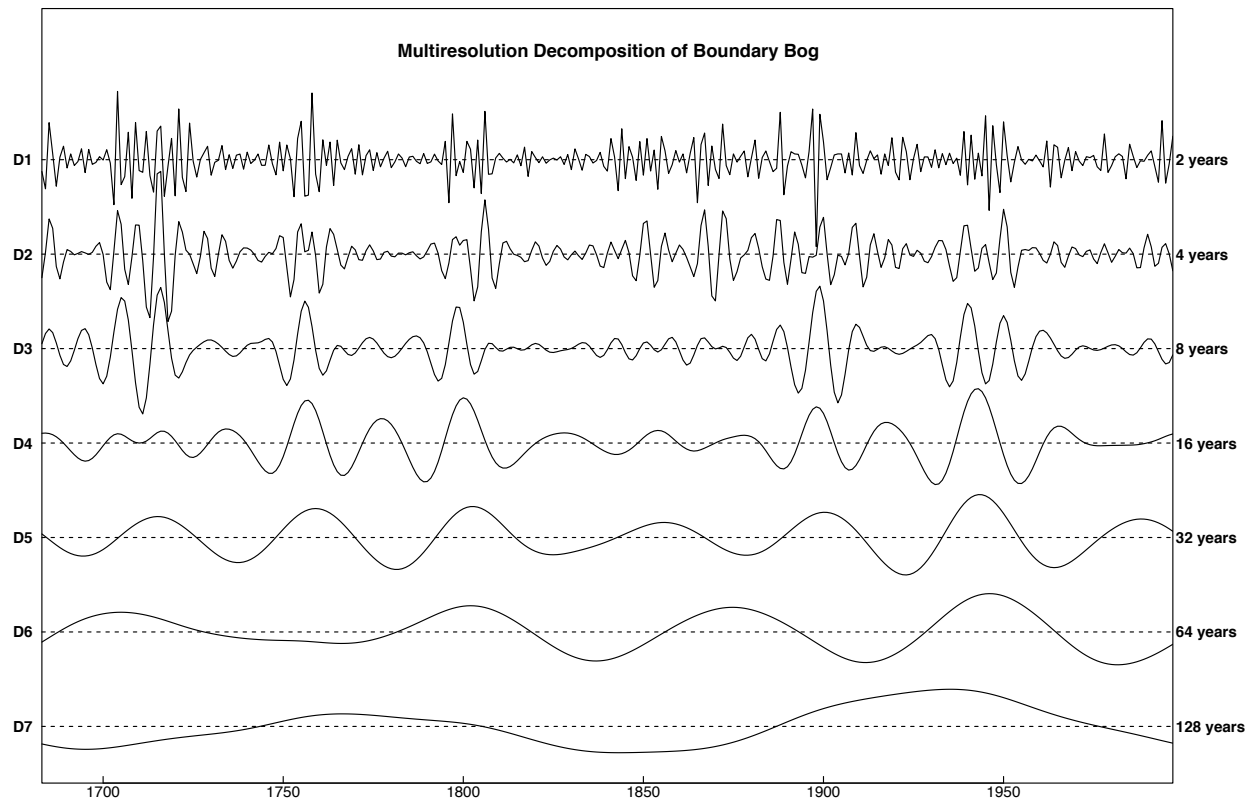


Figure 5.2. Example multiresolution decomposition of tree-ring chronology at Boundary Bog, Saskatchewan, Canada.

In figure 5.2, the line labeled D1 on the left and 2 years on the right represents the short-term variability over a 2-year time scale. D7 represents the variability over a 128-year time scale. This is an additive decomposition, so adding D1 through D7, plus a shift (not shown) produces the original tree-ring chronologies. The interest here is in the longer-term variability, beyond 12

years, therefore, the D1, D2, and D3 wavelet voices were not considered, leaving the D4, D5, D6, and D7 wavelet voices as potential explanatory variables.

To further examine the frequency bands expressed in the tree ring chronologies, a continuous wavelet analysis was done using a continuous Morlet wavelet transform (Bunn et al., 2014; Torrence and Compo, 1998). Figures B.5-B.8 in Appendix B depict continuous wavelet analysis and the colored portion of each figure shows a measure of wavelet power relative to white noise. Each continuous wavelet figure shows that the four sites have power in the 16, 32, 64, and 128-year time bands for at least part of the period of record. However, all or almost all of the 128-year time bands are within a cone of influence that occurs at the beginning and end of the time series, where edge effects are an issue. This indicates that the lengths of the tree-ring chronologies used are not long enough to have a reliable 128-year wavelet voice. Therefore, to model precipitation the D4 (16 years), D5 (32 years), and D6 (64 years) wavelet voices were used as potential explanatory variables.

#### ***5.2.3.1. Model Selection***

All subsets regression (Lumley, 2009) was used to examine potential 12-year moving average precipitation models using the D4, D5, and D6 subset of the wavelet voices of the four chronologies. All subsets regression performs an exhaustive search for the best subsets of the potential explanatory variables for predicting the response with a multiple regression model. The procedure examines all models with one explanatory variable and picks the best fit (or more than one depending on how many the user chooses to save), then examines all models with 2 explanatory variables and so on, up to the total number of possible explanatory variables or an upper limit set by the user. It was assumed that all wavelet voices of the four chronologies were potentially correlated with the seasonal precipitation in the five groups. The all subsets

regression modeling process dropped out the wavelet voices not correlated with a particular group and season.

All subsets regression provides measures of model quality: adjusted coefficient of multiple determination ( $R_a^2$ ), Schwartz's information criterion ( $BIC$ ), and Mallows's  $C_p$ .  $R_a^2$  allows for the comparison of models that have differing numbers of explanatory variables by penalizing models that have additional coefficients (Helsel and Hirsch 1995). The closer  $R_a^2$  is to 1 the better the model is considered, but this does not guarantee the model has good predictive capabilities.  $BIC$  takes into account goodness of fit of the model and applies a penalty for increasing the number of parameters in a model. It approximates the Bayes factor, which is a "summary of the evidence provided by the data in favor of one scientific theory, represented by a statistical model, as opposed to another" (Kass and Raftery, 1995). In model selection using  $BIC$ , the goal is to minimize  $BIC$ , while making a tradeoff between model fit and number of parameters in the model. The  $C_p$  criterion is a measure of the total mean squared error and an indicator of model bias (Neter et al., 1996). In comparing models, the models with the lowest  $C_p$  values are considered those with the least bias.

Given the large number of potential explanatory variables and results of exploratory analysis, the following additional steps were taken to refine the model selection process.

- Limit models to fewer potential explanatory variables (this favors using the  $BIC$  as selection criterion over  $R_a^2$  because  $BIC$  penalizes additional explanatory variables more than  $R_a^2$ , although  $R_a^2$  is still useful as a report of model quality).
- Some edge effects appeared at the ends of the precipitation predictions (because of greater uncertainty at the ends of the precipitation and tree-ring data), so the

precipitation data used to build the model were limited to a start date between 1888 and 1899, depending on the group, and ending in 1990.

- Precipitation predictions were done only for the period 1700-1990; this removed some of the edge effects attributed to the tree-ring chronologies where there were fewer cores in the early parts of their record.
- The seasonal 12-year running means were correlated with each other; therefore, to reduce correlation and leave out some data to test the models, the data used to select the precipitation models were thinned to every fourth year.
- The Durbin-Watson test was performed to examine autocorrelation of the residuals. In the Durbin-Watson test (Durbin and Watson 1950, 1951, and 1971; Zeileis and Hothorn, 2002), the null hypothesis is that the autocorrelation of the residuals is zero and it is tested against the alternative hypothesis that the residuals are autocorrelated. A statistically significant result is undesirable and indicates that the residuals are autocorrelated.
- The Breusch-Pagan test was performed to examine the variance of the residuals. In the Breusch-Pagan test (Breusch and Pagan, 1979; Zeileis and Hothorn, 2002), the null hypothesis is that the residuals are independent, normally distributed, with a constant variance. The alternative is that the variance is not constant. A statistically significant result is undesirable and indicates that the residuals are heteroskedastic, violating one of the underlying assumptions of regression (Neter et al., 1996).

In addition to the quantitative measures, a literature review was done of historical accounts of weather in the study area and of past tree-ring, precipitation, and streamflow studies that indicated periods of wet and dry conditions prior to 1900 (Brooks et al., 2003; Carlyle, 1984;

Case and MacDonald, 2003; Lapp et al., 2013; Rannie, 1998; Red River Basin Board, 2000; Sauchyn and Beaudoin, 1998; Severson and Sieg, 2006; St. George and Nielsen, 2002; St. George and Nielsen, 2003; St. George and Rannie, 2003; Thorleifson et al., 1998). Severson and Sieg (2006) and Brooks et al. (2003) summarized the work of a number of other studies. In both the U.S. and Canada, the eastern side of the study area is more information rich based largely on the work of Rannie (1998), who focused on the Red River Basin, and Severson and Sieg (2006), who focused on eastern North Dakota. When hindcasting precipitation outside the period of instrumental observation, models were examined in light of these past studies, keeping in mind that wet and dry periods would vary with respect to season, duration, and spatial extent.

### **5.3. Results of Cluster Analysis**

There was very little difference in clustering based on mean and median values and clusters were well defined using precipitation only. Using the mean resulted in more geographically cohesive cluster groups. Therefore, the variable subset chosen for effectiveness and parsimony was mean season 1 total precipitation, mean season 2 total precipitation, and mean season 3 total precipitation at each site with a minimum of 60 observations in each season over its period of record from 1900-2010.

The dendrogram (a complete graphical description of the hierarchical clustering) for the final cluster analysis is shown in figure 5.3. In the dendrogram, the vertical lines at the bottom (arranged so that branches of the dendrogram do not cross) represent the individual meteorological stations. Horizontal lines connecting clusters represent the merges of similar clusters. The y-axis represents the distance (in three-dimensional space defined by mean season 1 total precipitation, mean season 2 total precipitation, and mean season 3 total precipitation) between the two clusters being merged. The higher on the y-axis that merges occur, the more

distant the clusters are from each other in terms of mean seasonal precipitation. The AC of the HACA in this study was high, 0.97, indicating distinct clustering structure.

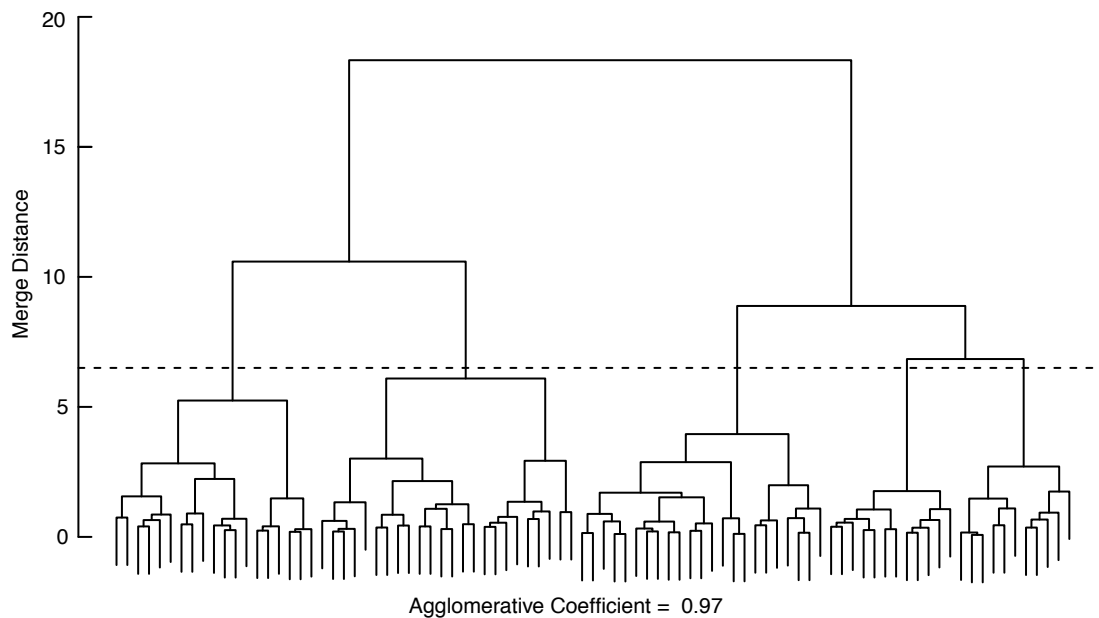


Figure 5.3. Dendrogram for cluster analysis with horizontal line indicating five groups of meteorological stations.

Determination of the number of cluster groups is subjective in that the analyst determines the number of groups by balancing interest in interpretable groups and avoidance of needless splitting of the data. The number of groups is determined by drawing a line across the dendrogram and examining the main clusters branching out beneath that line. Depictions of three, four, and five groups were plotted on maps and examined for reasonable climate similarity with each group having numerous meteorological stations (with the intent of having no micro clusters). By means of a dashed horizontal line, figure 5.3 shows the data divided into five groups. The five branches below the dashed line represent the major cluster groups. They are major cluster groups because the linkage distance at which they combine with each other is relatively large, indicating that there are relatively large Euclidean distances between the sites in

groups 1, 2, 3, 4, and 5. The clustering with five groups represented well the north-south gradient in winter precipitation and the east-west gradient in precipitation across the study area as shown in the boxplots of seasonal mean precipitation for each group (fig. 5.4).

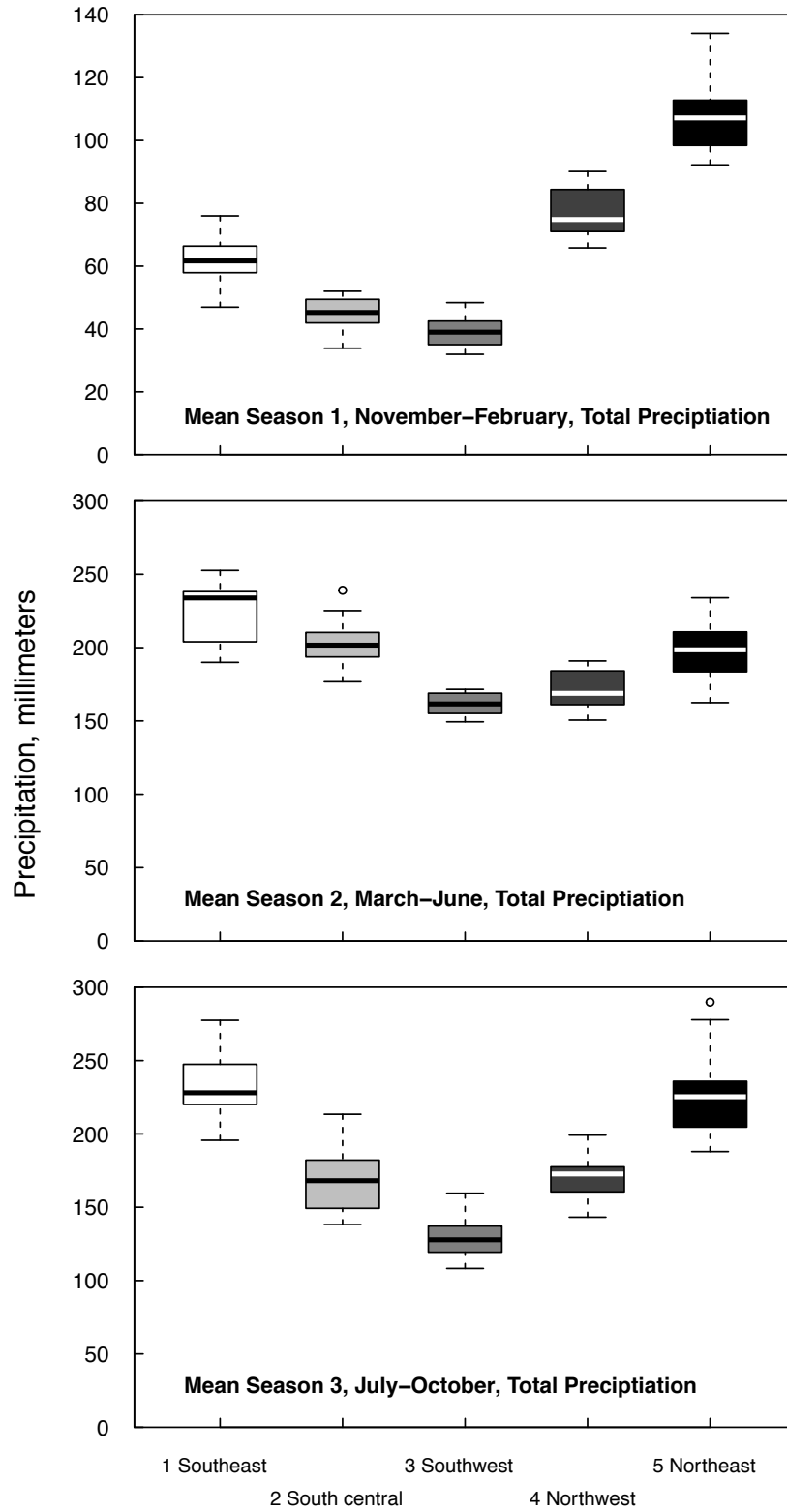


Figure 5.4. Boxplots of mean seasonal total precipitation for each group of meteorological stations.

The sites were mapped in GIS with their cluster group assignments, 1) southeast, 2) south central, 3) southwest, 4) northwest, and 5) northeast. Voronoi polygons (Voronoi, 1908) were drawn around each site used in the cluster analysis (Voronoi polygons are drawn so that every location within a polygon is closer to the meteorological station in that polygon than to any other meteorological station). Then, the polygons were extended as necessary to cover the entire study area and clipped to the study boundary. Each polygon was assigned to the cluster group of the meteorological station around which it was drawn. The numerous polygons were then dissolved in GIS so there were polygons for the meteorological stations in each group. Those sites with shorter periods of record were assigned to the cluster group in which they fell; figure 5.5 shows the final five clusters. Part of cluster 4 occurs within cluster 5. A higher density of meteorological stations in this area might result in a continuous cluster for cluster 4; however, the analysis indicated that the outlier station belonged in cluster 4 and it was subsequently grouped with the rest of cluster 4.

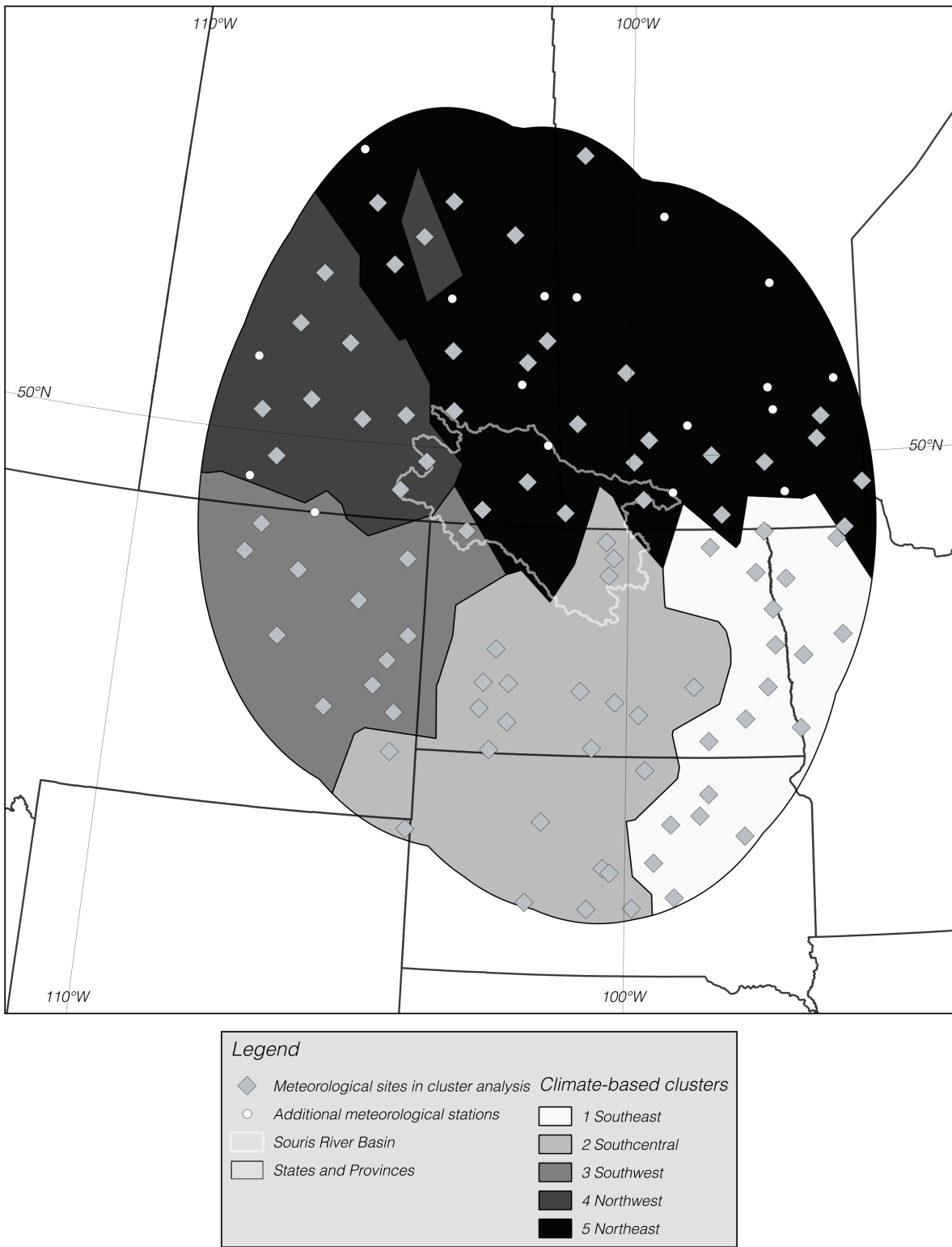


Figure 5.5. The five clusters of meteorological stations in the study area.

The nonparametric Kruskal-Wallis rank sum test (Higgins, 2004) was used to test whether all groups have the same mean annual precipitation distribution function or at least one of the groups has a different location parameter. For season 1, the Kruskal-Wallis test was statistically significant at the 0.01 significance level, which means at least one of the groups has a mean significantly different from the other means. The test was repeated for season 2 and season 3 precipitation and the results were statistically significant. Boxplots (fig. 5.4) visually confirm the differences.

#### **5.4. Results of Precipitation Modeling**

The equations for reconstructing the seasonal 12-year moving average precipitation for each season and cluster group are shown below where  $G_i$  represents the  $i$ th group and  $S_j$  represents the  $j$ th season; BB, Boundary Bog tree-ring chronology; TRNP, Theodore Roosevelt National Park tree-ring chronology; BCV, Burning Coal Vein tree-ring chronology; CB, Cedar Butte tree-ring chronology; D4, represents the 16-year wavelet voice in the associated tree-ring chronology; D5, 32-year wavelet voice; and D6, 64-year wavelet voice.

Model information and quality criteria are shown in table 5.1. The models generally show high coefficient of multiple determination indicating that they explain most of the variability in the 12-year moving average seasonal precipitation. Quality of the models varies with group and season, with better results in the more eastern groups and more difficulty modeling the drier, western areas. Group 3 in particular, the southwestern part of the study area, had low coefficients of multiple determination in seasons 2 and 3. In these seasons the residuals failed the test for serial correlation in the residuals (Durbin-Watson test), as did group 4, season 1. These results can indicate the need for additional explanatory variables, but adding variables did not improve

the models (not shown). Group 3, season 2, also failed the Breusch-Pagan test for constant variance.

$$G1S1 = 61.5 + 26.9(BB.D6) - 36.5(TRNP.D5) + 21.4(BCV.D6) - 8.3(CB.D4) + 28.2(CB.D5) \quad (\text{Eq. 5.1})$$

$$G1S2 = 219.5 + 19.0(BB.D5) - 366.2(TRNP.D6) + 51.4(CB.D4) + 377.0(CB.D6) \quad (\text{Eq. 5.2})$$

$$G1S3 =$$

$$223.5 - 19.7(BB.D4) + 15.5(BB.D5) - 108.3(BB.D6) + 258.6(TRNP.D5) - 204.3(BCV.D5) - 46.0(BCV.D6) + 37.2(CB.D4) + 64.8(CB.D5) \quad (\text{Eq. 5.3})$$

$$G2S1 = 45 + 32.1(BB.D6) - 6.3(TRNP.D4) - 15.7(TRNP.D5) - 93.9(TRNP.D6) + 27.9(BCV.D6) + 9.4(CB.D5) \quad (\text{Eq. 5.4})$$

$$G2S2 = 201.2 + 15.2(BB.D5) - 281.4(TRNP.D6) - 92.6(BCV.D6) + 38.2(CB.D4) + 333.2(CB.D6) \quad (\text{Eq. 5.5})$$

$$G2S3 = 159.8 - 19.2(BB.D4) + 19.2(BB.D5) - 34.9(BB.D6) + 112.5(TRNP.D6) + 95.6(CB.D5) \quad (\text{Eq. 5.6})$$

$$G3S1 = 43.2 + 3.2(BB.D4) + 15.1(BB.D6) - 257.41(TRNP.D6) - 28.3(BCV.D5) + 28.1(BCV.D6) + 37.8(CB.D6) \quad (\text{Eq. 5.7})$$

$$G3S2 = 161.4 + 17.4(BB.D5) - 346.3(TRNP.D6) - 293.7(CB.D6) \quad (\text{Eq. 5.8})$$

$$G3S3 = 121.9 + 13.7(BB.D5) + 105.4(CB.D5) \quad (\text{Eq. 5.9})$$

$$G4S1 = 78.3 - 12.2(BCV.D4) - 67.7(BCV.D6) \quad (\text{Eq. 5.10})$$

$$G4S2 = 167.2 - 14.9(BB.D4) + 92.9(BCV.D5) + 40.6(BCV.D6) - 30.5(CB.D5) \quad (\text{Eq. 5.11})$$

$$G4S3 = 168.0 - 117.9(BB.D6) + 232.1(TRNP.D5) - 298.1(BCV.D5) + 58.1(BCV.D6) \quad (\text{Eq. 5.12})$$

$$G5S1 = 105.1 + 9.3(BB.D5) - 9.3(BB.D6) + 33.6(TRNP.D5) - 8.2(BCV.D4) - 79.0(BCV.D6) + 28.3(CB.D5) + 139.4(CB.D6) \quad (\text{Eq. 5.13})$$

$$G5S2 = 198.1 - 24.7(BB.D4) + 78.0(TRNP.D5) - 216.7(TRNP.D6) - 30.8(BCV.D6) - 45.3(CB.D5) \quad (\text{Eq. 5.14})$$

$$G5S3 = 218.1 - 17.4(BB.D4) + 16.3(BB.D5) - 94.0(BB.D6) + 263.5(TRNP.D6) - 99.2(BCV.D6) + 48.6(CB.D5) \quad (\text{Eq. 5.15})$$

Table 5.1. Information and associated statistics for precipitation models.

Group	Season	Predictor variables	Calibration period, every fourth year in interval	$R^2$	$R^2_a$	Durbin-Watson test $p$ -value	Breusch-Pagan test $p$ -value
1	1	BB.D6, TRNP.D5, BCV.D6, CB.D4, CB.D5	1888-1990	0.78	0.74	0.446	0.267
	2	BB.D5, TRNP.D6, CB.D4, CB.D6	1888-1990	0.66	0.62	0.102	0.107
	3	BB.D4, BB.D5, BB.D6, TRNP.D5, BCV.D5, BCV.D6, CB.D4, CB.D5	1888-1990	0.84	0.78	0.045	0.570
2	1	BB.D6, TRNP.D4, TRNP.D5, TRNP.D6, CB.D5	1888-1990	0.71	0.64	0.765	0.949
	2	BB.D5, TRNP.D6, BCV.D6, CB.D4, CB.D6	1888-1990	0.64	0.58	0.016	0.630
	3	BB.D4, BB.D5, BB.D6, TRNP.D6, CB.D5	1888-1990	0.81	0.77	0.172	0.891
3	1	BB.D4, BB.D6, TRNP.D6, BCV.D5, BCV.D6, CB.D6	1890-1990	0.93	0.92	0.053	0.435
	2	BB.D5, TRNP.D6, CB.D6	1890-1990	0.38	0.32	0.001	0.005
	3	BB.D5, CB.D5	1890-1990	0.48	0.45	<0.001	0.235
4	1	BCV.D4, BCV.D6	1899-1990	0.66	0.63	0.001	0.290
	2	BB.D4, BCV.D5, BCV.D6, CB.D5	1899-1990	0.60	0.54	0.048	0.953
	3	BB.D6, TRNP.D5, BCV.D5, BCV.D6	1899-1990	0.84	0.81	0.014	0.459

Table 5.1. Information and associated statistics for precipitation models (continued).

Group	Season	Predictor variables	Calibration period, every fourth year in interval	$R^2$	$R^2_a$	Durbin-Watson test $p$ -value	Breusch-Pagan test $p$ -value
5	1	BB.D5, BB.D6, TRNP.D5, BCV.D4, BCV.D6, CB.D5, CB.D6	1888-1990	0.91	0.88	0.268	0.203
	2	BB.D4, TRNP.D5, TRNP.D6, BCV.D6, CB.D5	1888-1990	0.74	0.69	0.419	0.401
	3	BB.D5, BB.D6, TRNP.D6, BCV.D6, CB.D5	1888-1990	0.84	0.81	0.651	0.301

As an example, the model (Equation 5.2) for group 1 (southeastern group, mainly the Red River Basin), season 2 (March-June) is shown in figure 5.6. Using this model, modeled precipitation matches well with observed precipitation and corresponds well with known wet and dry periods. The early 1700s (approximately 1703-20) had periods of drought or dry years in the northern Great Plains and central North Dakota (Severson and Sieg, 2006). Lapp et al. (2013) documented 24 sustained droughts over the past 600 years in the northwestern Great Plains and found droughts in 1701-1708 and 1717-1721, which matches well with the severe drought shown in figure 5.6. Of the droughts they found, the most intense was the drought of 1717-1721, which also supports figure 5.6 showing the early 1700s drought being worse than the 1930s drought. St. George and Nielsen (2003) documented floods on the upper Red River in 1726, 1727, and 1741; 1753-62 was quite dry in parts of the northern Great Plains (Severson and Sieg, 2006); and from the 1820s to about 1861, conditions seem to have been quite wet. There were five successive high or very high runoff years on the Red River from 1823-28 and five successive high or very high runoff years again on the Red River 1847-52 (Thorleifson et al., 1998). The year 1849 stands out in records documented by Severson and Sieg (2006) as a very wet year, whereas 1852 saw one of the largest floods on the Red River at Winnipeg and extreme flooding on the Assiniboine River. The Red River again experienced a large flood at Winnipeg in 1861 (Red River Basin Board, 2000). St. George and Nielsen (2002) described a pronounced wet interval in the 1850s in southern Manitoba.

While predicted 12-year moving average precipitation stayed above the mean from the 1820s into the 1850s, there was a decline in the middle of this period (fig. 5.6). Case and MacDonald (2003) report “There is ample historical documentation of meteorological drought during the mid-1800s across the northern Great Plains (e.g., Mock, 1991; Blair and Rannie,

1994). Tree ring reconstructions of precipitation have also indicated drought during the mid-19<sup>th</sup> Century in the southern Canadian Prairies (Sauchyn and Beaudoin, 1998), Rocky Mountain foothills (Case and MacDonald, 1995), and Montane regions (Watson and Luckman, 2001).” This drought may have caused the dip in precipitation just before 1850 and the sudden shift from wet to dry conditions after 1850 (fig. 5.6).

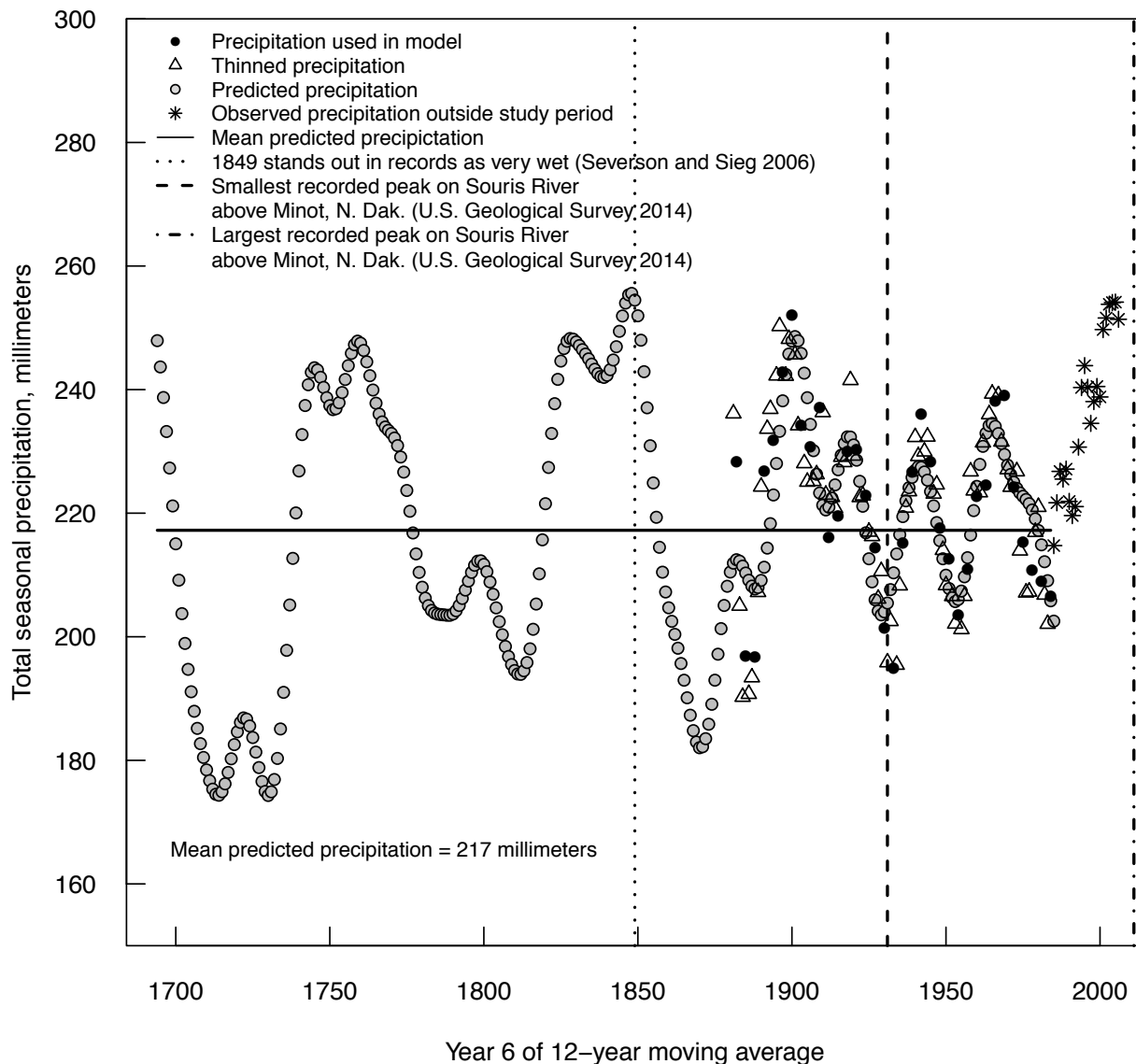


Figure 5.6. Group 1 (southeast), Season 2 (March-June) modeled and observed 12-year moving average precipitation.

Season 3 (July-October) 12-year moving average precipitation (Equation 5.15) is shown for group 5 (northeast; lower Red River Basin, southern Manitoba and southeastern Saskatchewan) in figure 5.7. The early part of the modeled precipitation shows a drought centered around 1750. St. George and Nielsen (2002) documented a severe drought in 1753 in southern Manitoba with annual precipitation estimated at more than two standard deviations below the mean. There appears to have been a widespread regional drought in the 1750s to the early 1760s. Meko (1982) found a period of drought or dry years in the western Great Plains from 1753-62 based on Ponderosa pine in North Dakota, South Dakota, Nebraska, Wyoming, and Montana. Lapp et al. (2013) found a sustained drought in the northwestern Great Plains from 1755-1761, and Stockton and Meko (1983) found a major historical drought in the mid-to-late 1750s in the Great Plains. There is another severe drought around 1800 (fig. 5.7). Thorleifson et al. (1998) described the period of 1792-1828 as one of “high variability” with numerous floods and “several drought episodes.” Rannie (1998) indicated that there was low runoff in the Assiniboine, Red, and Clearwater Rivers in 1800. In group 5 (fig. 5.7), further north than group 1 (fig. 5.6) and in a different season, the pronounced wet period during the 1800s started earlier, in this case in the 1820s. This suggests that the generally wetter period in the first half of the 1800s may have started with wetter falls. Wet falls provide antecedent conditions that contribute to large floods in the region (Ryberg et al., 2007) and may have contributed to the large floods documented on the Red and Assiniboine in the 1800s (Harrison and Bluemle 1980; Miller and Frink 1998; Rannie, 1998; Severson and Sieg, 2006). The modeled and observed precipitation match well and the wet period at the end of the record is able to be modeled.

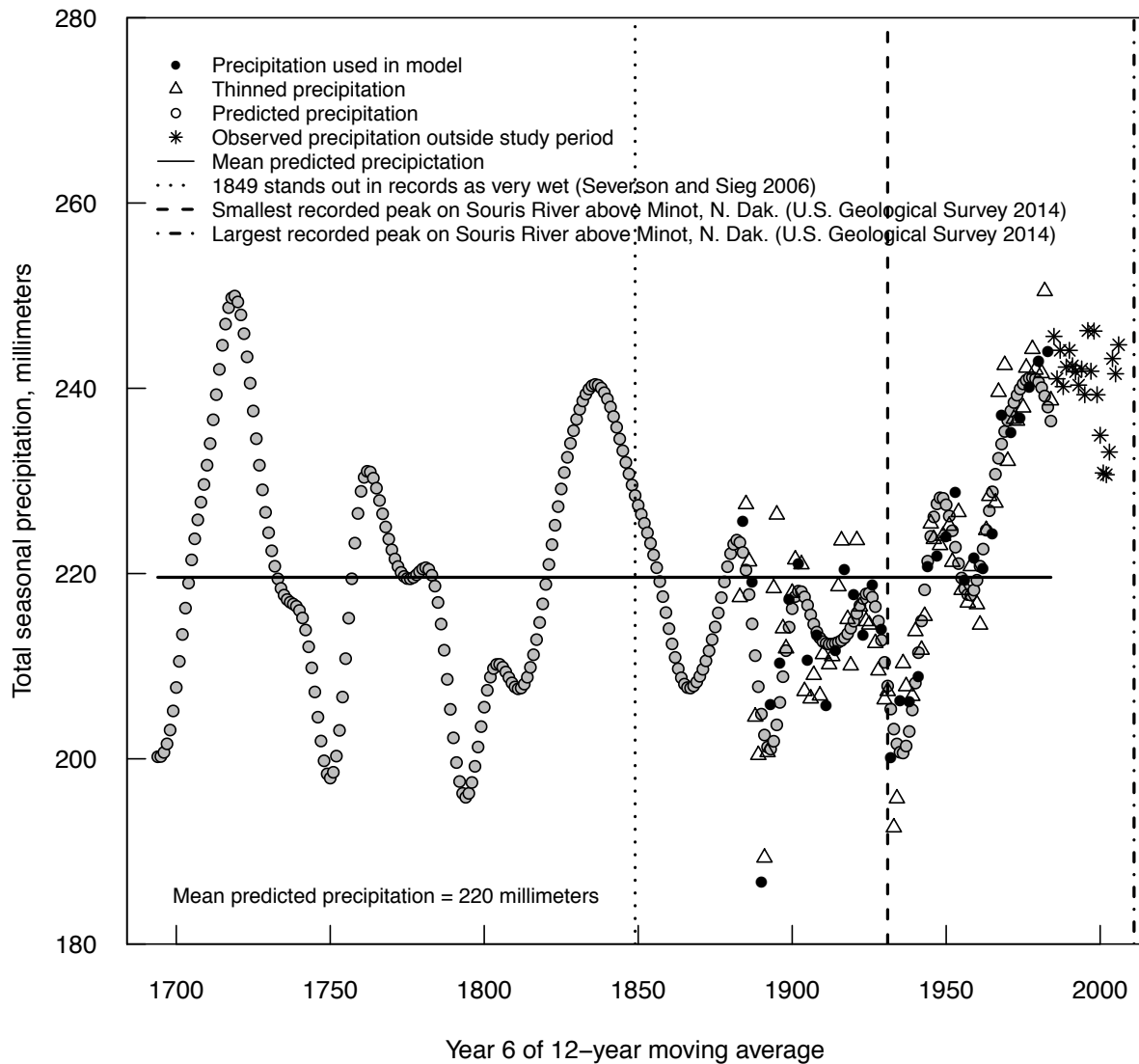


Figure 5.7. Group 5 (southern Manitoba and southeastern Saskatchewan), season 3 (July-October) modeled and observed 12-year moving average precipitation.

For season 1 (November-February), good historical or analytical accounts of snow amounts are difficult to obtain because blizzards can occur with highly variable snow amounts and season 1 is not a growing season; therefore, no graph is shown. The 1820s did see numerous large floods on the Red River (most likely driven by snowmelt) and there were accounts of

snowstorms in this decade. There were reports of deep snowpack near the Red River Settlement and throughout the southern Red River Basin in the winter of 1825-26 (St. George and Rannie, 2003). On December 20, 1826, a snowstorm described as “fearful” drove away the bison from the Pembina region, and resulted in the loss of many horses and 33 people (Severson and Sieg, 2006).

As a check of the models developed for the five groups, modeled precipitation from the three seasons (November-February, March-June, July-October) was added to get the total 12-year moving average precipitation for each group. Despite being modeled separately, the seasonal precipitation summed to reasonable annual totals. The seasonal total for groups 1 and 3 are shown in figure 5.8. The summed seasonal precipitation matched annual totals well in groups 1 and 5 and did less well in groups 3 and 4 where it matched general patterns but did not match the highs and lows; this is evidenced in the lower coefficients of multiple determination for groups 3 and 4 (table 5.1).

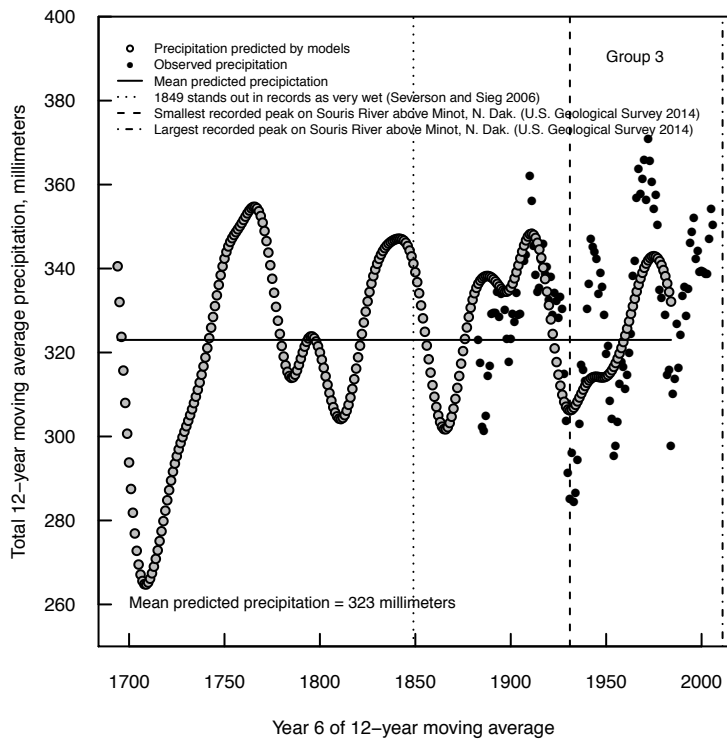
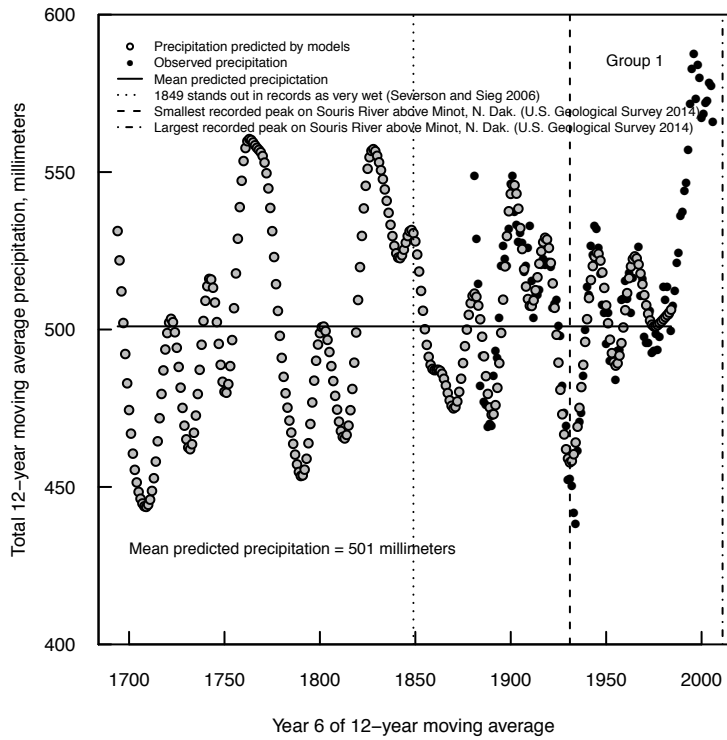


Figure 5.8. Twelve-year moving average annual precipitation for group 1 (southeast) and group 3 (southwest).

## 5.5. Conclusions

Using the multiresolution decomposition of the tree-ring chronologies in the study area shows that precipitation varies on long-term, multi-decadal time scales: 16, 32, and 64 years. The time scales vary with location in the study area and with season. The most frequently used tree-ring site in the precipitation regression models was Boundary Bog (indicated by BB in the equations and in table 5.1 and occurring in 14 of 15 equations). The most frequently used wavelet voice over all sites was the 64-year wavelet (indicated by D6 in the equations and in table 5.1 and occurring in 14 of 15 equations). While tree rings are more sensitive to drought conditions than wet conditions, the cluster groups within the greater Souris River Basin that were best modeled with the multiresolution decomposition of the tree-ring chronologies were those in the wettest part of the study area, groups 1 (southeast group, mainly the Red River Basin in the U.S.) and 5 (northeast group, southern Manitoba and southeastern Saskatchewan).

The modeled precipitation with the three seasons summed generally compares well with the observed data, showing that the individual seasonal models are good at predicting precipitation during the period of instrumental observation. The models also generally match low precipitation (high precipitation) with known drought (pluvial) periods. The model for group 3, the southwest, did the least well at matching observed precipitation (fig. 5.8). This group had some of the poorest seasonal models (table 5.1). However, the resulting modeled precipitation pattern seems reasonable, although it misses the wet period in the 1940s.

One issue is that the tree-ring chronologies did not have tree rings recent enough to model the wet period at the end of the precipitation period of record. The tree-ring record ends at approximately the same time as an abrupt change from dry to wet conditions in the early 1990s. However, the recent wet period seems to have started earlier in season 3, particularly for the

eastern side, groups 1 and 5. Season 3 for group 5 is an example in which the high precipitation in recent times started around 1990 in season 3 and was able to be modeled using the decomposed chronologies (fig. 5.7). The model also shows very high precipitation in the first half of the 1800s and historic accounts corroborate this. The recent wet period may be similar to that of the 1800s and be part of natural variability on a very long time scale and in many cases there probably are not enough instrumental data to detect it.

The modeled precipitation and the accounts of past pluvial and drought periods are characterized by sudden shifts from wet to dry and dry to wet. These sudden shifts have been documented elsewhere in the region and appear to be characteristic of climate in the northern Great Plains (Vance et al., 1992; Shapley et al., 2005; Vecchia, 2008). By describing regional long-term variability in seasonal precipitation, these results can be used to inform models of future Souris River streamflow, thereby helping the ISRB and the Souris River Flood Task Force evaluate future water-resource management options.

## **CHAPTER 6. TOTAL PHOSPHORUS CHANGES IN THE RED RIVER OF THE NORTH AT EMERSON, MANITOBA, AND FARGO, NORTH DAKOTA-MOORHEAD, MINNESOTA, 1970-2012**

With increased runoff in the past few decades (Ryberg et al., 2014; Hirsch and Ryberg, 2012), total phosphorus fluxes (loads) have increased in the Red River of the North (Red River). This is a concern, especially with respect to eutrophication issues in Lake Winnipeg, Manitoba, Canada. There is pressure at the State and International level to reduce phosphorus flux – an expensive proposition, depending on the method (controlling sources, settling ponds, buffer strips) and not always effective during spring runoff. The purpose of this study is to show how total phosphorus (TP) concentration and flux (load) have changed in the Red River over the period 1970-2012 and to illustrate how discharge affects flux. Results show that TP increases and decreases in concentration and flux are complex and differ at points on the Red River at Emerson, Manitoba, and Fargo, North Dakota-Moorhead, Minnesota, and that some of the increase in flux in recent years is mainly climatic – increased discharge (streamflow) in the past two decades has increased the TP flux. These results will be used in future work to perform causal analysis on temporal changes in TP.

### **6.1. Background**

The Red River of the North (Red River) Basin (fig. 6.1) is a hydrologic region where both water quality and water quantity are concerns. The river flows north into Manitoba, Canada, ultimately into Lake Winnipeg, so water quality is an International concern, particularly related to the nutrients phosphorus and nitrogen. Phosphorus is naturally occurring, widespread, and an essential nutrient for plant growth; however, there are anthropogenic sources as well and phosphorus is often the nutrient responsible for accelerated eutrophication (Mueller and Helsel,

1996). Eutrophication is the process “by which a body of water acquires a high concentration of nutrients... These typically promote excessive growth of algae. As the algae die and decompose, high levels of organic matter and the decomposing organisms deplete the water of available oxygen, causing the death of other organisms, such as fish. Eutrophication is a natural, slow-aging process for a water body, but human activity greatly speeds up the process” (Art, 1993). Eutrophication can have negative effects of undesirable tastes and odors, clogged pipes, and can cause declines in recreational use of water bodies, thereby negatively affecting tourism (Mueller and Helsel, 1996; Jones and Armstrong, 2001). Algal blooms also may produce toxins that are may create health risks for livestock, pets, and humans that drink the water (Jones and Armstrong, 2001).

Lake Winnipeg in Manitoba, Canada, was classified as eutrophic in 2000 and 2004 and hypereutrophic in all other years from 1999 to 2007 with annual mean TP concentration greater than 0.1 mg/L (Environment Canada and Manitoba Water Stewardship, 2011a). Hypereutrophic lakes are dominated by frequent and severe algal blooms and low transparency and usually reach this state as the result of human activities (U.S. Environmental Protection Agency, 2010).

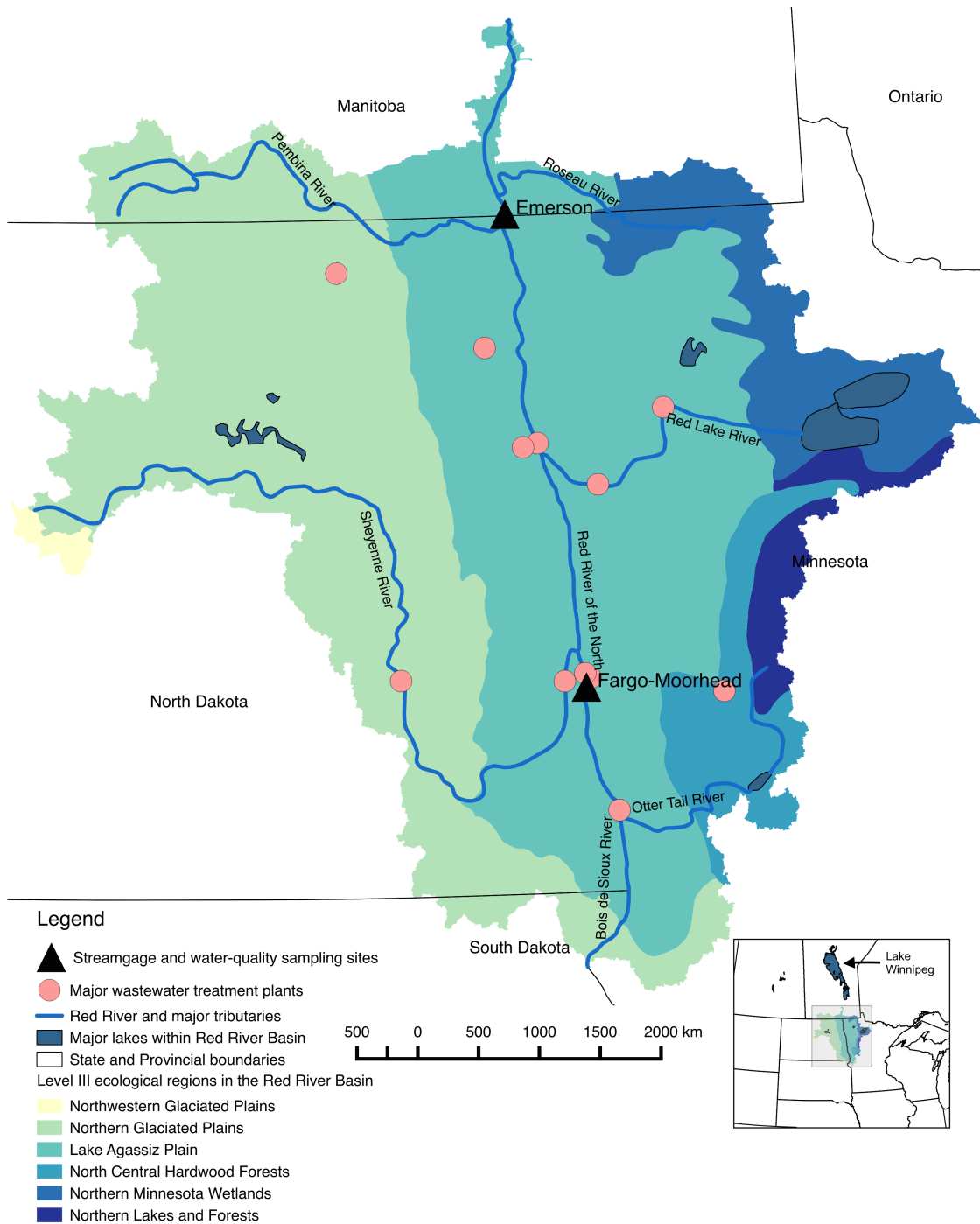


Figure 6.1. Red River of the North Basin, upstream of the confluence with the Assiniboine Basin at Winnipeg, Manitoba, Canada. (Political divisions, major rivers and lakes, and ecological regions from Commission for Environmental Cooperation (1997); selected streamgauge and water-quality sampling site locations from U.S. Geological Survey Water Data for the Nation, <http://dx.doi.org/10.5066/F7P55KJN>.)

Total phosphorus is the sum of all forms of phosphorus including dissolved (that portion that can pass through a filter at the time of water-quality sampling, including phosphate) and particulate (that portion adsorbed to sediment and in plant and animal tissue) phosphorus. Total phosphorus is not necessarily immediately available to plants, but an indication of potentially available amounts. Nonpoint sources of phosphorus include minerals, rocks, soil, fertilizer, and dead biomass, all of which can contribute excess phosphorus to streams through natural runoff and soil erosion (natural or as the result of tillage practices). The most common point source is sewage effluent (Hem, 1985; Mueller and Helsel, 1996). The U.S. Department of Agriculture Economic Research Service has estimated U.S. consumption (agricultural use) of plant nutrients (nitrogen, phosphate, and potash) from 1960-2011. The U.S. total for phosphate is shown in figure 6.2. The black line is a loess smooth line (Cleveland et al. 1992) that gives a general idea of the pattern in the data, removing some of the year-to-year variability (such as 2009 which appears to be underestimated). In addition, phosphate as a percent of total fertilizer used is shown in figure 6.3, with nitrogen and potash for comparison. The percent of phosphorus as total nutrient fertilizer used has declined since 1960, remaining relatively stable after the mid-1980s.

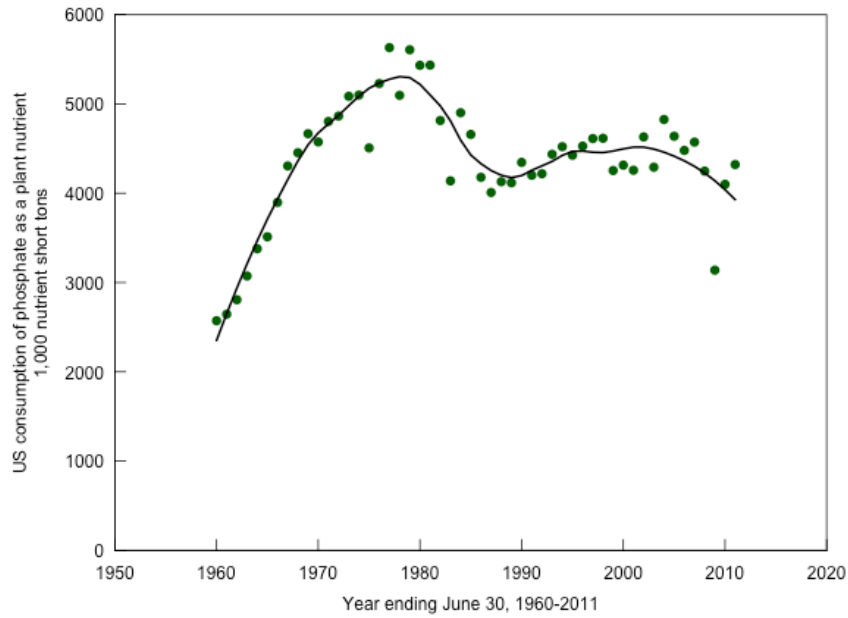


Figure 6.2. U.S. total consumption of the plant nutrient phosphate (U.S. Department of Agriculture Economic Research Service, 2013).

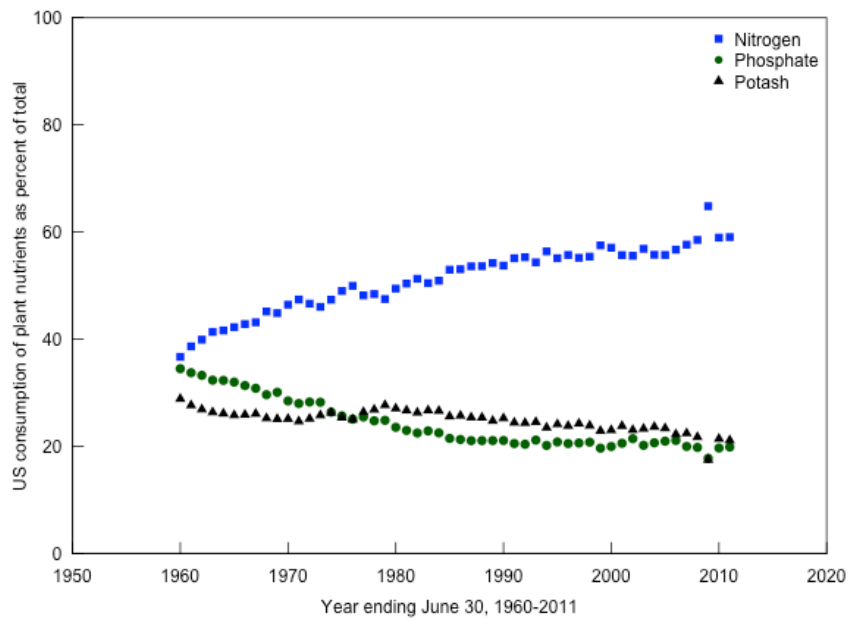


Figure 6.3. U.S. consumption of plant nutrients (fertilizer) as a percent of total consumption (U.S. Department of Agriculture Economic Research Service, 2013).

According to Mueller and Helsel (1996), the natural, or background, concentration of phosphorus in streams is usually less than 0.1 mg/L. The U.S. Environmental Protection Agency recommended criteria for TP is 0.07625 mg/L in rivers and streams in ecological region VI, Corn Belt and Northern Great Plains (U.S. Environmental Protection Agency, 2002). The Federal Water Pollution Control Act (now known as the Clean Water Act) was enacted in 1972 resulting in numerous efforts to improve water quality. About 0.3 million tons of phosphorus per year was discharged in sewage effluent during the period 1978-81 and surface-water phosphorus concentrations were highest downstream from urban areas (Mueller and Helsel (1996). From 1970 to 1992, urban streams experienced a “sustained decrease in phosphorus following mandated phosphorus controls in sewage-treatment-plant effluent. Phosphorus decreases were caused by limits on the phosphate content of detergent, which were established to reduce the amount of phosphorus input to treatment plants, and by additional treatment used in a few plants to remove phosphorus” (Mueller and Helsel, 1996). Prompted by concerns about phosphorus in lakes, Minnesota banned phosphorus in lawn fertilizers in 2005 (State of Minnesota, 2005).

Figure 6.4 depicts estimates of TP flux from wastewater treatment plants that discharge to streams upstream from Emerson and upstream from Fargo-Moorhead. The data represent 68 major and minor WWTPs in the U.S. portion of the Basin. The major WWTPs are defined as discharging more than 1 million gallons per day and are indicated in fig. 6.1. The estimates are from T. Ivahnenko of the U.S. Geological Survey (written communication, February 4, 2015) and were compiled from the U.S. Environmental Protection Agency Clean Watershed Needs Survey wastewater treatment and discharge information (U.S. Environmental Protection Agency, 2012). The data are an underestimate of TP flux, as North Dakota did not report minor WWTPs.

The TP flux has been fairly constant from 1980-2009, with a slight decline upstream from Fargo and Moorhead, but a slight increase for the entire U.S. portion of the Basin.

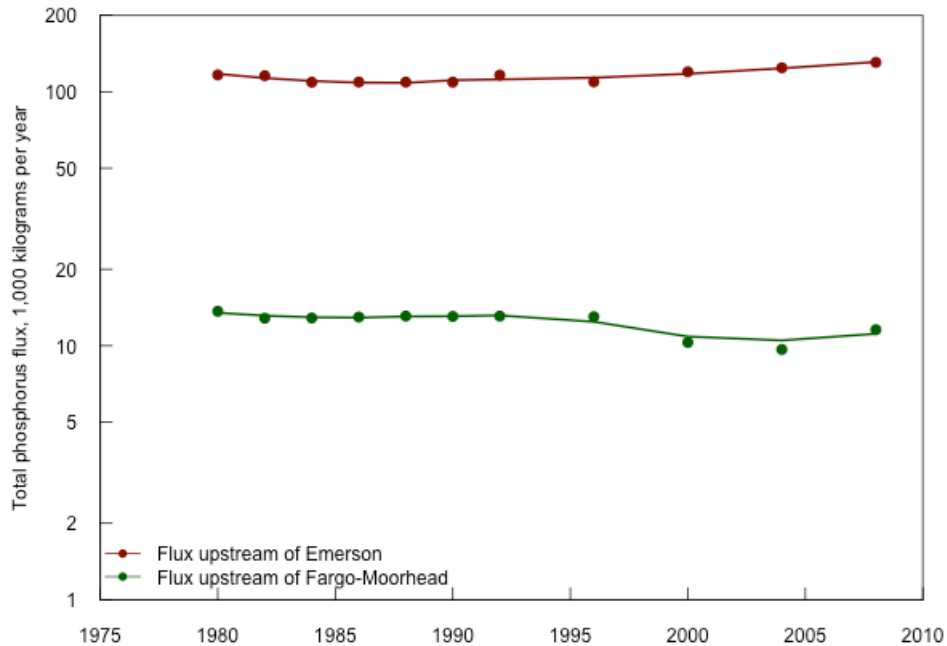


Figure 6.4. Estimated total phosphorus flux from wastewater treatment plants in the Red River of the North Basin.

While this research is focused on the Red River Basin upstream from Emerson, Manitoba (the United States portion of the Red River Basin), past research in the United States and Canada is important for understanding the larger phosphorus picture. One of the major concerns is that phosphorus flux from the Red River can have numerous consequences for Lake Winnipeg. Therefore, a literature review of past phosphorus trend studies in the U.S. and Canada is available in Chapter 2.5.

## 6.2. Discharge History and Variability Analysis

Discharge is an integral part to the TP concentration and flux story. High TP concentrations can occur at high discharge when snowmelt or rain-generated runoff washes manure, fertilizers, and soil into streams. High TP concentrations can also occur at low discharge when the stream is more influenced by wastewater treatment plant effluent. Droughts could influence what crops were grown in the Red River Basin. Wheat, for example, is much more drought tolerant than corn and planting wheat instead for corn (or soybeans) would reduce the amount of fertilizer needed. Tillage practices also could vary with climate, and hence hydrologic conditions. During periods of higher precipitation, farmers till fields to evaporate excess moisture. During dry periods, less fall tillage may occur and minimum till or no till methods, in which crops are planted in last year's crop residue, might be preferred, thereby reducing the potential for soil erosion, that may transport phosphorus to streams.

Discharge data were obtained from the U.S. Geological Survey online database Water Data for the Nation <http://dx.doi.org/10.5066/F7P55KJN>. The discharge analyses were performed using Exploration and Graphics for RivEr Trends (EGRET; Hirsch and De Cicco, 2014), a package for the statistical computing software R (R Core Team, 2014).

Figures 6.5-6.12 provide graphical discharge information for the Red River at Emerson and at Fargo-Moorhead. The first figure shown for each site (figs. 6.5 and 6.9) is the time series plot of discharge. The second figure for each site (figs. 6.6 and 6.10) shows the running standard deviation of the logarithm of daily discharge. "In the case of a system where discharge might be increasing over a period of years, this graphic provides a way of looking at the variability relative to that changing mean value. The standard deviation of the log discharge is much like a coefficient of variation, but it has sample properties that make it a smoother measure of

variability" (Hirsch and De Cicco, 2015). Additional information about interpreting the running standard deviation plot is provided by Hirsch and De Cicco (2015): "If, for example, the probability distribution of daily mean discharge were to have trended upwards (or downwards) over time, but had done so in a manner that all quantiles of the distribution had increased by the same percentage amount, then we would expect this graphic to show a horizontal line. If, on the other hand, the change in the probability distribution were such that there was a greater percentage change in the high end and (or) low end of the distribution, compared to the percentage change in the middle portion of the distribution, then this curve would slope upwards over time... this graphic can be useful and simple way of providing empirical evidence for hypotheses exploring the idea that increasing urbanization or increasing green house gas concentrations in the atmosphere are bringing about changes in hydrologic variability." The running standard deviation is a 12-year centered window (modified from the default of 15), so the first 6 and last 6 years of the data are cut off on the plot.

The third figure shown for each site (figs. 6.7 and 6.11) provides plots of four statistics: annual 1-day maximum daily mean discharge (maximum day), annual mean of the daily mean discharges (mean daily), annual median of the daily mean discharges (median daily), and annual minimum 7-day mean of the daily mean discharges (7-day minimum) and a smoothed version of those time series. The smoothed statistics are determined using weighted regression with a 12-year half window (24-year centered window). This means that in the weighted regressions, a point in the middle of the period will use weighted values of the logarithm of discharge 12 years before and 12 years after it. In this research, the weighted regression windows were modified from the default of 20 years (Hirsch and De Cicco, 2015) to 12 years for the discharge statistic estimates because a number of studies have identified a decadal-scale (greater than 7 years)

signal in precipitation (Cayan et al. 1998; Garbrecht and Rossel 2002; Small and Islam 2008; Small and Islam 2009; Ault and St. George 2010). Small and Islam (2008; 2009) identified a statistically significant signal in fall precipitation in the central U.S. with a periodicity of approximately 12 years, with the signal strongest in the Midwest and Great Plains. Ryberg et al. (2014) focused on long-term (multi-decadal) variability and thus shorter-term, quasi-periodic signals were treated as “nuisance” variability and smoothed out by using a 12-year moving average (backwards looking) when analyzing precipitation, potential evapotranspiration, and runoff. The research presented in Chapter 5 used a 12-year moving average (backwards looking) when modeling seasonal precipitation. The north central U.S. is subject to sudden shifts from wet to dry or dry to wet (Ryberg et al., 2014; Ryberg et al., submitted; Shapley et al. 2005; Vance et al 1992; Vecchia 2008) and the default estimation curves may be too gradual for highly variable prairie streams. The revised windows look 12 years back and 12 years forward for points in the center of the period of record; a point at the end of the record has higher weights extended back in time 24 years, but with the highest weights closest to the point. The resulting estimates of the discharge statistics match well institutional knowledge of changes in the Red River and the surrounding region. The intervening discharge from tributaries is also important to the understanding of variability in the Red River. Discharge analyses for major tributaries and other long-term streamgauge sites on the Red River are shown in Appendix C.

The fourth figure shown for each site (figs. 6.8 and 6.12) present decadal boxplots of discharge during and before the 1970-2012 analysis period. These highlight a drier period in the 1970s and a transition to generally higher discharge that occurred in the 1990s, as well as the general variability in discharge.

### 6.2.1. Red River at Emerson, Manitoba

The three plots described above are shown in figures 6.5 through 6.7 for the Red River at Emerson, Manitoba, as well as additional boxplots (fig. 6.8) to highlight changes in discharge over time. This region is highly variable in terms of climate and discharge and has stood out as an area with increasing trends in other studies that have related trends in flood magnitude to global carbon dioxide concentration and time (Hirsch and Ryberg, 2012; Peterson et al., 2013; Georgakakos et al., 2014). Figure 6.5 highlights intra-annual variability as well as longer term periods (of varying length) of relatively lower or higher discharge conditions.

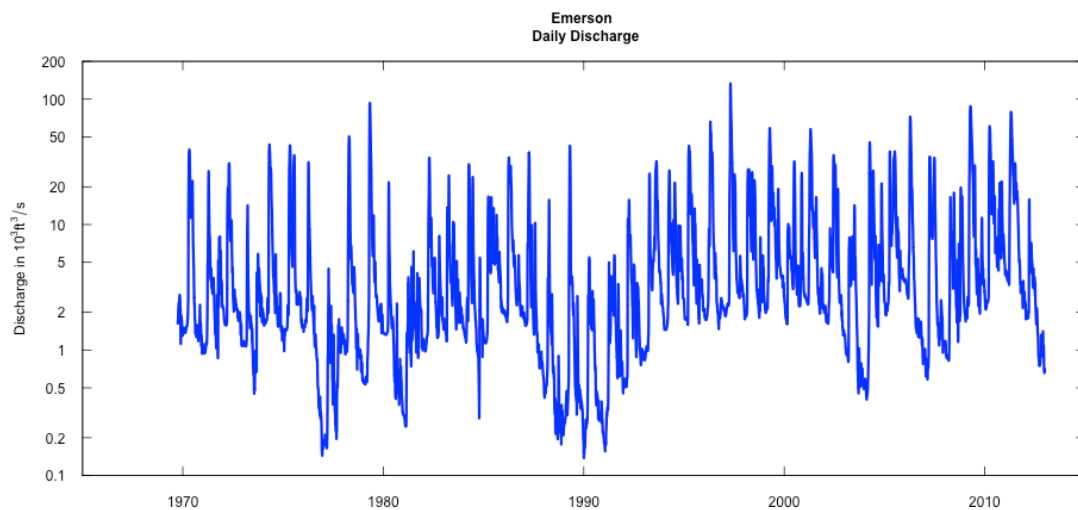


Figure 6.5. Time series plot of daily mean discharge for the Red River of the North at Emerson, Manitoba.

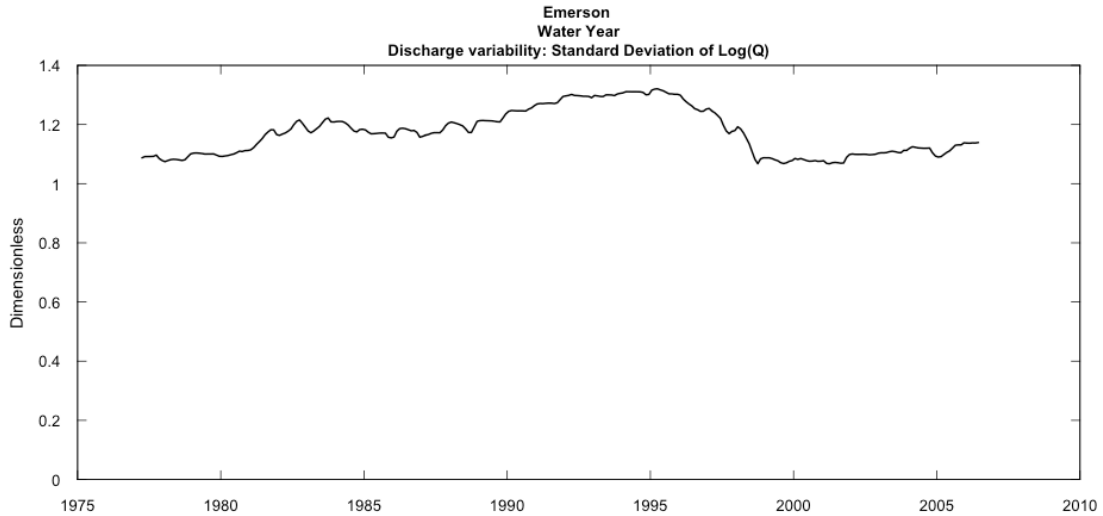


Figure 6.6. Running standard deviation of the logarithm of daily mean discharge (Q) for the Red River of the North at Emerson, Manitoba.

Starting in 1995, the moving discharge variability (fig. 6.6) shows a decline as maximum day, mean daily, median daily, and 7-day minimum discharge all increased (fig. 6.7). The maximum day and mean daily discharge increases tapered off at the end of the record (fig. 6.7), while the median daily and 7-day minimum continued to increase, with a slight decline in the slope occurring around 2000.

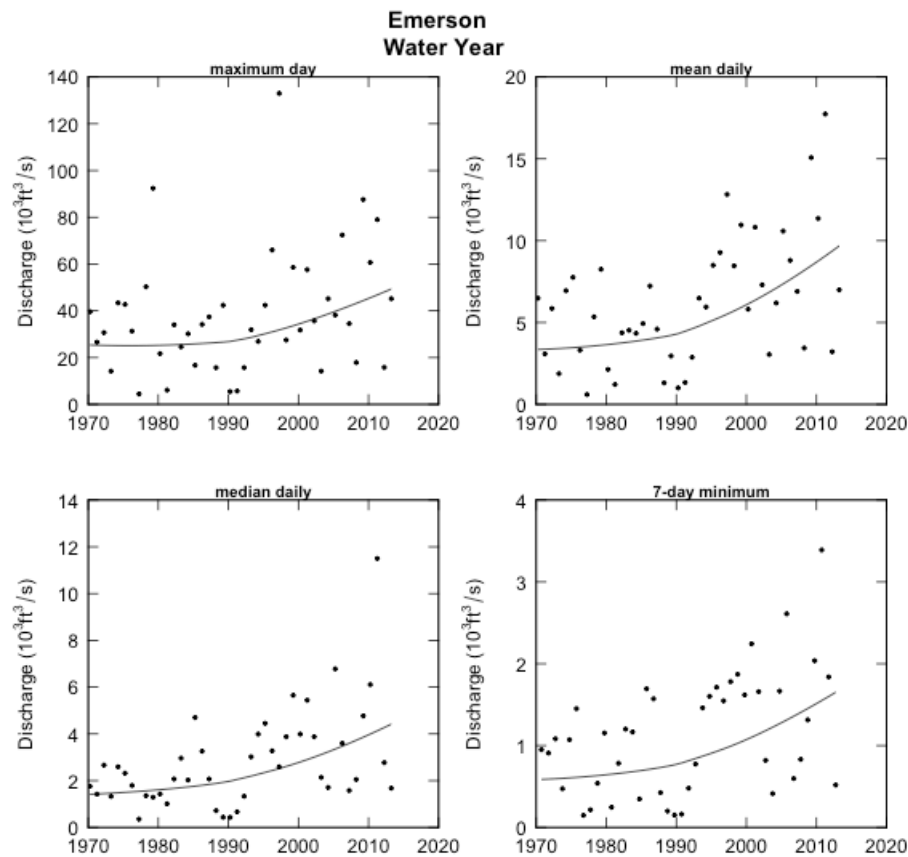


Figure 6.7. Plots of discharge statistics annual 1-day maximum daily mean discharge (maximum day), annual mean of the daily mean discharges (mean daily), annual median of the daily mean discharges (median daily), and annual minimum 7-day mean of the daily mean discharges (7-day minimum) for the Red River of the North at Emerson, Manitoba.

To emphasize how discharge varies over periods in this study, boxplots are shown in figure 6.8 for five decades during and before the 1970-2012 analysis period. The median flow in the second and third decades was about half that of the fourth and fifth decades. There was a drought in the late 1980s through early 1990s, then a sudden switch from dry to wet conditions in 1993 (Williams-Sether, 1999).

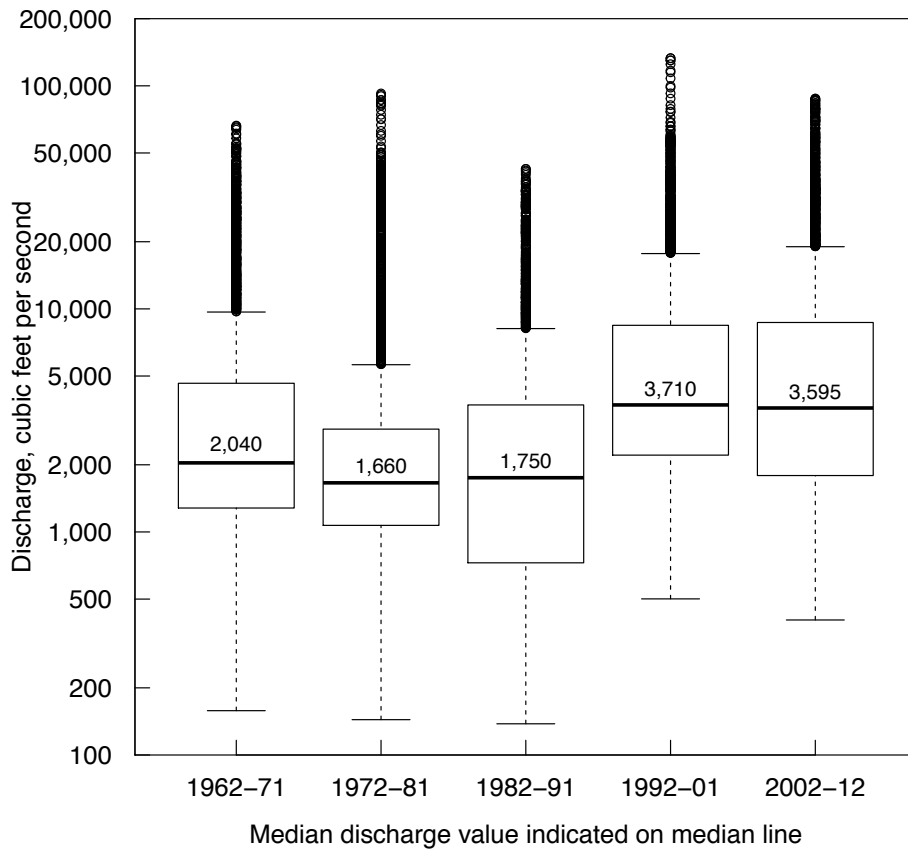


Figure 6.8. Decadal boxplots of daily mean discharge for the Red River of the North at Emerson, Manitoba.

### 6.2.2. Red River at Fargo, North Dakota-Moorhead, Minnesota

The Red River at Fargo, North Dakota-Moorhead, Minnesota, is upstream (south) of the site at Emerson and is upstream from the discharge points of the Fargo and Moorhead wastewater treatment plants (fig. 6.1). Figure 6.9 presents the daily discharge over the analysis period.

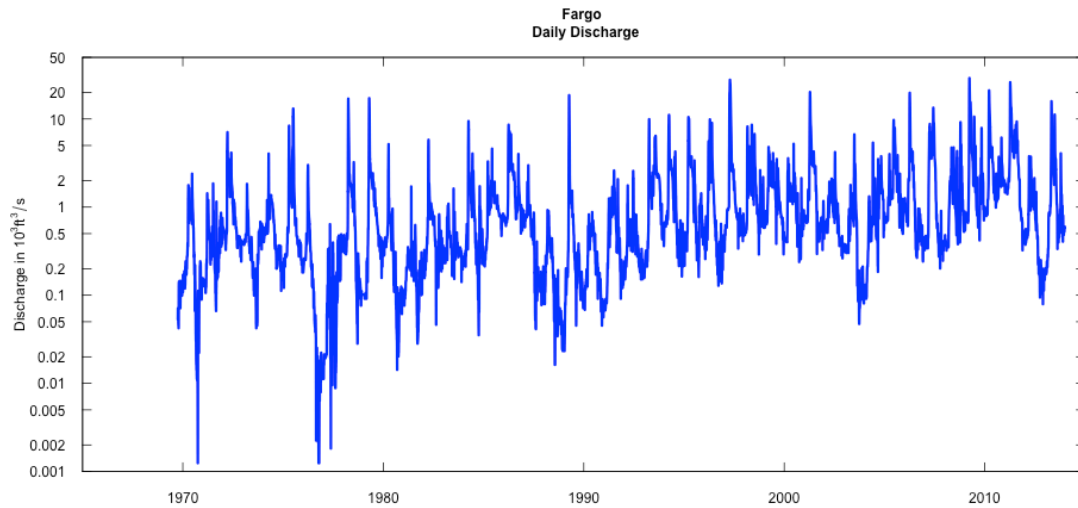


Figure 6.9. Time series plot of daily mean discharge for the Red River at Fargo, North Dakota, and Moorhead, Minnesota.

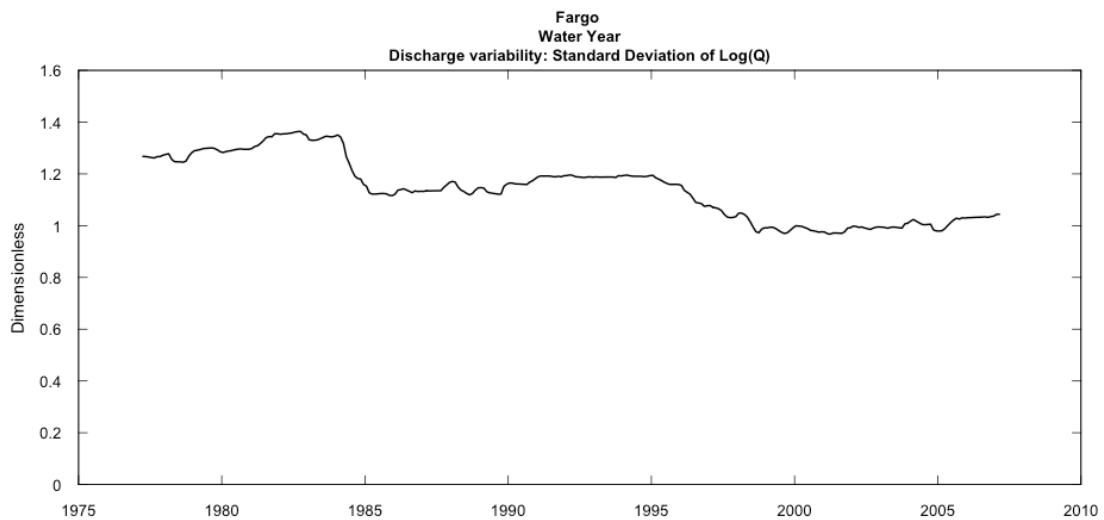


Figure 6.10. Running standard deviation of logarithm of daily mean discharge for the Red River at Fargo, North Dakota, and Moorhead, Minnesota.

Figure 6.10 shows that the Red River at Fargo-Moorhead has greater variability in discharge and was affected more by a 1970s drought than the Emerson site where the river has much higher discharge because of numerous tributaries between the two sites. The decline in variability in the 1980s was caused by the high end of the distribution having a smaller percentage change than the middle and lower portions of the distribution (during this period there were increases in the median daily and 7-day minimum discharge, but little change in the maximum day). Figure 6.10 also shows a decrease in variability from the mid 1990s to 2000, with the variability remaining fairly stable since then. This is because the maximum day, mean daily, median daily, and 7-day minimum (fig. 6.11, as well as other percentiles not shown in the figure) have increased in unison, resulting in less discharge variability.

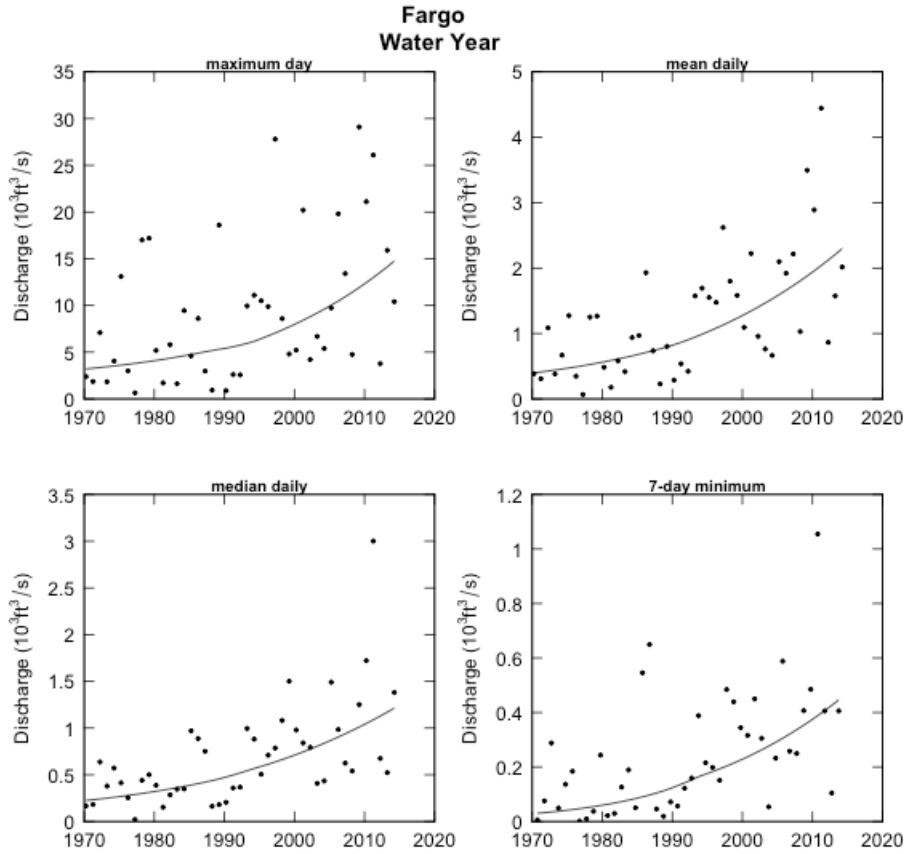


Figure 6.11. Plots of discharge statistics annual 1-day maximum daily mean discharge (maximum day), annual mean of the daily mean discharges (mean daily), annual median of the daily mean discharges (median daily), and annual minimum 7-day mean of the daily mean discharges (7-day minimum) for the Red River at Fargo, North Dakota, and Moorhead, Minnesota.

As with the Red River at Emerson, decadal boxplots (fig. 6.12) show two discharge regimes, a lower discharge period in the first three boxplots and a higher discharge period in the second two.

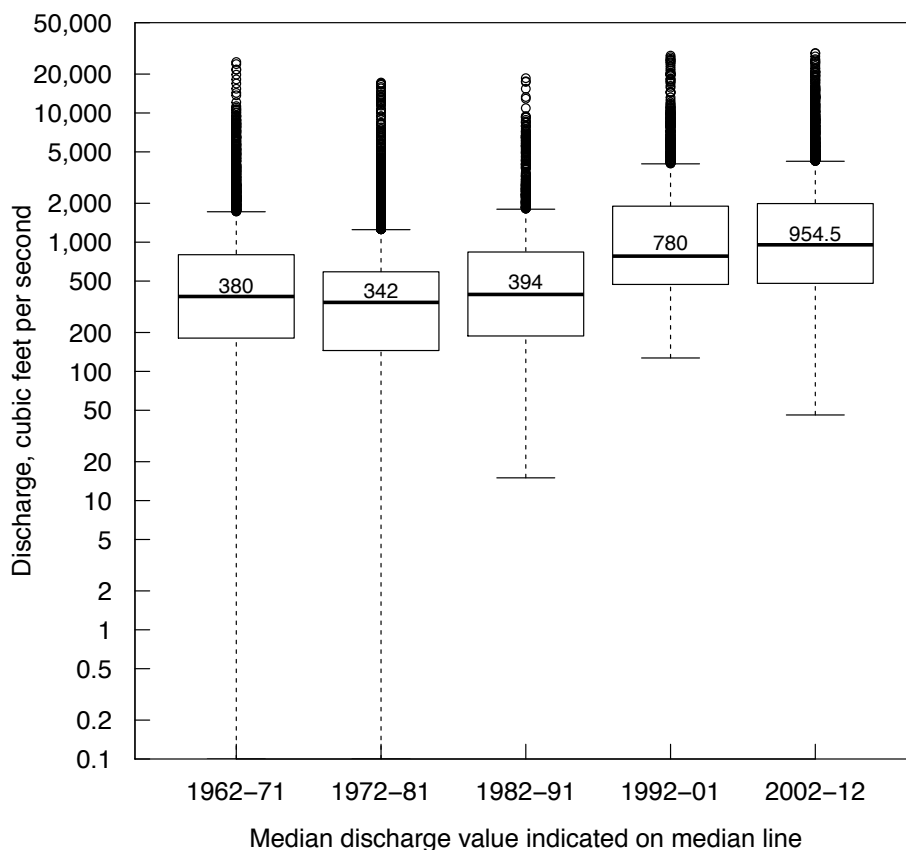


Figure 6.12. Decadal boxplots of daily mean discharge for the Red River at Fargo, North Dakota-Moorhead, Minnesota. Twelve discharge values of zero were replaced with 0.1 because of the use of a logarithmic scale.

### 6.3. Total Phosphorus Data

Four sources of data for TP concentrations in the Red River were identified: Environment Canada (EC; data that the U.S. Geological Survey had already because of ongoing projects with the International Joint Commission related to Red River water quality), U.S. Geological Survey (USGS) data available from the online Water Data for the Nation database <http://dx.doi.org/10.5066/F7P55KJN>, data from the Minnesota Pollution Control Agency (MPCA) Stream and Lake Information online database [http://cf.pca.state.mn.us/water/watershedweb/wdip/search\\_more.cfm](http://cf.pca.state.mn.us/water/watershedweb/wdip/search_more.cfm), and data from the North Dakota Department of Health (NDDH) online Surface Water Quality Data for North Dakota

database [http://www.ndhealth.gov/WQ/SW/Z8\\_SWData/viewer.html](http://www.ndhealth.gov/WQ/SW/Z8_SWData/viewer.html). The North Dakota State Water Commission's online water-quality data were also considered, but dissolved, rather than total, phosphorus was reported.

### **6.3.1. Red River of the North at Emerson, Manitoba**

Three sources of TP data were identified for the site at Emerson: EC (3,847 samples, 1960-2012), USGS (149 samples at Emerson, 1978-2004; 152 samples at Pembina, North Dakota, 1970-2013), and MPCA (110 samples, 1962-2009, with all but one prior to 1980). The various datasets were compared, where they overlapped, using the Kolmogorov-Smirnov test (Higgins, 2004). This is a nonparametric test for whether or not two populations differ in distribution. Since the Red River at Emerson, Manitoba, site represents TP transport from the U.S. to Canada, both EC and USGS are interested in this site and have done paired sampling in the past to verify that their methods would provide the same results. Duplicates were removed and the EC data were used as the default data to which everything else was compared because there were significantly more samples over longer period in the EC dataset than in any of the other sources. Results showed that the EC and USGS data at Emerson were from the same distribution; therefore, they were combined for the analysis. USGS data collected upstream at Pembina, North Dakota (just upstream from Emerson and indistinguishable from the site at Emerson on the scale of Figure 6.1), were compared, but the Kolmogorov-Smirnov test indicated that they were not from the same distribution. Initially this was surprising as some past studies have combined the two nearby sites (they are only about five miles apart with no notable surface-water addition between them); however, at least some of the USGS Pembina samples were grab samples, not equal-width increment samples (U.S. Geological Survey, 2006) that would result in a composite sample. The Pembina sampling site on the Red River is just downstream from the

inflow from the Pembina River and the two rivers are not well mixed at the sampling point (R. Nustad, USGS North Dakota Water Science Center Water-Quality Specialist, oral communication, March 2015). By the time the combined Pembina-Red River flow arrives at Emerson, it is well mixed. The combined EC-USGS data at Emerson were compared to the MPCA data and the Kolmogorov-Smirnov test indicated they were not from the same distribution (confirming what could be seen in exploratory data analysis, not shown, in which the MPCA data appeared biased slightly high compared to the other data). Figures 6.13-6.15 summarize the combined EC-USGS TP data for the Red River at Emerson.

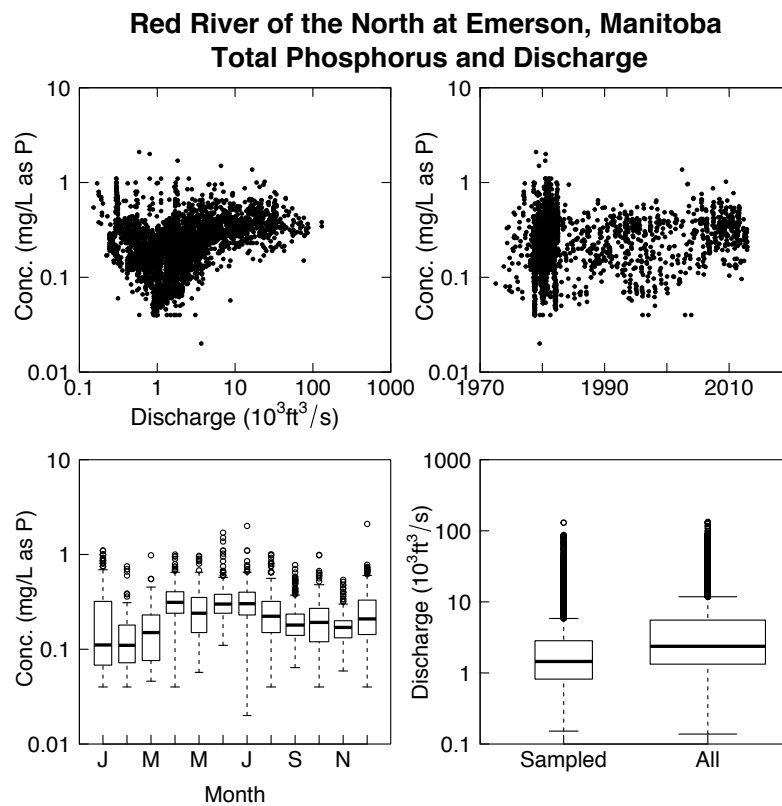


Figure 6.13. Total phosphorus concentration versus discharge, concentration versus time, boxplots of concentration by month, and boxplots of the sampled discharges and all daily discharges for the Red River of the North at Emerson, Manitoba.

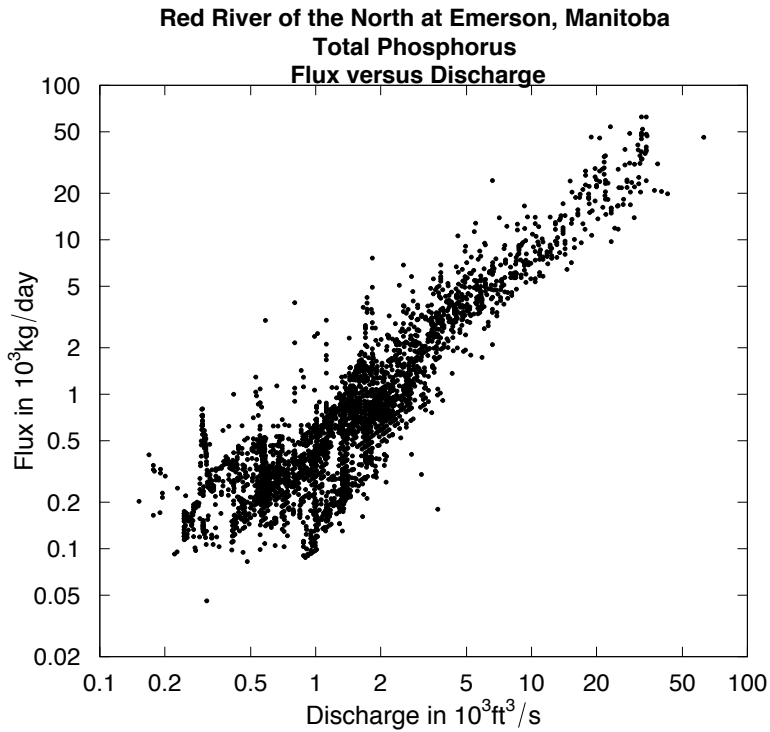


Figure 6.14. Observed log flux (load) versus discharge for the Red River of the North at Emerson, Manitoba.

While this site is very data rich, water-quality sampling intensity has changed over the years. The boxplots in figure 6.15 show the number of samples per decadal period. Sampling frequency was lowest in the 1960s, but was still greater than six per year. Then sampling intensity increased dramatically in the 1970s, as concerns about eutrophication of Lake Winnipeg were growing and phosphorus use was increasing. Sampling decreased after the 1970s; however, the number of samples per year still remained high compared to sampling at rivers in North Dakota (Galloway, 2012).

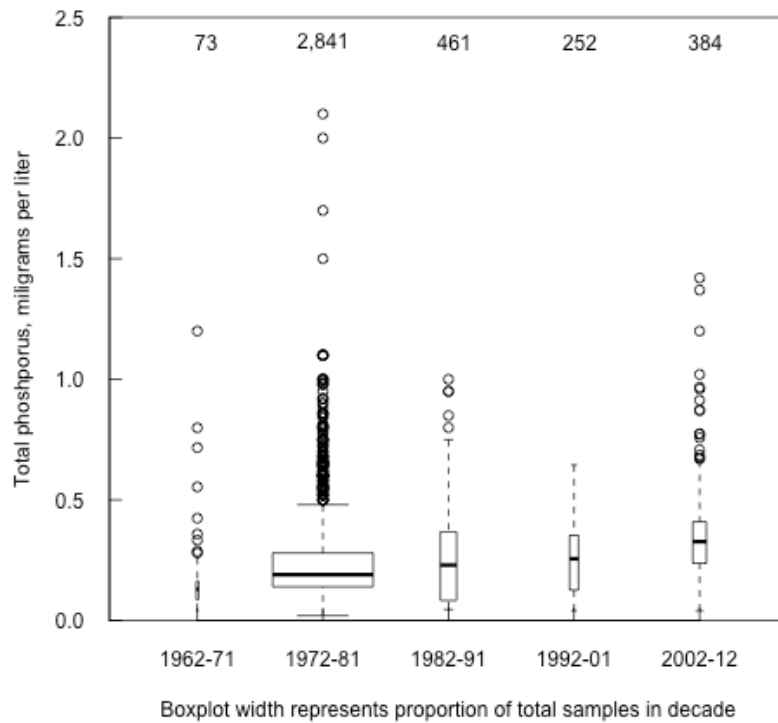


Figure 6.15. Decadal boxplots of total phosphorus for the Red River of the North at Emerson, Manitoba, including some samples prior to the 1970-2012 analysis period. Number of samples per period written above each boxplot.

### 6.3.2. Red River at Fargo, North Dakota, and Moorhead, Minnesota

Three sources of TP data were identified for Fargo-Moorhead: USGS (102 samples, 2003-2013), MPCA (at two nearby sites; 311 samples, 1971-2011 from the Main Avenue Bridge; 63 samples, 2001-2012 from the First Avenue North Bridge), and North Dakota Department of Health (16 samples, 1994-1996). MPCA data for the Red River Main Avenue Bridge, Moorhead, Minnesota, were used as the default data to which everything else was compared because there were significantly more samples over a longer period. The MPCA data at the two nearby sites were compared using the Kolmogorov-Smirnov test and deemed comparable. This is reasonable because the USGS samples from both of these bridges and

identifies it as one site, 05054000, Red River at Fargo, North Dakota. Using a combination of bridges as a sampling strategy in Fargo-Moorhead is common. For example, in a study of water-quality in the Red River at Fargo-Moorhead, 2003-05, location varied. "In 2003, samples were collected from the Main Avenue Bridge or the First Avenue Bridge. In 2004 and 2005, samples were collected from the First Avenue Bridge during high flow and from the walking-path bridge, between the gaging station and the Main Avenue Bridge, during low flow" (Ryberg, 2006). The MPCA data were combined and compared to the USGS and NDDH data. The MPCA and NDDH were from the same distribution and combined. The USGS data were not from the same distribution based on the Kolmogorov-Smirnov test and were dropped from further consideration.

Figures 6.16-6.18 summarize the combined TP data for the Fargo-Moorhead site. The plots highlight the long-term and seasonal variability in TP and the strong relation between flux and discharge.

**Red River of the North at Fargo, North Dakota–Moorhead, Minnesota  
Total Phosphorus and Discharge**

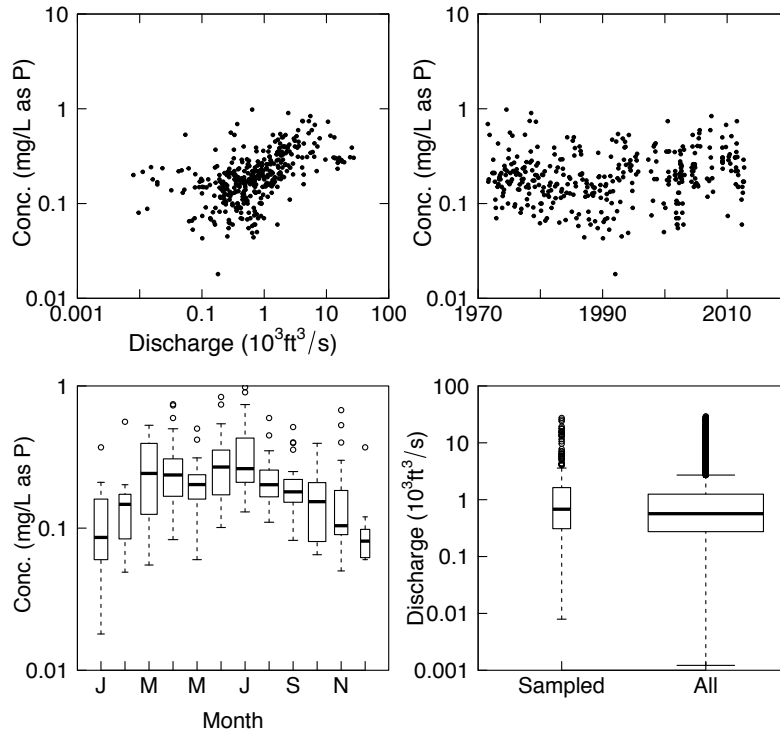


Figure 6.16. Total phosphorus concentration versus discharge, concentration versus time, boxplots of concentration by month, and side-by-side boxplots of the sampled discharges and all daily discharges for the Red River of the North at Fargo, North Dakota-Moorhead, Minnesota.

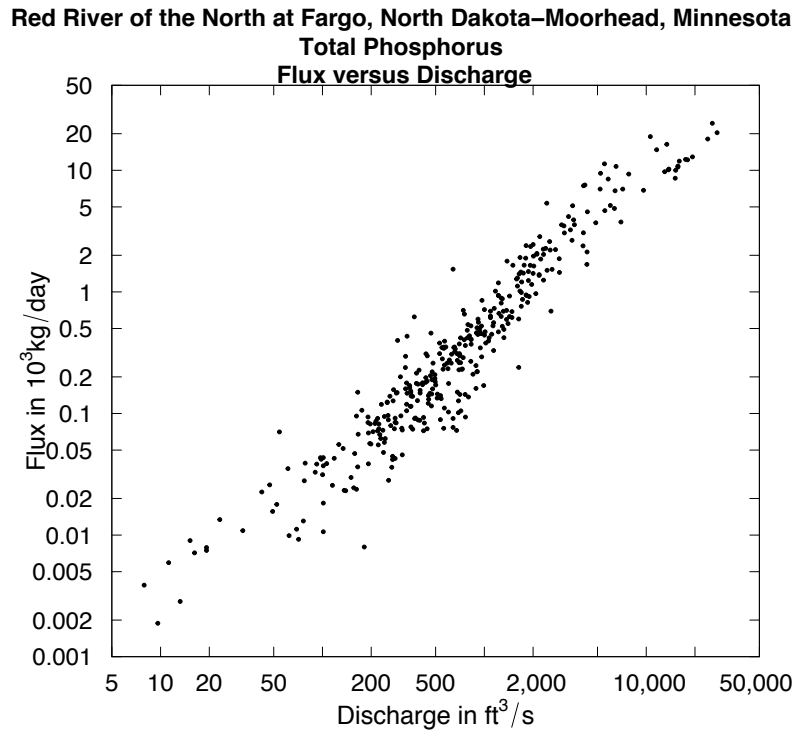


Figure 6.17. Observed log flux (load) versus log discharge for the Red River of the North at Fargo, North Dakota-Moorhead, Minnesota.

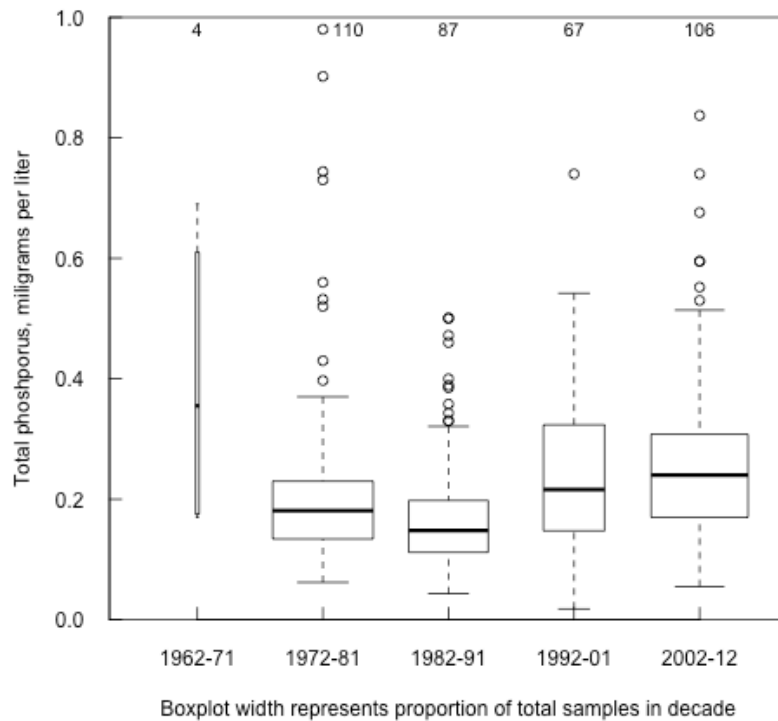


Figure 6.18. Decadal boxplots of total phosphorus for the Red River of the North at Fargo, North Dakota-Moorhead, Minnesota. Number of samples per period written above each boxplot.

#### 6.4. Weighted Regression on Time, Discharge, and Season - WRTDS

Total phosphorus is modeled using Weighted Regressions on Time, Discharge, and Season (WRTDS), a method for analysis that can be used to characterize trends in concentration and flux (Hirsch et al., 2010; Hirsch and De Cicco, 2014). WRTDS is a fairly new approach for analysis of surface-water water-quality datasets. The main requirements for data analysis are:

- More than 200 samples at a site.
- At least 20 years of sampling.
- A complete record of daily discharge (Hirsch et al., 2010).

WRTDS was designed to meet seven desired attributes for an analysis approach, summarized below from Hirsch et al. (2010).

- Provide a description of change.

- Do not assume that the flow versus concentration relation is constant with time, that is the approach should allow the relation to change over time.
- Allow for seasonality, but do not assume that seasonality is exactly the same from year-to-year (such as in multiple regression models that include cosine and sine terms to represent well documented seasonality, such as in nutrients, but that force seasonality to be the same every year; WRTDS uses sine and cosine terms, but their functional relation with concentration can change over time).
- Do not force a linear or quadratic or other specific function on the data over the entire analysis period that is the same for the entire discharge distribution.
- Provide consistent results for concentration and flux by removing some of the year-to-year variability caused by discharge.
- Provide estimates of the time series of concentrations and fluxes where the variation attributable to variation in discharge has been removed.
- Provide additional diagnostic tools such as graphical methods.

WRTDS combines water-quality and discharge data into an analysis that decomposes the record into four parts.

- A trend that is a "smooth function of time, typical of a moving average of a time series where the moving average is over a window of several years duration" (Hirsch et al., 2010).
- A seasonal component that "is a pattern that has a wavelength of a year but does not necessarily follow a set functional form (such as a sine wave). Its amplitude and phase shift and even its shape can change gradually over the years" (Hirsch et al., 2010).

- A discharge relation that is relatively smooth "The influence of discharge can evolve over time due to changes in the dominant processes... Over the period of record, changes in the relative importance of these processes can result in substantial changes in this relationship, but the changes are assumed to be gradual" (Hirsch et al., 2010).
- A random part that remains after the removal of the trend, seasonal, and discharge components.

The equations used in WRTDS are provided in Hirsch et al. (2010) and Hirsch and De Cicco (2015). The concentration is estimated across a rectangular grid based on time and discharge using weighted regression at each node of the grid with the model taking the form:

$$\log(c) = \beta_0 + \beta_1 q + \beta_2 T + \beta_3 \sin(2\pi T) + \beta_4 \cos(2\pi T) + \epsilon \quad (\text{Eq. 6.1})$$

where  $c$  is concentration in milligrams per liter,  $\beta$  are the regression coefficients,  $q$  is the logarithm of daily mean discharge,  $T$  is time, in decimal years, and  $\epsilon$  is the error (unexplained variation).

This equation is estimated at each node in the grid, so the  $\beta$  values vary at each node. The equation is fitted using a weighted Tobin model (Tobin, 1958; often referred to as Tobit regression) and can be used with censored data, although no data are censored in this study. The weights are determined using three metrics: distance in time, distance in log discharge units, and distance in season. Hirsch and De Cicco (2015) provide this example, "if we compare a sample value with  $q$  and  $T$  values of 3.0 and 1995.0, respectively, to a grid point with  $q$  value of 3.8 and a  $T$  value of 1997.25, then the distance in log discharge would be 0.8, the distance in time would be 2.25 years, and the distance in season would be 0.25 years. Weights are associated with each of these three distance measures by using the tricube weight function... The half window widths ... have default values of 2 (in log discharge units), 7 years, and 0.5 years... The overall weight

for any observation is the product of the three weights." In this study, the default half-window width of 7 years was changed to 6 to match with previous analyses of discharge as discussed above.

WRTDS uses the estimates of concentration in the grid to estimate daily concentration. The daily concentrations are then used to estimate daily flux:

$$\text{Flux} = c_d \times Q_d \times 86.4 \quad (\text{Eq. 6.2})$$

where Flux is the daily estimate of flux,  $c_d$  is the daily estimate of concentration, in mg/L,  $Q$  is daily mean discharge, stored in cubic meters per second ( $\text{m}^3/\text{s}$ ) in WRTDS (but able to be read in and output in other units), and 86.4 is the unit conversion that results in flux in kilograms per day (kg/d).

#### **6.4.1. Flow Normalization**

Some of the results presented are for concentration and flux, others are for flow-normalized concentration and flux. Hirsch and De Cicco (2015) discuss flow normalization as follows. "Estimates of daily concentration and daily flux are of great value and importance in terms of knowing the actual history of water quality in a river. Particularly where there is an interest in understanding the water quality or ecological condition in a receiving water body such as an estuary, lake, or reservoir, the variable of interest would be the history of flux integrated over periods such as months, seasons, or years. In addition, when the interest is in the concentrations of a pollutant that may have impacts on receptors such as biota or water supply intakes, then the history of concentration will be of interest. However, the history produced by the model will not describe the frequency of exceedances of water-quality criteria or standards, because the concentration estimates will have less variability than real records would [as this is the nature of regression models]. The concentration or flux estimates ... can be very strongly

influenced by the particular time history of flow conditions. For example, for a pollutant for which concentration increases with discharge, a high-flow period of a year or two near the end of the period of record can suggest deteriorating water quality. For those interested in evaluating the effectiveness of pollution control efforts, these types of results can seriously confound the analysis. The variability in concentration or flux that is related to discharge can overwhelm a true signal of change. Discharge-driven variability creates a large amount of apparent 'noise,' thus making the identification of trend virtually impossible. For those seeking information about 'progress' or 'effectiveness' or an understanding of how the watershed system is changing, what is needed are time histories that filter out the impact of year-to-year variation in discharge."

Flow normalization is described by the following equation

$$E[C_{fn}(T)] = \int_0^{\infty} w(Q, T) \times f_{T_s}(Q) dQ \quad (\text{Eq. 6.3})$$

where  $E[C_{fn}(T)]$  is the flow-normalized estimate of concentration for time  $T$  (a specific day of a specific year),  $w(Q, T)$  is the WRTDS estimate of concentration as a function of  $Q$  (discharge) and  $T$  (time, in years),  $f_{T_s}(Q)$  is the probability density function (pdf) of discharge, specific to a particular time of year, designated as  $T_s$ , and  $T_s$  is restricted to values between 0 and 1 (the fractional part of the time variable  $T$ ; Hirsch and De Cicco, 2015).

"Thus, the flow-normalized concentration on a specific day (a specific value of  $T$ ) is the integral of the fitted estimates of concentration as a function of discharge and time multiplied by the pdf of discharge for that day of the year... This process is repeated for every day in the period of record, and the results of the process become the time series of flow-normalized concentrations for the period of record. These daily values can be aggregated to monthly values by computing a mean of the flow-normalized values for the month and to yearly values by computing a mean of the flow-normalized values for the year. These monthly values will show

strong seasonality and will change gradually over time, but they will be free of any variation due to the occurrence of high- or low-flow conditions in any given month. Similarly, the annual values will show gradual change over time, but will be free of any variation due to the occurrence of high- or low-flow conditions in any given year" (Hirsch and De Cicco, 2015).

The flow-normalized flux is computed in a similar manner.

$$E[F_{fn}(T)] = 86.4 \times \int_0^{\infty} Q \times w(Q, T) \times f_{T_s}(Q) dQ \quad (\text{Eq. 6.4})$$

where  $E[F_{fn}(T)]$  is the flow-normalized flux for time  $T$  (a specific day of a specific year),  $Q$  is daily mean discharge in cubic meters per second, 86.4 is a conversion factor to determine flux in kilograms per day,  $w(Q, T)$  is the WRTDS estimate of concentration in mg/L as a function of  $Q$  (discharge) and  $T$  (time, in years),  $f_{T_s}(Q)$  is the probability density function (pdf) of discharge, specific to a particular time or year, designated as  $T_s$ , and  $T_s$  is restricted to values between 0 and 1 (the fractional part of the time variable  $T$ ; Hirsch and De Cicco, 2015).

Flow normalization assumes that for any given day of the year, the discharge distribution is stationary (Hirsch and De Cicco, 2015), that is the mean and variance do not change over time. However, as the above streamflow analyses show and has been documented elsewhere (Williams-Sether, 1999), there was a sudden switch from dry to wet in 1993. Thus, the flow-normalization process used in WRTDS would not be appropriate if the analysis were conducted over the entire 1970-2012 period, because of the very strong non-stationarity evident in the discharge data set. Given this very clear difference in discharge between these two periods, the WRTDS analyses of the Red River at Emerson and Fargo-Moorhead were divided into two slightly overlapping periods, 1970-1993 and 1993-2012. The year 1993 is included in both periods because the change happened mid-year 1993 and for some locations the increase in precipitation was seen more in 1994 than 1993 (Williams-Sether, 1999). Therefore, the

estimates of daily and annual concentration and flux differ for 1993 between the two analysis periods because the first period (1970-1993) experienced comparatively drier conditions while the second period (1993-2012) was wetter with higher runoff.

### **6.5. Results of WRTDS Analysis**

WRTDS requires a significant amount of data, 200 samples over 20 years. Many sites on the Red River do not have enough data. By far the richest data site is the Red River at Emerson, Manitoba, as it represents the discharge and TP flux exported to Canada from the U.S. and has been sampled extensively. Therefore, that site is presented first, followed by the upstream site at Fargo, North Dakota, and Moorhead, Minnesota. Data were analyzed with WRTDS from 1970-1993 and 1993-2012 because of the sudden switch from generally drier to generally wetter conditions in 1993. These two periods combined represent the maximal period of record available for this study at both sites.

#### **6.5.1. WRTDS Results for Red River at Emerson, Manitoba**

Figure 6.19 shows observed and estimated concentrations and fluxes for period 1 (1970-1993) and figure 6.20 shows the same for period 2 (1993-2012). The flow-normalized concentration (green line in lower-left of fig. 6.19) shows the large increase in TP in the 1970s, followed by a decline to the late 1980s, then a fairly stable concentration to 1993. The flow-normalized flux green line in lower right of fig. 6.19 shows a similar pattern with an increase to the early 1980s, followed by a decline to the late 1980s, followed by a slight increase to 1993.

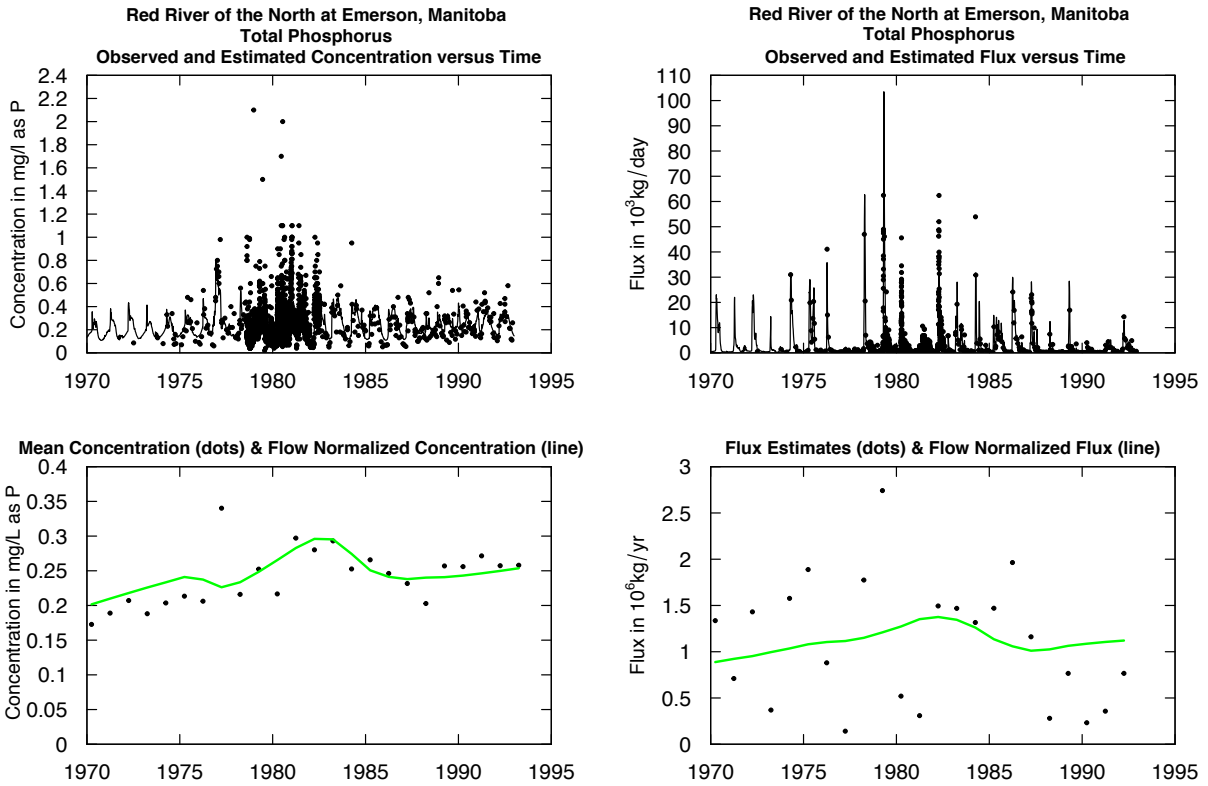


Figure 6.19. Observed and estimated total phosphorus concentrations and fluxes in the Red River of the North at Emerson, Manitoba, 1970-1993.

Observed and flow-normalized concentrations tend to be larger in the second period (fig. 6.20) and the estimates for 1993 is larger than they were in the 1970-1993 period. Despite increased streamflow in the recent period (fig. 6.7) flux has been fairly stable, with some decrease at the end of the period. With the discharge variability removed in the flow-normalized flux, the analysis shows what flux might look like if discharge had not been increasing at the end of the period of record and indicates that some improvements (likely related to agricultural and WWTP practices) may have been made, even if the actual fluxes do not reflect a reduction.

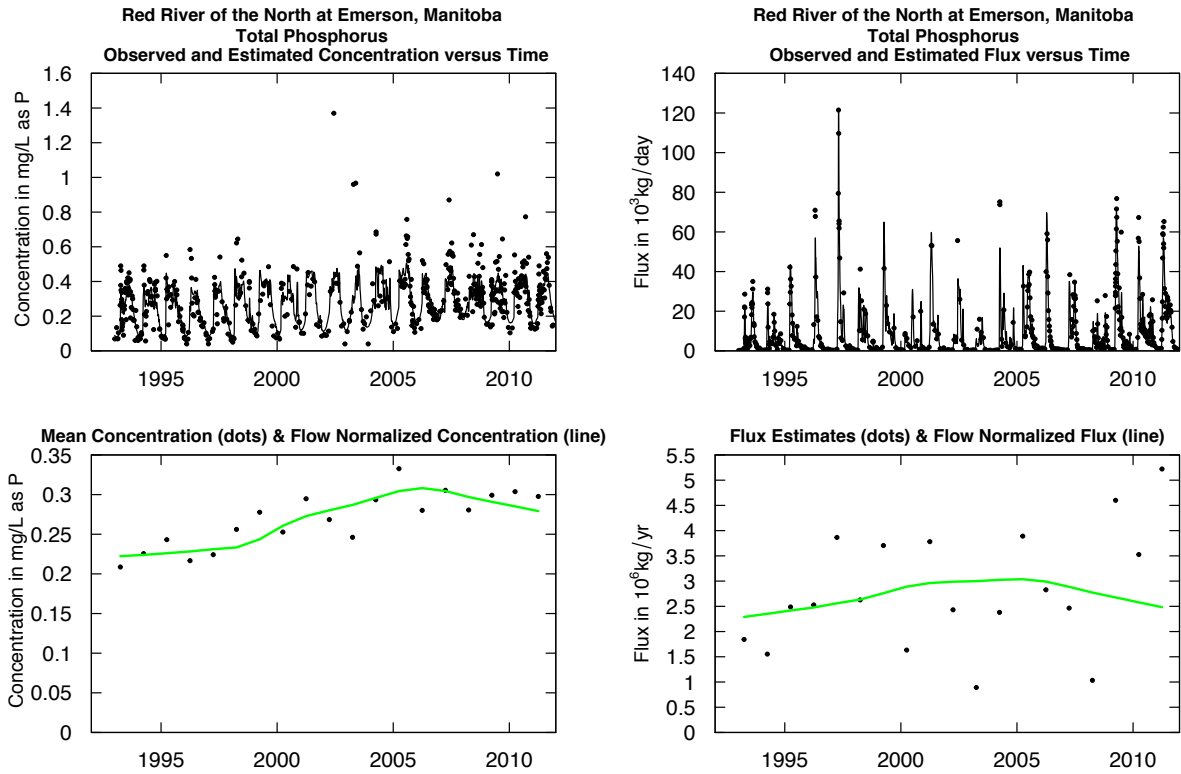


Figure 6.20. Observed and estimated total phosphorus concentrations and fluxes in the Red River of the North at Emerson, Manitoba, 1993-2012.

WRTDS provided a flux bias statistic of 0.00333 for period 1 and -0.0243 for period 2.

Values between -0.1 and +0.1 indicate that the bias in estimates of the long-term mean flux is likely to be less than 10 percent. Hirsch (2014) showed that the relation between the true bias and the flux bias statistic is nonlinear and rather imprecise, therefore, the flux bias statistic is not a basis for making corrections to flux estimates, but can identify cases that are likely to have severe biases. WRTDS also provides model diagnostic plots and those plots for both periods are provided in Appendix D.

### 6.5.1.1. Estimates of Concentration and Flux as a Function of Time and Discharge

Contour plots in figures 6.21 and 6.22 estimate concentration change over a time and discharge grid in each period, 1970-1993 and 1993-2012. The changes in color and pattern indicate in what seasons and discharges TP concentration increases or decreases have occurred.

Figure 6.21 shows increases in TP at almost all discharges during the growing season, which could be expected because of the increase in the use of phosphorus on the landscape (fig. 6.2). The largest increases were focused on the later part of the growing season and into the fall when plants are not taking up phosphorus and plant residue from harvested crops and from natural vegetation losing leaves increases the amount of available phosphorus in the soil, which then increases the amount of phosphorus available for transport. There were improvements in TP concentrations at low discharges in spring, possibly because of improvements in phosphorus control at WWTPs.

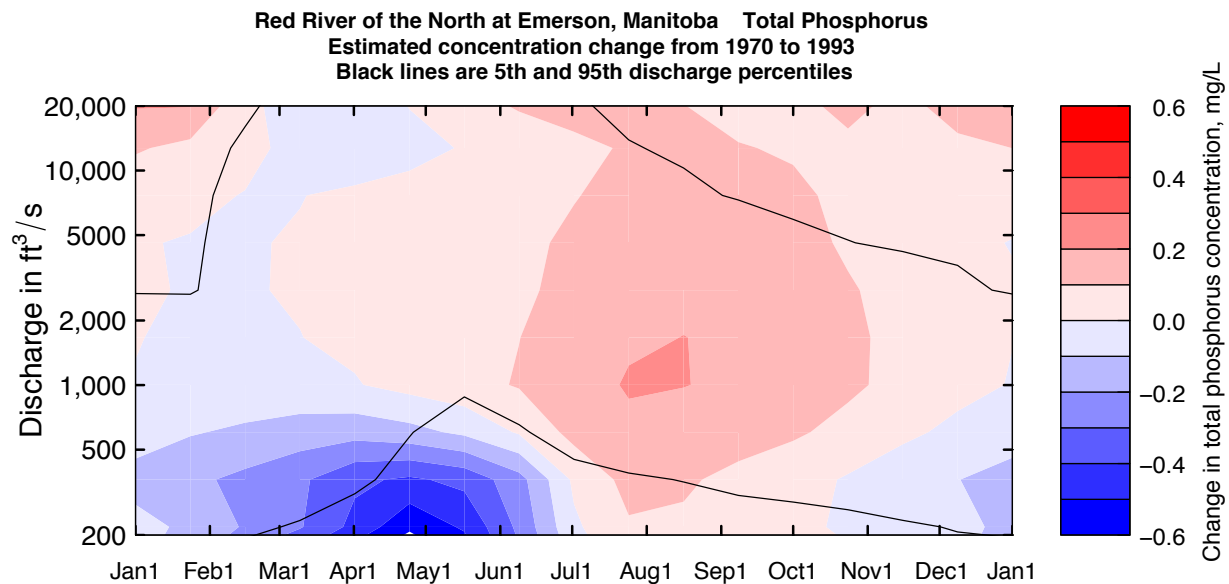


Figure 6.21. Estimated total phosphorus concentration change the Red River of the North at Emerson, Manitoba, from 1970 to 1993.

From 1993 to 2012 (fig. 6.22), there were increases in TP at lower discharges particularly in fall, winter, and spring. More investigation needs to be done as to the causal factors for this as TP flux from WWTPs has been quite stable (fig. 6.4). Potential causal factors that warrant future study include changes in cropping in the Red River Basin, such as an increase in the planting of corn that may contribute to additional phosphorus in the Basin or a change in the timing of phosphorus applications, increasing population in the Red River Basin, the unreported minor wastewater treatment plants in North Dakota, and a decrease in cropland in the Conservation Reserve Program.

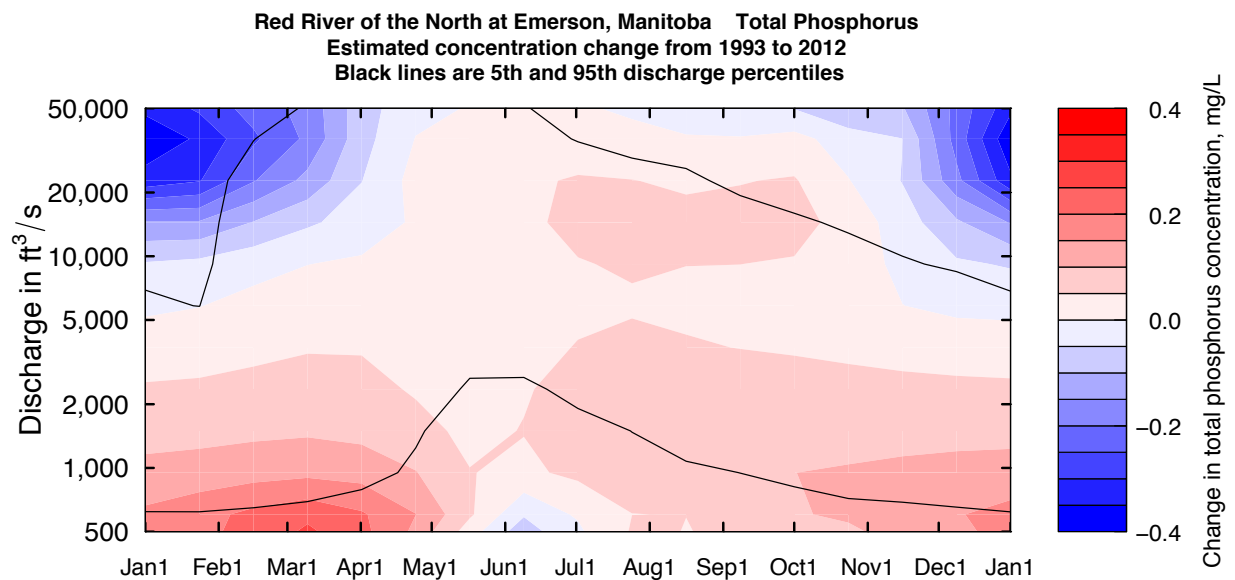


Figure 6.22. Estimated total phosphorus concentration change the Red River of the North at Emerson, Manitoba, from 1993 to 2012.

WRTDS estimates the concentration based on time, discharge, and season, and, therefore, can show how concentration at a particular discharge can change over time. Figures 6.23 and 6.24 estimate the TP concentrations on January 15, April 15, July 15, and October 15 of each year at the 25th, 50th, and 75th percentiles of discharge for each month over each period, 1970-

1993 and 1993-2012. For example, the percentiles used in the January 15 plot in figure 6.23 (upper-left) are calculated using all January streamflows from 1970 through 1993.

Figure 6.23 shows that for 1970-1993, the highest estimated concentrations are generally at the 75th percentile of discharge in April when phosphorus is transported to the river with spring runoff. The lowest concentrations tend to be in October, or when higher discharge occurs in January. When discharge is low in January (524 cfs, 25<sup>th</sup> percentile), water quality is influenced by effluent, and higher concentrations occur than at the 50th or 75th percentiles. In all four dates and at all three percentiles for each date, TP concentration increases in varying degrees from 1970 to the early 1980s, with the smallest increase (smallest slope) occurring January 15. During this period phosphate fertilizer use increased (fig. 6.2) and improvements were made at WWTPs, which matches with fig. 6.23 showing the smallest increase occurring in potentially effluent-dominated January and the largest concentrations occurring during the growing season.

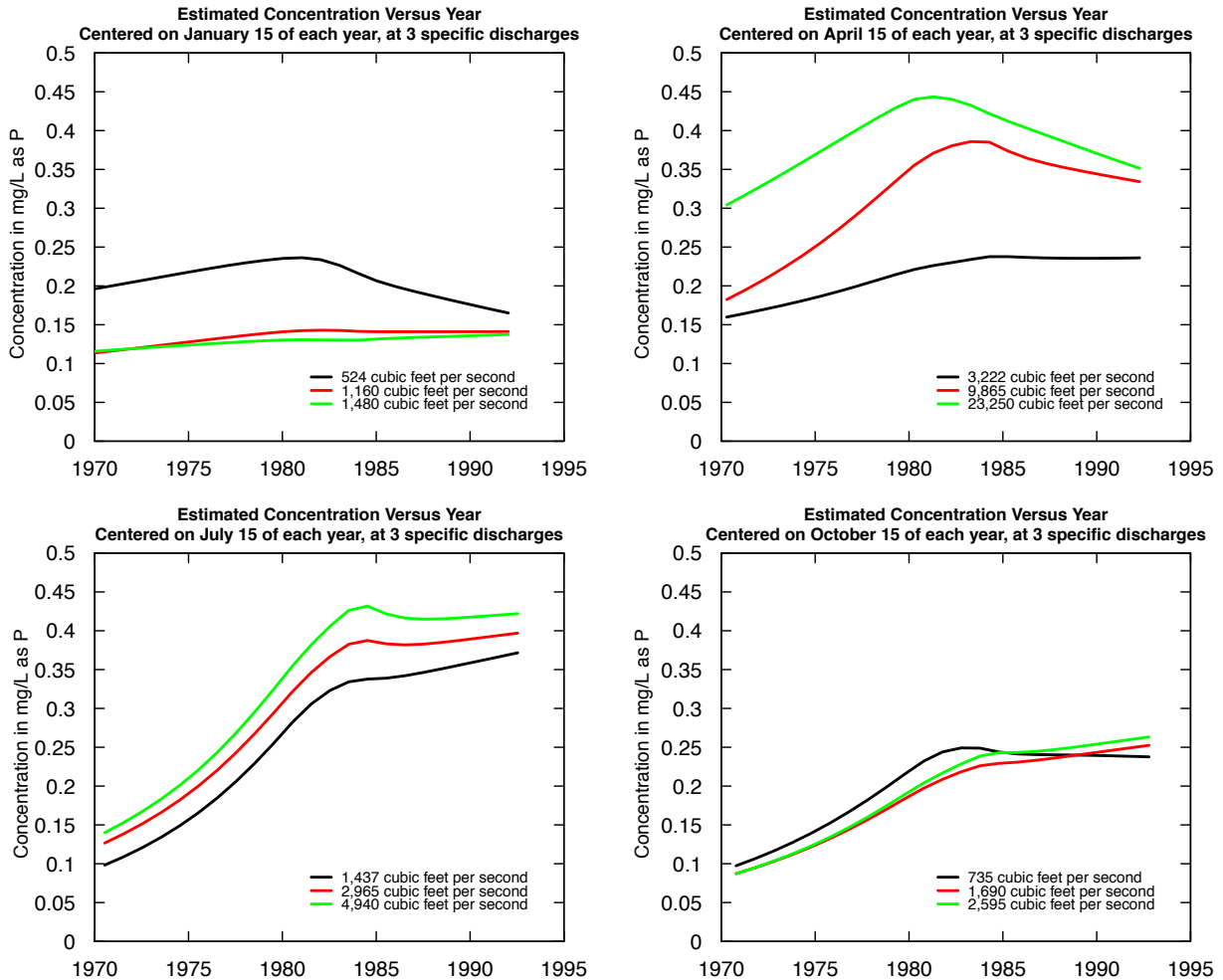


Figure 6.23. Estimated January 1, April 1, July 1, and October 1 total phosphorus concentration over time, at the 25th, 50th, and 75th percentiles of discharge for each month for the period 1970-1993, Red River of the North at Emerson, Manitoba.

Figure 6.24 shows continuing increases in concentrations from 1993 to 2003 or 2004 at which time there is an inflection point at all four dates followed by a change in slope; in the case of April and July, the concentration starts to decline, in the case of October, it has a slightly steeper increase. One potential factor for future investigation is the potential for a change in the timing of fertilizer application. Corn acres planted in the United States were approximately 79.3 million acres in 1992, increasing to 93.5 million acres in 2007 (U.S. Department of Agriculture, National Agricultural Statistics Service, 2013). Depending on the type of tillage used and other

individual factors such as soil type, fall application of phosphorus fertilizer can be the most effective period (Rehm, 2013).

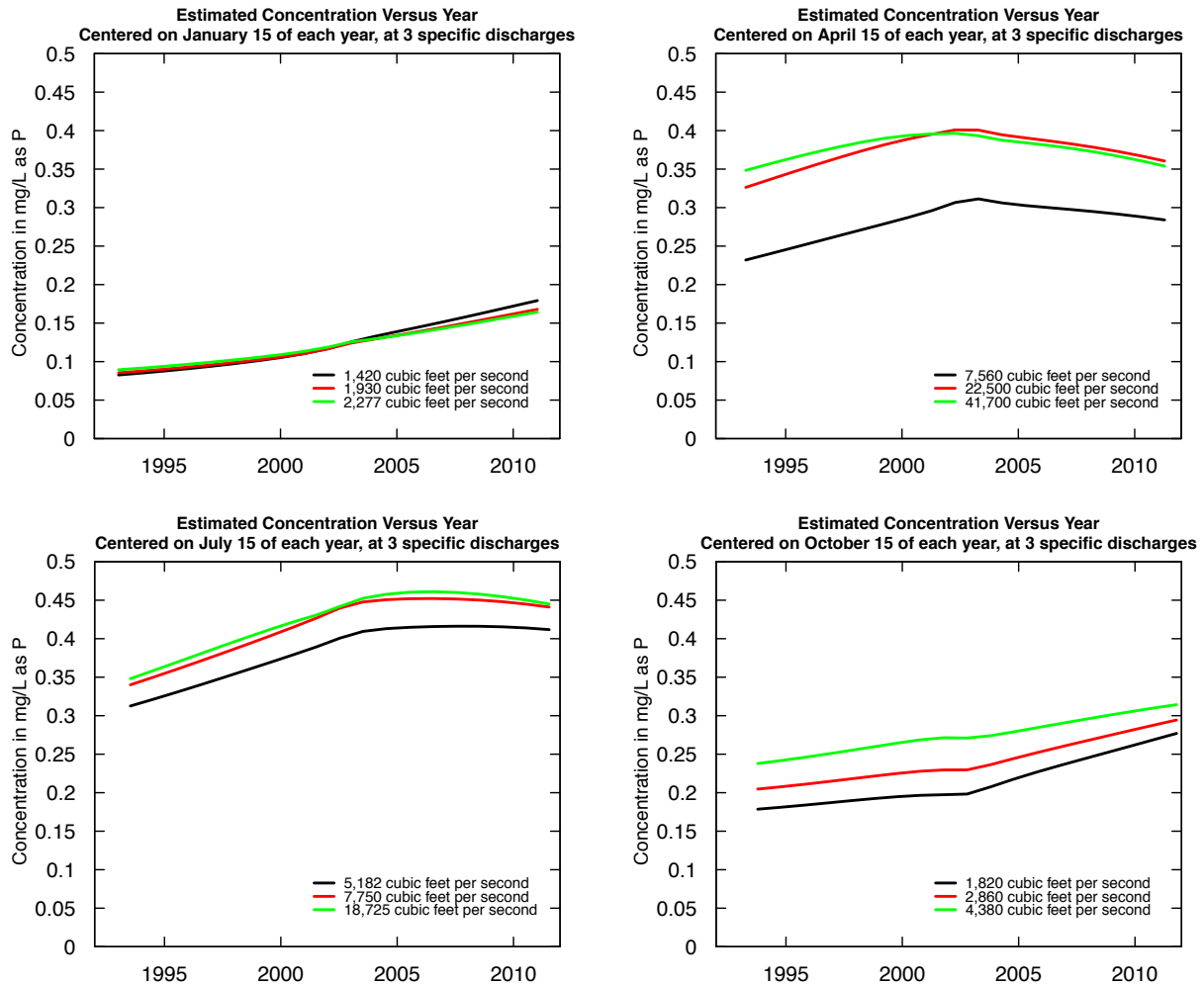


Figure 6.24. Estimated January 1, April 1, July 1, and October 1 total phosphorus concentration over time, at the 25th, 50th, and 75th percentiles of discharge for each month for the period 1993-2012, Red River of the North at Emerson, Manitoba.

### 6.5.1.2. Numerical Results

The following results show flow-normalized concentration (table 6.1) and flux (table 6.2) changes between specific years in each analysis period. Flow-normalized concentrations and fluxes consistently increased in the first half of period 1 (1970-1993) and decreased slightly in

the second half. In the second period (1993-2012), there were small increases in the first half of the period and small decreases in the second half of the period, similar to the shape of national agricultural phosphate use for that period (fig. 6.2).

Table 6.1. Changes in total phosphorus flow-normalized concentration between three time points in period 1, 1970-1993, and three time points in period 2, 1993-2012, for the Red River at Emerson, Manitoba.

Time span	Change, mg/L	Slope, mg/L/year	Change, percent	Slope, percent per year
1971 to 1981	0.073	0.0073	35	3.5
1971 to 1991	0.036	0.0018	17	0.87
1981 to 1991	-0.037	-0.0037	-13	-1.3
1993 to 2003	0.065	0.0065	29	2.9
1993 to 2012	0.051	0.0027	23	1.2
2003 to 2012	-0.014	-0.0016	-4.9	-0.54

mg/L, milligrams per liter,

Table 6.2. Changes in total phosphorus flow-normalized flux between three time points in period 1, 1970-1993, and three time points in period 2, 1993-2012, for the Red River at Emerson, Manitoba.

Time span	Change, kg/day	Slope, kg/day/year	Change, percent	Slope, percent per year
1971 to 1981	1,175	118	47	4.7
1971 to 1991	501	25	20	0.99
1981 to 1991	-675	-67	-18	-1.8
1993 to 2003	1,941	194	31	3.1
1993 to 2012	263	14	4.2	0.22
2003 to 2012	-1,678	-186	-20	-2.3

kg, kilograms

### 6.5.2. WRTDS Results for the Red River at Fargo, North Dakota-Moorhead Minnesota

Figure 6.25 shows observed and estimated concentrations and fluxes for period 1 (1970-1993) and figure 6.26 shows the same for period 2 (1993-2012). For period 1, the observed and flow-normalized (green line in lower-left of fig. 6.25) concentrations show a decline in TP in the

Red River at Fargo-Moorhead from 1970-1993. The flux is much more variable with years of comparatively high flux and more years with comparatively low flux. The flow-normalized flux (green line in lower-right of fig. 6.25) shows a fairly consistent flux across the period. The two, slightly overlapping analysis periods provide different estimates for the year 1993, showing the impact that discharge conditions have on the estimates. In the first period, estimates for 1993 are based on comparatively drier conditions, while in the second period the estimates for 1993 are based on wetter conditions.

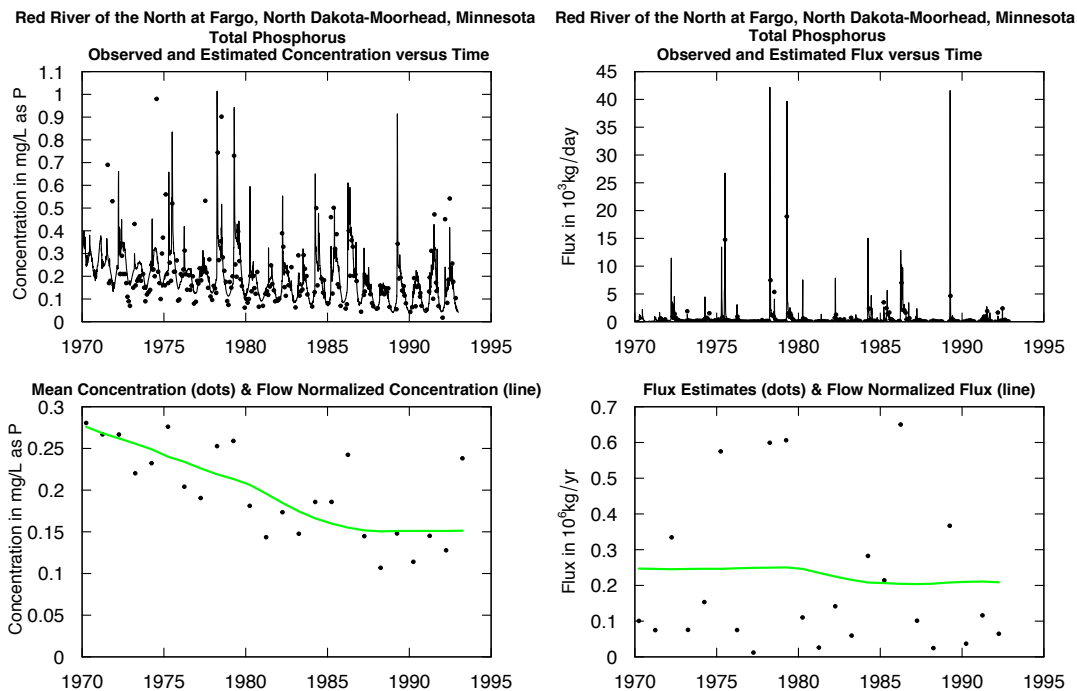


Figure 6.25. Observed and estimated total phosphorus concentrations and fluxes in the Red River of the North at Fargo, North Dakota-Moorhead, Minnesota, 1970-1993.

In the second period (fig. 6.26), flow-normalized concentration and flux have a similar pattern of level conditions from 1993 to about 2005, then a decline from about 2006 through 2012. WRTDS recommends at least 200 samples over 20 years; however, the second period (1993-2012) for Fargo-Moorhead had only 165 samples. Testing by Hirsch and De Cicco (2015) has shown that in some cases WRTDS can produce reliable estimates of mean concentrations or

mean fluxes with data sets as small as 60 samples spanning periods as short as a decade. Because the dataset for Fargo-Moorhead was much larger and longer than the case described in testing, it was used for this analysis.

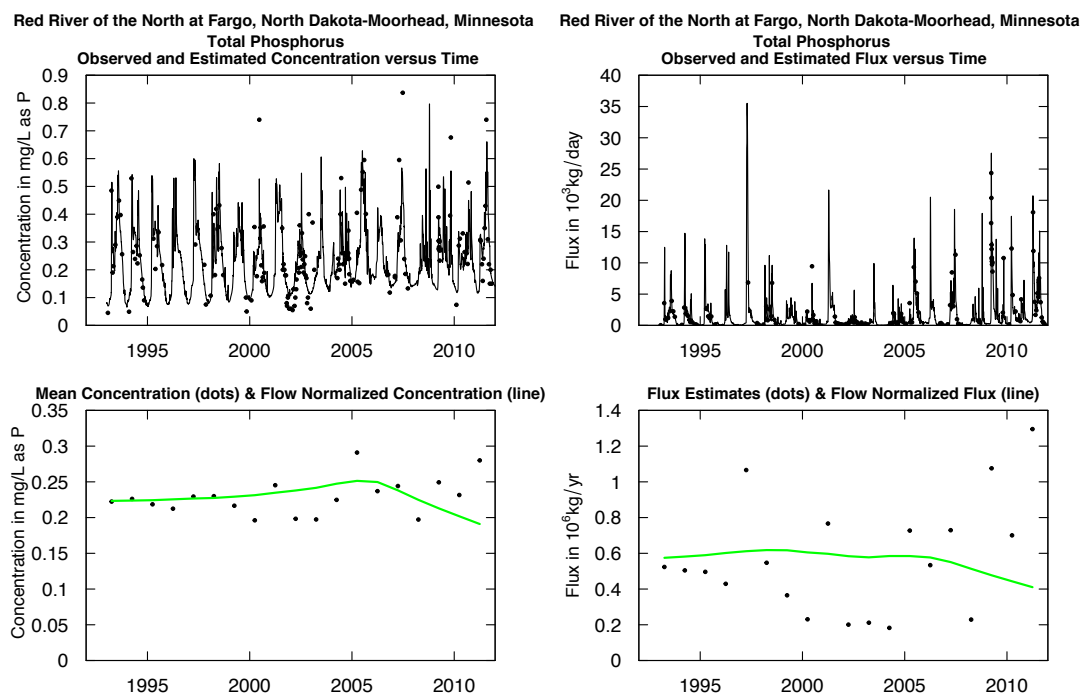


Figure 6.26. Observed and estimated total phosphorus concentrations and fluxes in the Red River of the North at Fargo, North Dakota-Moorhead, Minnesota, 1993-2012.

The flux bias statistic for the first period was 0.148, indicating that there may be some bias in the flux estimates. For the second period, the flux bias statistic was 0.0362. Diagnostic plots provided by the WRTDS modeling process are provided in Appendix D and do not indicate any obvious problems with the first period, other than one extremely large flux estimate that was much larger than the observed value.

### 6.5.1.1. Estimates of Concentration and Flux as a Function of Time and Discharge

Contour plots in figures 6.27 and 6.28 estimate concentration change over a time and discharge grid in the 1970-1993 and 1993-2012 periods. Figure 6.27 shows improvements in TP

over all days at almost all discharges below about 1,000 cubic feet per second (cfs). There are increases during the growing season above about 2,000 cfs, when TP could wash off the landscape. From 1993 to 2012 (fig. 6.28), there were improvements during high discharge in the winter and spring and at low discharge during midsummer. TP increases are estimated during low discharge in the winter and high discharge in the fall. More investigation needs to be done as to the causal factors for these changes.

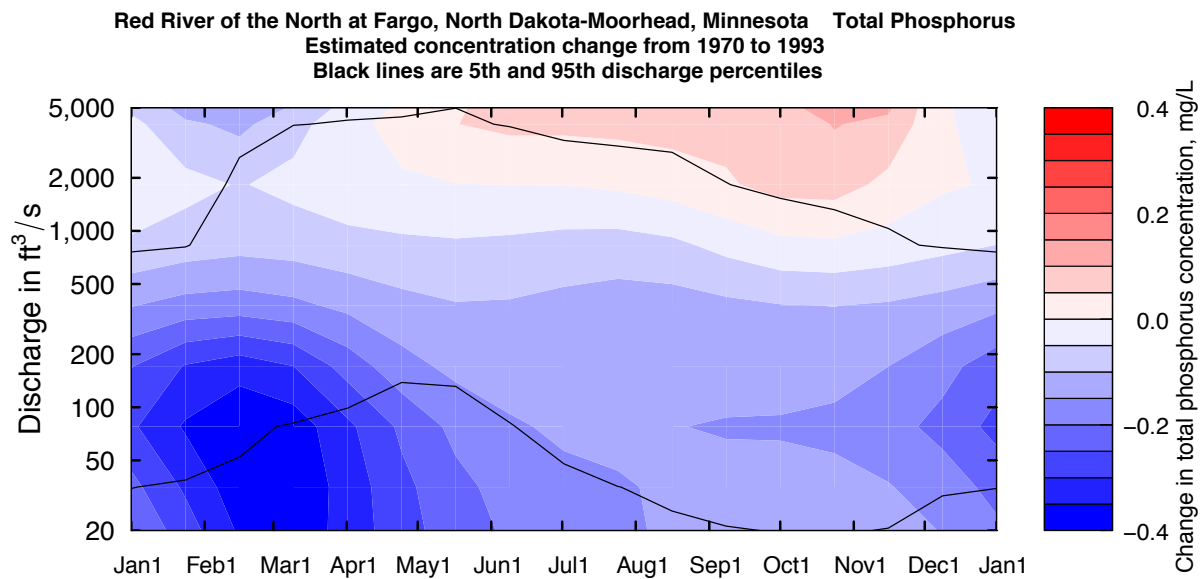


Figure 6.27. Estimated total phosphorus concentration change in the Red River of the North at Fargo, North Dakota-Moorhead, Minnesota, from 1970 to 1993.

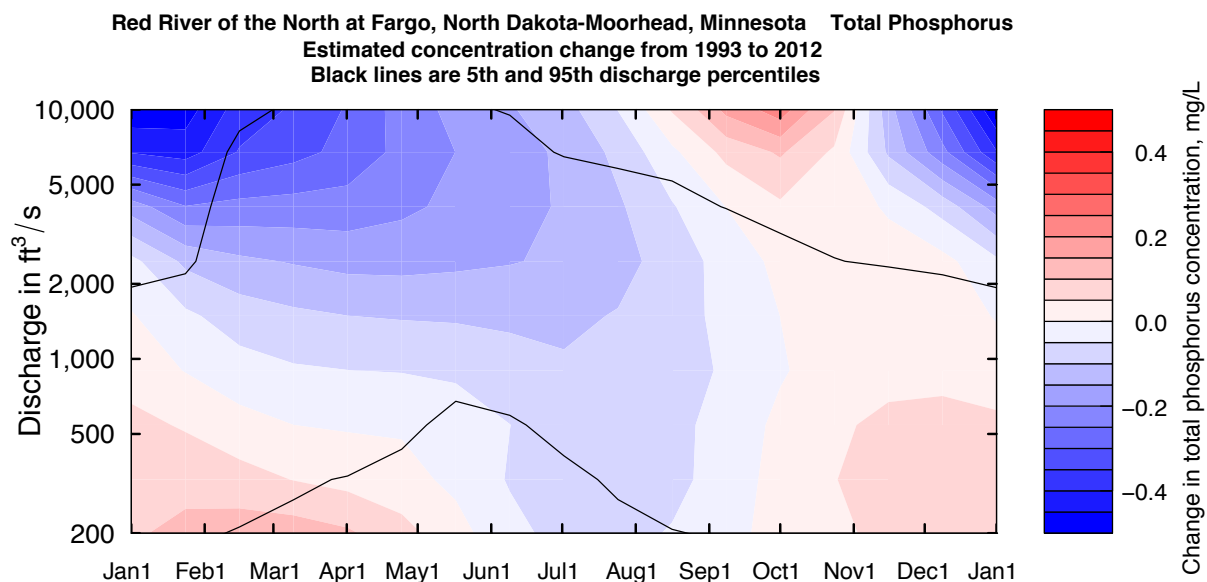


Figure 6.28. Estimated total phosphorus concentration change in the Red River of the North at Fargo, North Dakota-Moorhead, Minnesota, from 1993 to 2012.

Figures 6.29 and 6.30 show estimates of TP concentration at the 25th, 50th, and 75th percentiles of discharge for January 15, April 15, July 15, and October 15 of each analysis period. The percentiles are based on January, April, July, and October discharge percentiles for the two periods, 1970-1993 and 1993-2012. Figure 6.29 is consistent with the other results that show a decline in TP from 1970 to 1993 at Fargo-Moorhead. This decline was consistent at all three discharge values shown, representing the 25th, 50th, and 75th percentiles for January, April, July, and October. These declines are in contrast to increases for the same periods at Emerson. More examination of intervening influences is needed to understand these differences.

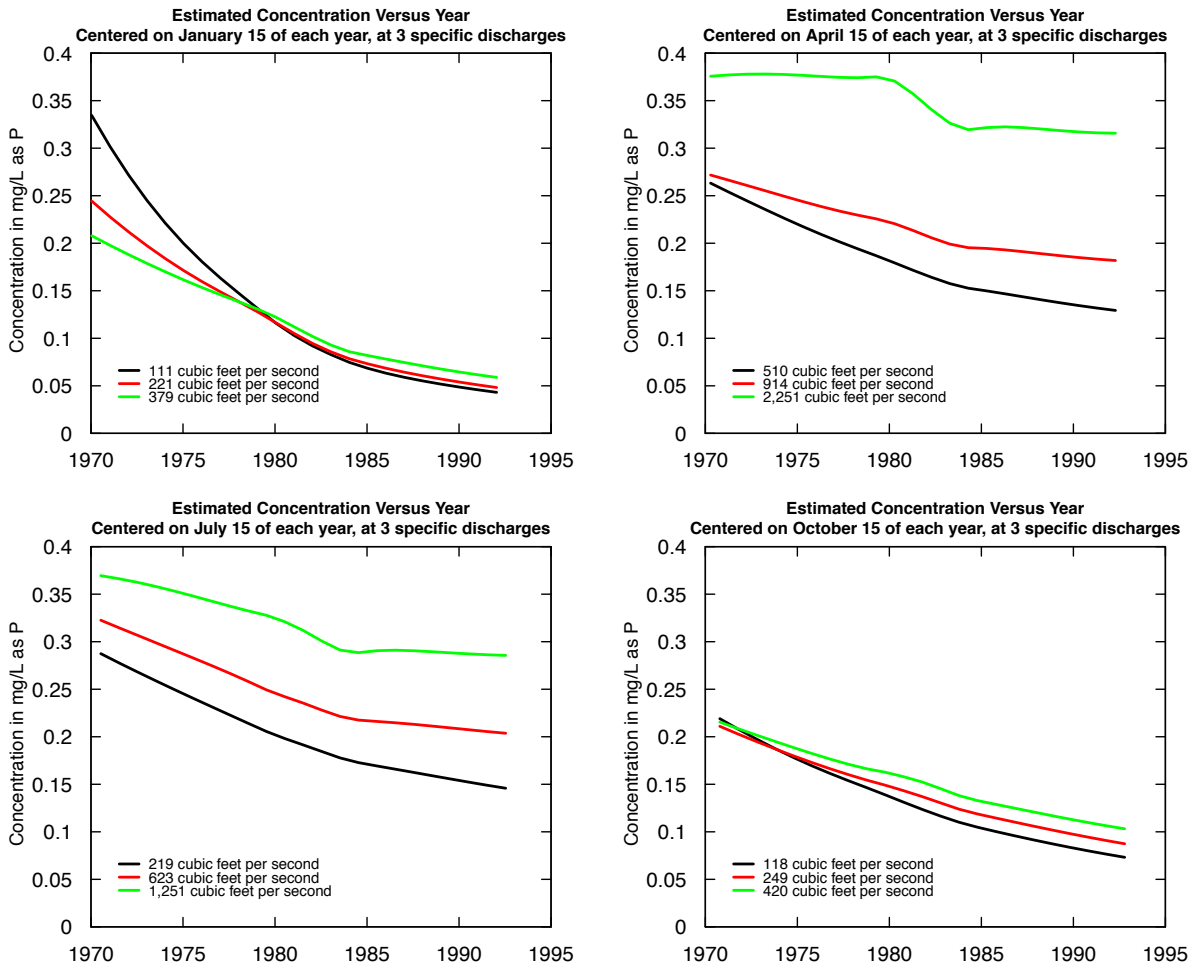


Figure 6.29. Estimated January 1, April 1, July 1, and October 1 total phosphorus concentration over time at the 25th, 50th, and 75th percentiles of discharge for each month for the period 1970-1993, Red River of the North at Fargo, North Dakota-Moorhead, Minnesota.

Generally steady to declining concentrations are shown in figure 6.30 for the 1993-2012 period, a period in which fertilizer use was more stable. The exception is the 75th percentile for April 15, which has shown an increase in concentration. These patterns also differ from Emerson during the same period and do not show the 2003-2004 inflection point.

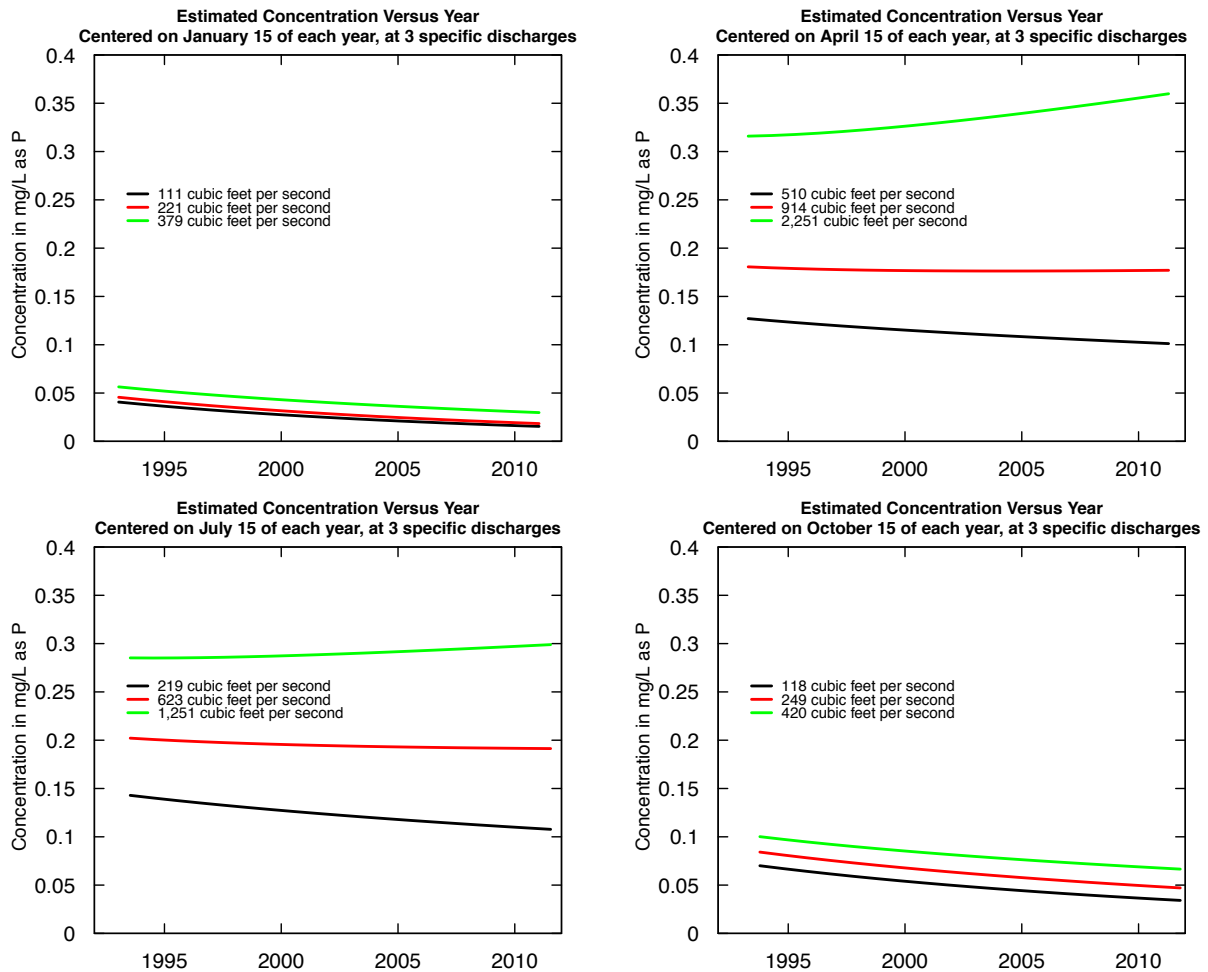


Figure 6.30. Estimated January 1, April 1, July 1, and October 1 total phosphorus concentration over time at the 25th, 50th, and 75th percentiles of discharge for each month for the period 1993-2012, Red River of the North at Fargo, North Dakota-Moorhead, Minnesota.

### 6.5.1.2. Numerical Results

The following tables (6.3 and 6.4) show flow-normalized concentration and flux changes between specific years in each analysis period (period 1, 1970-1993, and period 2, 1993-2012). Flow-normalized concentrations and fluxes consistently declined in all comparisons in period 1, which is a different pattern than that seen at Emerson. There were increases in the first half of the period 2 and decreases in the second half of the period, which is more like the results for Emerson.

Table 6.3. Changes in total phosphorus flow-normalized concentration between three time points in period 1, 1970-1993, and three time points in period 2, 1993-2012, for the Red River of the North at Fargo, North Dakota-Moorhead, Minnesota.

Time span	Change, mg/L	Slope, mg/L/year	Change, percent	Slope, percent per year
1971 to 1981	-0.073	-0.0073	-27	-2.7
1971 to 1991	-0.120	-0.0059	-44	-2.2
1981 to 1991	-0.045	-0.0045	-23	-2.3
1993 to 2003	0.018	0.0018	8.2	0.82
1993 to 2012	-0.043	-0.0022	-19	-1.0
2003 to 2012	-0.061	-0.0068	-25	-2.8

mg/L, milligrams per liter

Table 6.4. Changes in total phosphorus flow-normalized flux between three time points in period 1, 1970-1993, and three time points in period 2, 1993-2012, for the Red River of the North at Fargo, North Dakota- Moorhead, Minnesota.

Time span	Change, kg/day	Slope, kg/day/year	Change, percent	Slope, percent per year
1971 to 1981	-30	-3	-4.5	-0.45
1971 to 1991	-97	-4.8	-44	-0.72
1981 to 1991	-66	-6.6	-10	-1.0
1993 to 2003	7	0.7	0.44	0.044
1993 to 2012	-536	-28	-34	-1.8
2003 to 2012	-543	-60	-34	-3.8

kg, kilograms

## 6.6. Discussion

Total phosphorus concentration and flux (both standard and flow-normalized) increased in the 1970s at Emerson, Manitoba, indicating phosphorus was likely being transported to streams during runoff events. A very different pattern occurred at Fargo-Moorhead with declines in TP concentration, highly variable flux, and flat flow-normalized flux over the first period (1970-1993). The reason for the difference is not known at this time, but differences in agriculture in the northern and southern parts of the Basin are potential direction for future

research. While TP concentrations continually change, in the second period (1993-2012) they were generally decreasing during spring runoff at Emerson and Fargo-Moorhead, perhaps because of improved agricultural practices and declines in the use of phosphorus as fertilizer (figs. 6.2 and 6.3). Agricultural subsurface tile drains are often suggested as sources of phosphorus; however, tile drains decrease surface runoff and promote infiltration, where the phosphorus can bind to soil particulates. The resulting TP contribution from surface runoff and tile drainage is a complex pattern depending on soil characteristics and the tile drainage system. In a study in phosphorus rich soils in eastern Wisconsin (Ruark et. 2012), flow-weighted concentrations of TP were higher from surface water than from drain tiles and surface water was the dominant loss pathway for TP at each site studied. Tile drain TP contributed to total basin flux, but was lower than surface-runoff flux (Ruark et al., 2012). In a study of tile drains in the Red Lake River Basin (a tributary of the Red River upstream from Emerson), the Red Lake Watershed District found that TP from tile drainage was “minimal” and concluded that tile drains generally should have a positive impact on TP in the Red River Basin (with the unfortunate side effect of higher nitrate levels; Red Lake Watershed District, Red Lake River Watershed District, 2006 and 2009).

At Fargo-Moorhead, there was a large decline in January (low discharge) concentrations in 1970-1993 followed by a continued but more gradual decline in 1993-2012. The phaseout of phosphorus in laundry detergent in the U.S. was accomplished by 1994 (Litke, 1999), the State of Minnesota (2005) banned phosphorus use in lawn fertilizer in 2005, and phosphorus was removed from dishwasher detergent in the U.S. in 2010 (Shogren, 2010). These changes may have contributed to small declines in TP coming from WWTPs or to small seasonal declines in urban runoff. The TP story appears to be more complex at Emerson and investigation of the

intervening tributaries may help explain this, unfortunately, there are not enough data at most other sites for the type of analyses done here.

As with other work in the region that has addressed discharge (and climate) variability, this work highlights how variable discharge affects water resources. Total phosphorus flux is an ongoing concern, particularly for Lake Winnipeg. However, TP concentrations and fluxes when normalized for flow decreased at the end of the period of record for Emerson and Fargo-Moorhead, indicating that climate is an important contributor to flux – increased discharge caused by wetter conditions from 1993 through 2012, caused increases in the total amount of TP exported to Canada. Climate related changes in flux are difficult or costly to control (such as through the incorporation of settling ponds or buffer stripes); however, the flow normalizations show that, as agriculture has continued to be the dominant land use and population in the Basin has increased, flow-normalized flux at Fargo-Moorhead has declined. The pattern is not as clear at Emerson, indicating the importance of tributaries not studied here.

### **6.7. Future Research**

Work will be continued to relate the changes in TP at Emerson and Fargo-Moorhead to tributary TP concentrations and fluxes. Particularly in the first period (1970-1993), Emerson and Fargo-Moorhead show very different patterns that could likely be explained by tributary contributions between the two points. In addition, more work needs to be done to examine causal factors such as changes in WWTP practices, changes in agricultural practices, in-stream processes that may consume phosphorus or release it from bed sediment, and changes in Conservation Reserve Program acreage that might affect soil erosion and the transport of phosphorus to streams. This will help to scientifically identify ways that TP fluxes might be reduced in the future.

## CHAPTER 7. SUMMARY AND CONCLUSIONS

Brekke et al. (2009) stated, from a Federal perspective, that trend analysis related to climate change should be “conducted over large areas affected by similar weather systems.” Such analysis of climate related influences on streamflow and water quality were done for the north central U.S. and for specific Basins, the Red River of the North and the Souris River, that have International water-quantity and water-quality concerns as they are shared resources with Canada.

One of the key issues in the north central U.S. is that larger floods have tended to occur in the north central U.S. from the 1970s to the present. The attribution of these changes is of much interest: is this natural, long-term variability, is it climate-change driven? For future water resources management, understanding the reasons for these changes and the potential of long-term wet or dry periods is important. Therefore, long-term precipitation, temperature, and streamflow records were used to compare changes in precipitation and potential evapotranspiration to changes in runoff within 25 stream basins.

Runoff patterns are smoother than precipitation patterns in the region because the land surface provides a buffer to even out the variations in precipitation when it results in runoff. When precipitation increases during dry periods, some of the increased precipitation goes to ET, storage in soil, groundwater, and lakes rather than to the stream, until the water-storage capacity of the landscape is exceeded and excess precipitation is then lost to runoff. Likewise, when conditions are wet and precipitation decreases, moisture stored in the soil dampens the short-term variability in runoff. Nevertheless, if precipitation is intense (one anticipated impact of climate change) and exceeds the rate of infiltration, runoff can occur whether or not the soil is saturated.

Climate and soils conditions can help explain differences in basins in the north central U.S. respond to changes in precipitation. Soils in the Dakotas dry out more often than they do in Missouri for example and initial increases in precipitation in the northwest part of the study area go into soil storage while initial increases in precipitation in the south go into runoff. If a wet period is long enough in the northwest, the excess precipitation goes into runoff as well. The wet and dry periods are different in timing and duration in the winter-spring and summer-autumn seasons confirming that precipitation changes do not change uniformly over a calendar year, emphasizing the need for seasonal analysis. The changes are complex, each one different from the others (in length, severity, seasonality, and regional coverage).

Changes in runoff in the north central U.S. are closely related to changing precipitation patterns. Historical changes in the region appear to be more consistent with complex transient shifts in seasonal climatic conditions than with gradual climate change. Periods of highest flood risk and the magnitude of large floods are consistent with seasonal changes in precipitation combined with multi-year moisture-surplus conditions that become more important in the northern and western basins. This suggests that recent increases in runoff in this area are not primarily land-use change driven.

Although anthropogenic changes may be affecting climate and runoff in subtle ways not yet evident in the runoff records or climatic data analyzed in this paper, it appears that runoff changes for this region are consistent with observations in paleo-climatic records and with natural climatic variability related to long-term fluctuations in global ocean temperature and atmospheric pressure anomalies. Intervals between extreme wet or dry periods seem to be random rather than periodic, indicating nonlinear dynamical behavior. The dominant wet

climatic anomaly of the 20th century and the early 21st century and the increase in autumn precipitation beginning in mid-to-late 1970s may be another transient shift.

Climate variability expressed as precipitation is a major driver of changes in runoff. An additional important climate variable is temperature, expressed in this study as PET. Recent temperature increases in the January-June period would be expected to increase PET. PET tends to be somewhat higher for comparable precipitation values during the post-1970 periods compared with the pre-1970 periods. However, the changes are relatively small compared to the overall temporal variability of PET and very small compared with temporal variability in precipitation. Therefore, the PET increases turned out to be a negligible contributor to the water-balance analysis. Of course, larger temperature changes in future years may be important drivers of future runoff changes.

Overall, the scale of historical precipitation variability in both seasons is considerably larger than the scale of historical PET variability, so precipitation changes are expected to be the dominant driver of runoff changes. However, the water-balance analysis shows that both PET and precipitation are important for explaining historical runoff variability and they explain the majority of the spatial/temporal variability. Land-use/other effects may explain much of the remaining variability in seasonal runoff. While the water-balance may explain the climate effects on 7-day high runoff, the highly variable nature of 7-day high runoff makes it difficult to discern a relation between 7-day high runoff and relatively small land-use effects.

Researchers have linked a shift in the timing of runoff in “snowmelt-fed rivers” to a warming global climate. U.S. average temperature has increased across the country and trends toward earlier snowmelt runoff have been observed in New England, New York, and eastern North America, California and the western U.S., and Canada. At the same time, numerous

studies have reported increases in precipitation in all seasons, with the largest trends observed in fall. Consequently, at some locations, fall streamflow has been increasing. Increases in fall precipitation may or may not be represented in annual peak streamflow, especially in snowmelt-dominated areas where the typical peak still occurs in the spring. However, there is the possibility that a trend toward earlier snowmelt, or earlier spring, may be confounded by a concurrent increase in the occurrence of annual peaks in the summer or fall.

Annual peak streamflow data were divided into two populations, snowmelt/spring and summer/fall, to test the hypotheses that, because of changes in precipitation regimes, the odds of summer/fall peaks have increased and, because of temperature changes, snowmelt/spring peaks happen earlier.

The Palmer Hydrologic Drought Index (PHDI, a measure of long-term cumulative hydrological drought and wet conditions, which reflect groundwater conditions, reservoir levels, and other long-term hydrologic conditions) lagged 2 months was used to control for hydrologic droughts and wet periods that might occur randomly at the end of record and unduly influence a trend. When also controlling for difference in climate and location (based on climate zones and ecological regions), the odds of peaks occurring in the summer or fall are increasing. The coefficient for PHDI2 was negative, indicating that when PHDI2 is positive (long-term wet conditions two months earlier than the peak, such as a wet fall or winter snow accumulation) the odds of the peak of the year occurring in the summer or fall decrease (moisture storage favors snowmelt/spring peaks).

When examining the snowmelt/spring peak series for changes in the timing of the peak, evidence was found for a general change to earlier peaks in the northern regions of the study area. The likely cause for this is that the strongest U.S. surface air temperature warming in 1950-

2000 occurred in the spring over the northwestern U.S. and the northern plains. In northern portions of the study region, snowmelt/spring peaks are occurring earlier by 8.7 to 14.3 days. For summer/fall peaks there was little evidence for changes in timing beyond the north central (Red River Basin) portion of the study area.

Tree-ring chronologies and historical precipitation data in a region around the Souris River Basin, were analyzed to model past long-term variations of precipitation. Using multiresolution decomposition of the tree-ring chronologies in the study area to model long-term seasonal precipitation shows that precipitation varies on long-term, multi-decadal time scales: 16, 32, and 64 years. The time scales vary with location in the study area and with season. The most frequently used wavelet voice over all sites was the 64-year wavelet.

One issue is that the tree-ring chronologies did not have tree rings recent enough to model the wet period at the end of the precipitation period of record. The tree-ring record ends at approximately the same time as an abrupt change from dry to wet conditions in the early 1990s. However, the recent wet period seems to have started earlier in the summer and fall (July-October) and in some cases could be modeled using the decomposed chronologies. The models show very high precipitation in the first half of the 1800s and historic accounts corroborate this. The recent wet period may be similar to that of the 1800s and be part of natural variability on a very long time scale.

There is a growing awareness of the impact of climate variability or change on water quality. In the north central U.S., increases in TP concentrations occurred in the Red River of the North (which exports phosphorus to Canada) during high streamflow (discharge) in the 1970s (when phosphorus concentrations were increasing), indicating phosphorus was likely being transported to streams during runoff events. By the 2000s, TP had declined somewhat at high

streamflow (less phosphorus being transported to streams, perhaps because of improved agricultural practices and declines in the use of phosphorus as fertilizer).

As with other work in the region that has addressed discharge (and climate) variability, this work highlights how variable streamflow affects water resources. Total phosphorus flux (load, the amount transported in a stream, a function of concentration and discharge) has increased over time and is an ongoing concern, particularly for Lake Winnipeg. However, TP concentrations and fluxes show a different story when normalized for flow. Flow-normalized concentrations fluxes have decreased at Fargo, North Dakota-Moorhead, Minnesota, indicating that part of the reason for increased flux is climatic - increased discharge caused by wetter conditions from 1993 through 2012. This is a mixed message, as climate related changes in flux are difficult to control and are concerning; however, flow normalization shows that while population in the Basin has increased and corn acreage has increased, flow-normalized flux at Fargo-Moorhead has declined. The picture is more complex at Emerson, which shows an increase flow-normalized concentration and flux in the 1970s and 1980s followed by periods, decrease and increase, with a decrease since about 2005.

This research contributes to the quantification of the climate and land-use effects on streamflow and water quality. It also quantifies changes in seasonality and timing in peak streamflow. These changes provide new opportunities and risks for water managers and water users. In some cases, peak streamflow in summer and fall may be captured in reservoirs and help to extend irrigation or recreation seasons. However, changes have implications for the operation of flood-control dams. If a reservoir is normally drawn down in the fall to create storage for spring runoff, an increase in summer or fall peak streamflow may necessitate a change in the rules of operation. Lead time for flooding is also dramatically different between floods in the two

seasons. Floods generated by snowmelt usually have generous lead time for forecasting and flood-fighting operations. Floods generated by intense summer or fall precipitation do not have that kind of lead time. Understanding the nature of these changes is important to efficient water use and protection from the extremes of floods and droughts.

The modeled precipitation in the Souris River Basin region and the accounts of past pluvial and drought periods are characterized by sudden shifts from wet to dry and dry to wet. These sudden shifts have been documented elsewhere in the region and appear to be characteristic of climate in the northern Great Plains. By describing regional long-term variability in seasonal precipitation, these results will be used to inform future work.

### **7.1. Future Research**

Work will be continued to relate the changes in TP at Emerson, Manitoba, and Fargo, North Dakota-Moorhead, Minnesota to tributary TP concentrations and flux and anthropogenic causal factors such as changes in WWTP practices, changes in agricultural practices, in-stream processes that may consume phosphorus or release it from bed sediment, and changes in Conservation Reserve Program acreage that might affect soil erosion and the transport of phosphorus to streams. This will help to scientifically identify ways that TP fluxes might be reduced in the future.

## REFERENCES

- Allan, J.D., 1995, Stream ecology—structure and function of running waters: London, Chapman & Hall, 388 p.
- Allsopp, T.R., 1977, Agricultural weather in the Red River Basin of southern Manitoba over the period 1800 to 1975: Atmospheric Environment Service (CLI-3-77), Downsview, Ontario, 28 pp.
- America's Climate Choices: Panel on Advancing the Science of Climate Change, Board on Atmospheric Sciences and Climate, Division on Earth and Life Studies, National Research Council, 2010, Advancing the science of climate change: The National Academies Press, Washington, DC, 528 p.
- Andersen, J., Hilberg, S., and Kunkel, K., 2012, Historical Climate and Climate Trends in the Midwestern USA *in* U.S. National Climate Assessment Midwest Technical Input Report. J. Winkler, J. Andresen, J. Hatfield, D. Bidwell, and D. Brown, coordinators. Great Lakes Integrated Sciences and Assessments (GLISA) Center, accessed January 17, 2015, at [http://glisa.msu.edu/docs/NCA/MTIT\\_Historical.pdf](http://glisa.msu.edu/docs/NCA/MTIT_Historical.pdf).
- Andersen, T.K., and Shepherd, J.M., 2013, Floods in a changing climate: *Geography Compass*, 7(2), 95-115, DOI: 10.1111/gec3.12025.
- Art, H.W., 1993, Eutrophication, *in* Art, H.W., (ed.), A dictionary of ecology and environmental science (1st ed.): New York, New York, Henry Holt and Company, p. 196.
- Ault, T.R., and St. George, S., 2010, The magnitude of decadal and multidecadal variability in North American precipitation: *Journal of Climate*, v. 23, no. 4, p. 842–850, DOI: 10.1175/2009JCLI3013.1.

- Ball, T., 1992, Climatic change, droughts and their social impact – Central Canada, 1811-20, a classic example *in* C. R. Harington (ed.), *The Year Without a Summer? World Climate in 1816*: Canadian Museum of Nature, Ottawa, Ontario, p. 185-195.
- Bates, B.C., Kundzewicz, Z.W., Wu, S., Palutikof, J.P., (eds.), 2008, *Climate change and water*, IPCC Technical Paper VI, Geneva: Intergovernmental Panel on Climate Change Secretariat, 210 p.,  
[https://www.ipcc.ch/publications\\_and\\_data/\\_climate\\_change\\_and\\_water.htm](https://www.ipcc.ch/publications_and_data/_climate_change_and_water.htm).
- Blair, D., and Rannie, W.F., 1994, *Wading to Pembina: 1849 spring and summer weather in the Valley of the Red River of the North and some climatic implications*: *Great Plains Research*, v. 4, p. 3-26.
- Booy, C., and Lye, L.M., 1986, Accumulated basin storage as a factor in the correlation structure of annual peak flows on the Red River: *Canadian Journal of Civil Engineering*, v. 13, p. 365-374, DOI: 10.1139/l86-049.
- Borris, M., Viklander, M., Gustafsson, A.-M., and Marsalek, J., 2013, Modeling the effects of changes in rainfall event characteristics on TSS loads in urban runoff: *Hydrological Processes*, v. 28, no. 4, p. 1787-1796, DOI:10.1002/hyp.9729.
- Bourne, A., Armstrong, N., and Jones, G., 2002, A preliminary estimate of total nitrogen and total phosphorus loading to streams in Manitoba, Canada: *Manitoba Water Stewardship Manitoba Conservation Report 2002-04*, 49 p.,  
[http://www.gov.mb.ca/conservation/waterstewardship/water\\_quality/quality/nutrient\\_loading\\_report\\_2002-04\\_november\\_2002.pdf](http://www.gov.mb.ca/conservation/waterstewardship/water_quality/quality/nutrient_loading_report_2002-04_november_2002.pdf).

- Brekke, L.D., Kiang, J.E., Olsen, J.R., Pulwarty, R.S., Raff, D.A., Turnipseed, D.P., Webb, R.S., and White, K.D., 2009, Climate change and water resources management – A federal perspective: U.S. Geological Survey Circular 1331, 65 p., <http://pubs.usgs.gov/circ/1331/>.
- Breusch, T.S., and Pagan, A.R., 1979, A simple test for heteroscedasticity and random coefficient variation: *Econometrica*, v. 17, p. 1287-1294.
- Brier, G.W., 1950, Verification of forecasts expressed in terms of probability: *Monthly Weather Review*, v. 78, p. 1-3, DOI: 10.1175/1520-0493(1950)078<0001:VOFEIT>2.0.CO;2.
- Brooks, G.R., St. George, S. Lewis, C.F.M., Medioli, B.E., Nielsen, E., Simpson, S., and Thorleifson, L.H., 2003, Geoscientific insights into Red River flood hazards in Manitoba: Open-File Report 4473, Ottawa, Geological Survey of Canada, 36 pp.
- Bunn, A.G., 2008, A dendrochronology program library in R (dplR): *Dendrochronologia* v. 26, no. 2, p. 115-124, DOI: 10.1016/j.dendro.2008.01.002.
- Bunn, A.G., 2010, Statistical and visual crossdating in R using the dplR library: *Dendrochronologia* v. 28, no. 4, p. 251-258, DOI: 10.1016/j.dendro.2009.12.001.
- Bunn, A.G., Korpela, M., Biondi, F., Campelo, F., Mérian, P., Mudelsee, M., Qeadan, F., Schulz, M., and Zang, C., 2014, dplR: Dendrochronology Program Library in R: R package version 1.6.0.
- Bunn, A.G., Sharac, T.J., and Graumlich, L.J., 2004, Using a simulation model to compare methods of tree-ring detrending and to investigate the detectability of low-frequency signals: *Tree-Ring Research*, v. 60, no. 2, p. 77-90, DOI: 10.3959/1536-1098-60.2.77.
- Büntgen, U., Tegel, W., Heussner, K.-U., Hofmann, J., Kontic, R., Kyncl, T., and Cook, E.R., 2012, Effects of sample size in dendroclimatology: *Climate Research* v. 53, p. 263-269.

- Burn, D.H., Fan, L., Bell, G., 2008, Identification and quantification of streamflow trends on the Canadian Prairies: *Hydrological Sciences Journal*, v. 53, p. 538-549.
- Burns, D.A., Klaus, J., and McHale, M.R., 2007, Recent climate trends and implications for water resources in the Catskill Mountain region, New York, USA: *Journal of Hydrology*, v. 336, no. 1–2, p. 155–170, DOI: 10.1016/j.jhydrol.2006.12.019.
- Canada Department of Resources and Development, 1953, Report on investigations into measures of the reduction of the flood hazard in the greater Winnipeg area, Appendix B, History of Floods on the Red River, Red River Basin Investigation: Water Resources Branch, 124 p.
- Carbon Dioxide Information Analysis Center, 2014, Background: long-term daily and monthly climate records from stations across the contiguous United States, accessed May 12, 2014, at <http://cdiac.ornl.gov/epubs/ndp/ushcn/background.html>.
- Carlyle, W.J., 1984, Water in the Red River Valley of the North: *Geographical Review*, v. 74, no. 3, p. 331-358.
- Case, R.A., and MacDonald, G.M., 1995, A dendroclimatic reconstruction of annual precipitation on the western Canadian Prairies since A.D. 1505 from *Pinus flexilis James*: *Quaternary Research*, v. 44, no. 267-275.
- Case, R.A., and MacDonald, G.M., 2003, Tree ring reconstructions of streamflow for three Canadian Prairie rivers: *Journal of the American Water Resources Association*, v. 39, no. 3, p. 703-716.
- Cayan, D.R., Dettinger, M.D., Diaz, H.F., and Graham, N.E., 1998, Decadal variability of precipitation over western North America: *Journal of Climate*, v. 11, no. 12, p. 3148–3166, DOI: 10.1175/1520-0442(1998)011<3148:DVOPOW>2.0.CO;2.

- Cayan, D.R., Kammerdiener, S.A., Dettinger, M.D., Caprio, J.M., Peterson, D.H., 2001, Changes in the onset of spring in the western United States: *Bulletin of the American Meteorological Society*, v. 82, p. 399-415, DOI: 10.1175/1520-0477(2001)082<0399:CITOOS>2.3.CO;2.
- Christensen, V.G., 2007, Nutrients, suspended sediment, and pesticides in water of the Red River of the North Basin, Minnesota and North Dakota, 1990-2004: U.S. Geological Survey Scientific Investigations Report 2007-5065, 36 p., <http://pubs.usgs.gov/sir/2007/5065/>.
- City of Winnipeg, 2014, Sewer System – Combined sewers, accessed January 15, 2015, at <http://www.winnipeg.ca/waterandwaste/sewage/systemOperation.stm#combined>.
- Clark, R.H., 1950, Notes on Red River floods with particular reference to the flood of 1950: Manitoba Department of Mines and Natural Resources, Winnipeg, Manitoba, Canada.
- Cleveland, W.S., Grosse, E., and Shyu, W.M., 1992, Local regression models, *in* J.M. Chambers and T.J. Hastie (eds.), *Statistical Models in S*: Wadsworth & Brooks/Cole.
- Commission for Environmental Cooperation, 1997, *Ecological regions of North America—Toward a common perspective revised 2006*: Commission for Environmental Cooperation, Montreal, Quebec, Canada, 71 p. and map.
- Committee on Preparing for the Third Decade (Cycle 3) of the National Water Quality Assessment (NAWQA) Program, 2010, *Letter Report Assessing the USGS National Water Quality Assessment Program’s Science Framework*: Washington, D.C., The National Academies Press, ISBN 9780309149754, [http://www.nap.edu/openbook.php?record\\_id=12843](http://www.nap.edu/openbook.php?record_id=12843).

- Cook, B.I., Seager, R., and Miller, R., 2011, Atmospheric circulation anomalies during two persistent North American droughts: 1932–1939 and 1948–1957: *Climate Dynamics*, v. 36, no. 11–12, p. 2339–2355, DOI: 10.1007/s00382-010-0807-1.
- Deser, C., and Blackmon, M.L., 1993, Surface climate variations over the North Atlantic Ocean during winter: 1900–1989: *Journal of Climate*, v. 6, no. 9, p. 1743–1753, DOI: 10.1175/1520-0442(1993)006<1743:SCVOTN>2.0.CO;2.
- Dettinger, M.D., 2005, Changes in streamflow timing in the western United States in recent decades: U.S. Geological Survey Fact Sheet 2005-3018, [http://pubs.usgs.gov/fs/2005/3018/pdf/FS2005\\_3018.pdf](http://pubs.usgs.gov/fs/2005/3018/pdf/FS2005_3018.pdf).
- Dettinger, M.D., Cayan, D.R., 1995, Large-scale atmospheric forcing of recent trends toward early snowmelt runoff in California: *Journal of Climate*, v. 8, p. 606-623, DOI: 10.1175/1520-0442(1995)008<0606:LSAFOR>2.0.CO;2.
- Douglas, E.M., Vogel, R.M., and Kroll, C.N., 2000, Trends in floods and low flows in the United States – Impact of Spatial correlation: *Journal of Hydrology*, v. 240, p. 90-105.
- Durbin, J., and Watson, G.S., 1950, Testing for serial correlation in least squares regression I: *Biometrika*, v. 37, p. 409-428.
- Durbin, J., and Watson, G.S., 1951, Testing for serial correlation in least squares regression II: *Biometrika*, v. 38, p. 159-178.
- Durbin, J., Watson, G.S., 1971, Testing for serial correlation in least squares regression III: *Biometrika*, v. 58, p. 1-19, DOI: 10.1093/biomet/58.1.1.

- Easterling, D.R., Karl, T.R., Mason, E.H., Hughes, P.Y., and Bowman, D.P., 1996, United States Historical Climatology Network (USHCN) monthly temperature and precipitation data: Carbon Dioxide Information Analysis Center: ORNL/CDIAC-87, NDP-019/R3, Oak Ridge National Laboratory, U.S. Dept. of Energy, Oak Ridge, Tennessee.
- Environment Canada and Manitoba Water Stewardship, 2011a, State of Lake Winnipeg: 1999 to 2007: Government of Canada Report, 209 p.,  
[http://www.gov.mb.ca/conservation/waterstewardship/water\\_quality/state\\_lk\\_winnipeg\\_report/pdf/state\\_of\\_lake\\_winnipeg\\_rpt\\_technical\\_high\\_resolution.pdf](http://www.gov.mb.ca/conservation/waterstewardship/water_quality/state_lk_winnipeg_report/pdf/state_of_lake_winnipeg_rpt_technical_high_resolution.pdf).
- Environment Canada and Manitoba Water Stewardship, 2011b, State of Lake Winnipeg: 1999 to 2007 Highlights: Government of Canada Report, 16 p.,  
[http://www.gov.mb.ca/conservation/waterstewardship/water\\_quality/state\\_lk\\_winnipeg\\_report/pdf/state\\_of\\_lake\\_winnipeg\\_rpt\\_highlights\\_english.pdf](http://www.gov.mb.ca/conservation/waterstewardship/water_quality/state_lk_winnipeg_report/pdf/state_of_lake_winnipeg_rpt_highlights_english.pdf).
- Environment Canada, 2013, Manitoba – Red River floods, *in* Flooding Events in Canada – Prairie Provinces, accessed March 21, 2015, at <https://www.ec.gc.ca/eau-water/default.asp?lang=En&n=E0399791-1#MB>.
- Environment Canada, 2014, Adjusted and Homogenized Canadian Climate Data (AHCCD), accessed July 17, 2014, at <https://ec.gc.ca/dccha-ahccd/default.asp?lang=En&n=B1F8423A-1>.
- Falcone, J.A., 2011, GAGES-II Geospatial attributes of gages for evaluating streamflow: U.S. Geological Survey digital spatial dataset,  
[http://water.usgs.gov/GIS/metadata/usgswrd/XML/gagesII\\_Sept2011.xml](http://water.usgs.gov/GIS/metadata/usgswrd/XML/gagesII_Sept2011.xml).
- Ferro, C.A.T., 2007, Comparing probabilistic forecasting systems with the Brier Score: *Weather Forecasting*, v. 22, p. 1076–1088, DOI: 10.1175/WAF1034.1.

Galloway, J.M., 2014, Continuous water-quality monitoring and regression analysis to estimate constituent concentrations and loads in the Red River of the North at Fargo and Grand Forks, North Dakota, 2003–12: U.S. Geological Survey Scientific Investigations Report 2014–5064, 37 p., DOI:10.3133/sir20145064.x.

Galloway, J.M., Vecchia, A.V., Vining, K.C., Densmore, B.K., and Lundgren, R.F., 2012, Evaluation of water-quality characteristics and sampling design for streams in North Dakota, 1970-2008, 304 p., <http://pubs.usgs.gov/sir/2012/5216/>.

Garbrecht, J.D., and Rossel, F.E., 2002, Decade-scale precipitation increase in Great Plains at end of 20<sup>th</sup> century: *Journal of Hydrologic Engineering*, v. 7, no. 1, p. 64-75, DOI: 10.1061/(ASCE)1084-0699(2002)7:1(64).

Georgakakos, A., Fleming, P., Dettinger, M., Peters-Lidard, C., Richmond, T.C., Reckhow, K., White, K., and Yates, D., 2014, Chapter 3: Water Resources. *Climate Change Impacts in the United States: The Third National Climate Assessment*, J.M. Melillo, T.C. Richmond, and G. W. Yohe (eds.), U.S. Global Change Research Program, p. 69-112, DOI: 10.7930/J0G44N6T.

Guido, Z., 2010, Warmer means drier: Comparing the 2000s drought to the 1950s drought: *SW Climate Outlook*, v. 9, no. 2, p. 3-4.

Güler, C., Thyne, G.D., McCray, J.E., and Turner, K.A., 2002, Evaluation of graphical and multivariate statistical methods for classification of water chemistry data: *Hydrogeology Journal*, v. 10, p. 455-474.

Gunderson, Dan, June 18, 2010, Farmers, scientists struggle with Red River phosphorus: Minnesota Public Radio, Environment, accessed March 26, 2014, at <http://www.mprnews.org/story/2010/06/18/phosphorus-run-off-lake-winnipeg>.

- Gutowski, W.J., Hegerl, G.C., Holland, G.J., Knutson, T.R., Mearns, L.O., Stouffer, R.J., Webster, P.J., Wehner, M.F., Zwiers, F.W., 2008, Causes of observed changes in extremes and projections of future changes: Weather and climate extremes in a changing climate, CCSP synthesis and assessment product 3.3: U.S. Climate Change Science Program, 81–116.
- Hamon, W.R., 1961, Estimating potential evapotranspiration: *Journal of the Hydraulics Division, Proceedings of the American Society of Civil Engineers*, v. 87, p. 107–120.
- Harrell, F.E., Jr., 2014, rms: Regression modeling strategies: R package version 4.2-0, <http://CRAN.R-project.org/package=rms>.
- Harrison, S.S., and Bluemle, J.P., 1980, Flooding in the Grand Forks-East Grand Forks area: North Dakota Geological Survey Educational Series 12, Fargo, North Dakota.
- Hastie, T., Tibshirani, R., and Friedman, J., 2001, *The elements of statistical learning – Data mining, inference, and prediction*: Springer Science+Business Media, Inc., New York, 533 p.
- Heim, R.R., Jr., 2002. A review of twentieth-century drought indices used in the United States. *Bulletin of the American Meteorological Society*, v. 83, p. 1149-1165.
- Helsel, D.R., and Hirsch, R.M., 1995, *Statistical Methods in Water Resources*: Elsevier Science B.V., Amsterdam, 529 p.
- Hem, J.D., 1985, *Study and interpretation of the chemical characteristics of natural water*, (3rd ed.): U.S. Geological Survey Water-Supply Paper 2254, 264 p., <http://pubs.er.usgs.gov/usgspubs/wsp/wsp2254>.
- Higgins, J.J., 2004, *Introduction to modern nonparametric statistics*: Pacific Grove, California, Brooks/Cole-Thomson Learning, Inc., 366 p.

Hirsch, R.M, Moyer, D.L., and Archfield, S.A., 2010, Weighted regressions on time, discharge, and season (WRTDS), with an application to Chesapeake Bay River inputs: *Journal of the American Water Resources Association*, v. 46, no. 5, p. 857-880, DOI:

10.1111/j.1752-1688.2010.00482.x.

Hirsch, R.M. and Ryberg, K.R., 2012, Has the magnitude of floods across the USA changed with global CO2 levels?: *Hydrological Sciences Journal*, v. 57, no. 1, DOI:

10.1080/02626667.2011.621895.

Hirsch, R.M., 2014, Large biases in regression-based constituent flux estimates: Causes and diagnostic tools: *Journal of the American Water Resources Association*, v. 50, no. 6, p. 1401–1424, DOI: 10.1111/jawr.12195/full.

Hirsch, R.M., and De Cicco, L.A., 2014, EGRET: Exploration and Graphics for RivEr Trends (EGRET): R package version 2.1.0. <http://CRAN.R-project.org/package=EGRET>.

Hirsch, R.M., and De Cicco, L.A., 2015, User guide to Exploration and Graphics for RivEr Trends (EGRET) and dataRetrieval: R packages for hydrologic data (version 2.0, February 2015): *U.S. Geological Survey Techniques and Methods*, book 4, chap. A10, 93 p., DOI: 10.3133/tm4A10.

Hodgkins, G.A., and Dudley, R.W., 2006, Changes in the timing of winter–spring streamflows in eastern North America, 1913–2002: *Geophysical Research Letters*, v. 33, L06402, DOI: 10.1029/2005GL025593.

Hodgkins, G.A., Dudley, R.W., and Huntington, T.G., 2003, Changes in the timing of high river flows in New England over the 20th century: *Journal of Hydrology*, v. 278, p. 244-252. DOI: 10.1016/S0022-1694(03)00155-0.

- Hoerling, M., Eischeid, J., Easterling, D., Peterson, T., and Webb, R., 2010, Understanding and explaining hydro-climate variations at Devils Lake: A National Oceanic and Atmospheric Administration Climate Assessment, Silver Spring, Maryland.
- Homer, C.G., Huang, C., Yang, L., Wylie, B., and Coan, M., 2004, Development of a 2001 National Land Cover Database for the United States: Photogrammetric Engineering and Remote Sensing, v. 70, no. 7, p. 829-840.
- Hope, E.C., 1938, Weather and crop history in western Canada: Canadian Society of Technical Agriculturists (CSTA) Review, v. 16, p. 347-358.
- Insightful Corporation, 2001, S-PLUS 6 for Windows guide to statistics, volume 2: Seattle, Insightful Corporation, 622 pp.
- Intergovernmental Panel on Climate Change, 2007, Climate change 2007: The physical science basis: Contribution of Working Group I to the fourth assessment report of the Intergovernmental Panel on Climate Change, S. Solomon and D. Qin, et al., (eds.), Cambridge University Press, Cambridge, United Kingdom, and New York.
- International Souris River Board, 2013, Plan of Study for the Review of the Operating Plan Contained in Annex A of the 1989 International Agreement Between the Government of Canada and the Government of the United States: International Souris River Board, Task Force Report.
- Jensen, R.E, No Date, Climate of North Dakota, National Weather Service, North Dakota State University, Fargo, North Dakota: Published online, Northern Prairie Wildlife Research Center Online, Jamestown, North Dakota, <http://www.npwrc.usgs.gov/resource/habitat/climate/index.htm> (Version 02APR98).

- Jones, G., and Armstrong, N., 2001, Long-term trends in total nitrogen and total phosphorus concentrations in Manitoba streams: Manitoba Water Stewardship Manitoba Conservation Report 2001-07, 154 p.,  
[http://www.gov.mb.ca/conservation/waterstewardship/water\\_quality/quality/trend\\_report.pdf](http://www.gov.mb.ca/conservation/waterstewardship/water_quality/quality/trend_report.pdf).
- Karl, T.R., and Knight, R.W., 1998, Secular trends of precipitation amount, frequency, and intensity in the United States: *Bulletin of the American Meteorological Society*, v. 79, p. 231-241, DOI: 10.1175/1520-0477(1998)079<0231:STOPAF>2.0.CO;2.
- Kass, R.E., and Raftery, A.E., 1995, Bayes factors: *Journal of the American Statistical Association*, v. 90, no. 430, p. 773-795.
- Kaufman, L., and Rousseeuw, P.J., 1990, *Finding groups in data—An introduction to cluster analysis*: New York, Wiley, 368 p.
- Kemp, D.D., 1982, The drought of 1804-1805 in central North America: *Weather*, v. 37, no. 2, p. 34-41, DOI: 10.1002/j.1477-8696.1982.tb03543.x.
- Kottek, M., Grieser, J., Beck, C., Rudolf, B., Rubel, F., 2006, World map of Köppen-Geiger climate classification updated: *Meteorologische Zeitschrift*, v. 15, p. 259-263, DOI: 10.1127/0941-2948/2006/0130.
- Kundzewicz, Z.W., Graczyk, D., Maurer, T., Pinskiwar, I., Radziejewski, M., Svensson, C., and Szwed, M., 2005, Trend detection in river flow series – 1. Annual maximum flow: *Hydrological Sciences Journal*, v. 50, no. 5, p. 797-810.

- Laird, K.R., Cumming, B.F., Wunsam, S., Rusak, J.A., Oglesby, R.J., Fritz, S.C., and Leavitt, P.R., 2003, Lake sediments record large-scale shifts in moisture regimes across the northern prairies of North America during the past two millennia: *Proceedings of the National Academy of Sciences USA*, v. 100, no. 5, p. 2483–2488, DOI: 10.1073/pnas.0530193100.
- Lapp, S.L., St. Jacques, J.-M., Sauchyn, D.J., and Vanstone, J.R., 2013, Forcing of hydroclimatic variability in the northwestern Great Plains since AD 1406: *Quaternary International*, v. 310, p. 47-61.
- Lesnoff, M., and Lancelot, R., 2012, aod: analysis of overdispersed data: R package version 1.3, <http://cran.r-project.org/package=aod>.
- Lins, H.F., 2012, USGS Hydro-climatic data network 2009 (HCDN-2009): U.S. Geological Survey Fact Sheet 2012-3047, 4 p., <http://pubs.usgs.gov/fs/2012/3047/>.
- Lins, H.F., and Slack, J.R., 1999, Streamflow trends in the United States: *Geophysical Research Letters*, v. 26, no. 2, p. 227–230, DOI: 10.1029/1998GL900291.
- Litke, D.W., 1999, Review of phosphorus control measures in the United States and their effects on water quality: U.S. Geological Survey Water-Resources Investigations Report 99-4007, <http://pubs.usgs.gov/wri/wri994007/pdf/wri99-4007.pdf>.
- Lu, J., Sun, G., McNulty, S.G., and Amatya, D.M., 2005, A comparison of six potential evapotranspiration methods for regional use in the southeastern United States: *Journal of the American Water Resources Association*, v. 41, no. 3, p 621–633, DOI: 10.1111/jawr.2005.41.issue-3.
- Lumley, T. (using Fortran code by A. Miller), 2009, leaps: regression subset selection: R package version 2.9, <http://CRAN.R-project.org/package=leaps>.

- MacDonald, G.M., and Case, R.A., 2014, MacDonald - Boundary Bog - LALA - ITRDB CANA221, accessed July 16, 2014, at [https://www.ncdc.noaa.gov/cdo/f?p=519:1:::P1\\_STUDY\\_ID:3899](https://www.ncdc.noaa.gov/cdo/f?p=519:1:::P1_STUDY_ID:3899).
- Maechler, M., Rousseeuw, P., Struyf, A., Hubert, M., and Hornik, K., 2014, cluster—Cluster analysis basics and extensions: R package version 1.15.2.
- Mallat, S.G., 1989, A theory for multiresolution signal decomposition—The wavelet representation: IEEE Transactions on Pattern Analysis and Machine Intelligence, v. 11, no. 7, p. 674-693.
- Marquette, J., 1966, Voyages of Marquette: The Jesuit Relations, v. 59, accessed March 21, 2015, at <http://titan.iwu.edu/~matthews/marquett.html>.
- McCabe, G.J., and Clark, M.P., 2005, Trends and variability in snowmelt runoff in the western United States: Journal of Hydrometeorology, v. 6, p. 476–482, DOI: 10.1175/JHM428.1.
- McCabe, G.J., and Wolock, D.M., 2002, A step increase in streamflow in the conterminous United States: Geophysical Research Letters, v. 29, no. 24, p. 38-1-38-4, DOI: 10.1029/2002GL015999.
- McCabe, G.J., Palecki, M.A., and Betancourt, J.L., 2004, Pacific and Atlantic Ocean influences on multidecadal drought frequency in the United States: Proceedings of the National Academy of Sciences USA, v. 101, no. 12, p. 4136–4141, DOI: 10.1073/pnas.0306738101.
- Mekis, É and Vincent, L.A., 2011, An overview of the second generation adjusted daily precipitation dataset for trend analysis in Canada: Atmosphere-Ocean, v. 49, no. 2, p. 163-177.

- Meko, D. M., 1982, Drought history in the western Great Plains from tree rings: Proceedings of the International Symposium on Hydrometeorology, American Water Resources Association, p. 321-326.
- Meko, D., and Sieg, C.H., 2014a, Meko - Burning Coal Vein - PIPO - ITRDB ND001, accessed July 16, 2014, at [https://www.ncdc.noaa.gov/cdo/f?p=519:1:::P1\\_STUDY\\_ID:3932](https://www.ncdc.noaa.gov/cdo/f?p=519:1:::P1_STUDY_ID:3932).
- Meko, D., and Sieg, C.H., 2014b, Meko - Cedar Butte - PIPO - ITRDB SD004, accessed July 16, 2014, at [https://www.ncdc.noaa.gov/cdo/f?p=519:1:::P1\\_STUDY\\_ID:3935](https://www.ncdc.noaa.gov/cdo/f?p=519:1:::P1_STUDY_ID:3935).
- Meko, D., and Sieg, C.H., 2014b, Meko - Theodore Roosevelt National Park - JUSC - ITRDB ND006, accessed July 16, 2014, at [https://www.ncdc.noaa.gov/cdo/f?p=519:1:::P1\\_STUDY\\_ID:3969](https://www.ncdc.noaa.gov/cdo/f?p=519:1:::P1_STUDY_ID:3969).
- Melillo, J.M., Richmond, T.C., and Yohe, G.W. (eds.), 2014, Climate Change Impacts in the United States: The Third National Climate Assessment: U.S. Global Change Research Program, 841 pp. DOI: 10.7930/J0Z31WJ2.
- Menne, M.J., and Vose, R.S., 2011, Long-term daily and monthly climate records from stations across the contiguous United States: United States Historical Climatology Network, accessed August 24, 2011, at <http://cdiac.ornl.gov/epubs/ndp/ushcn/ushcn.html>.
- Menne, M.J., Williams, C.N., Jr., and Vose, R.S., 2014, United States Historical Climatology Network (USHCN) Version 2.5 serial monthly dataset. National Climatic Data Center, National Oceanic and Atmospheric Administration, accessed May 15, 2014, at [http://cdiac.ornl.gov/ftp/ushcn\\_v2.5\\_monthly/](http://cdiac.ornl.gov/ftp/ushcn_v2.5_monthly/).
- Miller, J.E., and Frink, D.L., 1984, Changes in response of the Red River of the North Basin, North Dakota-Minnesota: U.S. Geological Survey Water-Supply Paper 2243, 54 p.

- Milly, P.C.D., Dunne, K.A., and Vecchia, A.V., 2005, Global pattern of trends in streamflow and water availability in a changing climate: *Nature*, v. 438, no. 7066, p. 347–350, DOI: 10.1038/nature04312.
- Mock, C.J., 1991, Drought and precipitation fluctuations in the Great Plains during the late nineteenth century: *Great Plains Research*, v. 1, p. 26-57.
- Mueller, D.K., and Helsel, D.R., 1996, Nutrients in the Nation's waters – too much of a good thing?: U.S. Geological Survey Circular 1136, 24 p., <http://pubs.er.usgs.gov/publication/cir1136>.
- Nagelkerke, N., 1991, A note on a general definition of the coefficient of determination: *Biometrika*, v. 78, p. 691–692.
- NASA Earth Observatory, 2013, A decade of water, accessed May 15, 2014, at <http://earthobservatory.nasa.gov/IOTD/view.php?id=82266>.
- National Climate Assessment and Development Advisory Committee, January 2013, Draft climate assessment report: Draft report for public comment, U.S. Global Change Research Program, <http://ncadac.globalchange.gov/>.
- National Environmental Education Foundation, 2014, Climate Fact: Heat waves and extreme high daily low temperatures, accessed March 26, 2014, at <http://www.earthgauge.net/2012/climate-fact-heat-waves-and-extreme-high-daily-low-temperatures>.
- National Oceanic and Atmospheric Administration National Climate Data Center, 2014, Tree Ring, accessed July 16, 2014, at <http://www.ncdc.noaa.gov/data-access/paleoclimatology-data/datasets/tree-ring>.

National Park Service, 2015, Pick-Sloan Plan – Part one – The background, accessed March 21, 2015, at <http://www.nps.gov/mnrr/learn/historyculture/pick-sloan-plan-part-one-the-background.htm>.

Neter, J., Kutner, M.H., Nachtsheim, C.J., Wasserman, W., 1996, Applied linear statistical models, 4th ed.: WCB/McGraw-Hill, Boston, 1408 p.

North Dakota Department of Health, 1991, Standards of water quality for State of North Dakota, chapter 33-16-02: North Dakota Department of Health, 29 p.

Oudin, L., Hervieu, F., Michel, C., Perrin, C., Andréassian, V., Anctil, F., and Loumagne, C., 2005, Which potential evapotranspiration input for lumped rainfall-runoff model? Part 2. Towards a simple and efficient potential evapotranspiration model for rainfall-runoff modeling: *Journal of Hydrology*, v. 303, no. 1–4, p. 290–306, DOI: 10.1016/j.jhydrol.2004.08.026.

Peterson, T.C., Heim, R., Hirsch, R.M., Kaiser, D., Brooks, H., Diffenbaugh, N.S., Dole, R., Giovannetone, J., Guiguis, K., Karl, T.R., Katz, R.W, Kunkel, K., Lettenmaier, D., McCabe, G.J., Paciorek, C.J., Ryberg, K.R., Schubert, S., Silva, V.B.S., Stewart, B., Vecchia, A.V., Villarini, G., Vose, R.S, Walsh, J., Wolock, D., Wolter, K., Woodhouse, C.A., Wehner, M., and Wuebbles, D., 2013, Monitoring and understanding changes in heatwaves, coldwaves, floods and droughts in the United States: State of knowledge: *Bulletin of the American Meteorological Society*, v. 94, no. 6, p. 821-834, DOI: 10.1175/BAMS-D-12-00066.1.

- Pielke, R. A., Sr., Piman, A., Niyogi, D., Mahmood, R., McApline, C., Hossain, F., Goldewijk, K.K., Nair, U., Betts, R., Fall, S., Reichstein, M., Kabat, P., and de Noblet, N., 2011, Land use/land cover changes and climate: Modeling analysis and observational evidence: WIREs Climate Change, v. 2, no. 6, p. 828–850, DOI: 10.1002/wcc.144.
- Pielke, R.A., Sr., 2005, Land use and climate change: Science, v. 310, no. 5754, p. 1625–1626, DOI: 10.1126/science.1120529.
- R Core Team, 2014, R: A language and environment for statistical computing: R Foundation for Statistical Computing, Vienna, <http://www.R-project.org>.
- Rannie, W.F., 1998, A survey of hydroclimate, flooding, and runoff in the Red River Basin prior to 1870: Geological Survey of Canada Open-File Report 3705, Ottawa, 189 pp.
- Red Lake River Watershed District, 2006, Red Lake River Watershed farm to stream tile drainage water quality study: 2005-2006 Summary Brochure, accessed March 27, 2015, at <http://www.redlakewatershed.org/projects/Tile%20Drainage%20Study%20Brochure.pdf>.
- Red Lake River Watershed District, 2009, Red Lake River Watershed farm to stream tile drainage water quality study: Final Report, revision 3, accessed March 27, 2015, at <http://www.redlakewatershed.org/projects/Red%20Lake%20Watershed%20Farm%20to%20Stream%20Tile%20Drainage%20Study%20Final%20Report%20R3.pdf>.
- Red River Basin Board, 2000, Hydrology: Red River Basin Board Inventory Team Report, Moorhead, Minnesota, 71 pp.
- Regonda, S.K., Rajagopalan, B., Clark, M., Pitlick, J., 2005, Seasonal cycle shifts in hydroclimatology over the western United States: Journal of Climate, v. 18, p. 372–384, DOI: 10.1175/JCLI-3272.1.

- Rehm, G., 2013, Tips for applying phosphorus, potash this fall: Corn+Soybean Digest, accessed March 24, 2015, at <http://cornandsoybeandigest.com/fertilizer/tips-applying-phosphorus-potash-fall>.
- Ruark, M., Madison, A., Cooley, E., Stuntebeck, T., and Komiskey, M., 2012, Phosphorus loss from tile drains – Should we be concerned?: Proceedings of the 2012 Wisconsin Crop Management Conference, v. 51, p. 9-14, accessed March 27, 2015, at [http://www.soils.wisc.edu/extension/wcmc/2012/pap/Ruark\\_1.pdf](http://www.soils.wisc.edu/extension/wcmc/2012/pap/Ruark_1.pdf).
- Ryberg, K.R., 2006, Continuous water-quality monitoring and regression analysis to estimate constituent concentrations and loads in the Red River of the North, Fargo, North Dakota, 2003-05: U.S. Geological Survey Scientific Investigations Report 2006-5241, 35 p., <http://pubs.water.usgs.gov/SIR20065241>.
- Ryberg, K.R., Lin, W., and Vecchia, A., 2014, Impact of Climate Variability on Runoff in the North Central United States: Journal of Hydrological Engineering, v. 19, no. 1, p. 140-147, DOI: 10.1061/(ASCE)HE.1943-5584.0000775.
- Ryberg, K.R., Macek-Rowland, K.M., Banse, T.A., and Wiche, G.J., 2007, A history of flooding in the Red River Basin: U.S. Geological Survey General Information Product 55, 1 sheet, <http://pubs.usgs.gov/gip/2007/55/>.
- Sauchyn, D.J., and Beaudoin, A.B., 1998, Recent environmental change in the southwestern Canadian Plains: Canadian Geographer, v. 42, p. 337-353.
- Schilling, K.E., Chan, K.-S., Liu, H., and Zhang, Y.-K., 2010, Quantifying the effect of land use land cover change on increasing discharge in the Upper Mississippi River: Journal of Hydrology, v. 387, no. 3–4, p. 343–345, DOI: 10.1016/j.jhydrol.2010.04.019.

- Schilling, K.E., Jha, M.K., Zhang, Y.-K., Gassman, P.H., and Wolter, C.F., 2008, Impact of land-use and land cover change on the water balance of a large agricultural watershed: Historical effects and future directions: *Water Resources Research*, v. 44, no. 7, W00A09, DOI: 10.1029/2007WR006644.
- Schubert, S.D., Suarez, M.J., Pegion, P.J., Koster, R.D., and Bacmeister, J.T., 2004, On the cause of the 1930s Dust Bowl: *Science*, v. 303, no. 5665, p. 1855–1859, <http://dx.doi.org/10.1126/science.1095048>.
- Seaber, P.R., Kapinos, F.P., Knapp, G.L., 1987, Hydrologic unit maps: U.S. Geological Survey Water-Supply Paper 2294, 63 p., <http://pubs.usgs.gov/wsp/wsp2294/>.
- Service Assessment Team, 2012, The Missouri/Souris River floods of May-August 2011: U.S. Department of Commerce National Oceanic and Atmospheric Administration National Weather Service Assessment, 68 p., [http://www.nws.noaa.gov/os/assessments/pdfs/Missouri\\_floods11.pdf](http://www.nws.noaa.gov/os/assessments/pdfs/Missouri_floods11.pdf) (accessed January 2015).
- Sether, B.A., Berkas, W.R., and Vecchia, A.V., 2004, Constituent loads and flow-weighted average concentrations for major subbasins of the upper Red River of the North Basin, 1997-99: U.S. Geological Survey Scientific Investigations Report 2004-5200, 62 p., <http://pubs.usgs.gov/sir/2004/5200/>.
- Severson, K.E., and Sieg, C.H., 2006, The nature of eastern North Dakota – Pre-1880 historical ecology: North Dakota Institute for Regional Studies, Fargo, North Dakota, 308 p.

- Shapley, M.D., Johnson, W.C., Engstrom, D.R., and Osterkamp, W.R., 2005, Late Holocene flooding and drought in the Northern Great Plains, reconstructed from tree rings, lake sediments and ancient shorelines: *The Holocene*, v. 15, no. 1, p. 29–41, DOI: 10.1191/0959683605hl781rp.
- Shogren, E., 2010, Dishes still dirty? Blame phosphate-free detergent: NPR, December 15, 2010, accessed March 27, 2015, at <http://www.npr.org/2010/12/15/132072122/it-s-not-your-fault-your-dishes-are-still-dirty>.
- Simons, P.T., and King, F.V., 1922, Report on drainage and prevention of overflow in the valley of the Red River of the North: U.S. Department of Agriculture Bulletin 1017, 89 p.
- Small, D., Islam, S., 2008, Low frequency variability in fall precipitation across the United States: *Water Resources Research*, v. 44, W04426, DOI: 10.1029/2006WR005623.
- Small, D., Islam, S., 2009, A synoptic view of trends and decadal variations in autumn precipitation across the United States from 1948 to 2004: *Journal of Geophysical Research*, v. 114, D10102: DOI: 10.1029/2008JD011579.
- Smith, T.J., and McKenna, C.M., 2013, A comparison of logistic regression pseudo  $R^2$  indices: *Multiple Linear Regression Viewpoints*, v. 39, no. 2, p. 17-26.
- Snedecor, G.W., and Cochran, W.G., 1989, *Statistical Methods*, 8th Edition: Iowa State University Press, Ames, 503 p.
- St. George, S., and Nielsen, E., 2002, Hydroclimatic change in southern Manitoba since A.D. 1409 inferred from tree rings: *Quaternary Research*, v. 58, p. 103-111.
- St. George, S., and Nielsen, E., 2003, Palaeoflood records for the Red River, Manitoba, Canada, derived from anatomical tree-ring signatures: *The Holocene* v. 13, no. 4, p. 547-555.

- St. George, S., and Rannie, W., 2003, The causes, progression and magnitude of the 1826 Red River flood in Manitoba: *Canadian Water Resources Journal*, v. 28, no. 1, p. 99-120.
- State of Minnesota, 2005, Phosphorus turf fertilizer use restrictions: Office of the Revisor of Statutes, State of Minnesota, Ch. 18, Art. C, Sec. 60.
- Stewart, I.T., Cayan, D.R., Dettinger, M.D., 2005, Changes toward earlier streamflow timing across western North America: *Journal of Climate*, v. 18, p. 1136–1155, DOI: 10.1175/JCLI3321.1.
- Stockton, D.W., and Meko, D.M., 1983, Drought recurrence in the Great Plains reconstructed from long-term tree-ring records: *Journal of Climate and Meteorology*, v. 22, p. 17-29, DOI: 10.1175/1520-0450(1983)022<0017:DRITGP>2.0.CO;2.
- Thorleifson, H., Brooks, G., Hanuta, I., Kroker, S., Matile, G., Nielsen, E., Prévost, C., and Rannie, W., 1998, Red River flooding: evolutionary geomorphic trends and evidence for major floods in recent centuries: Manitoba Energy and Mines, Geological Services Report of Activities (NTS 62H/W), p. 186-195.
- Thornthwaite, C.W., and Holzman, B., 1942, Measurement of evaporation from land and water sources, U.S. Department of Agriculture Technical Bulletin 817, 143 p.
- Tobin, J., 1958, Estimation of relationships for limited dependent variables: *Econometrica - Journal of the Econometric Society*, p. 24-36.
- Tomer, M.D., and Schilling, K.E., 2009, A simple approach to distinguish land-use and climate-change effects on watershed hydrology: *Journal of Hydrology*, v. 376, no. 1–2, 24033, DOI: 10.1016/j.jhydrol.2009.07.029.

- Tornes, L.H., 2005, Water quality of streams in the Red River of the North Basin, Minnesota, North Dakota, and South Dakota, 1970-2001: U.S. Geological Survey Scientific Investigations Report 2005-5095, 81 p., <http://pubs.water.usgs.gov/sir20055095/>.
- Tornes, L.H., and Brigham, M.E., 1994, Nutrients, suspended sediment, and pesticides in waters of the Red River of the North Basin, Minnesota, North Dakota, and South Dakota, 1970-90: U.S. Geological Survey Water-Resources Investigations Report 93-4231, 62 p., <http://pubs.er.usgs.gov/publication/wri934231>.
- Torrence, C. and Compo, G.P., 1998, A practical guide to wavelet analysis: Bulletin of the American Meteorological Society, v. 79, no. 1, p. 61–78.
- Trenberth, K.E., 1999, Conceptual framework for changes of extremes of the hydrological cycle with climate change: Climate Change, v. 42, no. 1, p. 327–339.
- U.S. Department of Agriculture Economic Research Service, 2013, Fertilizer use and price data set, accessed March 4, 2015, at <http://www.ers.usda.gov/data-products/fertilizer-use-and-price.aspx#26718>.
- U.S. Department of Agriculture National Agricultural Statistics Service, 2013, National statistics for corn—Acres planted: U.S. Department of Agriculture database, accessed November 15, 2013, at [http://quickstats.nass.usda.gov/results/08638011-B478-3942-B44F-FA130ADDE283?pivot=short\\_desc](http://quickstats.nass.usda.gov/results/08638011-B478-3942-B44F-FA130ADDE283?pivot=short_desc).
- U.S. Environmental Protection Agency, 2002, Summary table for the nutrient criteria documents, 3 p., <http://www2.epa.gov/sites/production/files/2014-08/documents/criteria-nutrient-ecoregions-sumtable.pdf>.

- U.S. Environmental Protection Agency, 2010, Trophic states of l, chap 5 *of* U.S. Environmental Protection Agency National Lakes Assessment - A Collaborative Survey of the Nation's Lakes: EPA 841-R-09-001, p. 43-46, accessed March 21, 2015, at [http://www.epa.gov/owow/LAKES/lakessurvey/pdf/nla\\_chapter5.pdf](http://www.epa.gov/owow/LAKES/lakessurvey/pdf/nla_chapter5.pdf).
- U.S. Environmental Protection Agency, 2012, Clean watersheds needs survey overview, accessed April 14, 2015, at <http://water.epa.gov/scitech/datait/databases/cwns/>.
- U.S. Environmental Protection Agency, 2013, Primary distinguishing characteristics of level III ecoregions of the continental United States, accessed January 31, 2015, at [ftp://ftp.epa.gov/wed/ecoregions/us/Eco\\_Level\\_III\\_descriptions.doc](ftp://ftp.epa.gov/wed/ecoregions/us/Eco_Level_III_descriptions.doc).
- U.S. Geological Survey, 1952, Floods of 1950 in the Red River of the North and Winnipeg River basins: U.S. Geological Survey Water Supply Paper 1137-B, accessed January 17, 2015, at <http://pubs.er.usgs.gov/publication/wsp1137B>.
- U.S. Geological Survey, 2006, Collection of water samples (ver. 2.0): U.S. Geological Survey Techniques of Water-Resources Investigations, book 9, chap. A4, September 2006, accessed April 9, 2015, at <http://pubs.water.usgs.gov/twri9A4/>.
- U.S. Geological Survey, 2009, Red River flow in Fargo at highest level ever recorded for November: USGS News Release, accessed Jan. 11, 2012, at <http://www.usgs.gov/newsroom/article.asp?ID=2344>.
- U.S. Geological Survey, 2014a, Explanations for the National water conditions, accessed August 24, 2014, at [http://water.usgs.gov/nwc/explain\\_data.html](http://water.usgs.gov/nwc/explain_data.html).
- U.S. Geological Survey, 2014b, Peak Streamflow for North Dakota, accessed December 15, 2014, at <http://nwis.waterdata.usgs.gov/nd/nwis/peak/>.

- U.S. Geological Survey, 2015a, Peak Streamflow for the Nation USGS 05054000 RED RIVER OF THE NORTH AT FARGO, ND, accessed January 17, 2015, at [http://nwis.waterdata.usgs.gov/nwis/peak?site\\_no=05054000&agency\\_cd=USGS&format=html](http://nwis.waterdata.usgs.gov/nwis/peak?site_no=05054000&agency_cd=USGS&format=html).
- U.S. Geological Survey, 2015b, Peak Streamflow for the Nation USGS 05082500 RED RIVER OF THE NORTH AT GRAND FORKS, ND, accessed January 17, 2015, at [http://nwis.waterdata.usgs.gov/nwis/peak?site\\_no=05082500&agency\\_cd=USGS&format=html](http://nwis.waterdata.usgs.gov/nwis/peak?site_no=05082500&agency_cd=USGS&format=html).
- U.S. Geological Survey, 2015c, Peak Streamflow for the Nation USGS 05117500 SOURIS RIVER ABOVE MINOT, ND, accessed January 17, 2015, at [http://nwis.waterdata.usgs.gov/nwis/peak?site\\_no=05117500&agency\\_cd=USGS&format=html](http://nwis.waterdata.usgs.gov/nwis/peak?site_no=05117500&agency_cd=USGS&format=html).
- U.S. Geological Survey, 2015d, Peak Streamflow for the Nation USGS 06342500 MISSOURI RIVER AT BISMARCK, ND, accessed January 17, 2015, at [http://nwis.waterdata.usgs.gov/nwis/peak?site\\_no=06342500&agency\\_cd=USGS&format=html](http://nwis.waterdata.usgs.gov/nwis/peak?site_no=06342500&agency_cd=USGS&format=html).
- U.S. Geological Survey, 2015e, USGS water data for the nation, accessed January 17, 2015, at <http://waterdata.usgs.gov/nwis>.
- Upham, W., 1895, The glacial Lake Agassiz: U.S. Geological Survey Monograph 25, 658 p.
- Vance, R.E., Mathewes, R.W., and Clague, J.J., 1992, 7,000-year record of lake-level change on the northern Great Plains: A high-resolution proxy of past climate: *Geology*, v. 20, p. 879-882.

- Vecchia, A.V., 2005, Water-quality trend analysis and sampling design for streams in the Red River of the North Basin, Minnesota, North Dakota, and South Dakota, 1970-2001: U.S. Geological Survey Scientific Investigations Report 2005-5224, 54 p., <http://pubs.usgs.gov/sir/2005/5224/>.
- Vecchia, A.V., 2008, Climate simulation and flood risk analysis for 2008–40 for Devils Lake, North Dakota: U.S. Geological Survey Scientific Investigations Report 2008–5011, Reston, Virginia, <http://pubs.usgs.gov/sir/2008/5011/>.
- Vincent, L. A., Wang, X.L., Milewska, E.J., Wan, H., Yang, F., and Swail, V., 2012, A second generation of homogenized Canadian monthly surface air temperature for climate trend analysis: *Journal of Geophysical Research*, v. 117, D18110, DOI:10.1029/2012JD017859.
- Voronoi, G., 1908, Nouvelles applications des paramètres continus à la théorie des formes quadratiques: *Journal für die Reine und Angewandte Mathematik*, v. 133, p. 97–178, DOI: 10.1515/crll.1908.133.97.
- Walsh, J., Wuebbles, D., Hayhoe, K., Kossin, J., Kunkel, K., Stephens, G., Thorne, P., Vose, R., Wehner, M., Willis, J., Anderson, D., Doney, S., Feely, R., Hennon, P., Kharin, V., Knutson, T., Landerer, F., Lenton, T., Kennedy, J., Somerville, R., 2014, Ch. 2: Our Changing Climate, *in* Melillo, J.M., Richmond T.C., Yohe, G.W, (eds.), *Climate Change Impacts in the United States: The Third National Climate Assessment*, U.S. Global Change Research Program, p. 19-67, DOI: 10.7930/J0KW5CXT.

- Wang, H., Schubert, S., Suarez, M., Chen, J., Hoerling, M., Kumar, A., Pegion, P., 2009, Attribution of the seasonality and regionality in climate trends over the United States during 1950–2000: *Journal of Climate*, v. 22, p. 2571-2590, DOI: 10.1175/2008JCLI2359.1.
- Watson, E., and Luckman, B.H., 2001, Dendroclimatic reconstruction of precipitation for sites in the southern Canadian Rockies: *The Holocene*, v. 11, p. 203-213.
- Westerling, A., 2005, climdiv: U.S. climate division data, R package version 0.3, accessed July 11, 2014, at <http://ulmo.ucmerced.edu/data/R/climdiv/>.
- Wettstein, J.J., Littell, J.S., Wallace, J.M., Gedalof, Z., 2011, Coherent region-, species-, and frequency-dependent local climate signals in Northern Hemisphere tree-ring widths: *Journal of Climate*, v. 24, p. 5998-6012.
- Whitcher, B., 2013, waveslim—Basic wavelet routines for one-, two- and three-dimensional signal processing: R package version 1.7.3, <http://CRAN.R-project.org/package=waveslim>.
- Whitfield, 2012, Floods in future climates: a review, *Journal of Flood Risk Management*, v. 5, no. 4, 336-365, DOI: 10.1111/j.1753-318X.2012.01150.x.
- Wigley, T.M.L., Briffa, K.R., and Jones, P.D., 1984, On the average value of correlated time series, with applications in dendroclimatology and hydrometeorology: *Journal of Climate and Applied Meteorology*, v. 23, p. 201-213.
- Will, G.F., 1946, Tree ring studies in North Dakota: North Dakota Agricultural College, Fargo, Agricultural Experiment Station Bulletin 338.
- Williams-Sether, T., 1999, From dry to wet, 1988-97, North Dakota: U.S. Geological Survey Fact Sheet 075-99, 4 p., <http://pubs.er.usgs.gov/publication/fs07599>.

- Williams-Sether, T.J., 2004, Regression equations for estimating concentrations of selected water-quality constituents for selected gaging stations in the Red River of the North Basin, North Dakota, Minnesota, and South Dakota: U.S. Geological Survey Water-Resources Investigations Report 03-4291, 33 p., <http://pubs.water.usgs.gov/wri034291/>.
- Wishart, D.J. (ed.), 2004, Encyclopedia of the Great Plains. University of Nebraska Press: Lincoln, Nebraska, 940 p.
- Yang, S., Ding, X., Zheng, D., and Li, Q., 2007, Depiction of the variations of Great Plains precipitation and its relationship with tropical central-eastern Pacific SST: *Journal of Applied Meteorology and Climatology*, v. 46, no. 2, p. 136–153, DOI: 10.1175/JAM2455.1.
- Zeileis, A., Hothorn, T., 2002, Diagnostic checking in regression relationships: *R News*, v. 2, no. 3, p. 7-10.
- Zhang, L., Walker, G.R., and Dawes, W.R., 2002, Water balance modelling: concepts and applications, *in* McVicar, T.R., Rui, L., Walker, J., Fitzpatrick, R.W., and Changming, L. (eds.), *Regional Water and Soil Assessment for Managing Sustainable Agriculture in China and Australia*, ACIAR Monograph No. 84, p. 31–47.
- Zhang, W. and Rao, Y.R., 2012, Application of a eutrophication model for assessing water quality in Lake Winnipeg: *Journal of Great Lakes Research*, v. 38, p. 158-173.
- Zhang, X., Harvey, K.D., Hogg, W.D., Yuzyk, T.R., 2001, Trends in Canadian streamflow: *Water Resources Research*, v. 37, p. 987-998.
- Zhang, Y.-K., and Schilling, K. E., 2006, Increasing streamflow and baseflow in Mississippi River since the 1940s: Effect of land-use change: *Journal of Hydrology*, v. 324, no. 1–4, p. 412–422, DOI: 10.1016/j.jhydrol.2005.09.033.

**APPENDIX A. SUPPORTING MATERIAL FOR CHAPTER 4 CHANGES IN SEASONALITY AND TIMING OF PEAK STREAMFLOW IN SNOW AND SEMI-ARID CLIMATES OF THE NORTH-CENTRAL UNITED STATES, 1910-2012**

The following material provides additional background on how the study area was determined, how streamgages and peaks were selected, and how the time series of annual snowmelt/spring and summer/fall peaks were determined, as well as results of trend analysis in magnitude and timing at individual streamgages.

**A.1. Study Area**

The Water-Resources Regions (Seaber et al., 1987) used to define the study area are depicted in figure A.1.

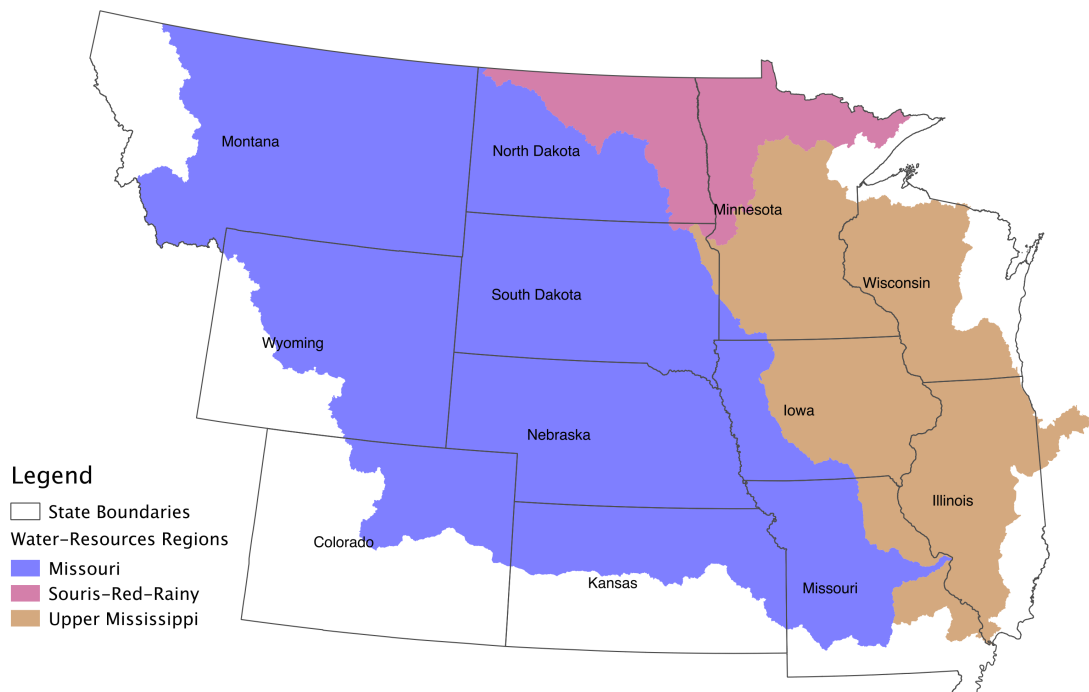


Figure A.1. Water-Resources Regions (Seaber et al., 1987) within the study area.

Five climate classes from the Köppen-Geiger classification system (Kottek et al., 2006) occur in the study area. The two major climate types are snow and arid, represented by D and B in this classification system. The climate classes are further differentiated by their precipitation and temperature conditions. The snow climate has two precipitation conditions—fully humid (f) and winter dry (w)—and each of the precipitation conditions has two temperature conditions—hot summer (a) and warm summer (b). For the arid climate, there is only one precipitation and one temperature condition, Steppe (S) and cold arid (k), respectively. The climate classifications for the study area are listed in table A.1 and shown in figure A.2.

Table A.1. Köppen-Geiger classification system (Kottek et al., 2006) representing the five climate classes in the study area.

Major Climate	KG label	Precipitation conditions	KG label	Temperature conditions	KG label	Final KG class label
Snow	D	fully humid	f	hot summer	a	Dfa
				warm summer	b	Dfb
		winter dry	w	hot summer	a	Dwa
				warm summer	b	Dwb
Arid	B	Steppe	S	cold arid	k	BSk

KG, Köppen-Geiger

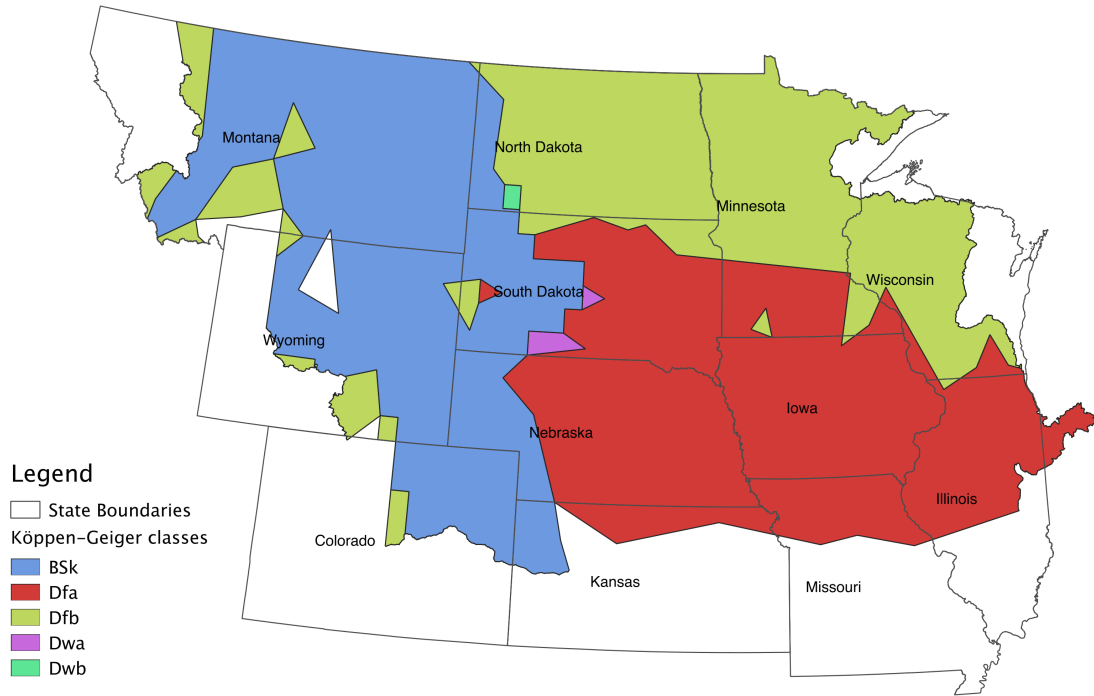


Figure A.2. Köppen-Geiger climate classes (Kottek et al., 2006) used within the study area. The white hole in Wyoming extending slightly into Montana is an arid climate with desert precipitation and cold arid temperature and was left out because of the desert designation.

Three level II ecological regions (Commission for Environmental Cooperation, 1997) were used to further define the study area. They are depicted in figure A.3 and all are subregions of the Level I ecological region 9, Great Plains. The Great Plains are described by the Commission for Environmental Cooperation (1997) as an ecological region “found in the central part of the continent and extends over the widest latitudinal range of any single North American ecological region. It is ... relatively continuous... This ecological region is distinguished particularly by the following characteristics: relatively little topographic relief; grasslands and a paucity of forests; and subhumid to semiarid climate.”

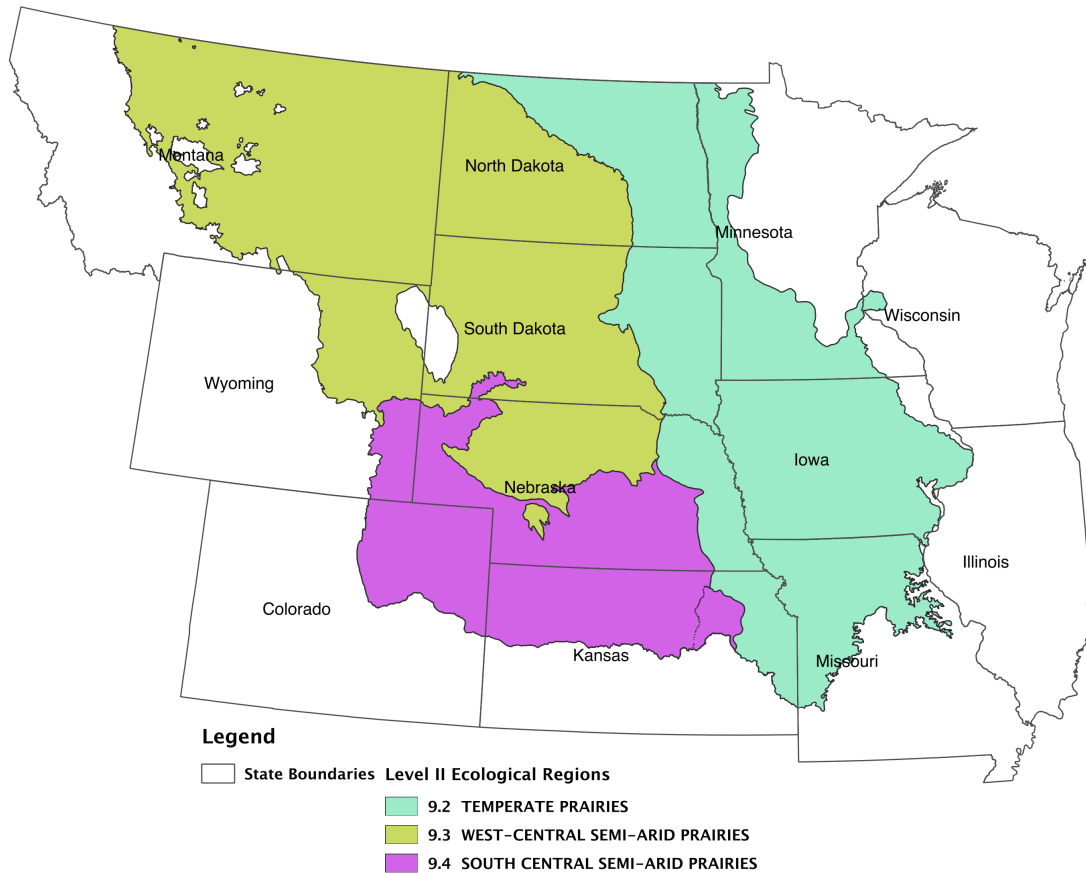


Figure A.3. Level II Ecological regions (Commission for Environmental Cooperation, 1997) within the study area. The white holes within the study area are mountainous ecological regions that were removed.

The intersections of the climate classes with the ecological regions within the Water-Resources Regions formed regions, each of similar climate and topography. The climate classes Dwa and Dwb (very small classes in figure A.2) were so small that they were not meaningful in this study and after examination of their characteristics were included in the Dfa and Dfb climate classes, respectively, that partially surrounded them. This created seven regions (fig. A.4), some with discontinuous areas, but each region has similar climate and topography. These seven regions focused the study area on the semi-arid and snow climate, plains regions of the north central U.S. This process of refining the study area removed mountainous areas (shown as white

holes in the figs. A.2, A.3, and A.4) and forested areas. Peak streamflow should be considered separately for mountainous areas because of their large altitude changes and different climate. Removing the forested areas in Minnesota is consistent with Ryberg et al. (2014) who found that basins in northern Minnesota (Group A in Ryberg et al.) had differences in precipitation-runoff response as compared to others in the study “because of land cover (group A basins included large contributions from forested areas and substantial surfacewater storage; see fig. S2) and the influence of Lake Superior.”

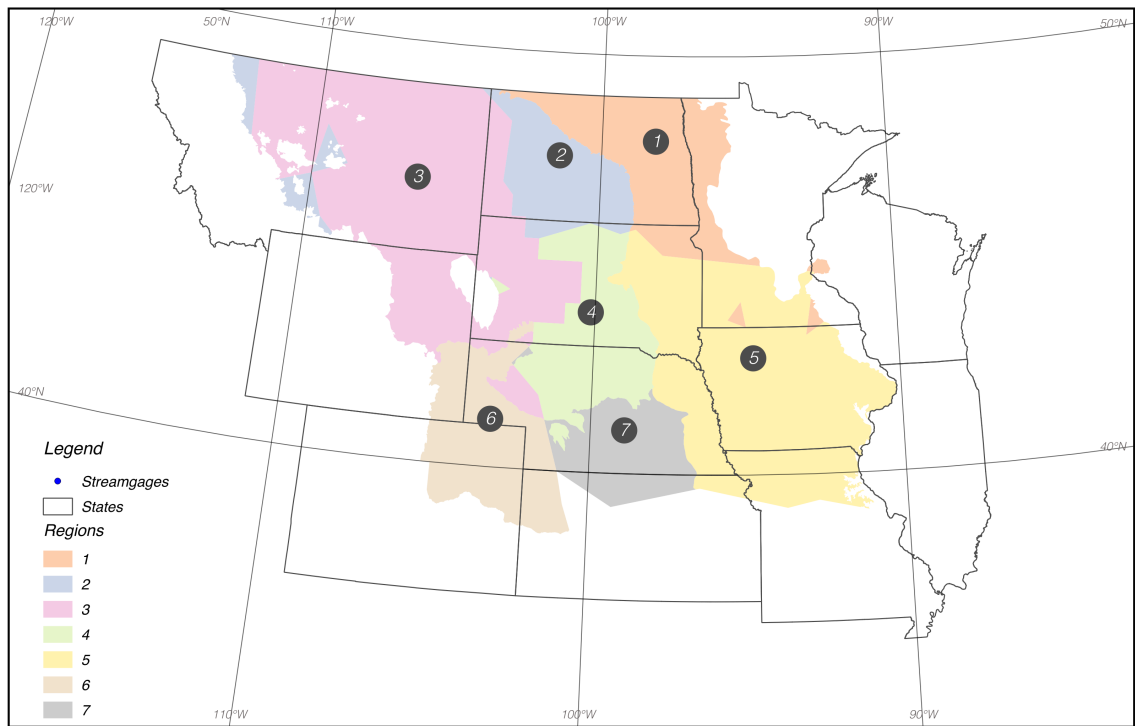


Figure A.4. Seven groups used in study, each of similar climate and topography.

## A.2. Streamgage Selection

Peak streamflow data for the states in the study were downloaded from the USGS Water Data for the Nation web site (<http://waterdata.usgs.gov>) on January 21, 2014. The list of possible streamgages for streamgages and years of data used were further reduced by using only those

peaks considered unregulated (regulation indicated by peak streamflow qualification code of 5 or 6), were not from dam failure (qualification code 3), did not have uncertainty as to the date of the peak (qualification code A, year of occurrence unknown or inexact, or B, month or day of occurrence unknown), had a defined drainage area, were below 4,000 feet, had a drainage area less than 60,000 square miles, were not on the Missouri, Yellowstone, or Platte rivers whose peaks are affected by mountain snowmelt (mountain snowmelt coming later than the snowmelt on the plains and prairies).

Some of the streamgages were unregulated early in their period of record and later regulated, only the unregulated peaks were used. Some of the streamgages have a short period of record, but they were required to have at least 15 unregulated peaks. The streamgages with fairly short periods of record vary in their range of observed years, but provide additional information across the period of record for each group.

There is a great deal of spatial correlation in the streamgages. Some are on the same stream and many are in the same eight-digit hydrologic unit (HUC, or cataloging unit: “a geographic area representing part or all of a surface drainage basin, a combination of drainage basins, or a distinct hydrologic feature,” Seaber et al., 1987). Therefore, to reduce spatial correlation, the potential streamgages were thinned in the following manner. For streamgages in the same HUC, the streamgage with the longest period of record for peak streamflow was retained and the remaining streamgage(s) was (were) removed. If one or more sites within the same HUC had the same period of record, the streamgage with the largest drainage area was retained. Exceptions to these rules occurred when the streamgages in the same HUC had non-overlapping periods of record, or overlapped by at most 3 years. This in essence extended the

period of record for those HUCs. Examples of exception are shown below. Paired streamgages are in the same 8-digit hydrologic unit and both were retained.

Table A.2. Examples of streamgages in same 8-digit hydrologic unit with overlapping periods of record where both were retained for the study.

USGS Streamgage Identification Number	Name of Streamgage	Beginning of Period of Record	End of Period of Record
04021205	Floodwood River above Floodwood, Minnesota	1972	1987
04019500	East Swan River near Toivola, Minnesota	1954	1971
06294995	Armells Creek near Forsyth, Montana	1975	1995
06295050	Little Porcupine Creek near Forsyth, Montana	1958	1973
06354500	Beaver Creek at Linton, North Dakota	1950	1989
06354580	Beaver Creek below Linton, North Dakota	1990	2011

### A.2.1. Additional Comments on Streamgage Selection

Streamgages were chosen based on codes in the peak-flow file rather than the streamgages listed in the Geospatial Attributes of Gages for Evaluating Streamflow database (GAGES II; Falcone, 2011) or the USGS Hydro-Climatic Data Network (HCDN-2009; Lins, 2012) for a number of reasons. First, HCDN-2009 is a subset of the GAGES-II and GAGES-II only includes streamgages whose basins lie within the U.S. Given the location of our study area, we wanted to include some streamgages with basin areas partially in Canada and they would never make the GAGES II or HCDN-2009 lists. Second, using only HCDN-2009 would result in poor coverage in the north central U.S. We wanted the results to be relevant to what people are experiencing on the landscape and at National Weather Service flood forecast points, not just the more pristine areas. Third, we eliminated peaks with codes 3, 5, 6, A, B, C, respectively defined as discharge affected by dam failure; discharge affected to unknown degree by regulation or

diversion; discharge affected by regulation or diversion; year of occurrence is unknown or not exact; month or day of occurrence is unknown or not exact; all or part of the record affected by urbanization, mining, agricultural changes, channelization, or other (U.S. Geological Survey, 2014a). Fourth, in Ryberg et al. (2014; with a similar study area), we found that seasonal climate effects explained 73 to 87 percent of variability in 7-day high runoff for January-June and land-use/other effects were not significant. In July-December, we found that seasonal climate effects explained 76-85 percent of 7-day high runoff with land-use other effects small (but significant). This finding was consistent with Zhang and Schilling (2006), who argued that land-use changes would tend to affect baseflow more than high flow. We contend the timing and seasonality of peak streamflow in the north central U.S. is mainly influenced by climate.

We did compare our list of streamgages to the GAGES-II and HCDN-2009 lists; 71% of our streamgages are GAGES-II streamgages, and 10 % are HCDN-2009 streamgages. One reason for the low HCDN-2009 percentage is that some of the streamgages used might meet some of the HCDN criteria, but are no longer operated. For example, a gage may have been operated early in the period of this study, a dam was put in (and subsequent peaks were coded as 5 or 6, or the gage was discontinued) and a gage may have been installed upstream to monitor unregulated flow. In this example, the original gage would not be in HCDN-2009 because it was discontinued, but we would use its early, unregulated peaks and the gage upstream to represent that geographic area. Another example is the case of moved streamgages, such as 06354500, Beaver Creek at Linton, North Dakota, operated 1950-1989, and 06354580 Beaver Creek below Linton, North Dakota, operated 1990-present. In this case, the original streamgage would not be in HCDN-2009 because it has been discontinued (assuming it met other criteria) and the new

streamgage would not be in HCDN-2009 because it did not have a complete 20 years of continuous record when HCDN-2009 was created.

### **A.3. Information about Regions**

Table A.3 contains additional summary information about the seven regions. The number of streamgages varies with each region; however, the median drainage areas are similar. Given the range of possible snowmelt/spring and summer/fall peak Julian dates, their median values are fairly similar across regions.

Table A.3. Additional information about each region in the study area.

Region	Number of Streamgages	Drainage Area			Snowmelt/Spring Peaks Julian Date			Summer/Fall Peaks Julian Date		
		Minimum	Median	Maximum	Minimum	Median	Maximum	Minimum	Median	Maximum
1	47	27.2	770.0	23,560	46	94	126	127	172	321
2	21	59.0	523.0	8,310	17	81	117	118	161	314
3	83	11.1	470.0	20,722	5	79	109	110	160	345
4	18	14.2	752.5	9,920	2	80	114	115	165	361
5	92	10.7	792.0	44,800	1	78	106	107	168	365
6	9	74.0	455.0	3,555	2	68	90	96	180	353
7	39	27.2	770.0	23,560	19	72	96	97	173	321

Because streamgages of variable period of record were used, the peaks were divided into two groups, 1910-1961 and 1962-2012 for each region. The average peak location was calculated for each group-period and plotted on a map. Region 2 has some streamgages in a discontinuous area at the western edge of the study area, so region 2 was divided into two subregions for this purpose. The majority of peaks for region 2 are represented by the average peak locations near the label in the eastern part of region 2 (fig. A.5); however, a second set of average peak locations for region 2 is shown for the discontinuous area on the western edge of the study area. The peak locations in all cases are very close to each other, indicating that the spatial coverage is similar in the first half of the record to that in the second half (fig. A.5).

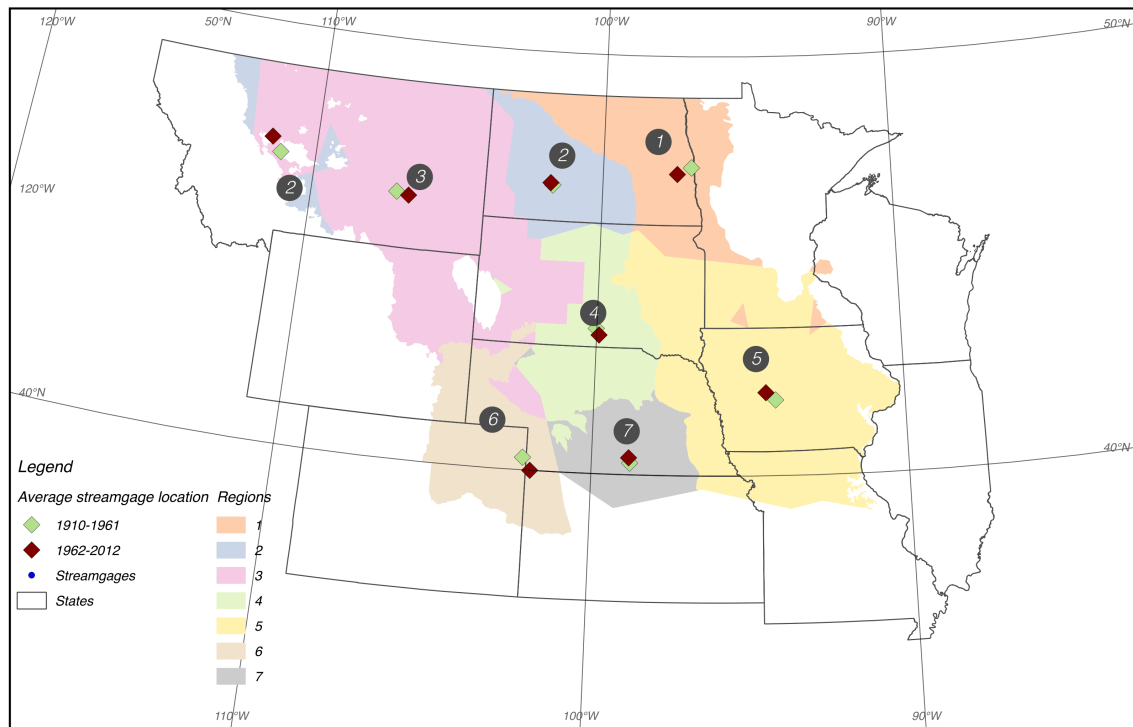


Figure A.5. Average streamgage locations for each region (region 2 divided into eastern and western parts) for the period 1910-1961 and 1962-2012.

#### **A.4. Creation of Annual Snowmelt/Spring and Summer/Fall Peak Streamflow Series**

Two annual peak times series, one of snowmelt/spring peaks the other of summer/fall peaks were created. When the peak of record for a particular year occurred during the snowmelt/spring period for the region a streamgage was in, that peak went into the snowmelt/spring series for that streamgage and the maximum daily value (where available) during the summer/fall period went into the summer/fall peak series for that streamgage. When the annual peak occurred during summer/fall, that peak went into the summer/fall series and the maximum daily value (where available) during the snowmelt/spring period was used in the series of snowmelt/spring peaks. Daily values were not always available for all water years, so the number of peaks in each series for a given streamgage is not necessarily the same.

The maximum daily value does not always occur on the same date as the peak, but it should not be biased earlier or later and is used here as an estimate of the seasonal peak. On some occasions, the maximum daily value occurred over several days. If it occurred over two days, the first day was selected as the date the peak. If it lasted over three days, the middle day was selected as the date of the peak. If it lasted over four days, day 2 was used, and if it lasted over five days, day 3 was used as the date for the annual peak.

#### **A.5. Regression to Examine Timing and Magnitude of Peaks at Individual Streamgages**

To further examine changes in timing and magnitude of peaks, individual long-term streamgages were selected using the criteria of Hirsch and Ryberg (2012) to obtain streamgages with at least 85 years of recorded peaks. Daily values were not always available for all water years, so the number of peaks in each series was counted and those with less than 85 peaks in each series were eliminated in order maintain records of 85 years or longer. Linear regression was performed on the Julian date of each series for each streamgage and on the logarithm of

streamflow of each series for each streamgage to examine changes in the timing of peaks and changes in magnitude. Regression was done with and without the lagged PHDI to determine if antecedent conditions made a difference in peak timing or magnitude.

The model used was:

$$Y = X\beta + \epsilon \quad (\text{Eq. A.1})$$

where  $Y$  is the matrix of annual regional Julian dates,  $X\beta$  is the matrix algebra representation of the observations of the explanatory variables ( $X$ ) and model parameters ( $\beta$ ), and  $\epsilon$  is the model error.

#### **A.5.1. Changes in Timing and Magnitude of Snowmelt/Spring Peaks at Individual Streamgages**

Of 25 individual long-term streamgage streamgages analyzed, three had negative trends in Julian date timing and are shown in figure A.6. Streamgages with solid down arrows have statistically significant ( $p$ -value  $\leq 0.01$ ) negative trends in the Julian date for the snowmelt/spring peak, that is the peak is occurring earlier (Julian date getting smaller over time). No streamgages had significant positive trends. The streamgages with statistically significant earlier (negative) trends were all in the northern tier of the study region, consistent with the regional results (fig. 4.3), and were Wild Rice River at Twin Valley, Minnesota (USGS streamgage identification number 05062500); Thief River near Thief River Falls, Minnesota (05076000); and Musselshell River at Harlowton, Montana (06120500).

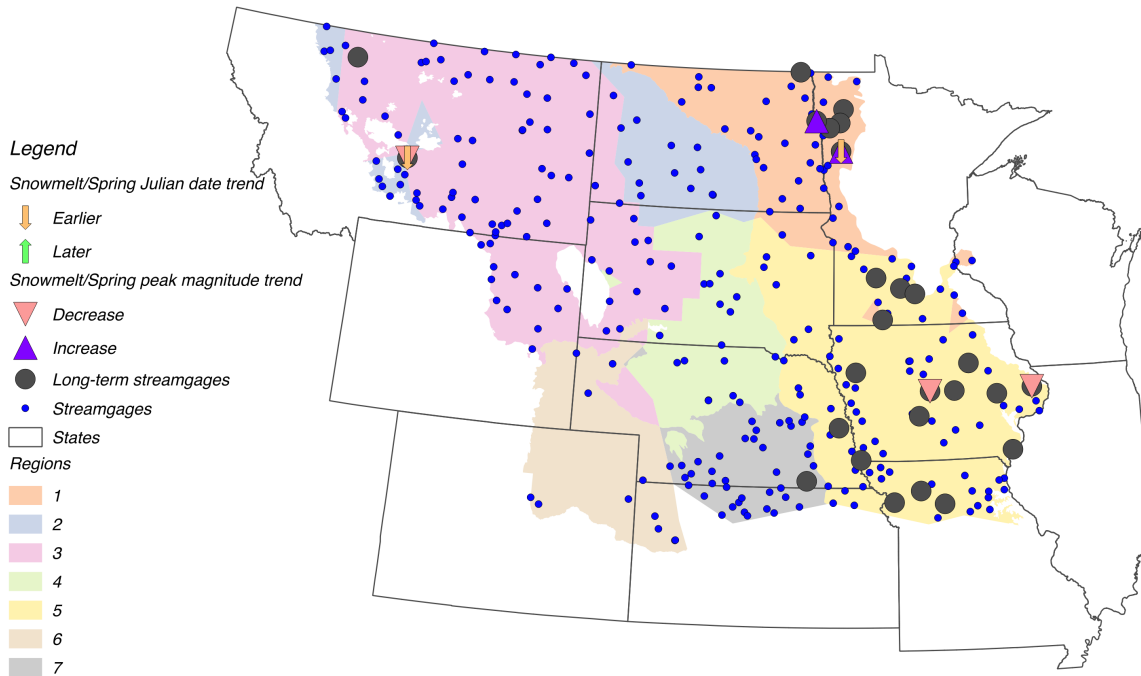


Figure A.6. Trends in snowmelt/spring Julian date and magnitude of peaks at long-term streamgages, after adjusting for antecedent conditions.

When adjusting for antecedent wet or dry conditions (by including PHDI2 in the regression model), which could occur at the end of the period of record and influence the trend, just Wild Rice River at Twin Valley, Minnesota, and Musselshell River at Harlowton, Montana, had negative coefficients on the water year term, indicating earlier spring peaks and no additional streamgages had significant trends.

For regression of snowmelt/spring peak magnitude on water year, seven streamgages had significant trends. However, when adjusting the model for antecedent conditions, only five had significant trends. The following streamgages had statistically significant trends in water year after adjusting for antecedent wet or dry conditions: Wild Rice River at Twin Valley, Minnesota (05062500); Red River of the North at Grand Forks, North Dakota (05082500); Maquoketa River near Maquoketa, Iowa (05418500); South Skunk River near Ames, Iowa (05476000); and Musselshell River at Harlowton, Montana (06120500).

Two had positive coefficients and three had negative (fig. A.6). All of the positive coefficients, indicating a trend for larger snowmelt/spring peaks, were in region 1 and were in the Souris-Red-Rainy Water-Resources Regions (fig. A.1). This is similar to an area that stood out in Hirsch and Ryberg (2012) in a study on peak streamflow and global carbon dioxide.

#### **A.5.2. Changes in Timing and Magnitude of Summer/Fall Peaks at Individual Streamgages**

Of the individual long-term streamgage streamgages analyzed, the following streamgages had statistically significant trends toward later summer/fall peaks: Wild Rice River at Twin Valley, Minnesota (05062500) and Red Lake River at Crookston, Minnesota (05079000). When adjusting for antecedent wet or dry conditions, which could occur at the end of the period of record and influence the trend, the same two streamgages had a positive water year coefficient. These are both streamgages in region 1 which showed the trend toward later peaks (fig. A.7)

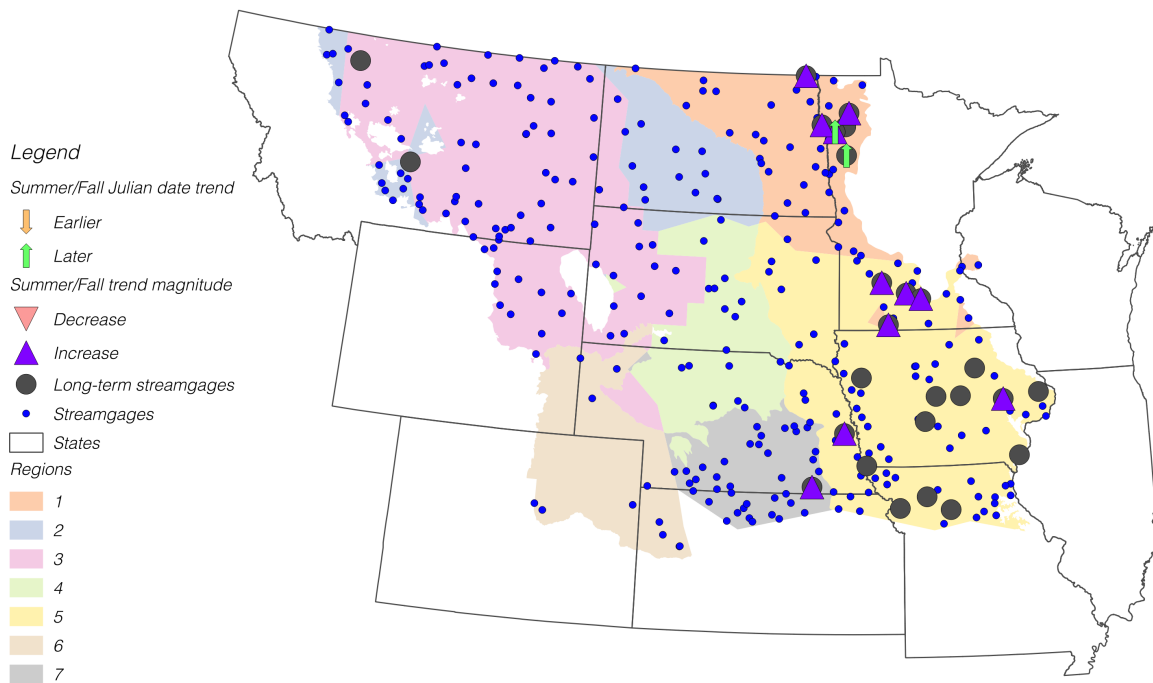


Figure A.7. Trends in summer/fall Julian date and magnitude of peaks at long-term streamgages, after adjusting for antecedent conditions.

For regression of summer/fall peak magnitude on water year, 14 streamgages had significant trends. However, when adding the PHDI2 term, only 11 streamgages had significant (0.01) trends in water year. All water year coefficients were positive indicating a trend toward larger summer/fall peaks. The streamgages with the significant trends are all on the eastern side of the study area and are: Thief River near Thief River Falls, Minnesota (05076000); Red Lake River at Crookston, Minnesota (05079000); Red River of the North at Grand Forks, North Dakota (05082500); Pembina River at Neche, North Dakota (05100000); Redwood River near Redwood Falls, Minnesota (05316500); Cottonwood River near New Ulm, Minnesota (05317000); Minnesota River at Mankato, Minnesota (05325000); Cedar River at Cedar Rapids, Iowa (05464500); Des Moines River at Jackson, Minnesota (05476000); Elkhorn River at Waterloo, Nebraska (06800500); and Little Blue River near Fairbury, Nebraska (06884000).

### **A.5.3. Summary of Changes in Timing and Magnitude at Individual Streamgages**

Examination of trends in timing and magnitude at individual streamgages is complicated by a lack of long-term unregulated streamgages. Peak magnitude at some streamgages did have significant trends, but was divided between those with upward and downward trends. The trend in magnitude, but not the trend in Julian date, of peaks was sensitive to antecedent wet and dry conditions, represented by the lagged Palmer Hydrologic Drought Index (PHDI).

For summer/fall peaks in that was little evidence for changes in timing beyond region 1, but magnitude had more changes that were sensitive to the lagged PHDI. Wang et al. (2009) found a “distinct precipitation enhancement” over the central U.S. in the summer and increases in fall precipitation in the majority of the U.S. While again limited by the number of long-term, unregulated streamgages, the trends in peak magnitude suggest that reported increases in summer and fall precipitation are evident in the record of annual peak streamflow in most areas of the north central U.S. When considering the timing of spring snowmelt, the annual streamflow peaks should be divided into spring/snowmelt peaks and summer/fall peaks. Then each separate population of peaks can be examined for changes.

Ultimately, the results at individual streamgages did not provide much additional information beyond that presented in Hirsch and Ryberg (2012) and Peterson et al. (2013) and, therefore, are presented in this Appendix.

**APPENDIX B. WAVELET ANALYSIS AND MULTIREOLUTION DECOMPOSITION  
FOR TREE-RING BASED ESTIMATES OF LONG-TERM SEASONAL  
PRECIPITATION IN THE SOURIS RIVER REGION OF SASKATCHEWAN, NORTH  
DAKOTA, AND MANITOBA**

The following figures are supporting information for Chapter 5 Tree-Ring Based Estimates of Long-Term Seasonal Precipitation in the Souris River Region of Saskatchewan, North Dakota, and Manitoba. Figures B.1-B.4 represent multiresolution decompositions of the tree-ring chronologies. Each figure represents a one-dimensional multiresolution analysis using a level  $J$  additive decomposition of the time series using the pyramid algorithm (Mallat, 1989) as implemented in the `dplr` package (Bunn et al., 2014). The additive decomposition is for each power of two in the period of record, where the number of powers is  $\text{trunc}(\log(nYrs)/\log(2)) - 1$ , where  $nYrs$  is the number of years in the tree-ring chronology. The R package `waveslim` (Whitcher, 2013) was used to do the multiresolution decomposition. Each "voice" is scaled by dividing by the standard deviation.

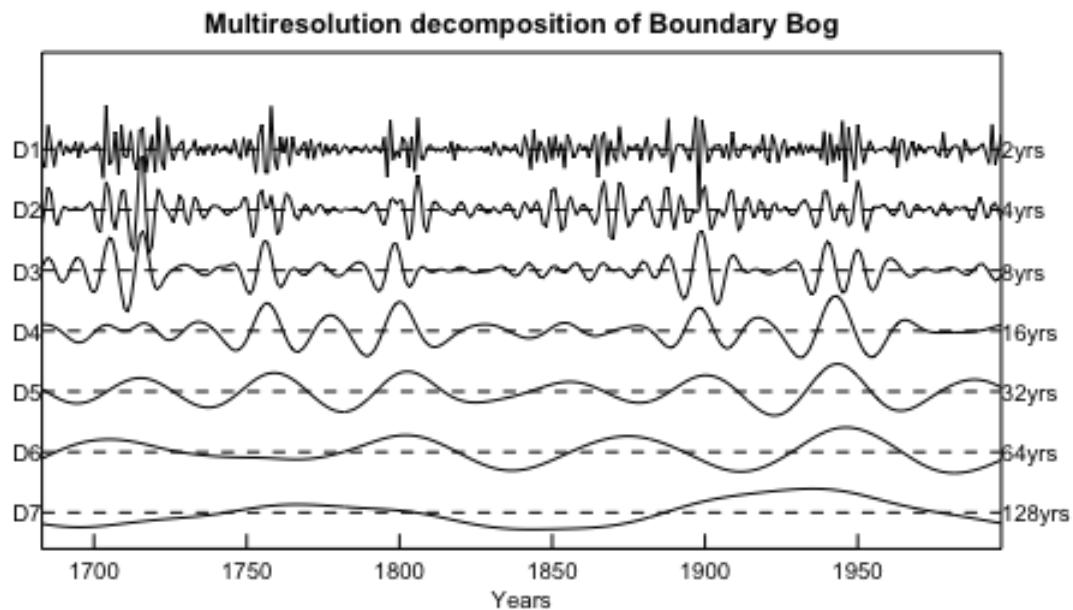


Figure B.1. Multiresolution decomposition for Boundary Bog tree-ring chronology (MacDonald and Case, 2014).

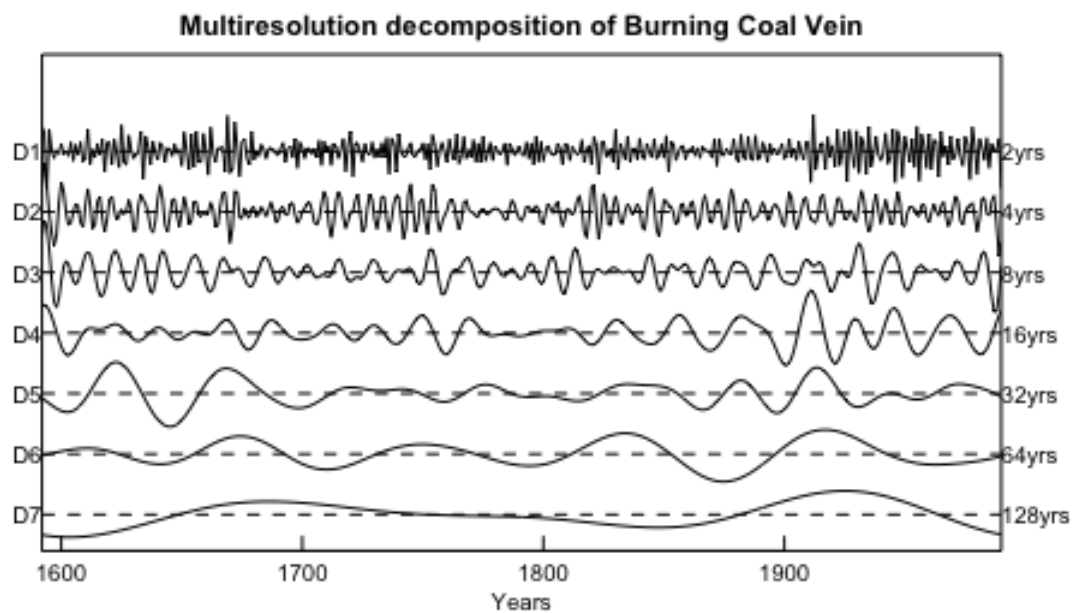


Figure B.2. Multiresolution decomposition for Burning Coal Vein tree-ring chronology (Meko and Sieg, 2014a).

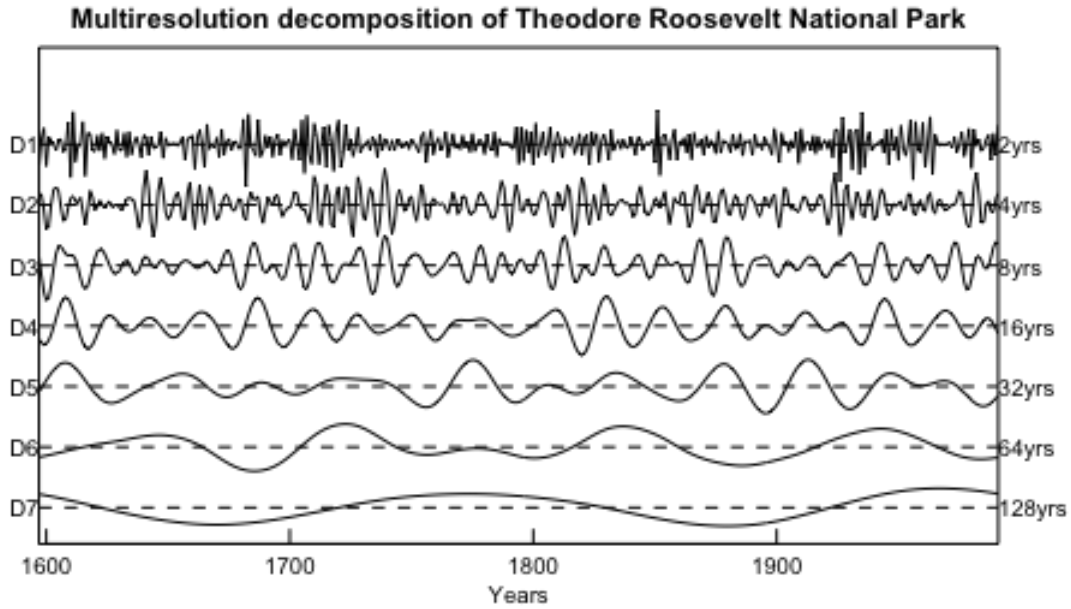


Figure B.3. Multiresolution decomposition for Theodore Roosevelt National Park tree-ring chronology (Meko and Sieg, 2014b).

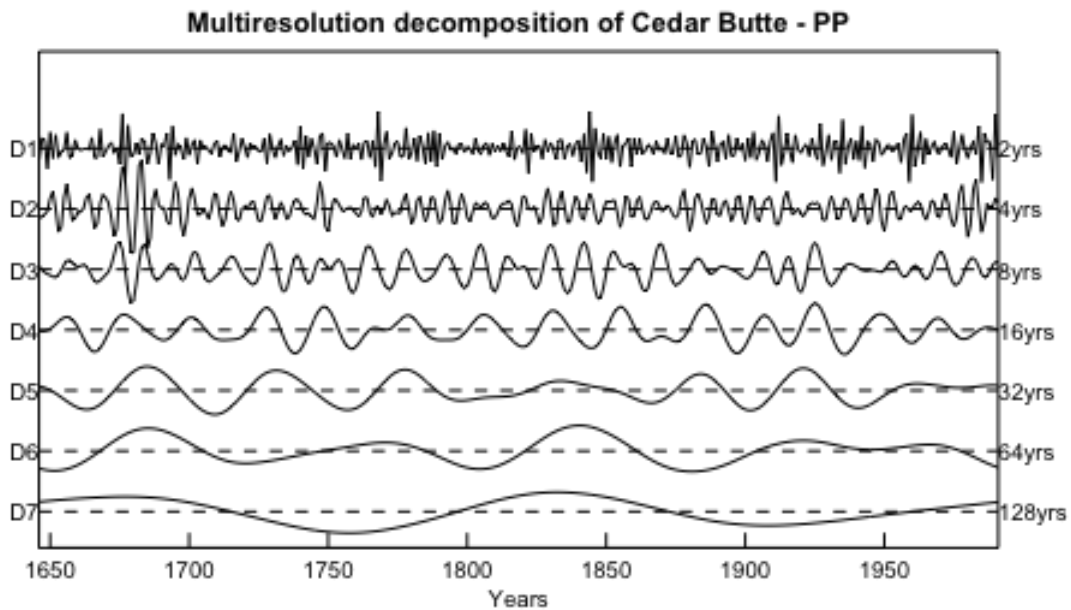


Figure B.4. Multiresolution decomposition for Cedar Butte tree-ring chronology (Meko and Sieg, 2014c).

Figures B.5-B.8 represent wavelet analyses that decompose the tree-ring chronologies into "time-frequency space" that allows one to "determine both the dominant modes of variability and how those modes vary in time" (Torrence and Compo, 1998). Wavelet analysis has been used in many climate-related studies, including subjects in tropical convection, El Niño-Southern Oscillation, atmospheric cold fronts, temperature, dispersion of ocean waves, wave growth and breaking, and turbulent flows (Torrence and Compo, 1998).

The colored portion of each figure shows the normalized wavelet power spectrum and shows a measure of wavelet power relative to white noise. The red and orange colors show where the power in the tree-ring series is concentrated. The wavelet function used is the Morlet, a common wavelet function (Torrence and Compo, 1998). Errors can occur at the beginning and end of the time series (Torrence and Compo, 1998), therefore, a cone of influence (area with black crosshatching) is shown in figures B.5-B.8.

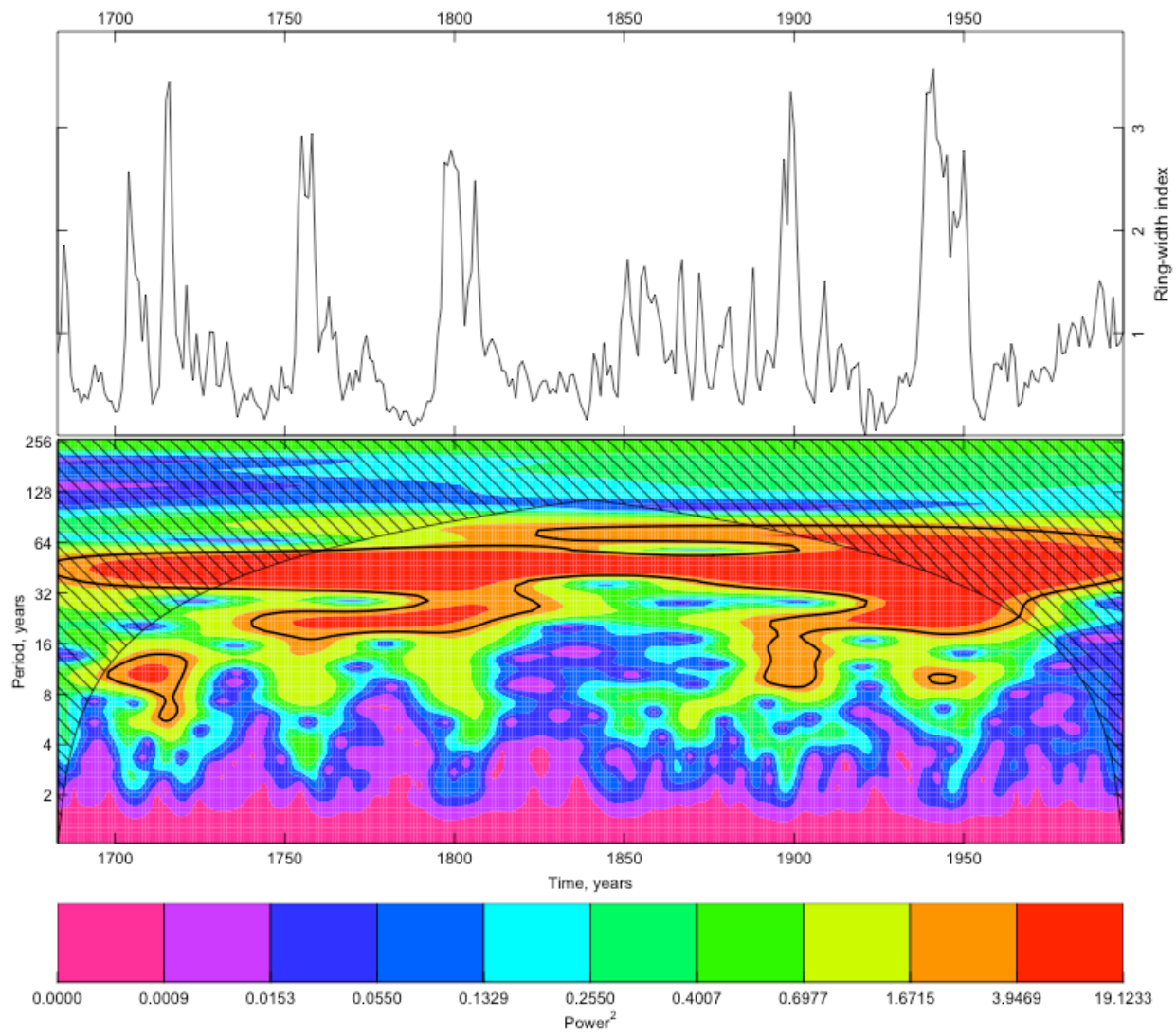


Figure B.5. Wavelet analysis for Boundary Bog tree-ring chronology (MacDonald and Case, 2014).

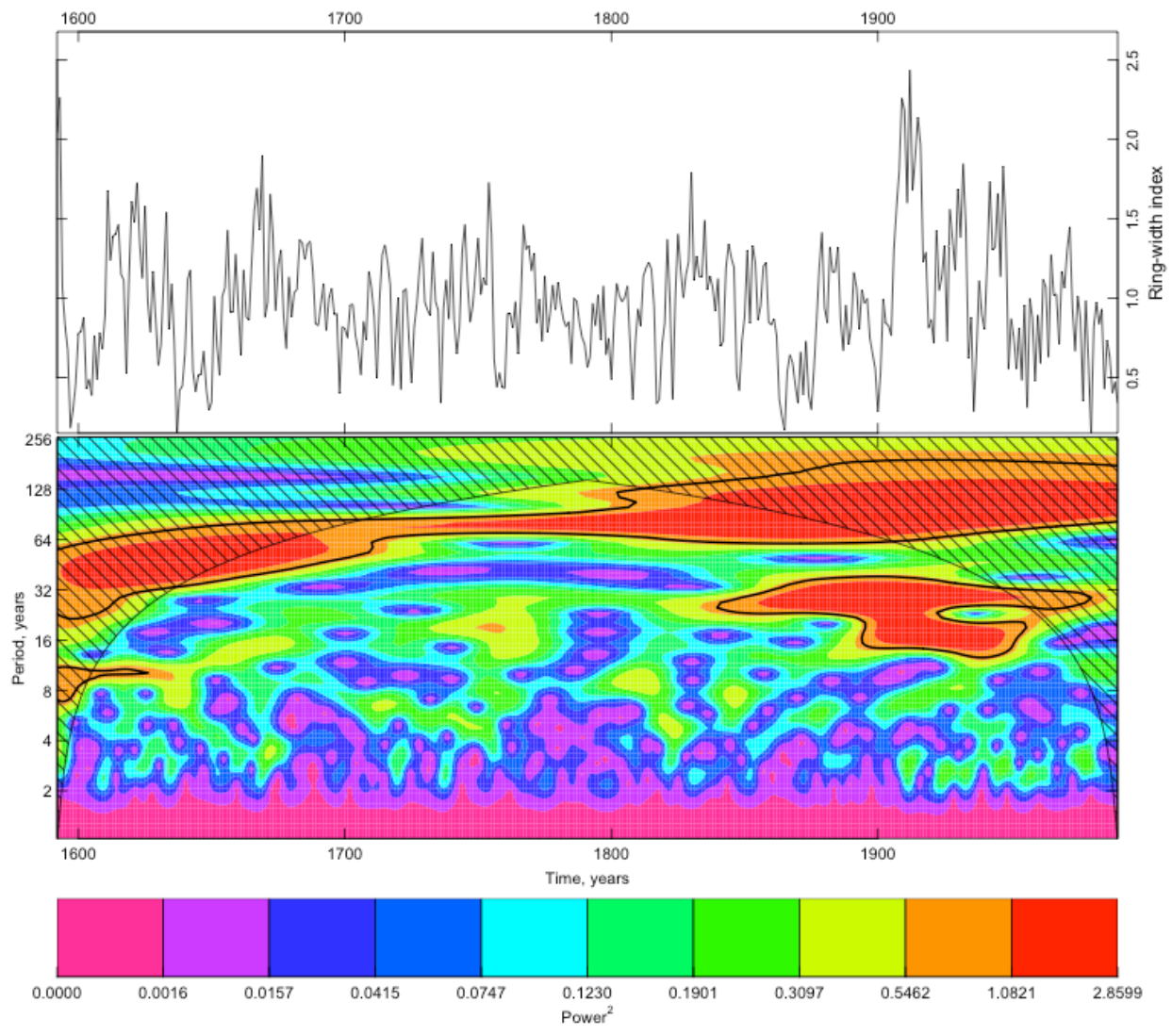


Figure B.6. Wavelet analysis for Burning Coal Vein tree-ring chronology (Meko and Sieg, 2014a).

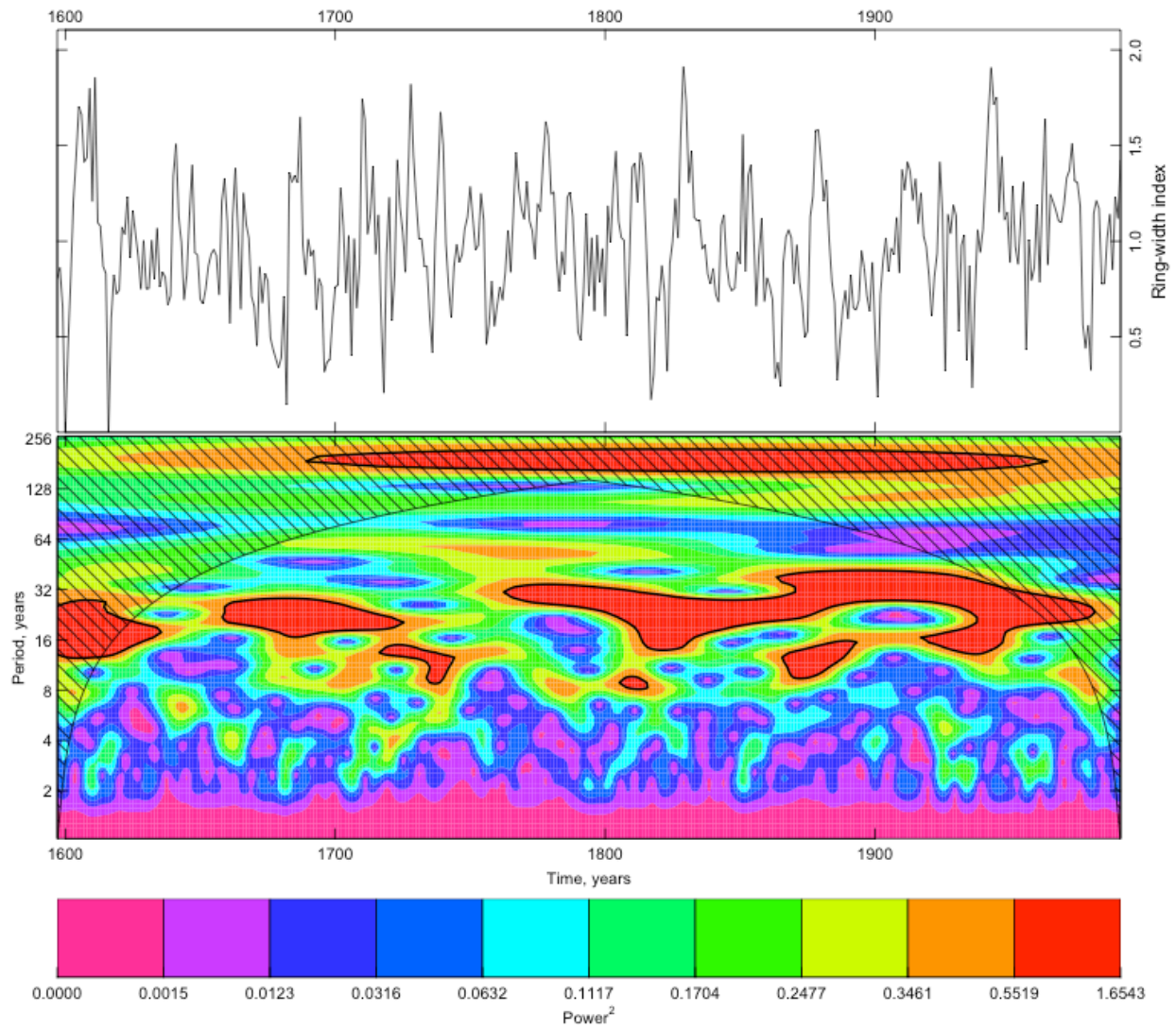


Figure B.7. Wavelet analysis for Theodore Roosevelt National Park tree-ring chronology (Meko and Sieg, 2014b).

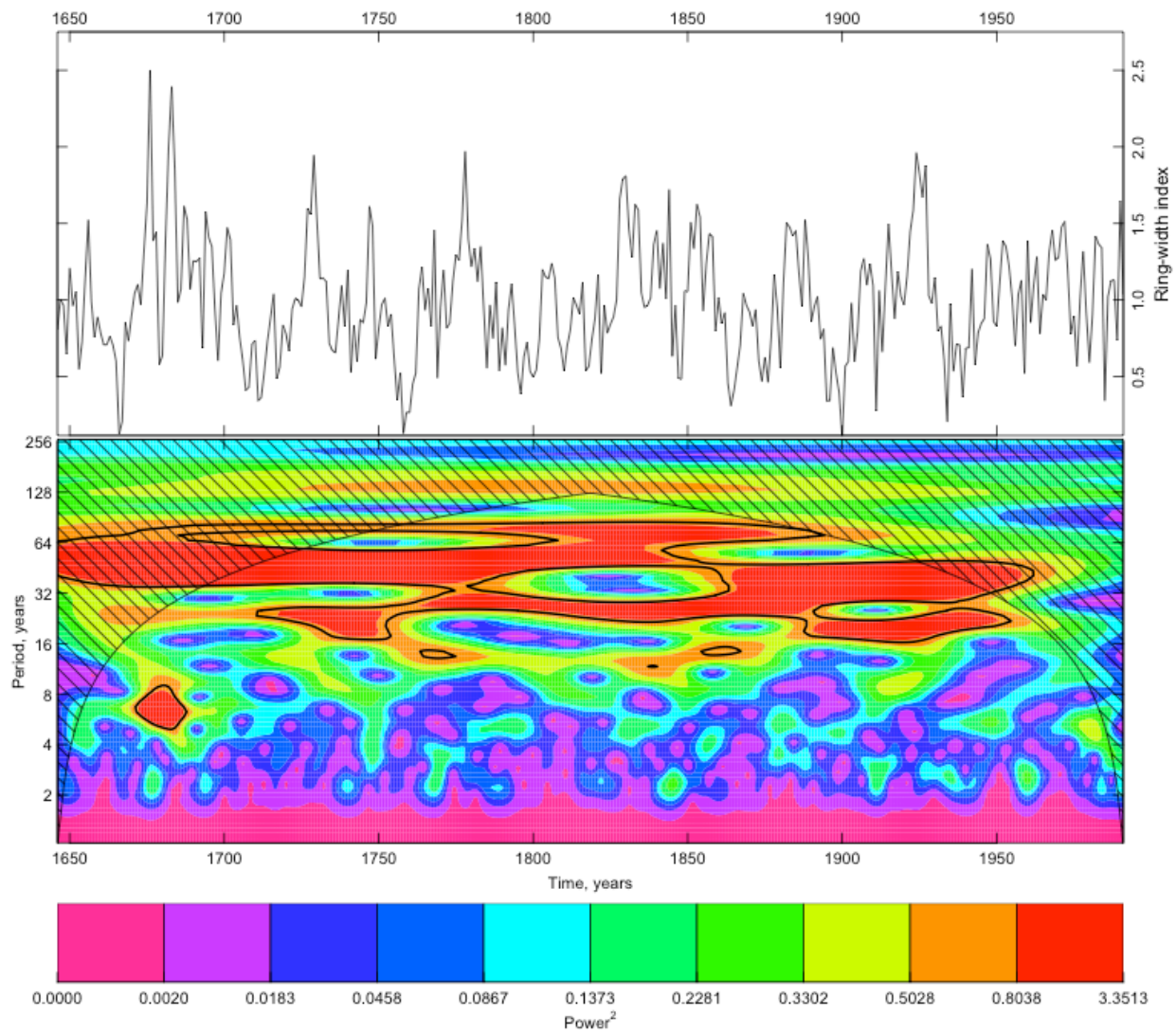


Figure B.8. Wavelet analysis for Cedar Butte tree-ring chronology (Meko and Sieg, 2014c).

**APPENDIX C. DISCHARGE ANALYSIS FOR LONG-TERM STREAMGAGES ON  
THE RED RIVER OF THE NORTH AND SELECTED TRIBUTARIES**

Discharge (streamflow) is an integral part to the total phosphorus (TP) concentration and flux trends and variability over time. High TP concentrations can occur at high discharge when snowmelt or rain-generated runoff washes manure, fertilizers, and soil into streams. High TP can also occur at low discharge when the stream is more influenced by wastewater treatment plant effluent. The following plots document discharge variability over time for the Red River of the North, and three major tributaries, at long-term streamgage sites.

Discharge data for sites in table C.1 were obtained from the U.S. Geological Survey online database Water Data for the Nation <http://dx.doi.org/10.5066/F7P55KJN>, March 10, 2015. The sites have varying periods of record for daily discharge, but the analysis ends for all sites on or before September 30, 2014.

Table C.1. U.S. Geological streamgage numbers and names, listed in downstream direction along the Red River of the North, used for discharge analysis.

Streamgage identification number	Name
05051500	Red River of the North at Wahpeton, North Dakota
05051522	Red River of the North at Hickson, North Dakota
05054000	Red River of the North at Fargo, North Dakota
05059500	Sheyenne River at West Fargo, North Dakota (beginning in water year 1993 includes the combined flows from the Sheyenne River at West Fargo and the Sheyenne River Diversion at West Fargo)
05064500	Red River of the North at Halstad, Minnesota
05079000	Red Lake River at Crookston, Minnesota
05082500	Red River of the North at Grand Forks, North Dakota
05100000	Pembina River at Neche, North Dakota
05102500	Red River of the North at Emerson, Manitoba

The following discharge analyses were done using Exploration and Graphics for RivEr Trends (EGRET; Hirsch and De Cicco, 2015), a package for the statistical computing software R (R Core Team, 2014). The first plot at each streamgage is the time series plot of discharge. The second plot at each streamgage shows the running standard deviation of the log of daily discharge. "In the case of a system where discharge might be increasing over a period of years, this graphic provides a way of looking at the variability relative to that changing mean value. The standard deviation of the log discharge is much like a coefficient of variation, but it has sample properties that make it a smoother measure of variability" (Hirsch and De Cicco, 2015).

Additional information about interpreting the running standard deviation plot is provided by Hirsch and De Cicco (2015): "If, for example, the probability distribution of daily mean discharge were to have trended upwards (or downwards) over time, but had done so in a manner that all quantiles of the distribution had increased by the same percentage amount, then we would expect this graphic to show a horizontal line. If, on the other hand, the change in the probability distribution were such that there was a greater percentage change in the high end and (or) low end of the distribution, compared to the percentage change in the middle portion of the distribution, then this curve would slope upwards over time... this graphic can be useful and simple way of providing empirical evidence for hypotheses exploring the idea that increasing urbanization or increasing green house gas concentrations in the atmosphere are bringing about changes in hydrologic variability." The running standard deviation is a 12-year centered window, so the first 6 and last 6 years of the data are cut off on the plot.

The third plot provides graphical estimates of four statistics: annual 1-day maximum daily mean discharge (maximum day), annual mean of the daily mean discharges (mean daily), annual median of the daily mean discharges (median daily), and annual minimum 7-day mean of

the daily mean discharges (7-day minimum) and smoothed versions of those time series. The smoothed version is determined using weighted regression with a 12-year half window. This means that in the weighted regressions, a point in the middle of the period will use weighted values of log discharge 12 years before and 12 years after it. A point at the end of the record has higher weights extended back in time.

The windows were modified from the default of 15 years to 12 for the standard deviation and from 20 to 12 for the discharge statistic estimates because a number of studies have identified a decadal-scale (greater than 7 years) signal in precipitation (Cayan et al., 1998; Garbrecht and Rossel, 2002; Small and Islam, 2008; Small and Islam, 2009; Ault and St. George, 2010). Small and Islam (2008; 2009) identified a statistically significant signal in autumn precipitation in the central U.S. with a periodicity of approximately 12 years, with the signal strongest in the Midwest and Great Plains. Ryberg et al. (2014) focused on long-term (multi-decadal) variability and thus shorter-term, quasi-periodic signals were treated as “nuisance” variability and smoothed out by using a 12-year moving average when analyzing precipitation, potential evapotranspiration, and runoff. Chapter 5 used a 12-year moving average when modeling seasonal precipitation. This region is subject to sudden shifts from wet to dry or dry to wet (Chapter 3 and 5; Ryberg et al., 2014; Shapley et al., 2005; Vance et al 1992; Vecchia, 2008) and the default estimation curves may be too gradual for highly variable prairie streams. The resulting estimates of the discharge statistics match institutional knowledge of changes in the Red River and the surrounding region and show well the fluctuations caused by droughts during the period of record at these sites.

### C.1. Red River of the North at Wahpeton, North Dakota

Figures C.1-C.3 highlight the drought of the 1970s that increased variability as it affected flow quantiles differently, with a more noticeable drop in seven-day minimum discharge than in the maximum daily discharge.

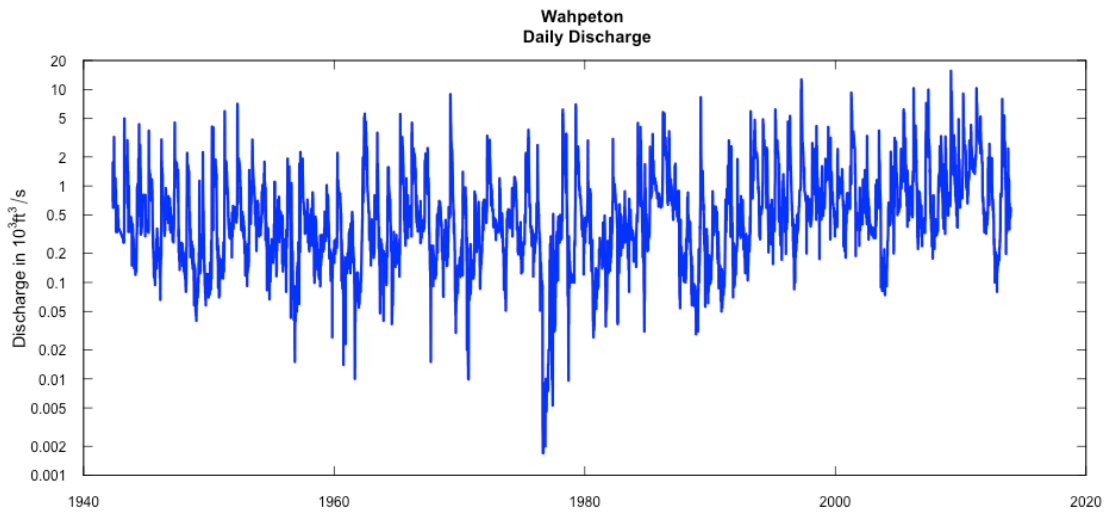


Figure C.1. Discharge for period of record ending September 30, 2014, Red River of the North at Wahpeton, North Dakota.

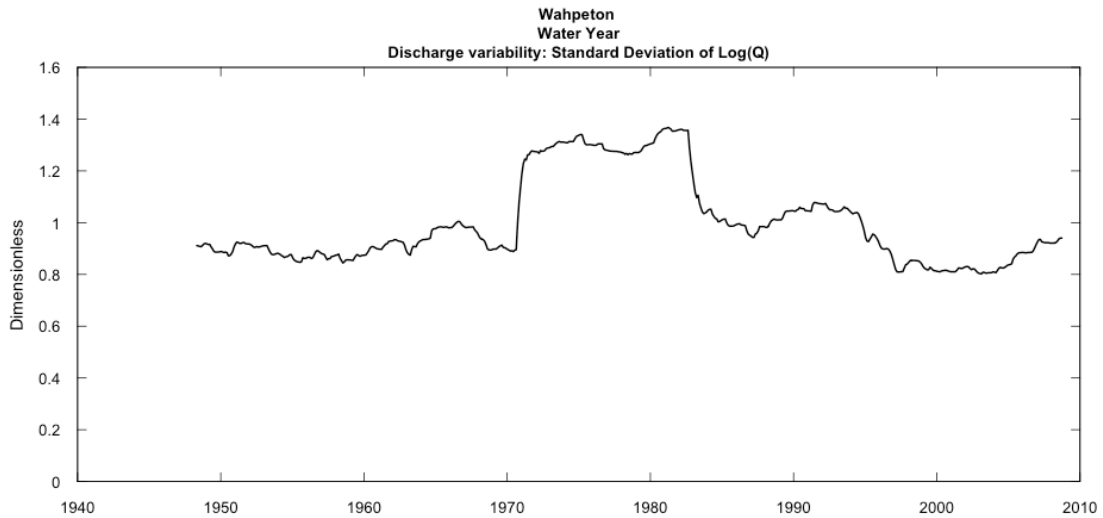


Figure C.2. Running standard deviation of logarithm of daily mean discharge (Q) for the Red River of the North at Wahpeton, North Dakota.

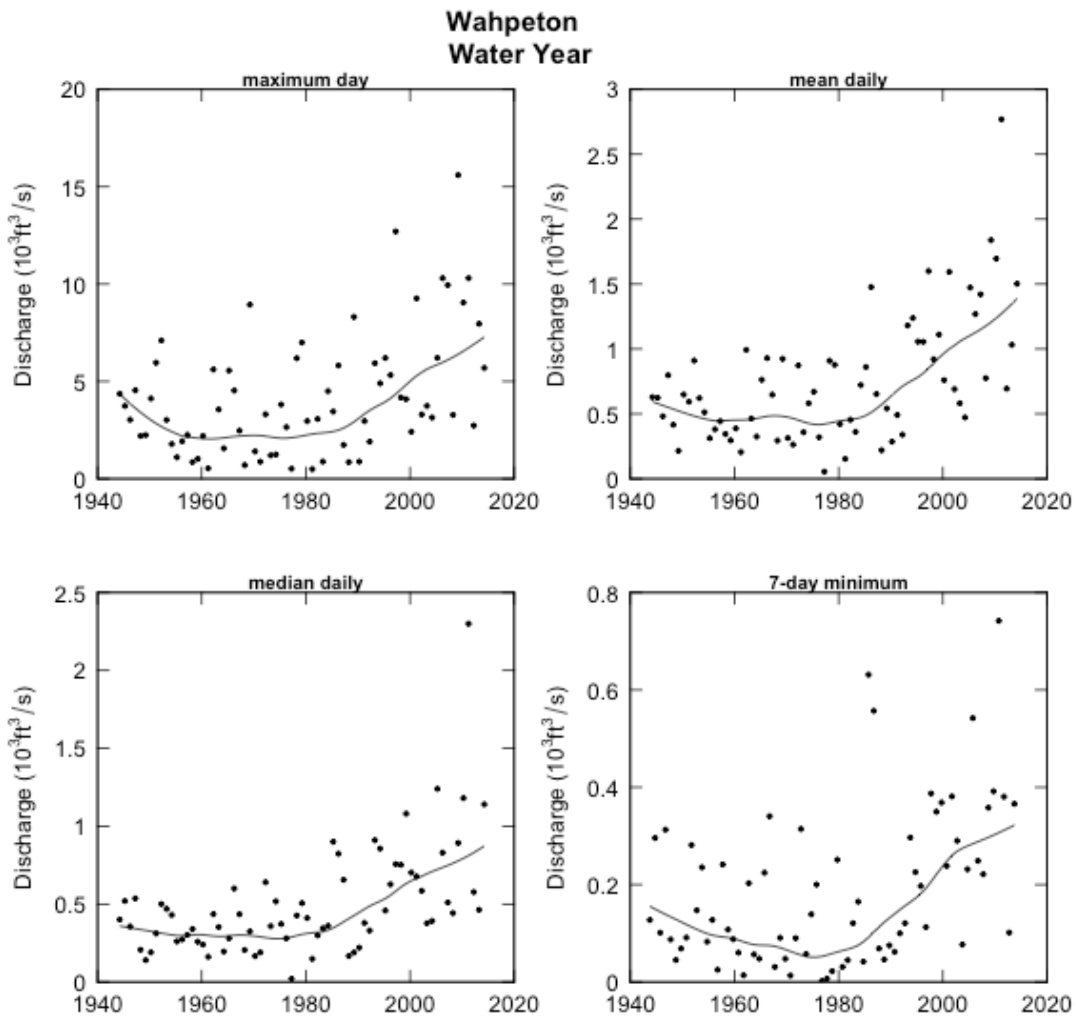


Figure C.3. Annual 1-day maximum daily mean discharge (maximum day), annual mean of the daily mean discharges (mean daily), annual median of the daily mean discharges (median daily), and annual minimum 7-day mean of the daily mean discharges (7-day minimum), Red River of the North at Wahpeton, North Dakota.

## C.2. Red River of the North at Hickson, North Dakota

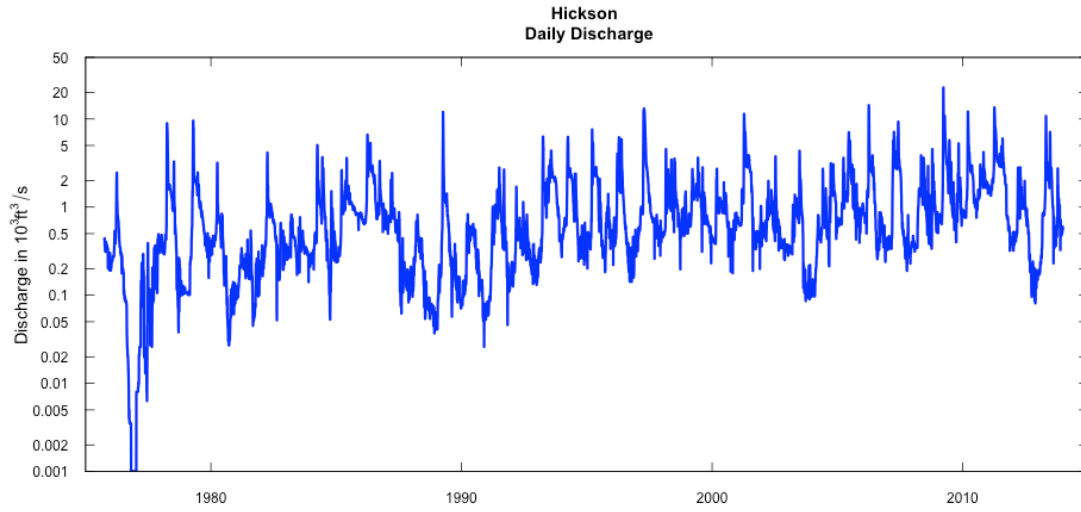


Figure C.4. Discharge for period of record ending September 30, 2014, Red River of the North at Hickson, North Dakota.

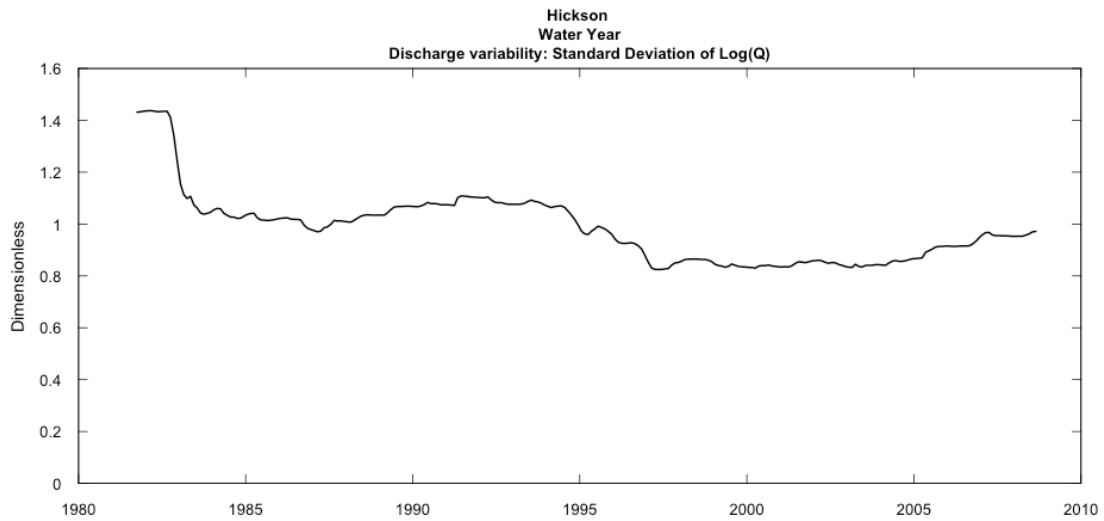


Figure C.5. Running standard deviation of logarithm of daily mean discharge (Q) for the Red River of the North at Hickson, North Dakota.

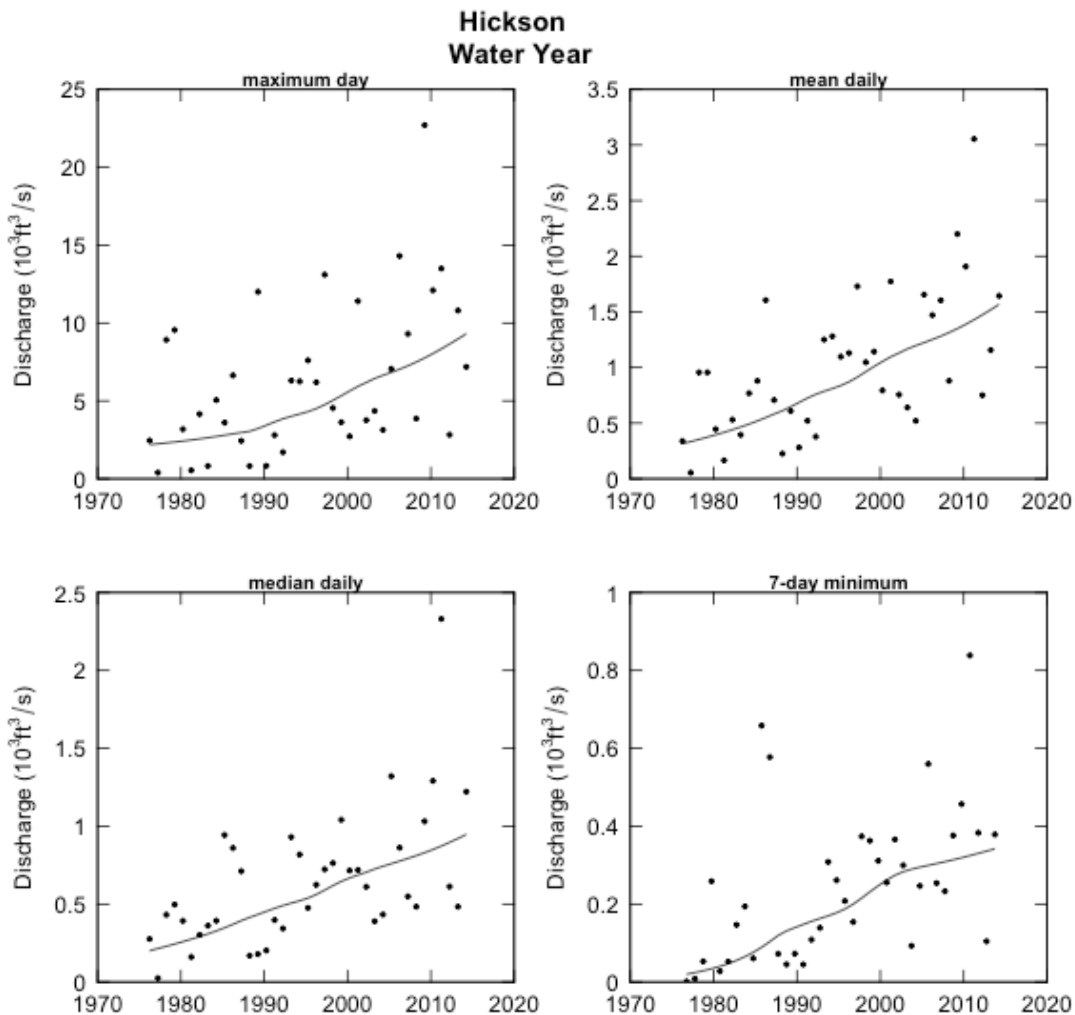


Figure C.6. Annual 1-day maximum daily mean discharge (maximum day), annual mean of the daily mean discharges (mean daily), annual median of the daily mean discharges (median daily), and annual minimum 7-day mean of the daily mean discharges (7-day minimum), Red River of the North at Hickson, North Dakota.

### C.3. Red River of the North at Fargo, North Dakota

The widespread 1930s drought is the dominant feature in figures C.7-C.9. Also notable is the recent increase in annual 1-day maximum daily mean discharge (maximum day), annual mean of the daily mean discharges (mean daily), annual median of the daily mean discharges (median daily), and annual minimum 7-day mean of the daily mean discharges (7-day

minimum). Since all of these measures of discharge are going up at the end of the record in a similar manner (fig. C.9), the variability in discharge is low at the end of the record (near 1, fig. C.8).

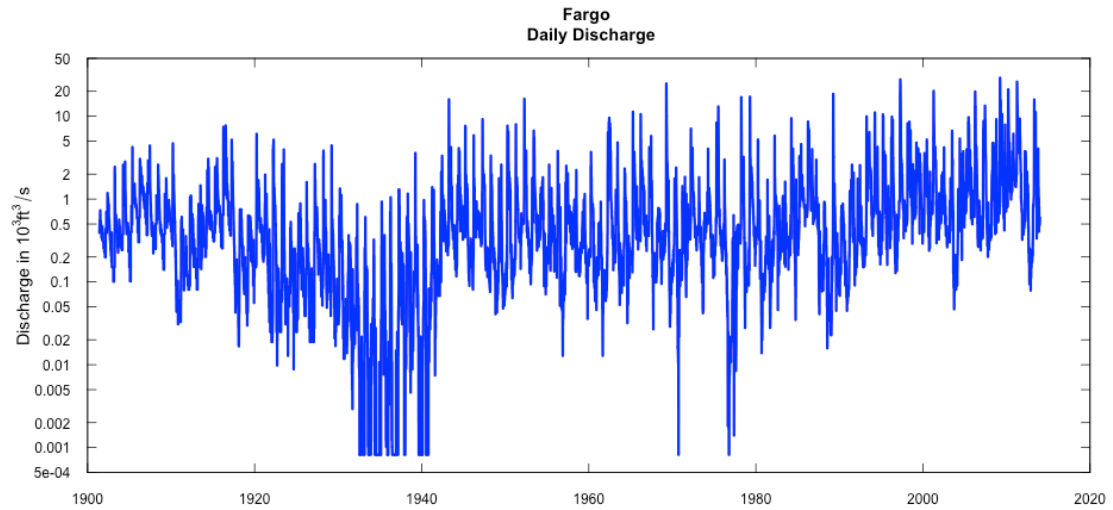


Figure C.7. Discharge for period of record ending September 30, 2014, Red River of the North at Fargo, North Dakota.

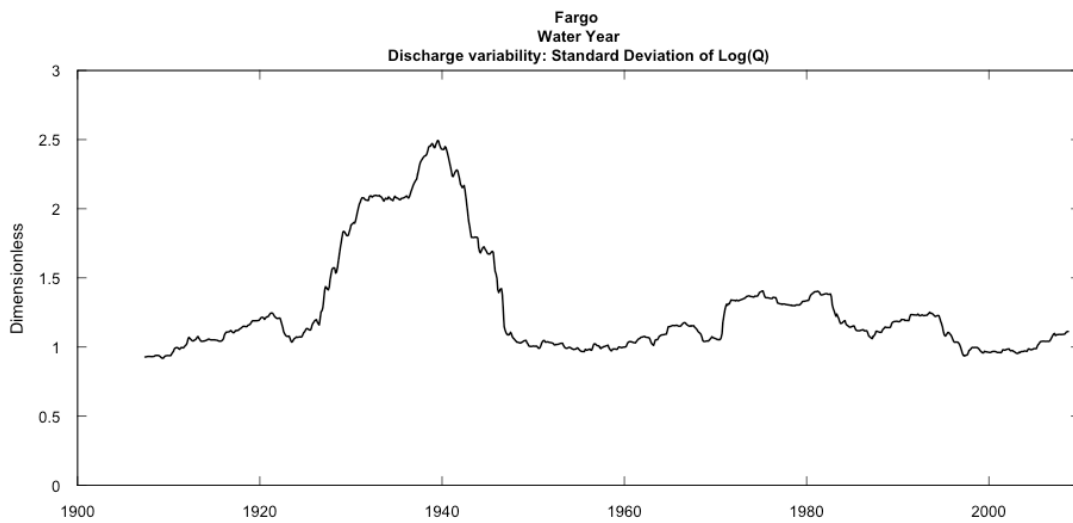


Figure C.8. Running standard deviation of logarithm of daily mean discharge ( $Q$ ) for the Red River of the North at Fargo, North Dakota.

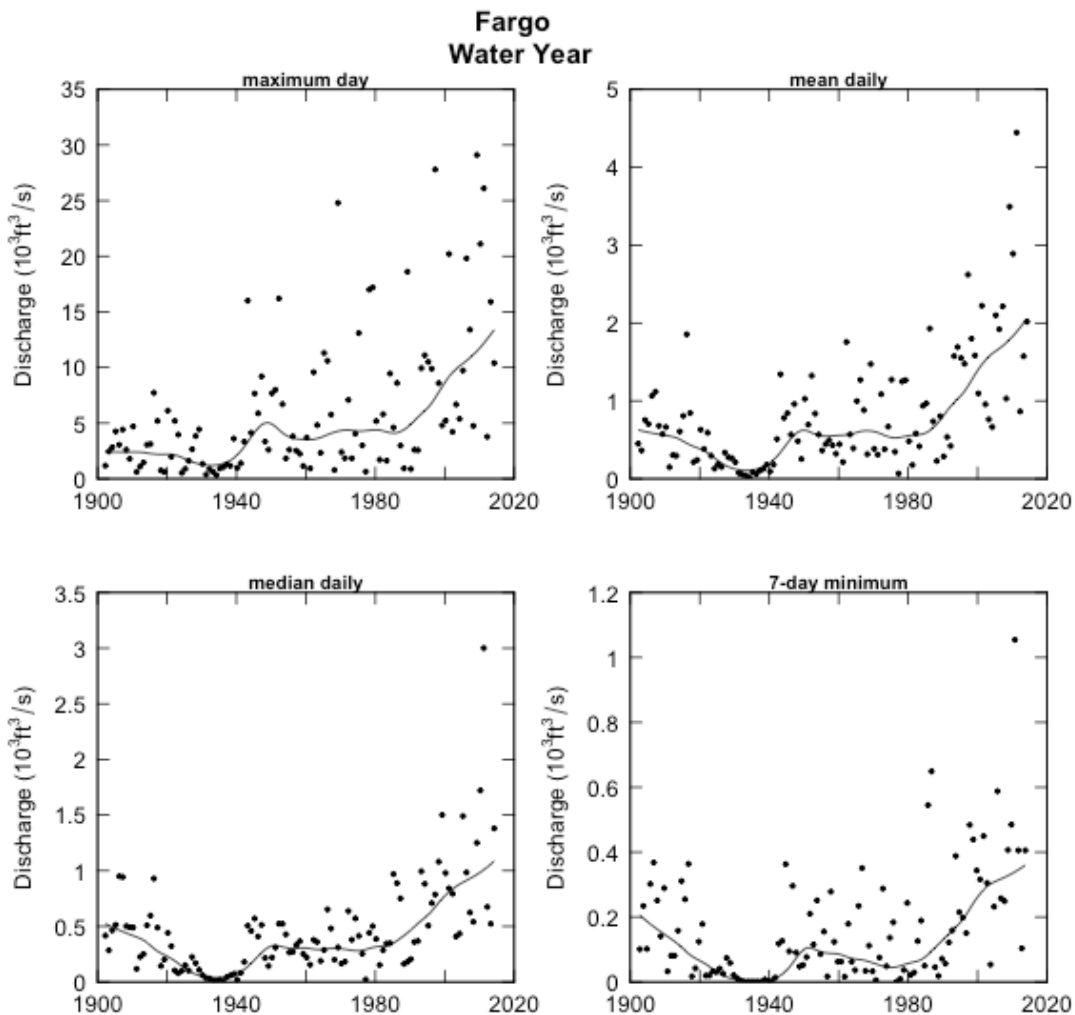


Figure C.9. Annual 1-day maximum daily mean discharge (maximum day), annual mean of the daily mean discharges (mean daily), annual median of the daily mean discharges (median daily), and annual minimum 7-day mean of the daily mean discharges (7-day minimum), Red River of the North at Fargo, North Dakota.

#### C.4. Sheyenne River at West Fargo, North Dakota

This streamgage had daily observations in 1903-05, and 1919, then a continuous record started in water year 1930. Figures C.10 and C.11 are presented from 1930 to the present and the entire period is depicted in C.12 for comparison purposes, although the smoothing line does not continue back to the early 1900s.

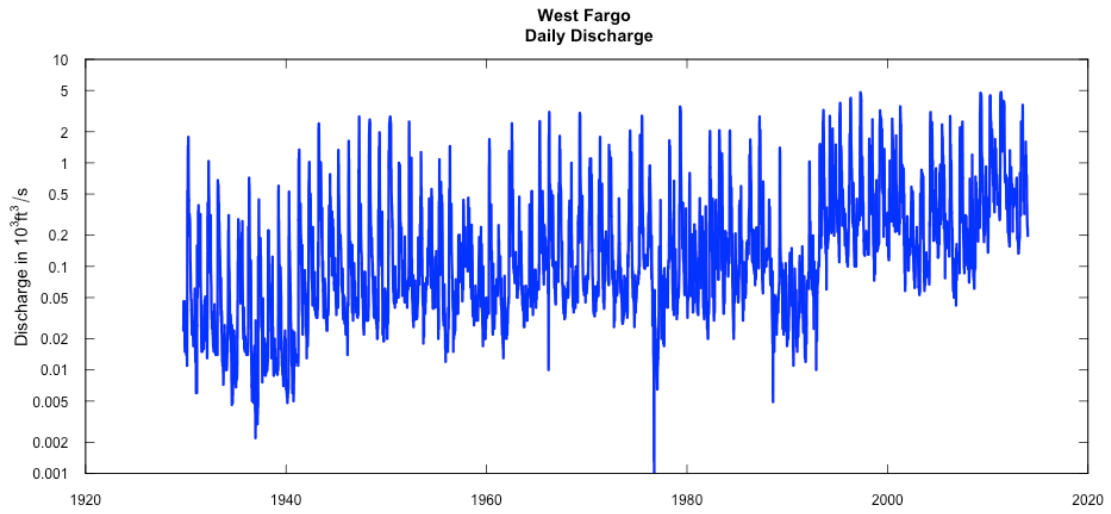


Figure C.10. Discharge for period of record ending September 30, 2014, Sheyenne River West at Fargo, North Dakota.

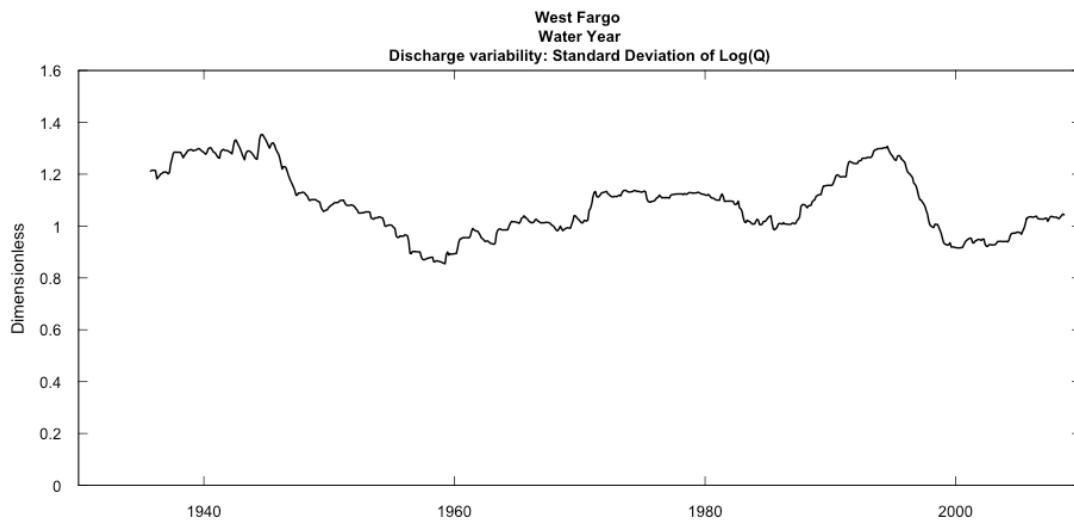


Figure C.11. Running standard deviation of logarithm of daily mean discharge (Q) for the Sheyenne River at West Fargo, North Dakota.

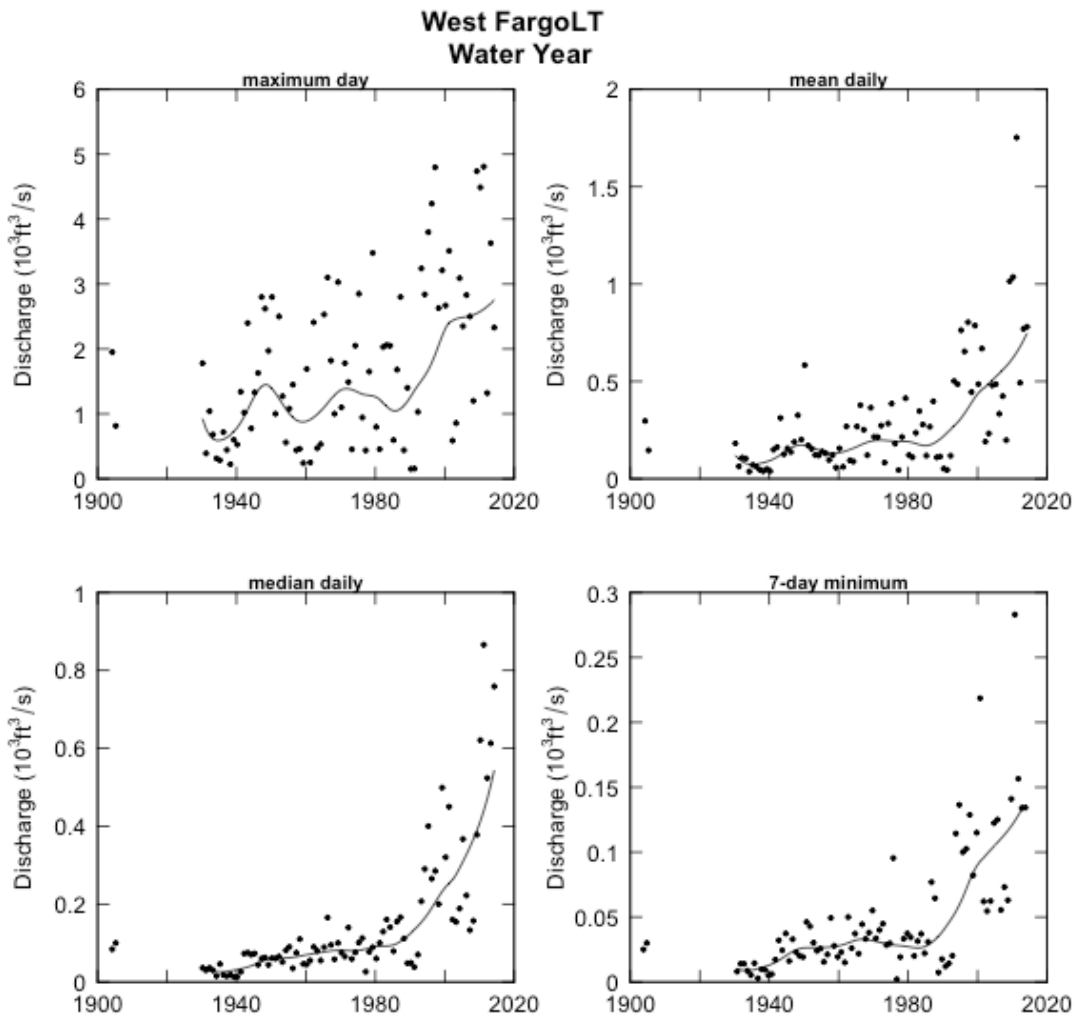


Figure C.12. Annual 1-day maximum daily mean discharge (maximum day), annual mean of the daily mean discharges (mean daily), annual median of the daily mean discharges (median daily), and annual minimum 7-day mean of the daily mean discharges (7-day minimum), Sheyenne River at West Fargo, North Dakota.

### C.5. Red River of the North at Halstad, Minnesota

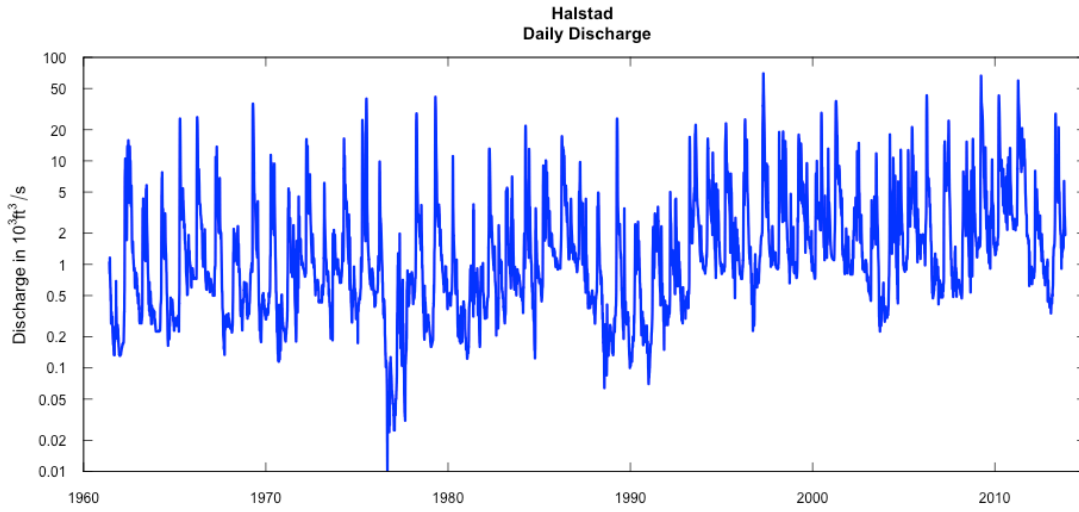


Figure C.13. Discharge for period of record ending September 30, 2014, Red River of the North at Halstad, Minnesota.

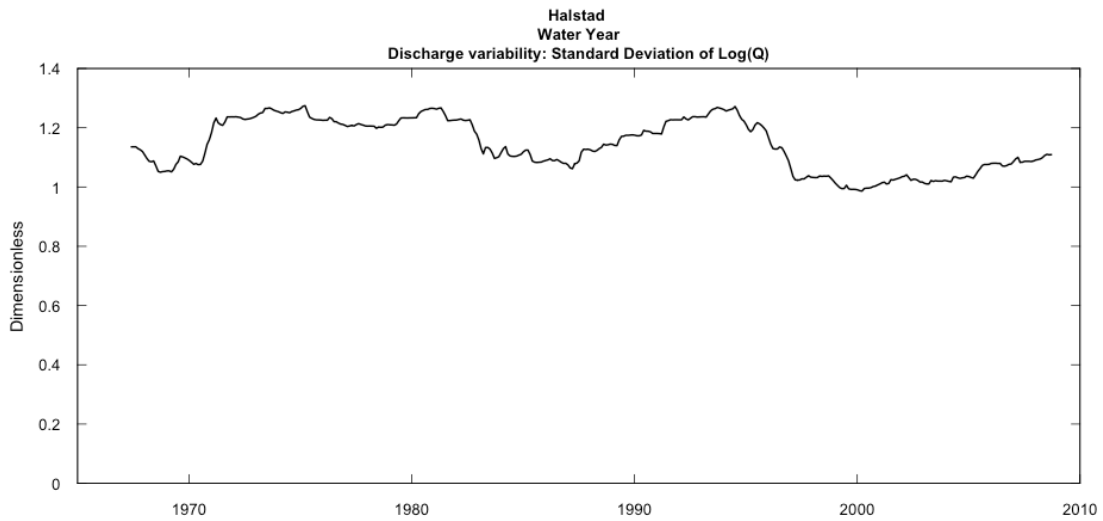


Figure C.14. Running standard deviation of logarithm of daily mean discharge ( $Q$ ) for the Red River of the North at Halstad, Minnesota.

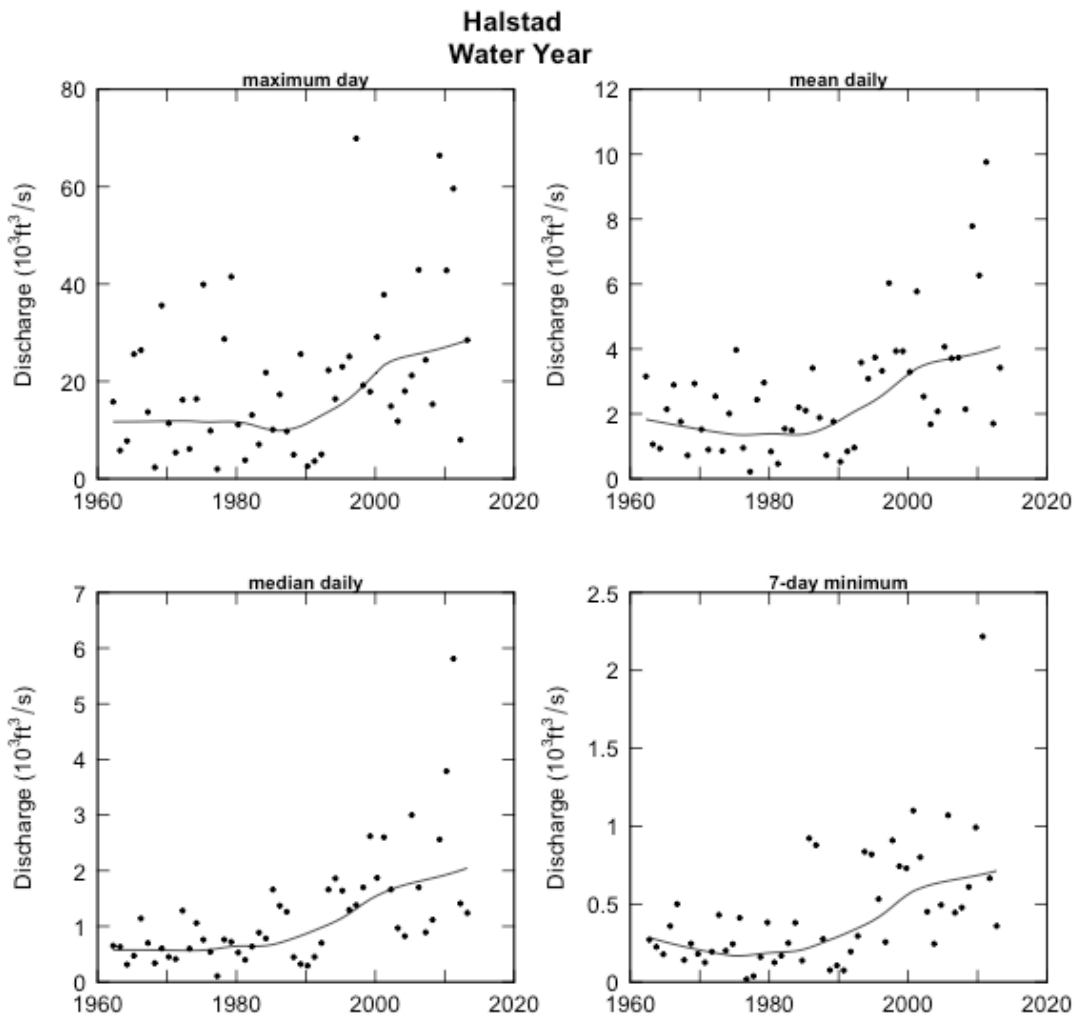


Figure C.15. Annual 1-day maximum daily mean discharge (maximum day), annual mean of the daily mean discharges (mean daily), annual median of the daily mean discharges (median daily), and annual minimum 7-day mean of the daily mean discharges (7-day minimum), Red River of the North at Halstad, Minnesota.

### C.6. Red Lake River at Crookston, Minnesota

The Red Lake River in Minnesota has a different period of variability than does the Red River upstream at Fargo, North Dakota. The Red Lake River has what looks like a quasi-periodic signal in the statistics of discharge shown in figure C.18. There are dams on the Red Lake River; however, the USGS does not indicate that any of the peaks recorded at five streamgages on the

Red Lake River are affected by regulation (which would be indicated by a peak-streamflow qualification code of 5, discharge affected to unknown degree by regulation or diversion, or 6, discharge affected by regulation or diversion; <http://nwis.waterdata.usgs.gov/mn/nwis/peak>, accessed March 10, 2015).

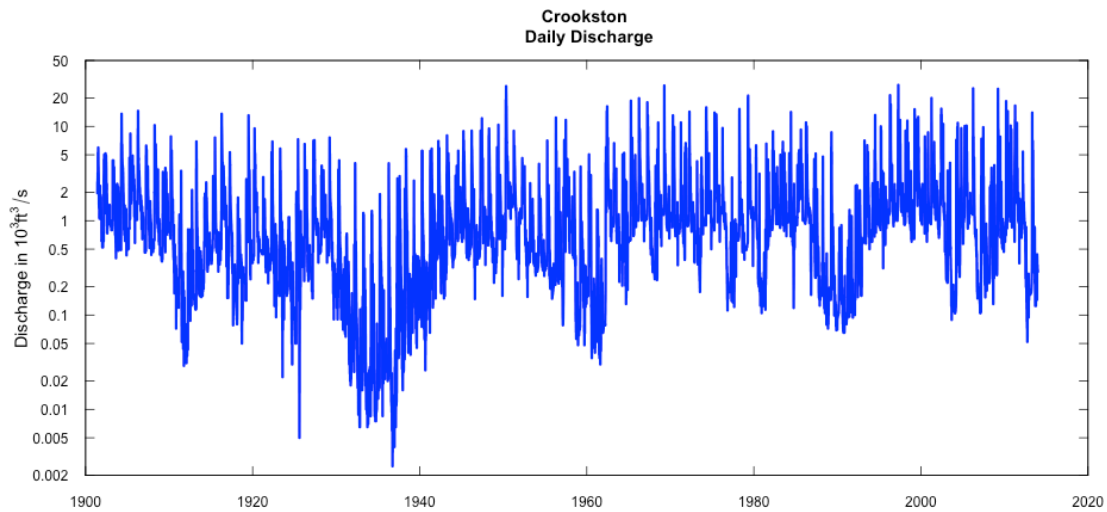


Figure C.16. Discharge for period of record ending September 30, 2014, Red Lake River at Crookston, Minnesota.

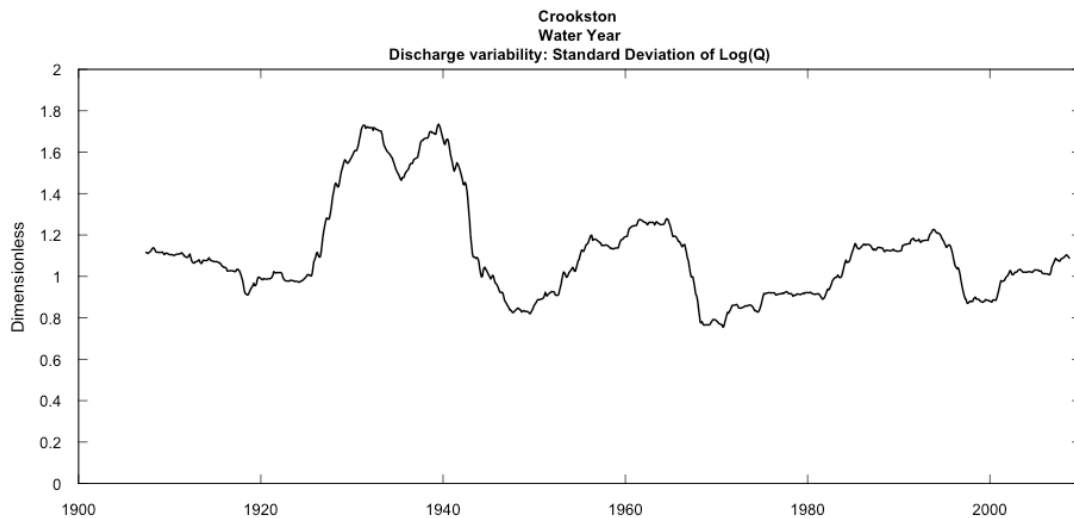


Figure C.17. Running standard deviation of logarithm of daily mean discharge (Q) for the Red Lake River at Crookston, Minnesota.

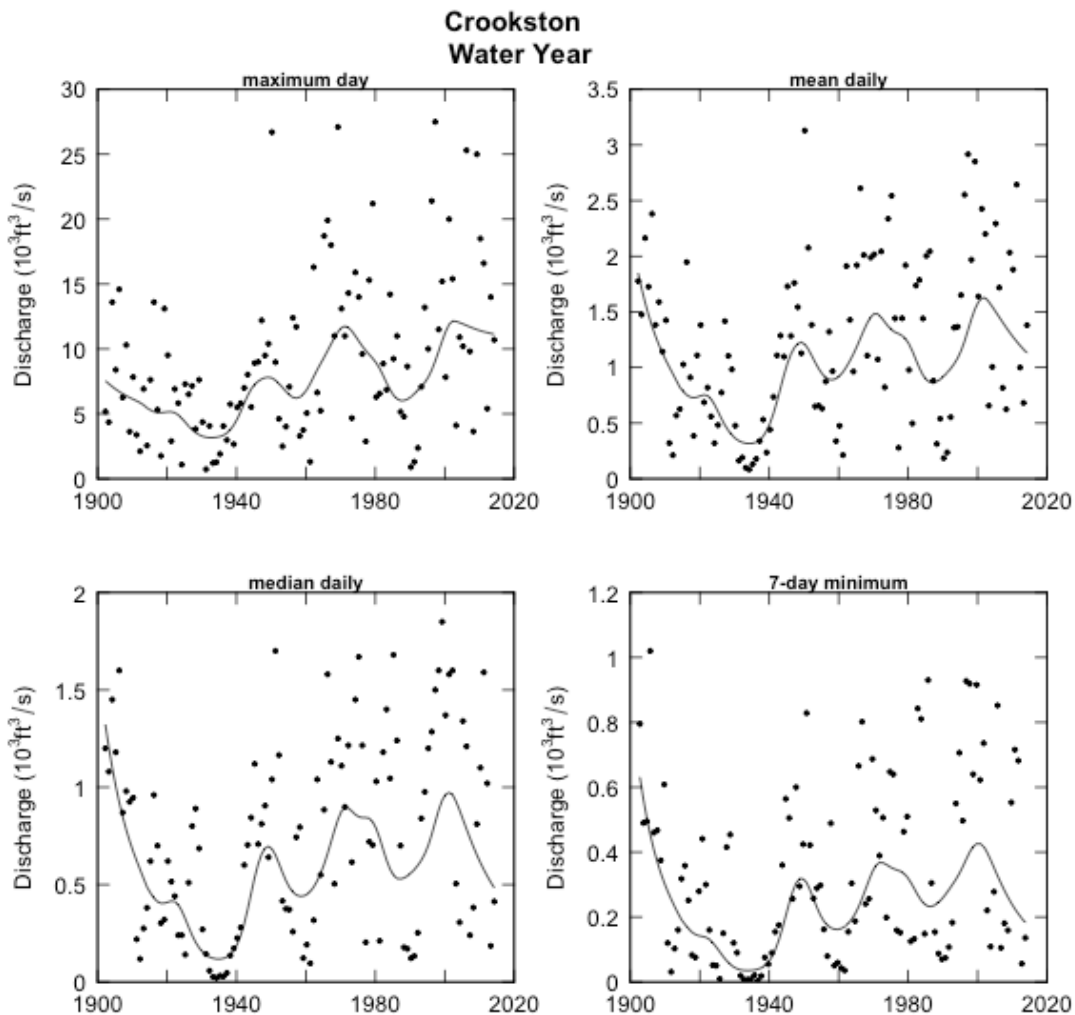


Figure C.18. Annual 1-day maximum daily mean discharge (maximum day), annual mean of the daily mean discharges (mean daily), annual median of the daily mean discharges (median daily), and annual minimum 7-day mean of the daily mean discharges (7-day minimum), Red Lake River at Crookston, Minnesota.

### C.7. Red River of the North at Grand Forks, North Dakota

Comparing the plots for the Red River at Grand Forks (figs. C.19-C.21) to the plots for the Red River at Fargo (C.7-C.9) and the Red Lake River (figs. C.16-C.18) shows how the Red Lake River influences the Red River at Grand Forks.

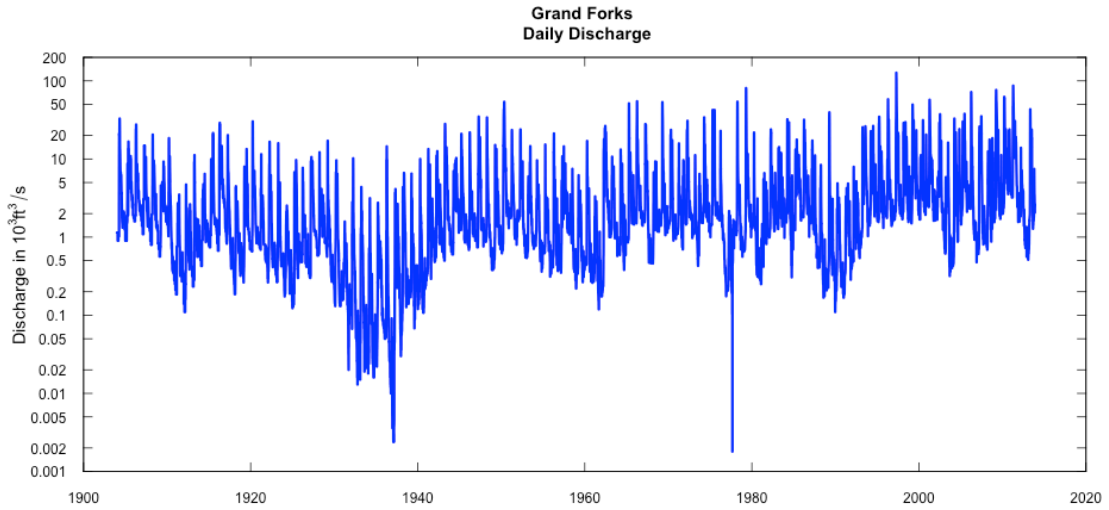


Figure C.19. Discharge for period of record ending September 30, 2014, Red River of the North at Grand Forks, North Dakota.

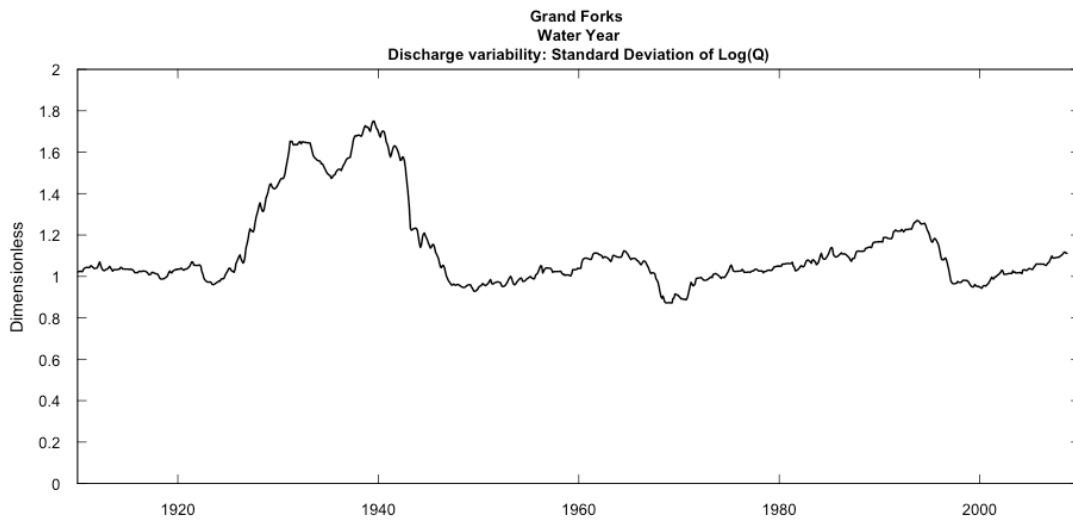


Figure C.20. Running standard deviation of logarithm of daily mean discharge (Q) for the Red River of the North at Grand Forks, North Dakota.

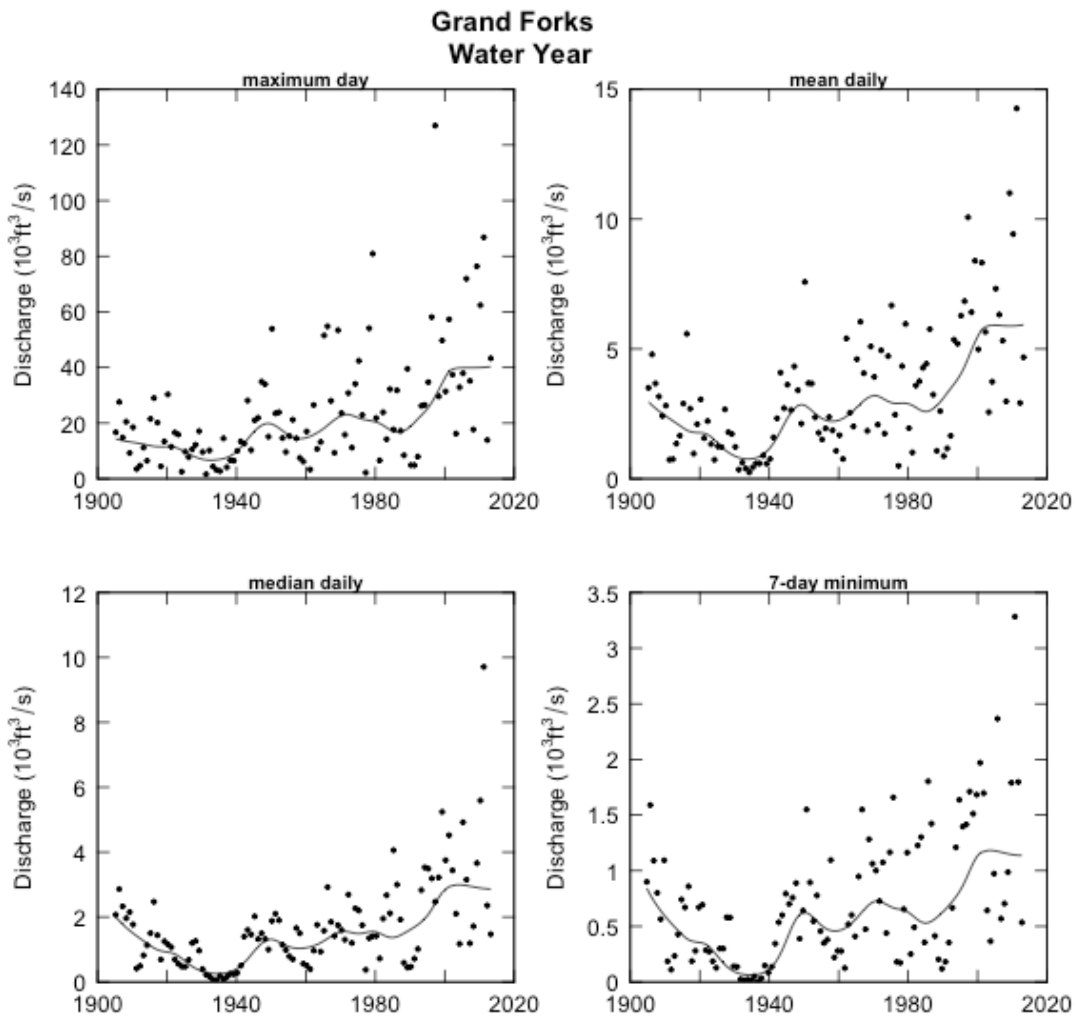


Figure C.21. Annual 1-day maximum daily mean discharge (maximum day), annual mean of the daily mean discharges (mean daily), annual median of the daily mean discharges (median daily), and annual minimum 7-day mean of the daily mean discharges (7-day minimum), Red River of the North at Grand Forks, North Dakota.

### C.8. Pembina River at Neche, North Dakota

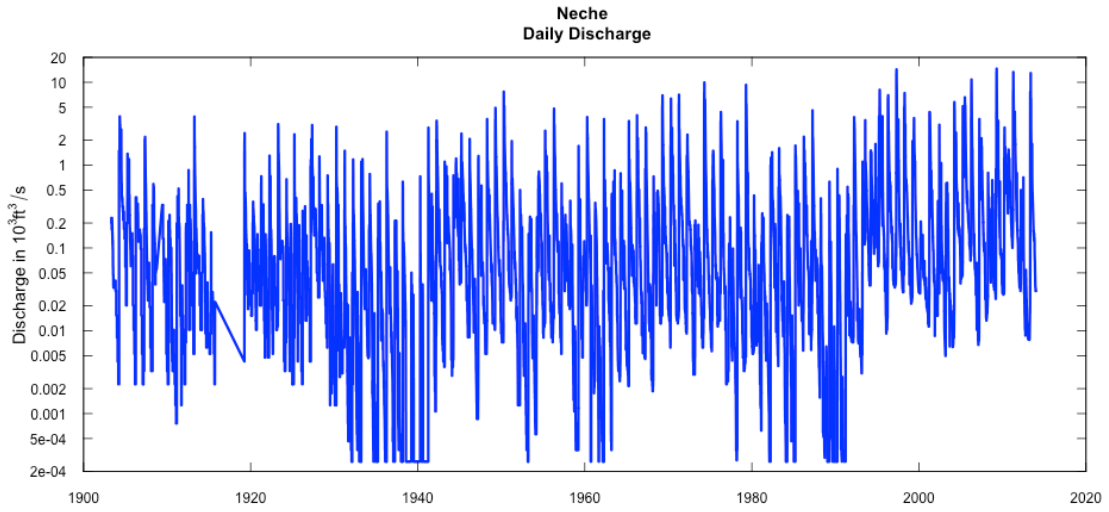


Figure C.22. Discharge for period of record ending September 30, 2014, Pembina River at Neche, North Dakota.

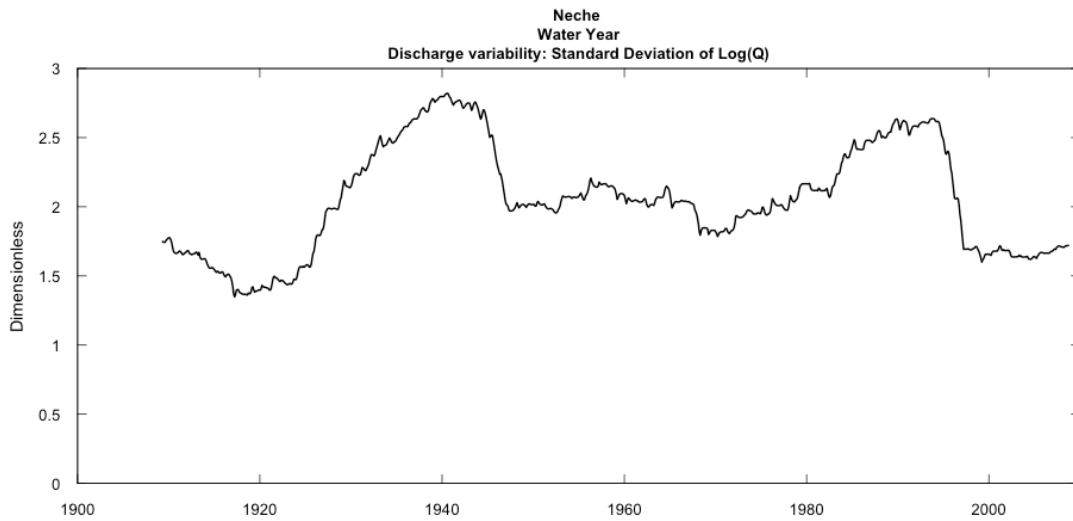


Figure C.23. Running standard deviation of logarithm of daily mean discharge ( $Q$ ) for the Pembina River at Neche, North Dakota.

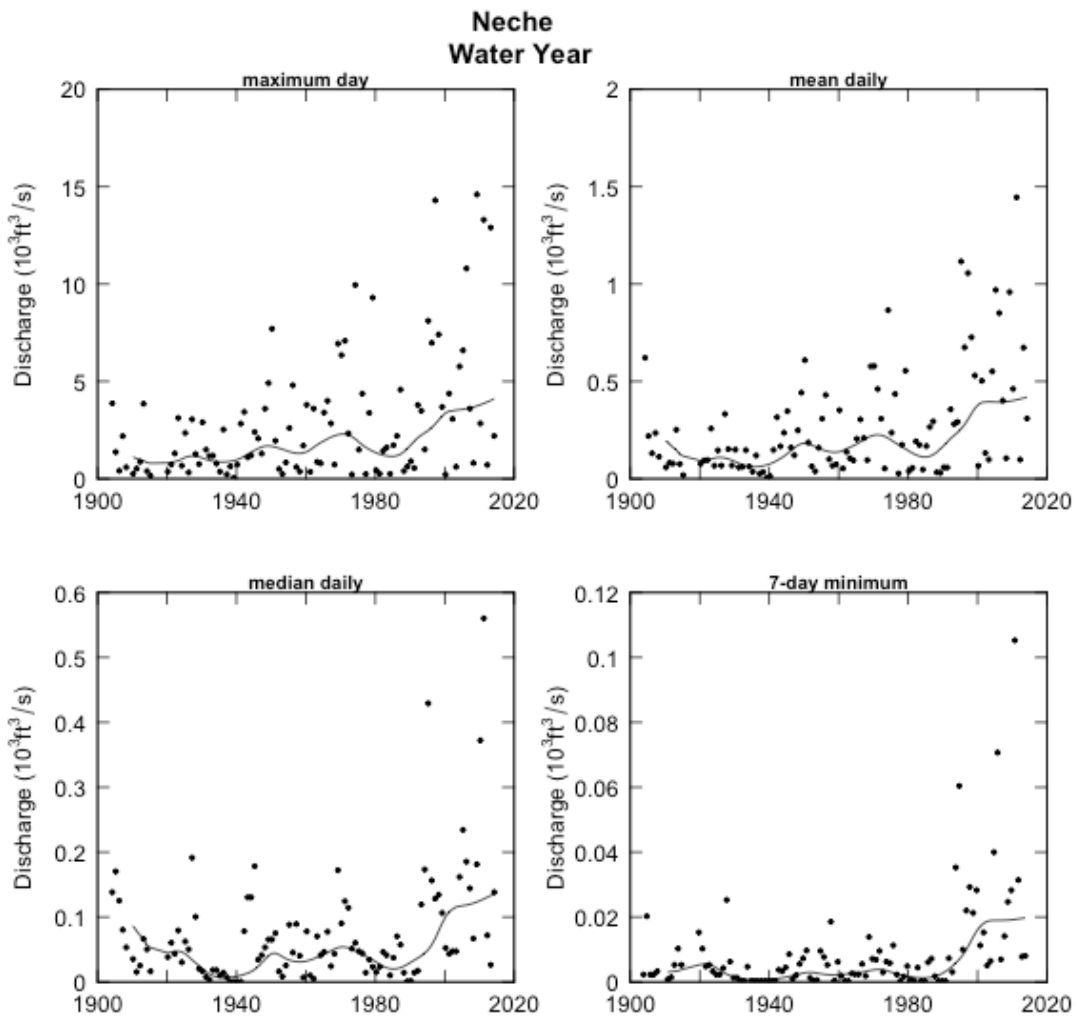


Figure C.24. Annual 1-day maximum daily mean discharge (maximum day), annual mean of the daily mean discharges (mean daily), annual median of the daily mean discharges (median daily), and annual minimum 7-day mean of the daily mean discharges (7-day minimum), Pembina River at Neche, North Dakota.

### C.9. Red River of the North at Emerson, Manitoba

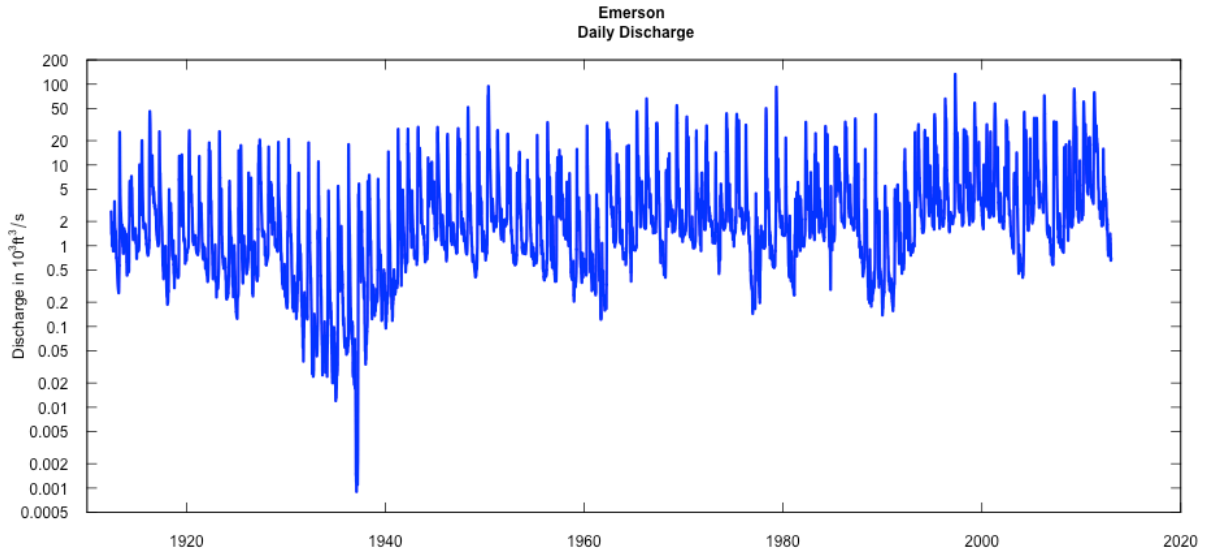


Figure C.25. Discharge for period of record ending September 30, 2014, Red River of the North at Emerson, Manitoba.

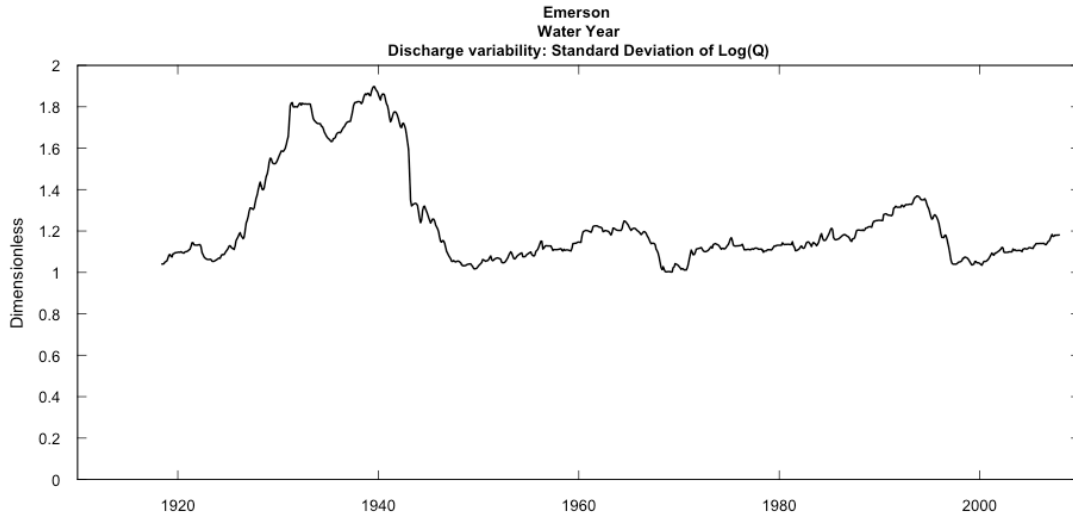


Figure C.26. Running standard deviation of logarithm of daily mean discharge ( $Q$ ) for the Red River of the North at Emerson, Manitoba.

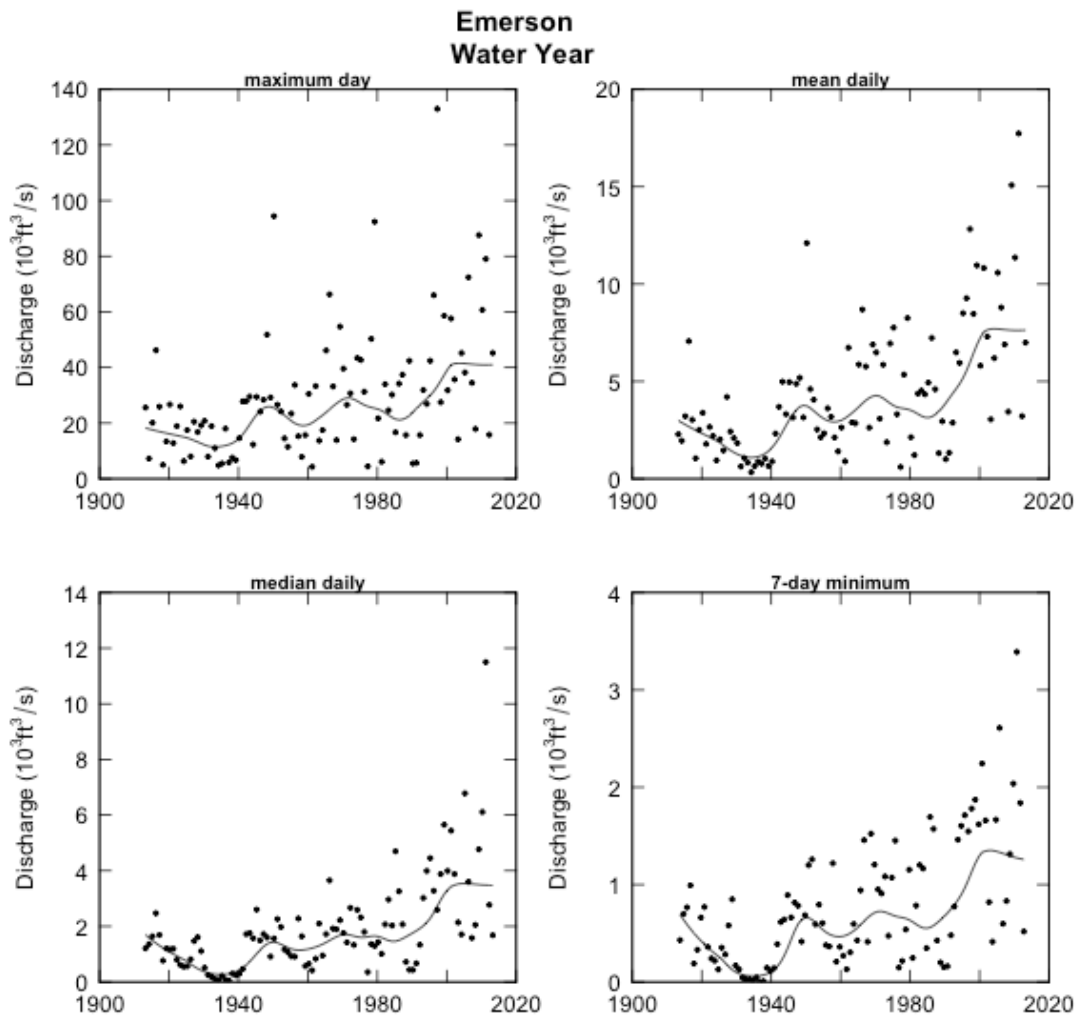


Figure C.27. Annual 1-day maximum daily mean discharge (maximum day), annual mean of the daily mean discharges (mean daily), annual median of the daily mean discharges (median daily), and annual minimum 7-day mean of the daily mean discharges (7-day minimum), Red River of the North at Emerson, Manitoba.

In examining the statistics (fig. C.27) one can still see the influence of the Red Lake River (fig. C.18) in the pattern of the Red River at Emerson, Manitoba.

**APPENDIX D. DIAGNOSTIC PLOTS FOR WEIGHTED REGRESSIONS ON TIME,  
DISCHARGE, AND SEASON (WRTDS) ANALYSES OF TOTAL PHOSPHORUS IN  
THE RED RIVER OF THE NORTH AT EMERSON, MANITOBA, AND FARGO,  
NORTH DAKOTA-MOORHEAD, MINNESOTA**

Following are the diagnostic plots produced by the software package Exploration and Graphics for RivEr Trends (EGRET; Hirsch and De Cicco, 2014) when it performs the Weighted Regressions on Time, Discharge, and Season (WRTDS) analysis for the site on the Red River at Emerson, Manitoba, and the site on the Red River at Fargo, North Dakota, and Moorhead, Minnesota.

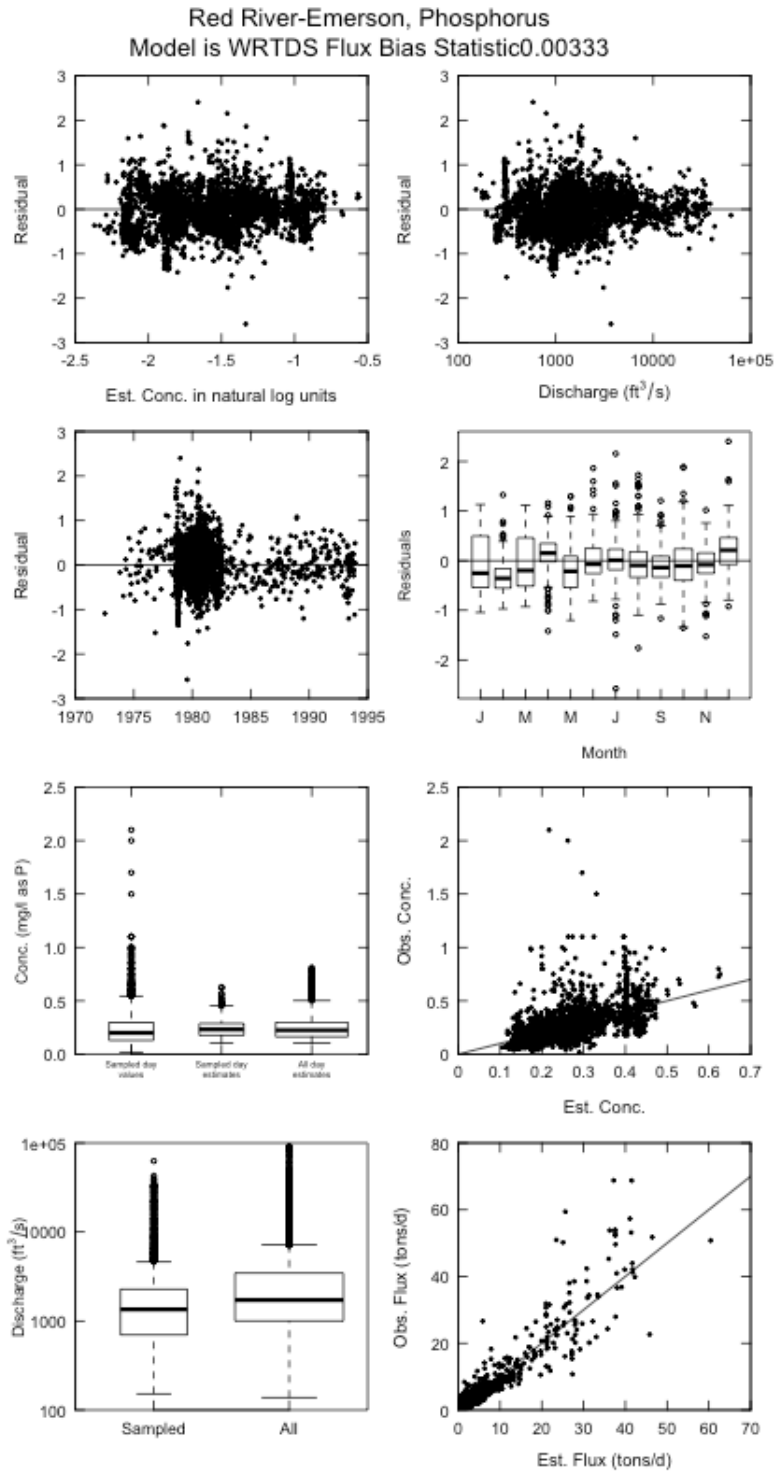


Figure D.1. WRTDS diagnostic plots for 1970-1993 total phosphorus model for the Red River of the North at Emerson, Manitoba.

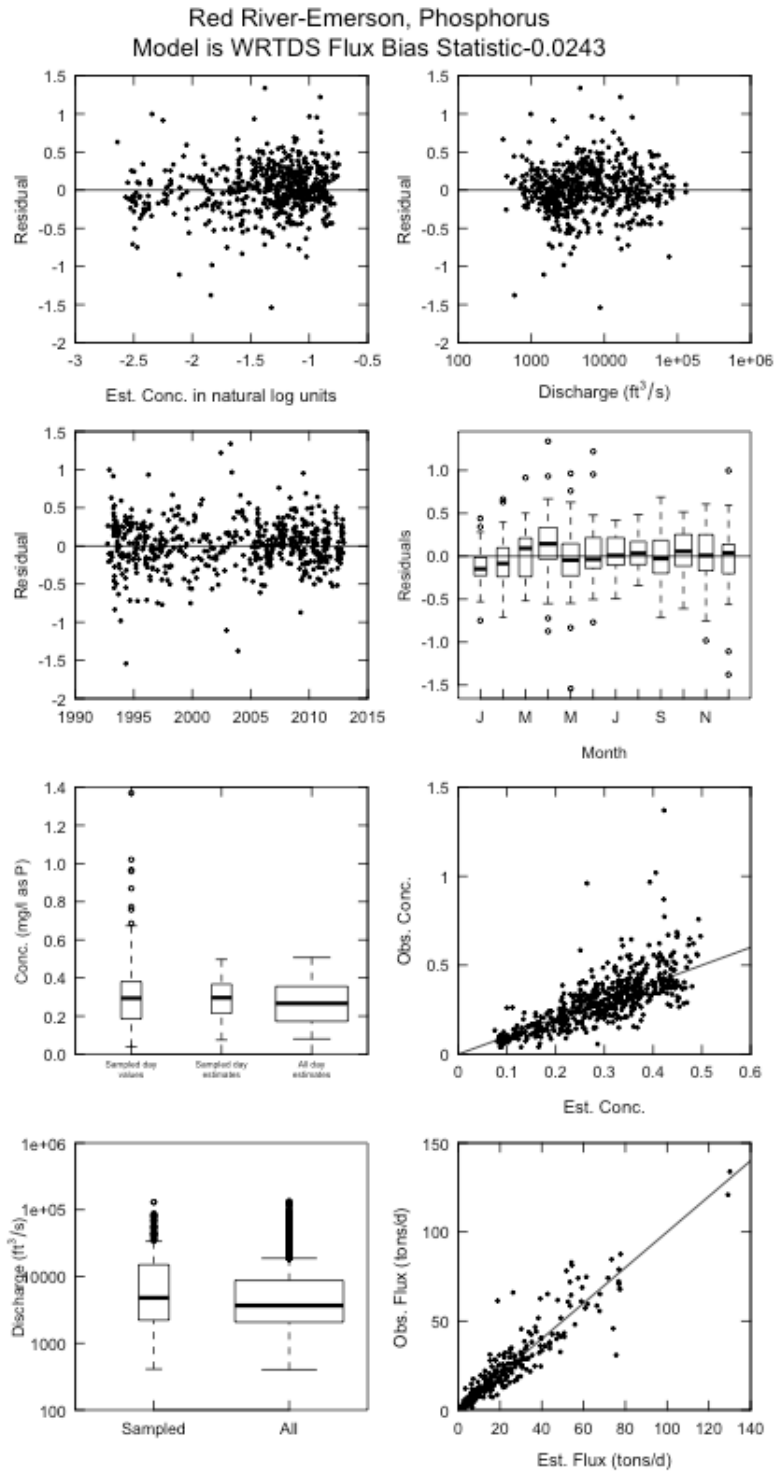


Figure D.2. WRTDS diagnostic plots for 1993-2012 total phosphorus model for the Red River of the North at Emerson, Manitoba.

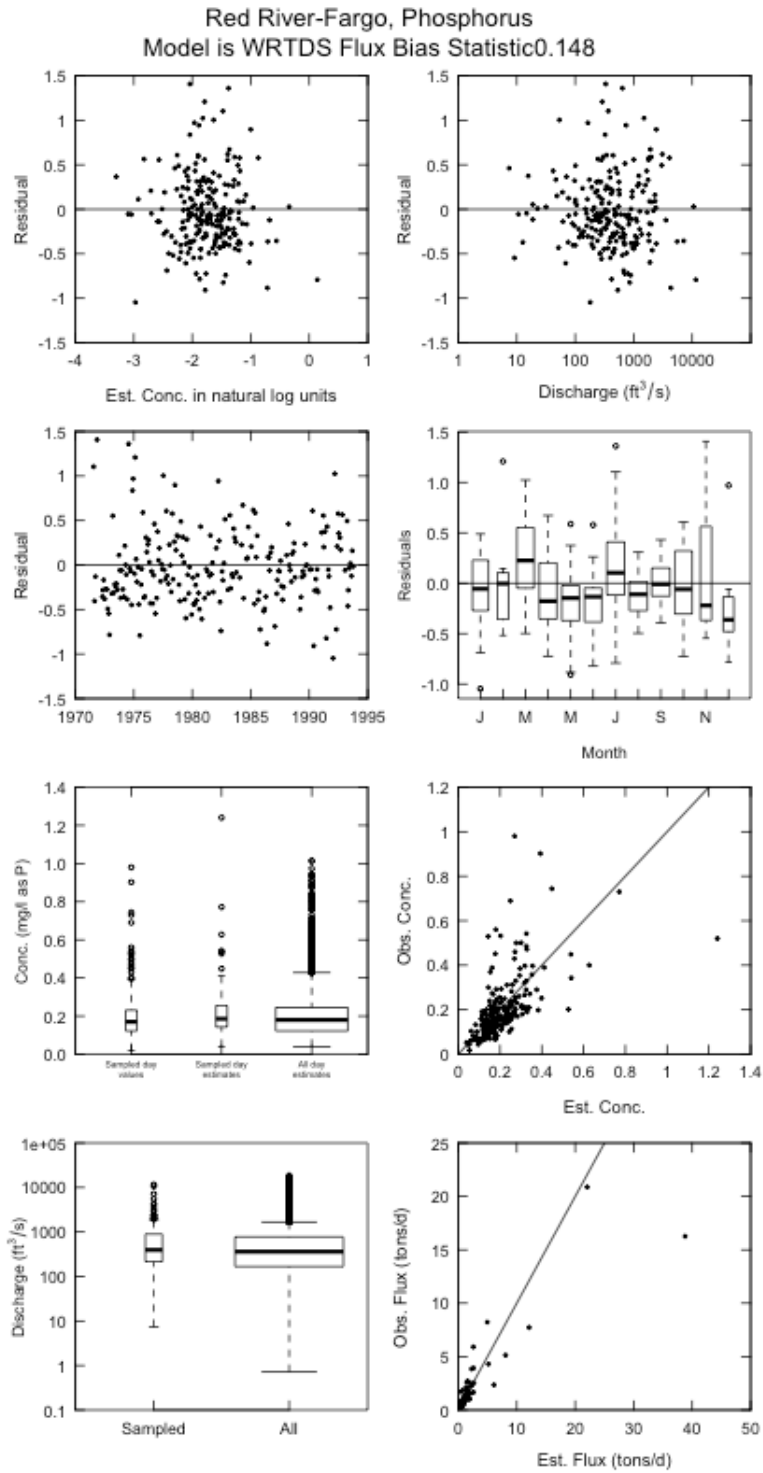


Figure D.3. WRTDS diagnostic plots for 1970-1993 total phosphorus model for the Red River of the North at Fargo, North Dakota-Moorhead, Minnesota.

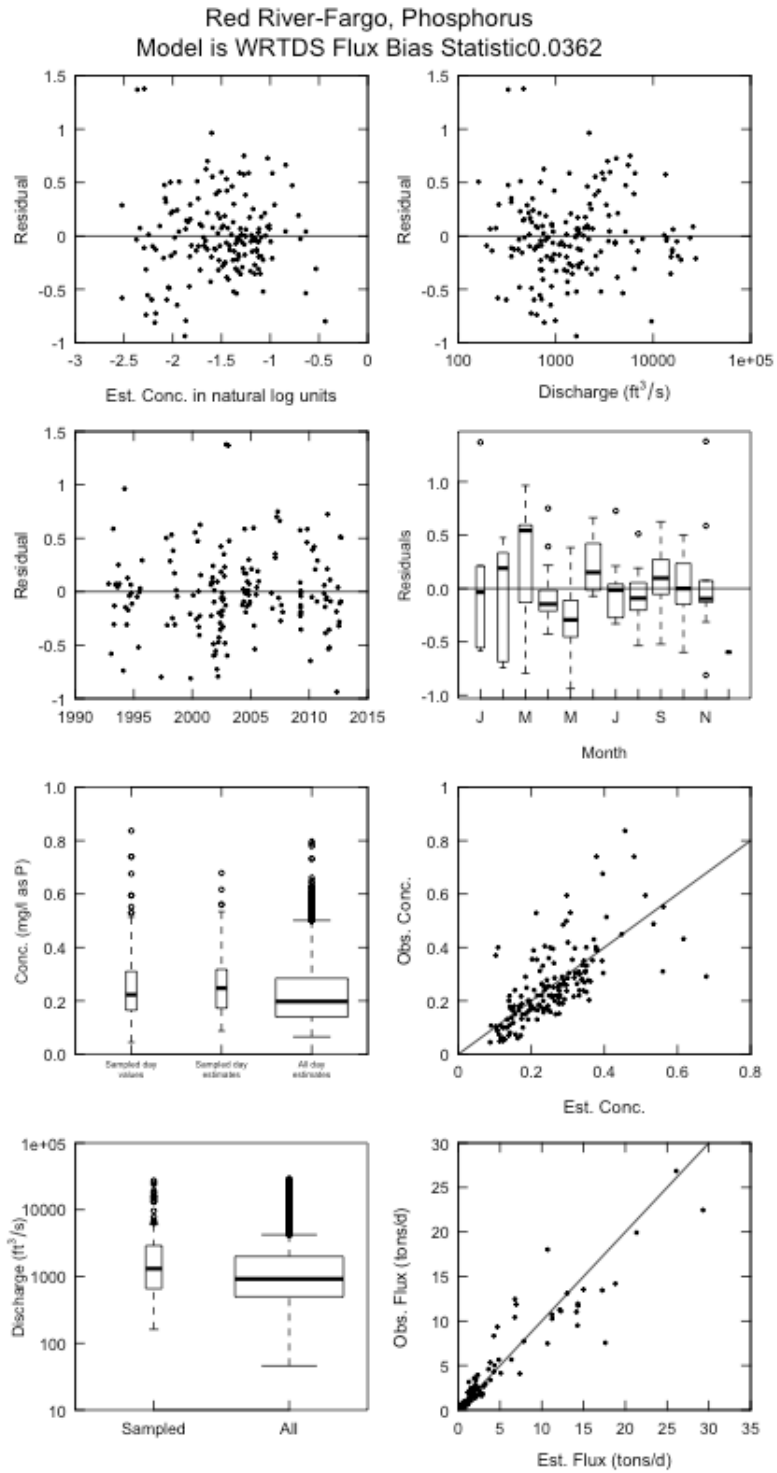


Figure D.4. WRTDS diagnostic plots for 1993-2012 total phosphorus model for the Red River of the North at Fargo, North Dakota-Moorhead, Minnesota.